Mathematical Methods for Reflector Design

Maurice Maes

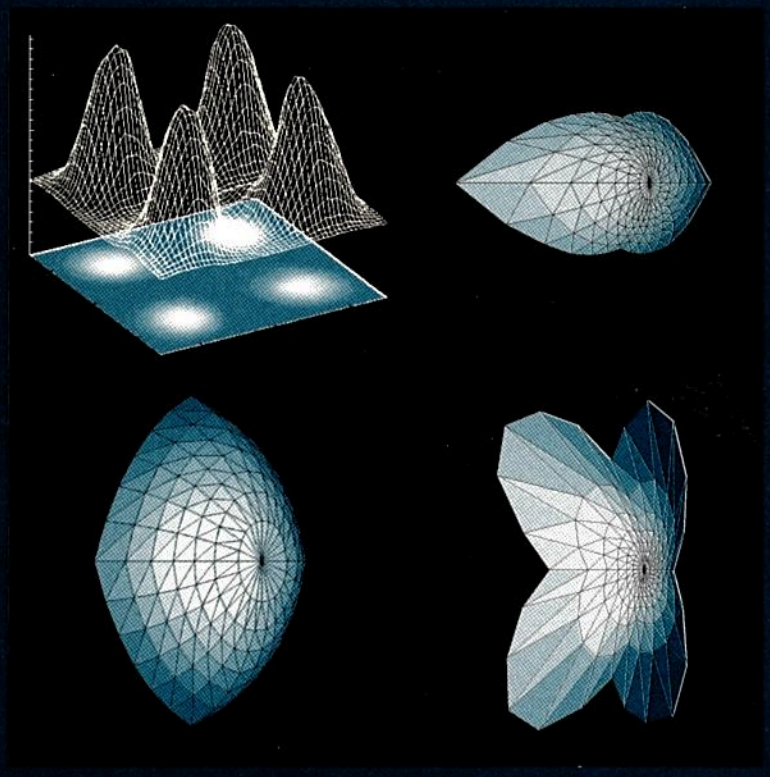

STELLINGEN

behorende bij het proefschrift

Mathematical Methods for Reflector Design

door Maurice Maes

I

Tweemaal differentieerbare, enkelvoudig samenhangende spiegeloppervlakken die in combinatie met een puntbron als lamp geen oneindige intensiteiten in het gereflecteerde licht opleveren, worden in dit proefschrift geclassificeerd op grond van de kromming van het golffront van het gereflecteerde licht. Convexe en concave golffronten corresponderen met wat men in de praktijk convergente en divergente stralengangen noemt.

[Dit proefschrift, Hoofdstuk 6, Stelling 6.5.4.]

II

Dát we zoveel klassificeren, is 'n gevolg van ons weinig weten en beperkt verstand. Om over 't weinige, dat onder ons waarnemingsvermogen valt, te heersen, hebben wy de toepassing van 't *divide et impera* nodig.

[Multatuli, *Ideeën*, Derde Bundel (1871), uit Idee **600**.]

III

Voor hyperbolische stralengangen is er geen gangbare term in de verlichtingswereld. Dit illustreert het feit dat dit type oplossingen daar nog onbekend is en nauwelijks gebruikt wordt. Voor optisch ontwerpers liggen hier mogelijkheden tot vernieuwing.

IV

Laat $\bar{\theta}\colon [t_1, t_2] \to \mathbb{R}$ een gladde, niet-dalende functie zijn, en laat f een gladde, oneven functie zijn met een convexe, niet-negatieve afgeleide. Wat is dan de maximale waarde van de functionaal $J(\theta) = \int_{t_1}^{t_2} f(s + \theta(s))\, ds$ over alle $\theta\colon [t_1, t_2] \to \mathbb{R}$ die 'rearrangements' zijn van $\bar{\theta}$? Als $||\bar{\theta}'||_\infty < 2$ en als $\bar{\theta}'(t) = \frac{1}{2}$ voor slechts een eindig aantal waarden t, dan is de optimale θ analytisch te beschrijven. Deze functie is dan V-vormig, en continu op de linker vleugel van de V.

[Dit proefschrift, Hoofdstuk 4.]

V

Laat een bolvormige lichtbron gecentreerd geplaatst zijn op de symmetrie-as van een kegelvormige reflector. Afhankelijk van de hoek waaruit men in de optiek kijkt, is het deel van de reflector dat licht weerkaatst hetzij één ringvormig gebied, of het bestaat uit twee, onderling niet met elkaar verbonden, enkelvoudig samenhangende gebieden.

[Dit proefschrift, Hoofdstuk 5.]

VI

Het in de praktijk gangbare gebruik van vierhoekige facetten bij het ontwerpen van reflectoren, is zeer ongeschikt wanneer er geen sprake is van rotatie- of cylindersymmetrie.

VII

Een vuistregel in de straatverlichting is dat de maximale afstand tussen twee lantaarnpalen 6 maal de hoogte bedraagt. Theoretisch is die afstand 2π maal de hoogte.

VIII

In de studie van topologische eigenschappen van digitale beelden, heeft men geprobeerd topologieën op digitale beelden te definiëren, zodat samenhangende verzamelingen in de topologische zin samenvallen met verzamelingen pixels die via buurpixels aan elkaar verbonden zijn. De resultaten in [1] en [2] behandelen speciale gevallen van de vraag: voor welke grafen kan men een topologie op de verzameling hoekpunten definiëren zodanig dat de samenhangende verzamelingen in graaftheoretische en in topologische zin samenvallen? Dit zijn precies de 'comparability' grafen, d.w.z. grafen waarvan de zijden transitief oriënteerbaar zijn [3]. Uit deze stelling volgen de resultaten van [1] en [2] onmiddellijk.

[[1] Solution to Problem 5712, *The American Mathematical Monthly* **77**, 1970, p. 1119.
[2] J.-M. Chassery, Connectivity and Consecutivity in Digital Pictures, *Computer Graphics and Image Processing*, **9**, 1979, pp. 294-300.
[3] M.J.J.J.B. Maes en H.D.L. Hollmann, niet gepubliceerd manuscript, 1991.]

IX

Anything is a work of art, if you take the time to frame it.

[Jack Hardy, from the album "*Through*", 1991.]

X

The front row is not for the fragile.

[Nick Cave, Groningen, 1982.]

Mathematical Methods for Reflector Design

Cover:
Hyperbolic, convergent and divergent reflectors which all three produce a light distribution consisting of four isolated peaks.

Mathematical Methods for Reflector Design

ACADEMISCH PROEFSCHIFT

ter verkrijging van de graad van doctor
aan de Universiteit van Amsterdam,
op gezag van de Rector Magnificus
Prof.dr. J.J.M. Franse,
ten overstaan van een door
het college van dekanen ingestelde commissie
in het openbaar te verdedigen in de Aula der Universiteit
op maandag 6 oktober 1997, te 13.00 uur

door

Maurice Jérôme Justin Jean-Baptiste Maes

geboren te Maastricht

Promotor: Prof.dr. P.W. Hemker
Co-promotor: Dr. S.M. Verduyn Lunel

CIP-gegevens Koninklijke Bibliotheek, Den Haag
Maes, M.J.J.J.B.
Mathematical Methods for Reflector Design
Proefschrift Universiteit van Amsterdam,-Met lit. opg.,
-Met samenvatting in het Nederlands.
ISBN 90-74445-36-5
Trefw.: reflector ontwerp

The work described in this thesis has been carried out
at the PHILIPS RESEARCH LABORATORIES Eindhoven,
the Netherlands, as part of the Philips Research Programme.

"Herinner u — of weet, als ge dit nooit mocht hebben vernomen — dat wiskunde in-genen-dele 'n zogenaamd droog vak is..."
Multatuli, *Ideeën*, Derde Bundel (1871), uit Idee **599**.

Voor mijn ouders:
Math Maes en Leny Maes - van Loo

Acknowledgments

This work on reflector design has been carried out at the Philips Research Laboratories in the Applied Mathematics Group. It was part of a long-term research project for the Central Development department of Philips Lighting.

I'd like to thank Marten Sikkens, former group leader of the Optical Design group, for his long time support of, and confidence in my approach. A complete list of optical designers who have helped me finding the right problems to solve would become too long. Throughout the years, I have enjoyed working with Johan Ansems, Gerard Harbers, Ton van Hees, Herman Muller, Dennis van Oers, Jelle Schuurmans, and many others.

Several people have helped with the realization of computer tools for reflector design, based on my methods. In particular, I'd like to thank Rob Kettler and Christ Vriens for their work on the 2D design tool we developed. For the 3D tool, I am highly indebted to Marjan Driessen, who also reviewed an earlier version of this thesis, and who proposed many improvements.

My friend Eisso Atzema has critically read this work, found several errors, and made many useful suggestions to improve the text. Henk Hollmann and Hans Melissen have reviewed an early version of Chapter 4, which was co-written by Guido Janssen. I'd like to thank Guido for this cooperation, and for thoroughly reviewing this thesis.

It is a pleasure for me to express my gratitude to my promotor Piet Hemker for many useful discussions and suggestions concerning the presentation of my results. I would also like to thank my co-promotor Sjoerd Verduyn Lunel, as well as Sebastiaan van Strien, for taking the time to listen to my presentations and to read this thesis.

I am indebted to my former and present group leaders Kees Stam and Menno Treffers, for giving their support to write this thesis.

This thesis has been typeset with LaTeX. Special thanks are due to Ronald van Rijn, Jurgen Rusch and Henk Hollmann for providing templates and for helping me out with all my LaTeX questions.

Contents

Chapter 1

Introduction

1.1 Reflector Design in Practice

This thesis describes some of the results of a long-term research project on reflector design, carried out within Philips Research Laboratories. A basic problem in lighting technology is to design an optical system that illuminates a certain object in a prescribed manner. In many lighting systems, the proper design of a reflector is essential to obtain a required lighting effect. The reflector design problem is that of finding a reflector which, in combination with a known light source, produces a required light distribution, under several additional conditions such as geometric constraints.

For Philips Lighting, reflector design has applications in a wide variety of products such as road or playground lighting systems, but also e.g. in Liquid Crystal Display back-lighting and in Projection TV.

Practical reflector design has long been a matter of craftsmanship. Presently, computer tools are more and more used to speed up the design process, and to come to new or better reflectors. Let us have a look at the practical design process, and see where exactly computer tools based on mathematical methods can contribute. The overall design process generally consists of the following four steps.

The first step is that of the *problem specification*. The requirements of a customer are translated into a problem formulation for the designer. The requirements will always consist of a desired lighting effect and of geometrical constraints on the lighting system. Additionally, economic, aesthetical, and even strategic or legal considerations may be important. The designer's role starts with translating these requirements to the choice of a light source, and to a more formal specification of geometric constraints and of a required illuminance for the system.

The second step is that of a *simplification* of the problem. In its most general form, the reflector design problem is too difficult to handle. So reflection is usually assumed to be specular and light sources are assumed to be geometrically simple. For instance, in the case of Low Voltage Halogen or UHP lamps one can safely assume the light source to be a point source. Also, in initial stages the problem is often treated two-dimensionally. Very often, designers choose for reflectors consisting of planar facets.

The third step, and this is the most difficult step, is to *achieve a correspondence between facets and parts of the required light distribution*, such that all the contributions of the facets add up to the required distribution, while the facets form a connected surface satisfying the prescribed geometric constraints. Usually it is attempted to do this in such a way that multiple reflections do not occur and that reflected rays do not re-enter the light source. Typically, this step is very time-consuming, and is usually one of trial and error. In this third step, mathematical insight and computer tools based on mathematical methods can contribute significantly.

The fourth step is that of *verification*, which may either be done on a computer (e.g. by ray-tracing), or at a later stage by prototyping and measuring. For ray-tracing, many computer programs have become available in recent years.

1.1.1 The Aim of our Research and of this Thesis

The aim of our research project has been to assist the optical designer's design process by a better theoretical understanding of the subject, as well as by implementing new design methods in computer tools. Our research project has resulted in dedicated computer tools for 2D and 3D problems with small light sources.

We have focussed on contributing to the third design step, by a mathematical approach to the problem, rather than by trial and error. To allow mathematical treatment, we too have had to make several simplifying assumptions, usually quite similar to those of the designers. Most importantly, we have assumed light sources to be very small. Our assumptions will be discussed in more detail in Section 2.3.

In this thesis, I give an overview of the mathematics behind the methods we employed. A mathematical understanding of the problem is in my opinion crucial in order to discover successful heuristic methods to actually solve the problem. In the 2D case, I give a complete overview of our method, as well as of practical and mathematical issues which play a role. In the 3D case, this thesis is restricted to results that give a better insight into the problem, and which formed the basis for our heuristic approach, but our actual method had to be excluded here.

As the readers of this thesis will notice, various mathematical disciplines are being applied to reflector design. I have attempted to write this thesis such that

it is accessible to readers with a general mathematical background. Whenever more specific knowledge is required, necessary definitions as well as references are included.

1.2 Other Approaches; Literature Overview

Literature on reflector design for non-imaging optics is relatively sparse. Optical design for lighting applications has always been, and still is, a speciality that is mainly exercised by practical craftsmen. The scientific world has always had little interest in non-imaging optics, as compared to that in imaging optics.

When it comes to literature on reflector design, we can distinguish between articles dealing with specific solutions for practical problems, and those dealing with more general design methods for a wider range of applications. We are interested in the latter. We can then distinguish between the literature which deals with the *direct problem* and that which deals with the *inverse problem*. The direct problem is the problem of calculating the achieved light distribution for a given source and reflector, while the inverse problem concerns computing the reflector, given the lamp and the required light distribution. Examples of articles dealing with the direct problem are [5, 31, 32, 40]. We will however mainly be concerned with the inverse problem.

General methods for the inverse problem can be subdivided into the following three categories:

- optimization methods,
- heuristic methods that attempt to formalize or automate the divide-and-conquer approach for facetted reflectors,
- approaches based on a mathematical description in terms of partial differential equations of the problem for point sources and smooth reflector surfaces.

These categories will be discussed in more detail below. Let us first mention two older publications that give an overview of the state of the art at the times they were written.

An early standard work for optical designers is the book by Elmer [7]. This book is very much written from the practical viewpoint, and does not really have a mathematical approach to the problem. Weis [41] gives an overview of what is known in the field by the late 70s. It appears that for 2D problems with point sources, the basic solution is well-known, and published several times, e.g. in [1, 15, 45]. For 3D problems with point sources, Weis mentions some work that had

been done mainly in the USSR. The more important developments in the 1970s, published by Schruben [34] and by Westcott et al. (see below) are not mentioned. For area sources, the inverse problem has only been dealt with for special, mostly spherical or cylindrical sources, and usually for rotationally symmetric reflectors. For more general cases, only the direct problem is considered.

It needs no explication that computer technology has had a big impact on optical design methods. For the direct problem, fast methods based on ray tracing or the calculation of view factors have become available. This in turn has opened opportunities for methods based on optimization. When we have a description of a class of reflectors by a limited set of parameters, we can try to find an optimal set of parameters by doing many tests (i.e. direct calculations) while changing the parameters in a clever way. This has proven to be feasible for 2D problems, see e.g. [20, 27]. In the 3D case, this approach has not yet been very successful. The direct methods usually are not yet fast enough to get reasonable computing times. Suitable parametric descriptions of reflectors are not obvious, and the difficulty to provide good initial guesses for new problem classes is another bottleneck.

The availability of computers has also led to methods that try to automate the time-consuming divide-and-conquer approach, see e.g. [26]. It is relatively easy to automatically direct individual facets of a facetted reflector in such a way that the sum of the contributions of the facets resembles the required distribution. The hard part however, is to do this in such a way that a nicely shaped connected reflector surface is obtained, especially if certain geometric constraints have to be satisfied as well. What is usually lacking in heuristic approaches to achieve this, is an understanding of what sort of light distributions or ray paths can actually be realised by connected surfaces. This understanding can only come from a more analytical, mathematical approach. For point sources, the fundamentals in this field have been established in the literature that we will discuss in the next section.

1.2.1 Literature on the Monge-Ampère Approach

The Monge-Ampère equation first appears in relation to reflector design for point sources in an article by Schruben [34] in 1972. In that article, the near field problem is considered: the required distribution is defined as an illuminance on a plane, as opposed to the far field problem, where required intensities are defined on angles. Schruben derives the non-linear partial differential equation that describes the problem, thus expressing it as a singular elliptic Monge-Ampère boundary-value problem. In the second half of the 1970s, Westcott and others at the University of Southampton study the far field problem, having applications to microwave antenna design in mind.

Westcott and Norris [44] apply techniques of differential geometry to derive the Monge-Ampère equation. Elliptic and hyperbolic solutions are being distinguished, and related to the number of caustic surfaces that may occur. As a special case, even azimuthal symmetric fields are considered and numerical solutions for this class of problems are presented in [28]. The hyperbolic case is further studied in [3, 43]. A derived set of quasi-linear equations is solved by a numerical finite differences method.

Later, complex coordinates are used [2, 4]. These simplify notation, but do not seem to help in finding actual solutions to the problem. From the theoretical viewpoint, questions of existence and uniqueness remain unanswered. For practical purposes, a bottleneck is the unavailability of good initial data, as pointed out in the conclusions of [3].

In 1981, a first uniqueness result for 3D far field problems is obtained by Marder [24]. It is shown that in the elliptic case, there are at most 2 solutions, provided that either the incident of the reflected ray cone satisfies a convexity condition. This condition is always fulfilled if one of the cones is circular. When both cones are circular, and luminous intensities are close to radially symmetric (in some Hölder norm), then the existence of solutions can be proven, as was done by Oliker [29] in 1987.

1.3 The Contents of this Thesis

Let us now summarize the contents of this thesis.

In Chapter 2, we introduce some Lighting terminology, and we define the 3D reflector design problem. We make several simplifying assumptions, such that the problem allows a mathematical formulation that gives hope to find actual solutions of the problem. The most important assumption is that we consider the light source to be a point source. The Law of Reflection, and Conservation of Energy are formulated.

If the 3D problem as sketched in Chapter 2 has rotational symmetry, then it allows a 2D treatment. The same applies to a cylindrically symmetric problem with an infinite line source. Chapter 3 deals with 2D problems. It will be shown that in 2D, when we consider reflectors which produce smooth ray paths, then there are at most two solutions corresponding to convergent and divergent ray paths. However, when reflectors are allowed to be only piecewise smooth, then infinitely many solutions may exist. We may then consider practically relevant constraints, such as constraints on the size of the reflector.

This has led to the study of smallest and largest 2D reflectors that solve a given problem. Chapter 4 is completely dedicated to this optimization problem.

We have slightly generalized the optimization problem that we consider, and consequently this chapter is to a large extent independent of the others.

The same holds for Chapter 5 which is the only chapter that deals with the direct problem: that of computing the achieved light distribution for a given source and reflector. In this chapter we consider 2D facetted reflectors with spherical and cylindrical area sources. We show that in these cases intensities and illuminances can be computed analytically, so direct calculations can be done much faster than by straightforwardly using ray tracing methods.

It is not until Chapter 6 that we return to the actual 3D problem that we started with. Rather than directly trying to solve the actual problem — which boils down to solving a non-linear partial differential equation of the Monge-Ampère type — we will classify the types of solutions that may occur. These types correspond to hyperbolic and elliptic ray paths, where in the elliptic case we can further distinguish between convergent and divergent ray paths. Some fixed point properties of these ray path types will be deduced. These results give insight in the geometry of the ray paths, and have proven to be helpful in finding actual solutions to the problem.

Finally, in Appendix A, we present a few examples of reflectors that have been designed by heuristic methods, based on the theory in this thesis.

Chapter 2

3D Mathematical Problem Statement

2.1 Introduction to the 3D Problem Statement

This chapter introduces the 3D reflector design problem for point sources that we will consider. It is limited to the formulation of the problem and the basic laws that play a role in reflector design. The 2D problems of the following chapter may refer to a rotationally symmetric special case of the problem sketched here. In Chapter 6, we will return to the 3D problem in more detail.

2.2 Lighting Terminology

We recall the basic notions of Lighting Theory that we will use. The terminology in Lighting Theory can easily lead to confusion. This is partly due to the fact that it has changed in the course of time, so different books may use different symbols, names or units in the same context. We adopt the terminology used by Keitz [14], unless indicated otherwise. For more details we refer to this book.

The *luminous flux* Φ of a light source is the radiated energy per second, where the energy is evaluated on the basis of the impression which it induces in the eye. The usual unit of luminous flux is the *lumen (lm)*.

For a *point source*, the *luminous intensity*, or just *intensity* I is the luminous flux per solid angle. So the total intensity of the source and the intensity in a certain direction are given by

$$I_{tot} = \frac{\Phi}{4\pi} \quad \text{and} \quad I = \frac{d\Phi}{d\Omega}, \tag{2.1}$$

respectively, where $d\Omega$ is an infinitesimal solid angle. The unit of intensity is the *candela (cd)*.

The luminous flux received per unit area of an illuminated surface is called the *illumination* (as it is called by Keitz and many others) or the *illuminance* (as it is called in more modern books on Lighting standards). The symbol for illuminance is E. The total illuminance of a surface S, and the illuminance at a certain point of the surface, are given by

$$E_{tot} = \frac{\Phi}{S} \quad \text{and} \quad E = \frac{d\Phi}{dS}, \tag{2.2}$$

respectively. The unit of illuminance is *lux*.

Now, for point sources, it follows from (2.2) and (2.1) that $E\,dS = I\,d\Omega$. Consequently, illuminance and intensity are related by the *inverse square law*, which is

$$E = \frac{I\cos\alpha}{d^2}, \tag{2.3}$$

where E is the illuminance in a point on a surface at a distance d to the source, and α is the angle between the normal to the surface at that point, and the line joining the point and the source.

For area sources, the brightness of the source is given by *the quotient of the luminous intensity divided by the apparent surface of the light source*. This used to be called *brightness* and denoted by the symbol B, but the modern term is *luminance*, denoted by the symbol L. The standard unit of luminance is the *stilb*, but several other units are used as well. For a plane surface or a surface element S, we find the luminance in direction α given by

$$L_\alpha = \frac{I_\alpha}{S\cos\alpha},$$

where I_α is the intensity in direction α. The source is said to be a *uniform diffuser* or a *perfect diffuser* if L_α is constant (and thus $L_\alpha = L_0$ for all α). This is the case if for all α we have

$$\frac{I_\alpha}{\cos\alpha} = I_0,$$

where I_0 is the intensity of the source in the direction perpendicular to the surface. This latter equation is known as *Lamberts law*. A perfect diffuser is also often said to be a surface radiating in accordance with Lamberts law. For a surface element or a plane surface that is perfectly diffuse, the relation between I_0 and the flux emitted by that surface is given by

$$\pi I_0 = \Phi.$$

There is one more definition that we need. Note that we have defined the intensity distribution for point sources only. To define the intensity for area sources, it makes sense to define it in such a way that the inverse square law holds in the limiting case that the screen is moved infinitely far away from the source. So we define I by

$$I = \lim_{d \to \infty} \frac{Ed^2}{\cos \alpha},$$

where d and α may be measured relative to any fixed point on the source (the choice of this point has no effect).

While I is the symbol we will use for the luminous intensity of the source, we will write G for the required or achieved far field intensity of the source in combination with a reflector. In Chapters 3 and 4, we will consider 2D problems, and the 2D analogues of I, G and E, will be denoted $\mathcal{I}$, $\mathcal{G}$ and $\mathcal{E}$.

2.3 Problem Simplification; Restrictions

As already indicated in the introduction, the reflector design problem in its most general form cannot be modelled or solved by mathematical methods. We therefore have to make several assumptions that simplify the problem. We now give a more detailed overview of these assumptions, which may differ from chapter to chapter. In the introduction to each chapter we will be more precise about the specific assumptions we make.

The Light Source. In the 3D case, we assume that the light source is a point source with an arbitrary intensity profile. In the 2D case of Chapter 3, the 2D point source of arbitrary intensity represents either a 3D point source with a rotationally symmetric intensity, or it represents a line source of infinite length and homogeneous intensity. When studying the direct problem for area sources in Chapter 5, we also consider infinite Lambertian cylinders, and Lambertian spheres as light sources.

The Reflector. The reflector is assumed to be a specularly reflecting surface, with a fixed reflection coefficient ρ. In the 3D case, this surface is assumed to be smooth and simply connected. In the 2D case, we consider reflectors represented by *piecewise* smooth curves.

The Required Light Distribution. The required distribution can either be an intensity distribution defined on angles (the far field problem), or an illuminance

on the screen (the near field problem). In both cases, we do not consider infinite intensities. In the 3D case, we only consider far field problems. When we have a screen in the 2D case, this screen refers to a planar disc or strip in 3D.

Other Constraints. We generally do not bother with multiple reflections, or with reflected light re-entering the light source, although in the 2D case we do give this subject some attention. Geometric constraints get special attention in the 2D case, in the 3D case these are not really considered. Practical matters as aesthetics, manufacturability, heat problems etc. are not considered here.

2.4 Notation for 3D Point Source Problems

In this section we define and introduce the notation for the 3D model problem. Since we are dealing with a point source, it is natural to define the design problem in spherical coordinates relative to this source.

Suppose we have a rectangular xyz-coordinate system in $\mathbb{R}^3$, with a point source located at the origin. Rays that are emitted from the source and incident on the reflector are represented by unit vectors

$$\mathbf{v} := \mathbf{v}(t, u) := (\cos t, \sin t \cos u, \sin t \sin u), \tag{2.4}$$

for $t \in [0, \pi]$ and $u \in [0, 2\pi]$. The reflector surface $\mathbf{r}(t, u)$ is given by

$$\mathbf{r} := \mathbf{r}(t, u) := f(t, u)\mathbf{v}(t, u), \tag{2.5}$$

where f is twice differentiable, strictly positive, and where $f(t, 0) = f(t, 2\pi)$ for all t. The function f and the surface $\mathbf{r}$ are defined on some fixed t, u domain, usually of the form $t \in [t_1, t_2]$ and $u \in [0, 2\pi]$. Note that the representation (2.5) is well-defined for $t = 0$ only if $f_u = \frac{\partial}{\partial u} f(t, u) = 0$ at $t = 0$, i.e. $f(0, u)$ is constant.

A reflected ray is denoted by the vector $\mathbf{w}$ (of unit length), which is often given in spherical coordinates θ, ϕ as follows,

$$\mathbf{w} := \mathbf{w}(\theta, \phi) := (-\cos\theta, \sin\theta \cos\phi, \sin\theta \sin\phi), \tag{2.6}$$

for $\theta \in [0, \pi]$ and $\phi \in [0, 2\pi]$.

2.5 The Law of Reflection

The reflector surface $\mathbf{r}(t, u) = f(t, u)\mathbf{v}(t, u)$ has normal

$$\mathbf{n} = \mathbf{n}(t, u) = \frac{\mathbf{r}_t \times \mathbf{r}_u}{|\mathbf{r}_t \times \mathbf{r}_u|}, \tag{2.7}$$

where $\mathbf{r}_t = \frac{\partial}{\partial t}\mathbf{r}(t, u)$ and $\mathbf{r}_u = \frac{\partial}{\partial u}\mathbf{r}(t, u)$.

According to the law of reflection, incident and reflected rays form equal angles with the normal to the surface in the point of incidence. So we have

$$\mathbf{v}.\mathbf{n} = -\mathbf{w}.\mathbf{n}, \tag{2.8}$$

or equivalently any of the following three expressions

$$\mathbf{w} = \mathbf{v} - 2(\mathbf{v}.\mathbf{n}).\mathbf{n}, \tag{2.9}$$

$$\mathbf{v} = \mathbf{w} - 2(\mathbf{w}.\mathbf{n}).\mathbf{n}, \tag{2.10}$$

$$\mathbf{n} = \frac{\mathbf{v} - \mathbf{w}}{\sqrt{2 - 2(\mathbf{v}.\mathbf{w})}}. \tag{2.11}$$

2.6 Conservation of Energy; Problem Statement

Now let G be a required far field intensity pattern for the *reflected* light, let I be the luminous intensity of the point source and let ρ be the reflection coefficient of the reflector. We will consider the problem of finding a specular reflector that in combination with the source produces the far field intensity G. Let the reflector surface be described by a function f as above on a given t, u domain.

Let us assume we have a one-to-one correspondence between incident and reflected rays. Then the reflector produces the required intensity if and only if for all $\mathbf{v}$ and corresponding $\mathbf{w}$, we have

$$G(\mathbf{w})|d\Omega| = \rho I(\mathbf{v})|d\Omega'|, \tag{2.12}$$

where $d\Omega'$ and $d\Omega$ are solid angles corresponding to incident and reflected ray cones, respectively. We have

$$d\Omega' = [\mathbf{v}, \mathbf{v}_t, \mathbf{v}_u]\,\mathrm{d}t\,\mathrm{d}u = \sin t\,\mathrm{d}t\,\mathrm{d}u, \tag{2.13}$$

$$d\Omega = [\mathbf{w}, \mathbf{w}_\theta, \mathbf{w}_\phi]\,\mathrm{d}\theta\,\mathrm{d}\phi = -\sin\theta\,\mathrm{d}\theta\,\mathrm{d}\phi, \tag{2.14}$$

where the *scalar triple product* $[\mathbf{a}, \mathbf{b}, \mathbf{c}]$ for vectors

$$\mathbf{a} = (a_1, a_2, a_3),\ \mathbf{b} = (b_1, b_2, b_3) \text{ and } \mathbf{c} = (c_1, c_2, c_3)$$

is defined by

$$[\mathbf{a}, \mathbf{b}, \mathbf{c}] := \mathbf{a}.(\mathbf{b} \times \mathbf{c}) = \begin{vmatrix} a_1 & b_1 & c_1 \\ a_2 & b_2 & c_2 \\ a_3 & b_3 & c_3 \end{vmatrix}.$$

So $[\mathbf{v}, \mathbf{v}_t, \mathbf{v}_u]$ and $[\mathbf{w}, \mathbf{w}_\theta, \mathbf{w}_\phi]$ are Jacobians. When we evaluate these, we can write the energy conservation equation as

$$G(\mathbf{w}) \sin\theta \, \mathrm{d}\theta \, \mathrm{d}\phi = \rho I(\mathbf{v}) \sin t \, \mathrm{d}t \, \mathrm{d}u. \tag{2.15}$$

Now, for a given function f, we have the reflected rays $\mathbf{w}$ given by (2.9), and f is a solution to the design problem if (2.15) holds in al directions. Of course, such a reflector can only be found if the condition of *global* conservation of energy is satisfied. So we should have

$$\iint G(\mathbf{w}) \sin\theta \, \mathrm{d}\theta \, \mathrm{d}\phi = \iint \rho I(\mathbf{v}) \sin t \, \mathrm{d}t \, \mathrm{d}u. \tag{2.16}$$

where the integration is over the appropriate domains.

Chapter 3

2D Problems with Point Sources

3.1 Introduction to 2D Problems

In this chapter we will see that the rotationally symmetric special case of the 3D problem of the previous chapter allows a 2D simplification, and it can be solved easily. Also, cylindrically symmetric problems with line sources are treated similarly. We consider both near and far field problems.

When we restrict ourselves to reflectors which produce smooth ray paths, then there will usually be exactly two solutions to the problem: those with convergent and divergent ray paths, respectively. However, when we allow the ray paths to be only piecewise smooth, then infinitely many solutions can be found, and one can pay attention to other conditions such as the absence of multiple reflections, or geometric constraints.

In our study of 2D problems, we will give many examples and consider a few specific problems, such as the uniform illumination of a circular disc.

3.2 2D Problem Statement

3.2.1 The Rotationally Symmetric Case

In this section we describe the rotationally symmetric 3D near field problem which allows a 2D treatment. Consider Figure 3.1. Suppose we have a Euclidean xyz-coordinate system in $\mathbb{R}^3$, with a point source located at the origin with a luminous intensity $I(t, u)$ in direction $(\cos t, \sin t \cos u, \sin t \sin u)$ which is rotationally symmetric around the x-axis, i.e. it does not depend on u and we can write $I(t)$ instead of $I(t, u)$.

Furthermore, suppose we have fixed angles $t_1, t_2 \in [0, \pi)$ with $t_1 < t_2$ (often

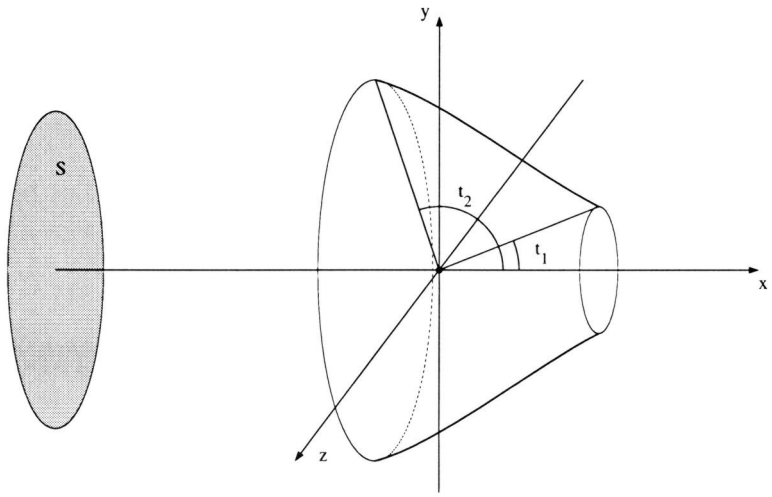

Figure 3.1: *The rotationally symmetric case.*

we will have $t_1 = 0$). Then a rotationally symmetric reflector around the x-axis between angles t_1 and t_2 can be described by a surface in $\mathbb{R}^3$ with parametrization

$$\mathbf{r}(t, u) := f(t)(\cos t, \sin t \cos u, \sin t \sin u), \tag{3.1}$$

where $t \in [t_1, t_2]$ and $u \in [0, 2\pi]$, and f is a continuous positive function.

Now, suppose that we have a screen that is represented by a disk S of the form

$$S := \{(x, y, z) \in \mathbb{R}^3 \mid x = -h,\ y^2 + z^2 \leq y_2^2\} \tag{3.2}$$

for a fixed distance h, and for fixed radius y_2. We first derive a formula for the direct illumination on the screen.

Proposition 3.2.1. *The direct illumination E_1 on S, caused by the source of intensity $I(\theta)$, in direction $(-\cos\theta, \sin\theta\cos\phi, \sin\theta\sin\phi)$ (again I does not depend on ϕ) is given by*

$$E_1(y, z) = I(\theta)\frac{h}{(y^2 + z^2 + h^2)^{3/2}} = I(\theta)\frac{\cos^3\theta}{h^2}, \tag{3.3}$$

where θ, ϕ and y, z are related by $y = h\tan\theta\cos\phi$ and $z = h\tan\theta\sin\phi$.

Proof. A ray from the origin in direction $(-\cos\theta, \sin\theta\cos\phi, \sin\theta\sin\phi)$ intersects S in a point $(-h, y, z)$ if and only if

$$y = h\tan\theta\cos\phi \text{ and } z = h\tan\theta\sin\phi,$$

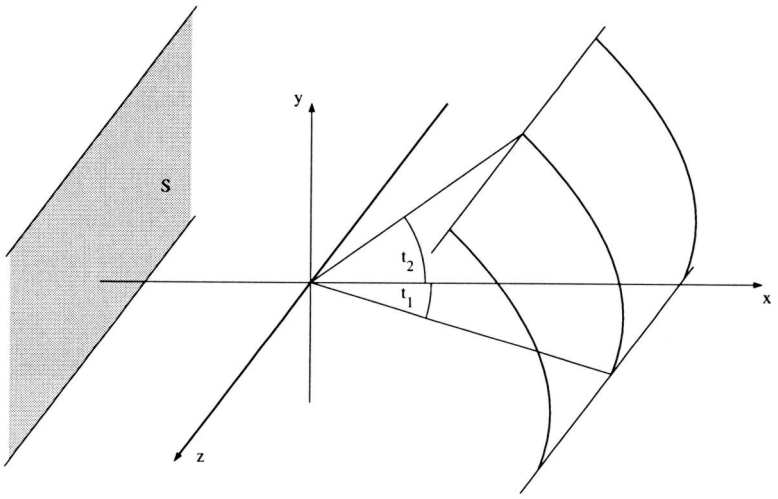

Figure 3.2: *The cylindrically symmetric case.*

so

$$\theta = \arctan \frac{\sqrt{y^2 + z^2}}{h}. \tag{3.4}$$

The proposition is now a consequence of the inverse square law (2.3). □

Now let E be a required illumination on S which is constant on circles in S with center $(-h, 0, 0)$, so E is of the form

$$E(y, z) = e(y^2 + z^2) \tag{3.5}$$

for some function $e : [0, y_2] \to \mathbb{R}^+$. We assume that e is a non-negative, integrable function. We may assume that E is the required illumination *for the reflected light only*: the direct light is known by the above proposition and can be subtracted. We will consider the problem of determining a reflector of the form (3.1) that realizes this required illumination E. In Section 3.2.5 we will show that this problem can be solved by solving a corresponding 2D problem.

3.2.2 The Cylindrically Symmetric Case

We now describe the cylindrically symmetric 3D near field problem which allows a 2D treatment. Consider Figure 3.2. Suppose that we have a rectangular xyz-coordinate system in $\mathbb{R}^3$, and that we have a linear, infinitely long light source l that coincides with the z-axis, of uniform radiation. This means that a line element dl at position $(0, 0, s)$ can be seen as a point source with intensity $I_1(\theta, \chi)$

in directions $(-\cos\theta \sin\chi, \sin\theta \sin\chi, \cos\chi)$ of the screen, and with intensity $I_2(t, \chi)$ in directions $(\cos t \sin\chi, \sin t \sin\chi, \cos\chi)$ of the reflector. The uniformity of l implies that this intensity distribution is independent of s.

Furthermore, suppose we have fixed angles $t_1, t_2 \in (-\pi, \pi)$ with $t_1 < t_2$. Then a cylindrical reflector for l between angles t_1 and t_2 can be described by a surface parameterized by

$$\mathbf{r}(t, z) = (f(t)\cos t,\ f(t)\sin t,\ z), \tag{3.6}$$

where f is a continuous positive function of $t \in [t_1, t_2]$, and where $z \in \mathbb{R}$.

Now, suppose that we have an infinite strip S (representing the screen) given by

$$S := \{(x, y, z) \in \mathbb{R}^3 \mid x = -h,\ y_1 \le y \le y_2\} \tag{3.7}$$

for fixed distance h and heights y_1 and y_2. We first derive a formula for the direct illumination on the screen. The following proposition was shown by Kruijer [17, p. 15].

Proposition 3.2.2. *The direct illumination E_1 on S, caused by the source l as described above, equals*

$$E_1(y, z) = \frac{h}{y^2 + h^2} I_1^*(\theta) = \frac{\cos^2\theta}{h} I_1^*(\theta), \tag{3.8}$$

for any z, where θ and y are related by $y = h\tan\theta$, and where

$$I_1^*(\theta) := \int_0^\pi I_1(\theta, \chi)\sin\chi\, d\chi.$$

Proof. Consider a point $(-h, y, z) \in S$ and take an infinitesimal line element dl at position $(0, 0, s)$. A ray from dl in direction

$$(-\cos\theta \sin\chi, \sin\theta \sin\chi, \cos\chi)$$

intersects S in $(-h, y, z)$ if and only if

$$\begin{aligned} y &= h\tan\theta, \\ z &= s + \frac{h}{\cos\theta \tan\chi} \end{aligned}$$

so

$$\theta = \arctan\frac{y}{h}, \tag{3.9}$$

$$\chi = \arctan\frac{\sqrt{y^2 + h^2}}{z - s}, \tag{3.10}$$

where in (3.10) we have $\chi = \pi/2$ if $z = s$. Then the element dl contributes

$$dE_1(y, z) = I_1(\theta, \chi) \sin \chi \left| \frac{\partial(y, z)}{\partial(\theta, \chi)} \right|^{-1} ds = I_1(\theta, \chi) \sin^3 \chi \frac{h}{(y^2 + h^2)^{3/2}} ds$$

to the illumination in the point $(-h, y, z)$. Therefore, the contribution of the whole line equals

$$E_1(y, z) = \frac{h}{(y^2 + h^2)^{3/2}} \int_{-\infty}^{\infty} I_1(\theta, \chi) \sin^3 \chi \, ds.$$

From (3.10) it follows that this equals

$$E_1(y, z) = \frac{h}{y^2 + h^2} \int_0^{\pi} I_1(\theta, \chi) \sin \chi \, d\chi.$$

□

Now suppose we have a required illumination E on S which is independent of z, so E is of the form

$$E(y, z) = e(y) \tag{3.11}$$

for some function $e : [y_1, y_2] \to \mathbb{R}^+$. We again assume that e is a non-negative, integrable function. We may assume that E is the required illumination *for the reflected light only*: the direct light is known by the above proposition and can be subtracted. We will consider the problem of determining a reflector of the form (3.6) that realizes this required illumination E. In Section 3.2.5 we will show that this problem can be solved by solving a corresponding 2D problem.

3.2.3 Geometry of the 2D Near Field Problem

We now introduce some notation for the 2D problem; see Figure 3.3. We assume that a point source is located in the origin of a rectangular xy-coordinate system. The directions of the rays that are emitted from the source are given in radians. As in Section 2.4, there is a subtlety in the notation we use. Those rays that are incident on the reflector are denoted by Arab letters, usually t or s, and they are measured clockwise relative to the positive direction of the x-axis. Reflected rays, and those emitted rays that are not incident on the reflector, are denoted by Greek letters, usually θ or ψ, and they are measured counterclockwise relative to the negative direction of the x-axis.

We can describe the reflector by a function $f : [t_1, t_2] \to \mathbb{R}^+$, where the reflector is located between angles t_1 and t_2, with $t_1 < t_2$, and where $f(t)$ is the distance from the source to the reflector in direction t. The corresponding reflector point is denoted $\mathbf{r}(t)$, i.e.

$$\mathbf{r}(t) = f(t)(\cos t, \sin t), \tag{3.12}$$

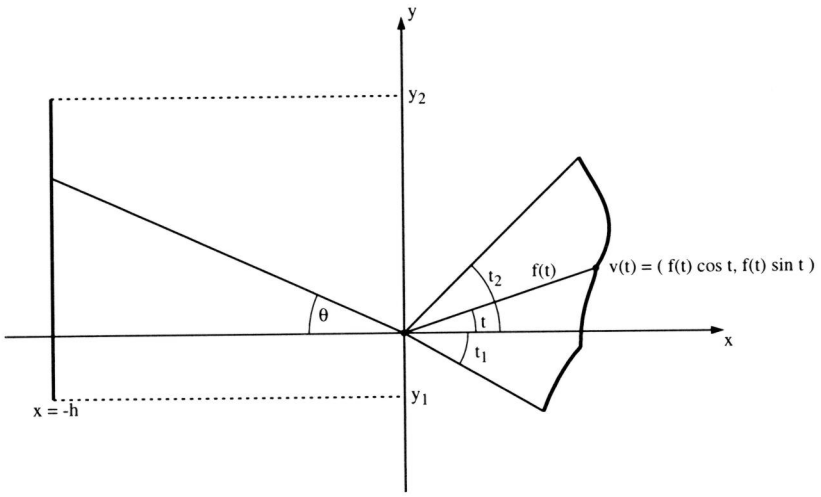

Figure 3.3: *The geometry of the 2D problem.*

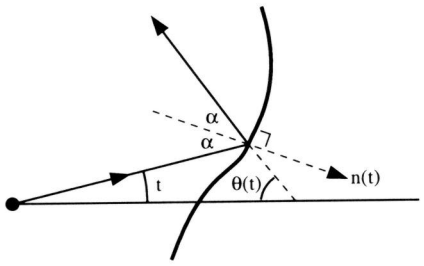

Figure 3.4: *Illustration of the law of reflection.*

so the reflector corresponds to the curve $\mathbf{r} : [t_1, t_2] \to \mathbb{R}^2$. In the case of a near field problem, the screen is represented by a segment of the line $x = -h$ between heights y_1 and y_2 ($y_1 < y_2$).

The direction of a ray that is reflected from the point $\mathbf{r}(t)$, is denoted $\theta(t)$.

Consider Figure 3.4 in which the 2D law of reflection is illustrated. As was found by Keller [15], it can be formulated conveniently as

$$\frac{\dot{f}(t)}{f(t)} = \tan\left(\frac{t + \theta(t)}{2}\right), \tag{3.13}$$

where we assume that the derivative $\dot{f}(t)$ exists.

The height at which the reflected ray enters the screen is denoted $y(t)$. The relation between $y(t)$ and $\theta(t)$ in terms of t and f is as follows:

$$\frac{y(t) - f(t)\sin t}{h + f(t)\cos t} = \tan\theta(t). \tag{3.14}$$

Combining (3.13) and (3.14) gives $y(t)$ expressed in terms of t and f. We get

$$\frac{\dot{f}(t)}{f(t)} = \tan\left(\frac{t}{2} + \frac{1}{2}\arctan\left(\frac{y(t) - f(t)\sin t}{h + f(t)\cos t}\right)\right). \tag{3.15}$$

3.2.4 The Direct Problem and Infinite Intensities

In this section we consider the so-called 'direct problem', i.e. the problem to determine the intensity distribution $\mathcal{G}$ (or the illuminance $\mathcal{E}$) when the reflector f is known.

We first consider the far field case. Suppose we have a reflector described by a function f which is *twice* differentiable in all but at most a finite number of points. Then we find from (3.13) that

$$\theta(t) = 2\arctan\left(\frac{\dot{f}(t)}{f(t)}\right) - t, \tag{3.16}$$

and

$$\dot{\theta}(t) = \frac{2\ddot{f}f - 3\dot{f}^2 - f^2}{f^2 + \dot{f}^2}, \tag{3.17}$$

where we write f instead of $f(t)$, etc.

Suppose that θ is increasing on an interval $S = [s_1, s_2]$. Let the contribution of that interval to the intensity distribution be called $\mathcal{G}_S$. We have

$$\int_{\theta(s_1)}^{\theta(t)} \mathcal{G}_S(\psi)\, d\psi = \int_{s_1}^{t} \mathcal{I}(s)\, ds \tag{3.18}$$

for all $t \in S$. Differentiating (3.18) with respect to t gives

$$\mathcal{G}_S(\theta(t))\,\dot{\theta}(t) = \mathcal{I}(t), \tag{3.19}$$

so

$$\mathcal{G}_S(\theta(t)) = \frac{\mathcal{I}(t)}{\dot{\theta}(t)}. \tag{3.20}$$

Similarly, we find $\mathcal{G}_S(\theta(t)) = -\mathcal{I}(t)/\dot{\theta}(t)$ if θ is decreasing on S. Note that if $\mathcal{I}(t) = 1$ for all t, i.e. if the source has a uniform distribution, then

$$\mathcal{G}_S(\theta(t)) = |\dot{\theta}(t)|^{-1}. \tag{3.21}$$

It follows that if $\dot{\theta}(t) \to 0$, then $\mathcal{G}_S(\theta(t)) \to \infty$. Consequently, we find that if θ is differentiable, and if infinite intensities are not allowed, then θ must either be strictly increasing or strictly decreasing.

Note that from (3.16) it follows that the ray path $\theta(t)$ is not influenced by scaling of the reflector: replacing f by cf for a positive constant c gives the same function $\theta(t)$, and therefore the same far field intensity.

An obvious example of a reflector which (theoretically) produces an infinite intensity is a parabola. The parabola with focal distance p, and with axis in direction θ_0 is given by the equation

$$f_{\text{par}}(t) = \frac{2p}{1 + \cos(t + \theta_0)}. \tag{3.22}$$

It is easily verified that in this case $\theta(t) = \theta_0$ and $\dot{\theta}(t) = 0$ for all t. The corresponding intensity distribution is then described by the Dirac function $\delta_{\theta_0} : \mathbb{R} \to \{0, \infty\}$, given by

$$\delta_{\theta_0}(\psi) = \begin{cases} \infty & \text{if } \psi = \theta_0, \\ 0 & \text{otherwise.} \end{cases} \tag{3.23}$$

In the near field case, we have a similar situation as in the far field case. Rewriting (3.15) gives

$$y(t) = (h + f(t)\cos t)\tan(2\arctan\frac{\dot{f}(t)}{f(t)} - t) + f(t)\sin t. \tag{3.24}$$

Now if y is monotonic on some interval S, we find that this interval realizes an illumination

$$\mathcal{E}_S(y(t)) = \frac{\mathcal{I}(t)}{|\dot{y}(t)|}. \tag{3.25}$$

It follows that if $\dot{y}(t) \to 0$, then $\mathcal{E}_S(y(t)) \to \infty$. Like parabolas in the near field case, now ellipses with focal points $(0, 0)$ and $(-h, y)$ correspond to reflectors that produce an infinite illuminance in $(-h, y)$.

3.2.5 Problem Statement

In this section we describe the general 2D problem that we are interested in. It is formulated such that it covers both cylindrically and rotationally symmetric problems as described above. Consider again the situation of the previous section.

Let $\mathcal{E} : [y_1, y_2] \to \mathbb{R}^+$ be a non-negative integrable function which describes the required illumination for the reflected light on the screen that is represented by the interval $[y_1, y_2]$ on the vertical $x = -h$. Also, let $\mathcal{I} : [t_1, t_2] \to \mathbb{R}^+$ be a non-negative integrable function which describes the intensity of the light source in the directions of the reflector. We may assume that $\mathcal{I}$ accounts for the *reflection coefficient* ρ of the reflector material as well, assuming that this coefficient is

constant (and not a function of e.g. the angle of incidence of a ray at the reflector). Indeed, a source of intensity I and a reflection coefficient ρ will have the same effect as a source of intensity ρI and a reflection coefficient equal to 1.

Furthermore, we assume that we have

$$\int_{y_1}^{y_2} \mathcal{E}(y)\,dy = \int_{t_1}^{t_2} \mathcal{I}(t)\,dt. \tag{3.26}$$

This condition is that of conservation of energy, and it is necessary for the problem that we will consider to have a solution. Now, informally speaking, the problem that we consider here is the following.

Problem 3.2.3. *Consider the situation described in Section 3.2.3, and let $\mathcal{E}$ and $\mathcal{I}$ be as defined above, satisfying (3.26). Given a point source of intensity distribution $\mathcal{I}$, find a reflector $f(t)$ between angles t_1 and t_2, such that it produces the illumination $\mathcal{E}$ on the interval $[y_1, y_2]$.*

3.2.6 From 3D to 2D

In this section we illustrate how the two 3D problems of Sections 3.2.1 and 3.2.2 can be solved in the 2D framework of the previous two sections. We start with the rotationally symmetric case.

We have a required distribution for the reflected light on the disk S given by (3.2), of the form $E(y, z) = e(y^2 + z^2)$. The intensity distribution of the source in the directions of the reflector is given by the function $I(t, u)$, and we may assume, as in the previous section, that this function has already been corrected for the reflection coefficient of the reflector material. The design problem has a solution only if

$$\int_S E(y, z)\,dy\,dz = \int_\Omega I(t, u)\,d\omega. \tag{3.27}$$

Here Ω is the set of directions of those rays that meet the reflector $\mathbf{r}$ (given by (3.1)), so $\Omega = \{(t, u) | t \in [t_1, t_2],\ u \in [0, 2\pi]\}$. We have $d\omega = \sin t\,dt\,du$. After substituting $y = r\cos\phi$, $z = r\sin\phi$, such that $dy\,dz = r\,dr\,d\phi$, we find

$$\int_0^{2\pi} \int_0^{y_2} e(r^2) r\,dr\,d\phi = \int_0^{2\pi} \int_{t_1}^{t_2} I(t, u) \sin t\,dt\,du, \tag{3.28}$$

so

$$\int_0^{y_2} e(r^2) r\,dr = \int_{t_1}^{t_2} I(t) \sin t\,dt. \tag{3.29}$$

The following result is a consequence of this relation.

Proposition 3.2.4. *Consider the 2D problem of Section 3.2.5 (using the variable r instead of y) with*

$$\mathcal{E}(r) = e(r^2)r \qquad \text{for all } r \in [0, y_2], \text{ and}$$
$$\mathcal{I}(t) = I(t)\sin t \qquad \text{for all } t \in [t_1, t_2].$$

Now if $f(t)$ is a curve that solves the 2D problem for this $\mathcal{E}$ and $\mathcal{I}$, then the reflector surface

$$\mathbf{r}(t, u) = f(t)(\cos t, \sin t \cos u, \sin t \sin u)$$

solves the 3-dimensional problem for E and I as defined in Section 3.2.1.

Proof. It suffices to prove this theorem for the case that $y(t)$ is strictly increasing. Let a ray in direction $(\cos t, \sin t \cos u, \sin t \sin u)$ meet the plane $x = -h$ in the point $(-h, y, z)$ after reflection. Because of the rotational symmetry, and because $y(t)$ is strictly increasing, we have a relation $(y, z) = (y(t, u), z(t, u))$ that is invertible. Then we have

$$E(y, z) = \frac{I(t, u)\sin t}{\left|\frac{\partial(y,z)}{\partial t,u}\right|}.$$

For the increasing function $y^+(t)$ in the rotationally symmetric case, we have

$$(y, z) = (y^+(t)\cos u, y^+(t)\sin u)$$

so

$$E(y, z) = \frac{I(t, u)\sin t}{\dot{y}^+(t)}$$

which proves the proposition, as follows from (3.25). □

For the cylindrically symmetric case of Section 3.2.2, conservation of energy per unit length is easily seen to be equivalent to

$$\int_{y_1}^{y_2} e(y)\,dy = \int_{t_1}^{t_2} I^*(t)\,dt, \tag{3.30}$$

where $I^*(t) := \int_0^\pi I(t, \chi)\sin\chi\,d\chi$, and we obtain the following result.

Proposition 3.2.5. *Consider the 2D problem of Section 3.2.5 with*

$$\mathcal{E}(u) = e(u) \qquad \text{for all } u \in [y_1, y_2], \text{ and}$$
$$\mathcal{I}(t) = \int_0^\pi I(t, \chi)\sin\chi\,d\chi \qquad \text{for all } t \in [t_1, t_2].$$

If $f(t)$ is a curve that solves the 2D problem for this $\mathcal{E}$ and $\mathcal{I}$, then the reflector surface

$$\mathbf{r}(t, z) = (f(t)\cos t, f(t)\sin t, z)$$

solves the 3-dimensional problem for E and I as in the cylindrically symmetric case of Section 3.2.2.

3.2.7 From Near Fields to Far Fields

It may happen that the distance h from the light source to the screen is much larger than the dimensions of the reflector to be designed. (Street or playground lighting are typical applications in which we have such a situation.) In that case we usually may describe the required illumination as an intensity distribution on the *angles* of the reflected rays. This intensity distribution can then be defined in such a way that, if all light would come directly from the light source, the correct illumination would be accomplished. Since the dimensions of the reflector are small compared to h, we may expect that the required illumination is approximated sufficiently accurately when the rays are reflected from the reflector rather than directly from the source. The reason why we would want to consider the far field problem is that the computation of the reflector and the description of some of its properties is easier for far than for near field problems.

For both rotationally and cylindrically symmetric problems, we can formulate the 3D far field problems, and then deduce a corresponding 2D problem. We may also start with the general 2D near field problem, and then deduce the corresponding far field problem. This gives the same result, and is somewhat easier.

Consider the required illumination $\mathcal{E}(y)$ on the interval $[y_1, y_2]$ on the vertical at distance h. On a small line element dy on this interval, an amount of light $\mathcal{E}(y)\,dy$ is required. Now, we may write $y = h\tan\theta$, and $dy = h/\cos^2\theta\,d\theta$, so

$$\mathcal{E}(y)\,dy = \mathcal{E}(h\tan\theta)\frac{h}{\cos^2\theta}\,d\theta. \tag{3.31}$$

Let $\theta_1 = \arctan(y_1/h)$ and $\theta_2 = \arctan(y_2/h)$. Then if the illumination $\mathcal{E}$ were to be realized by a light source located at the origin, it would have to produce the intensity distribution

$$\mathcal{G}(\theta) = \mathcal{E}(h\tan\theta)\frac{h}{\cos^2\theta}. \tag{3.32}$$

So we can prescribe the intensity distribution (3.32) for the reflected light. Note that we still have conservation of energy:

$$\int_{\theta_1}^{\theta_2} \mathcal{G}(\theta)\,d\theta = \int_{t_1}^{t_2} \mathcal{I}(s)\,ds. \tag{3.33}$$

In the rotationally symmetric case, we have

$$\mathcal{G}(\theta) = e(h^2\tan^2\theta)\frac{h^2\sin\theta}{\cos^3\theta} \tag{3.34}$$

and in the cylindrically symmetric case, we have

$$\mathcal{G}(\theta) = e(h\tan\theta)\frac{h}{\cos^2\theta}. \tag{3.35}$$

3.3 Monotonic Solutions for Far Field Problems

3.3.1 The Main Strategy

In this section we will consider the main strategy to solve the reflector design problem for far fields. We have a required intensity distribution $\mathcal{G}$ that is defined on *angles*, let us say on an interval $[\theta_1, \theta_2]$ with $\theta_1 < \theta_2$. Also, we have a function $\mathcal{I} : [t_1, t_2] \to \mathbb{R}$ describing the luminous intensity of the source in the directions of the reflector. In practice one will often have $t_1 \leq -\pi - \theta_1$ and $t_2 \geq \pi - \theta_2$, because then no light is 'lost': each ray is either directly emitted in the required interval, or it will meet the reflector. It is much more convenient however, to consider as well the case that $t_1 > -\pi - \theta_1$ and $t_2 < \pi - \theta_2$, and we do not bother about the light that is emitted into irrelevant directions.

The problem of designing a reflector between angles t_1 and t_2 for the above problem can of course only be solved if there is conservation of energy, i.e. if

$$\int_{\theta_1}^{\theta_2} \mathcal{G}(\theta)\, d\theta = \int_{t_1}^{t_2} \mathcal{I}(t)\, dt. \tag{3.36}$$

In order to present the global strategy to solve the problem, let us first assume that we have a reflector that realizes the required distribution. For each emitted ray t, let $\theta(t)$ be the direction of the reflected ray. We may describe this relation by a function $\theta : [t_1, t_2] \to [\theta_1, \theta_2]$. From (3.13) it then follows that the reflector is described by the function

$$f_\theta(t) = f_\theta(t_1) \exp\Big(\int_{t_1}^{t} \tan\Big(\frac{s + \theta(s)}{2}\Big)\, ds\Big). \tag{3.37}$$

Here we write $f_\theta(t)$ to emphasize that f depends on the choice of θ (and we will see later on that many feasible θ's may exist).

Now, consider an angular interval $[\psi_1, \psi_2] \subset [\theta_1, \theta_2]$, with $\psi_1 < \psi_2$. The required amount of light within $[\psi_1, \psi_2]$ equals

$$\int_{\psi_1}^{\psi_2} \mathcal{G}(\psi)\, d\psi.$$

Let $S_\theta[\psi_1, \psi_2]$ be the set of directions of emitted rays that are reflected into the interval $[\psi_1, \psi_2]$, i.e.

$$S_\theta[\psi_1, \psi_2] = \{t \mid \psi_1 \leq \theta(t) \leq \psi_2\}. \tag{3.38}$$

The corresponding amount of reflected light is equal to

$$\int_{S_\theta[\psi_1, \psi_2]} \mathcal{I}(s) ds.$$

So we find that

$$\int_{\psi_1}^{\psi_2} \mathcal{G}(\psi)\, d\psi = \int_{S_\theta[\psi_1,\psi_2]} \mathcal{I}(s) ds \tag{3.39}$$

for all ψ_1, ψ_2.

We see that if there is a reflector $f(t)$ that solves the problem, then the corresponding relation θ between incident and reflected rays satisfies (3.37) and (3.39). But the converse is also true: each function θ that satisfies (3.39) for all ψ_1 and ψ_2 defines a relation between incident and reflected rays that will produce the required luminous intensity distribution, if there is a reflector that accomplishes this relation. Now, by (3.37) there is a function $f(t)$ that suits our purposes in the sense that the corresponding reflector reflects the rays into the required directions, provided that multiple reflections do not occur.

In the following sections we will see how to find functions θ that satisfy (3.39). The choice of θ is an important design step, because it will influence the shape of the reflector. Moreover, it may be used to avoid reflected rays re-entering the light source (if, in practice, the finite dimensions of the source are taken into account) or to influence the angles of incidence on the screen, which may be important for near field problems.

From (3.13) it follows that if θ is continuous, then $\dot{f}$ is continuous, i.e. the reflector is smooth. In the following sections we will see that usually there are two (and only two) solutions such that θ is even differentiable: the unique increasing and decreasing θ's which correspond to divergent and convergent ray bundles, respectively.

3.3.2 Monotonic Solutions

In Section 3.2.4, we have first seen the relevance of the monotonicity of the functions describing the ray paths. In the figures in Section 3.3.3, monotonic ray paths are illustrated. The monotonic solutions have the advantage that they are easily computed and that the corresponding reflectors are smooth. To see how they can be found, let us first assume that we have such a solution, and then deduce the conditions it satisfies.

We start with the increasing solution, i.e. with an increasing function θ^+. Note that if θ^+ is increasing, then $\theta^+(t_1) = \theta_1$ and $\theta^+(t_2) = \theta_2$, and no two reflected rays intersect, so the ray bundle is divergent. Since θ^+ realizes the required distribution, we have for all t

$$\int_{\theta_1}^{\theta^+(t)} \mathcal{G}(\psi)\, d\psi = \int_{t_1}^{t} \mathcal{I}(s)\, ds. \tag{3.40}$$

Because $\mathcal{G}$ is integrable and positive, it has a strictly increasing anti-derivative P on $[\theta_1, \theta_2]$ with $P(\theta_1) = 0$. Also, $\mathcal{I}$ has an anti-derivative Q on $[t_1, t_2]$ with $G(t_1) = 0$. So we can write

$$P(\theta^+(t)) = Q(t). \tag{3.41}$$

Now, since P is strictly increasing, it has an inverse P^{-1}, and we find

$$\theta^+(t) = P^{-1}(Q(t)). \tag{3.42}$$

This uniquely defines θ^+ in terms of $\mathcal{G}$ and $\mathcal{I}$.

The decreasing case, corresponding to a convergent ray bundle, is treated similarly. Let us say we have a decreasing solution θ^-. We then find

$$\int_{\theta^-(t)}^{\theta_2} \mathcal{G}(\psi)\, d\psi = \int_{t_1}^{t} \mathcal{I}(s)\, ds, \tag{3.43}$$

so

$$P(\theta_2) - P(\theta^-(t)) = Q(t). \tag{3.44}$$

By (3.36) and by definition of P and Q, we have $P(\theta_2) = Q(t_2)$, so

$$\theta^-(t) = P^{-1}(Q(t_2) - Q(t)), \tag{3.45}$$

and this uniquely defines θ^- in terms of $\mathcal{G}$ and $\mathcal{I}$.

We can summarize the mathematical steps of the design process by the following diagram, where (a) and (d) are integrations, (b) is an inversion, and (c) is a simple substitution.

$$\left.\begin{array}{l} \mathcal{G} \xrightarrow{(a)} P \xrightarrow{(b)} P^{-1} \\ \mathcal{I} \xrightarrow{(a)} Q \end{array}\right\} \xrightarrow{(c)} \left\{\begin{array}{l} \theta^+ \xrightarrow{(d)} f_{\theta^+} \\ \theta^- \xrightarrow{(d)} f_{\theta^-} \end{array}\right. \tag{3.46}$$

In the following section, we give some examples.

3.3.3 Examples

In general, we may have to use numerical methods for the integration or inversion steps of (3.46) but we have chosen the examples such that the solutions can be found analytically. The examples do not only serve the purpose of illustrating the method of the previous section, but they also draw attention to particular properties of reflectors and special difficulties that may occur. Therefore, we have chosen examples that are relatively simple. In all examples we will assume that

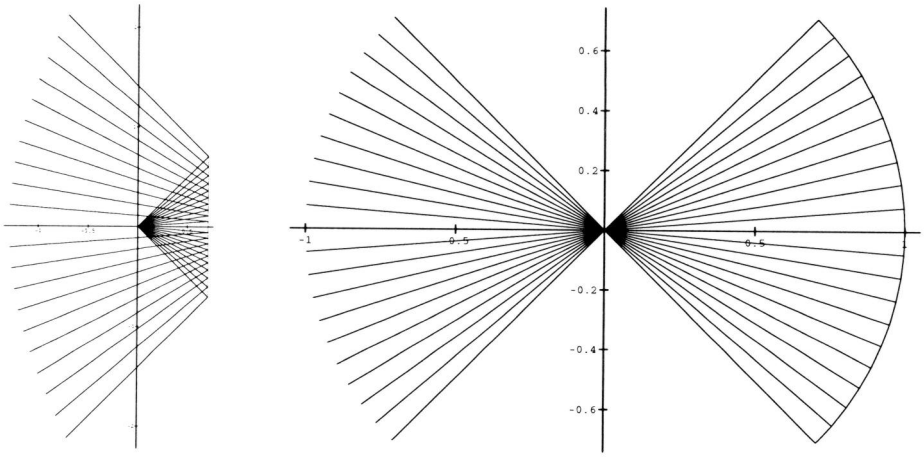

Figure 3.5: *Straight line and circle segments are the two monotonic solutions to Example 3.3.1.*

$\mathcal{I}(t) = 1$ for all $t \in [t_1, t_2]$. This corresponds to a cylindrically symmetric case with a uniform light source. In that case, we have $Q(t) = t - t_1$ for all $t \in [t_1, t_2]$, so $\theta^+(t) = P^{-1}(t - t_1)$, and $\theta^-(t) = P^{-1}(t_2 - t)$. Also, the far field problems are not presented as approximations to near field problems, but simply as problems on their own.

In each example, figures of the two monotonic solutions are shown. Incident and reflected rays are drawn at fixed angular intervals. Note that the increasing and decreasing solutions are not plotted on the same scale here, so the actual shapes are somewhat difficult to compare. In Section 3.4.1 however, the reflectors corresponding to both increasing and decreasing solutions for all examples will be plotted in one figure, along with several other solutions, such that their shapes can be compared.

Example 3.3.1. In this first example we require a uniform distribution of the reflected light. The two solutions will turn out to be the obvious ones. See Figure 3.5.

Problem:

t-range:	$[t_1, t_2]$	$= [-\pi/4, \pi/4]$
θ-range:	$[\theta_1, \theta_2]$	$= [-\pi/4, \pi/4]$
required distribution:	$\mathcal{G}(\psi)$	$= 1$ for all ψ
boundary condition:	$f(-\pi/4)$	$= 1$

Solution:

$$P(\psi) = \psi + \pi/4$$

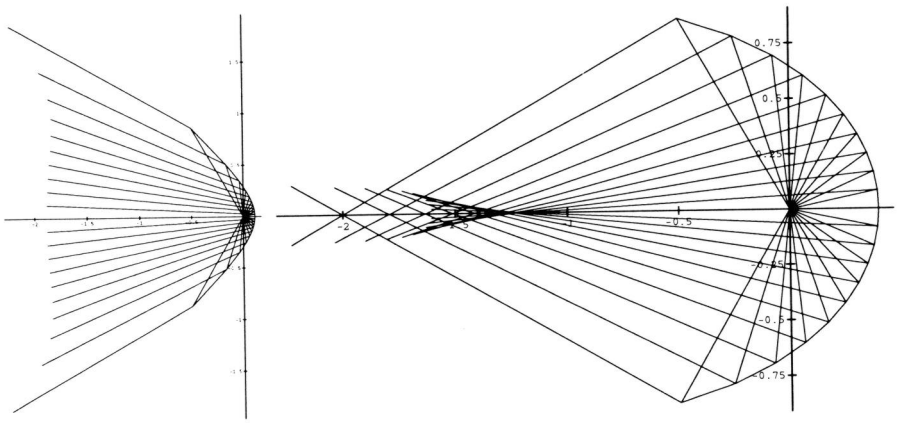

Figure 3.6: *The monotonic solutions to Example 3.3.2.*

$$
\begin{aligned}
P^{-1}(s) &= s - \pi/4 \\
\theta^+(t) &= P^{-1}(t + \pi/4) = t \\
\theta^-(t) &= P^{-1}(\pi/4 - t) = -t \\
f_{\theta^+}(t) &= \exp(\int_{-\pi/4}^{t} \tan s \, ds) = \tfrac{1}{2}\sqrt{2}/\cos t \\
f_{\theta^-}(t) &= 1 \\
\mathbf{r}_{\theta^+}(t) &= (\tfrac{1}{2}\sqrt{2}, \tfrac{1}{2}\sqrt{2}\tan t) \\
\mathbf{r}_{\theta^-}(t) &= (\cos t, \sin t)
\end{aligned}
$$

□

Example 3.3.2. Again we require a uniform distribution of the reflected light, but this time with other t- and θ-ranges. Explicit expressions for f_{θ^+}, etc. have been omitted. See Figure 3.6.

Problem:

t-range:	$[t_1, t_2]$	$= [-2\pi/3, 2\pi/3]$
θ-range:	$[\theta_1, \theta_2]$	$= [-\pi/6, \pi/6]$
required distribution:	$\mathcal{G}(\psi)$	$= 4$ for all ψ
boundary condition:	$f(-2\pi/3) = 1$	

Solution:

$$
\begin{aligned}
P(\psi) &= 4\psi + 2\pi/3 \\
P^{-1}(s) &= s/4 - \pi/6 \\
\theta^+(t) &= P^{-1}(t + 2\pi/3) = t/4 \\
\theta^-(t) &= -t/4
\end{aligned}
$$

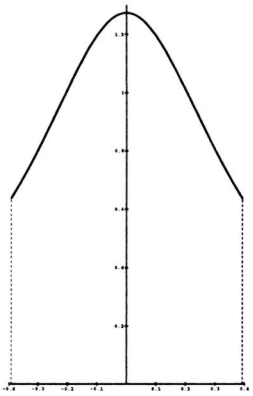

Figure 3.7: *The required distribution $\mathcal{G}$ of Example 3.3.3.*

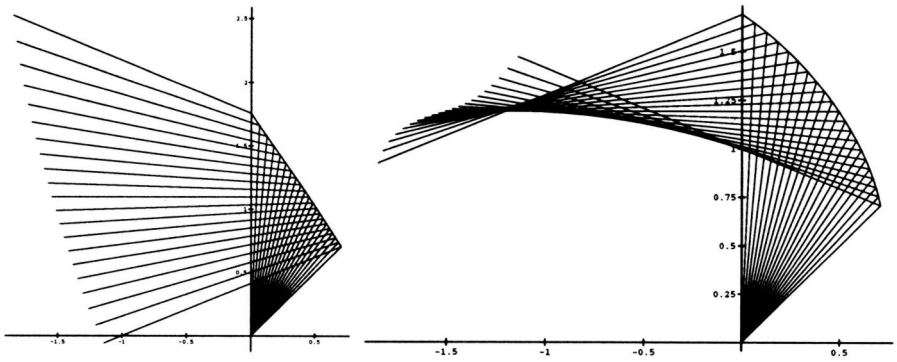

Figure 3.8: *The solutions to Example 3.3.3.*

□

Example 3.3.3. This time the required intensity distribution $\mathcal{G}$, sketched in Figure 3.7, is not uniform. In Figure 3.8 the two solutions are shown.
Problem:

t-range:	$[t_1, t_2]$	$= [\pi/4, \pi/2]$
θ-range:	$[\theta_1, \theta_2]$	$= [-\pi/8, \pi/8]$
required distribution:	$\mathcal{G}(\psi)$	$= \frac{4\pi}{\pi^2+64\psi^2}$
boundary condition:	$f(\pi/4)$	$= 1$

Solution:

$$\begin{aligned} P(\psi) &= \frac{1}{2}\arctan(8\psi/\pi) + \pi/8 \\ P^{-1}(s) &= \frac{\pi}{8}\tan(2s - \frac{\pi}{4}) \end{aligned}$$

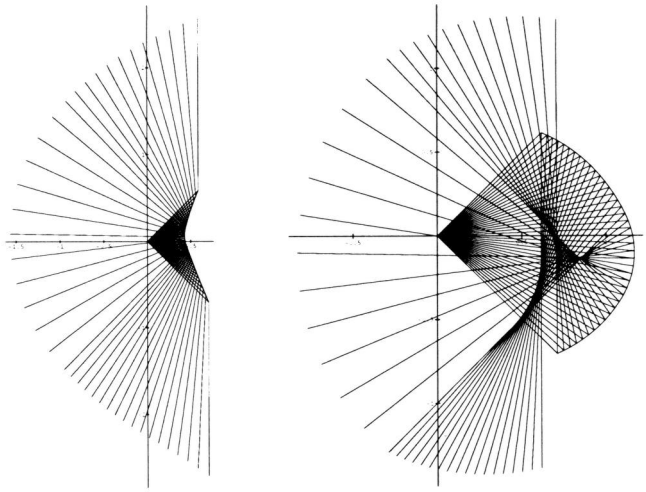

Figure 3.9: *The left reflector realizes the required step function distribution of Example 3.3.4; the right reflector does not because of multiple reflections.*

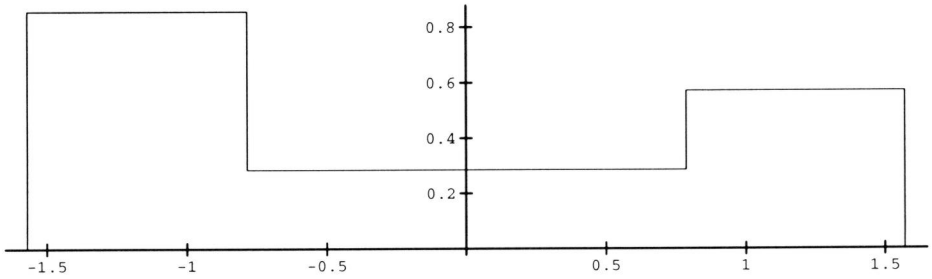

Figure 3.10: *The step function distribution of Example 3.3.4.*

$$\begin{aligned} \theta^+(t) &= \frac{\pi}{8}\tan(2t - \frac{3\pi}{4}) \\ \theta^-(t) &= -\theta^+(t) \end{aligned}$$

□

Example 3.3.4. The required distribution in this example is a step function, as shown in Figure 3.10. The two monotonic solutions illustrate two phenomena that can occur: reflectors being convex and multiple reflections, see Figure 3.9. The decreasing solution is incorrect because some reflected rays meet the reflector twice, and the effect of the second reflection is ignored.
Problem:

t-range: $[t_1, t_2] = [-\pi/4, \pi/4]$

$$
\begin{array}{lll}
\theta\text{-range:} & [\theta_1, \theta_2] & = [-\pi/2, \pi/2] \\
\text{required distribution:} & \mathcal{G}(\psi) & = \begin{cases} 6/7 & \text{if } \psi \in [-\pi/2, -\pi/4] \\ 2/7 & \text{if } \psi \in [-\pi/4, \pi/4] \\ 4/7 & \text{if } \psi \in [\pi/4, \pi/2] \end{cases} \\
\text{boundary condition:} & f(-\pi/4) & = 1
\end{array}
$$

Solution:

$$
P(\psi) = \begin{cases} 6\psi/7 + 3\pi/7 & \text{if } \psi \in [-\pi/2, -\pi/4] \\ 2\psi/7 + 2\pi/7 & \text{if } \psi \in [-\pi/4, \pi/4] \\ 4\psi/7 + 3\pi/14 & \text{if } \psi \in [\pi/4, \pi/2] \end{cases}
$$

$$
P^{-1}(s) = \begin{cases} 7s/6 - \pi/2 & \text{if } s \in [0, 3\pi/14] \\ 7s/2 - \pi & \text{if } s \in [3\pi/14, 5\pi/14] \\ 7s/4 - 3\pi/8 & \text{if } s \in [5\pi/14, \pi/2] \end{cases}
$$

$$
\theta^+(t) = \begin{cases} 7t/6 - 5\pi/24 & \text{if } t \in [-\pi/4, -\pi/28] \\ 7t/2 - \pi/8 & \text{if } t \in [-\pi/28, 3\pi/28] \\ 7t/4 + \pi/16 & \text{if } t \in [3\pi/28, \pi/4] \end{cases}
$$

$$
\theta^-(t) = \begin{cases} -7t/4 + \pi/16 & \text{if } t \in [-\pi/4, -3\pi/28] \\ -7t/2 - \pi/8 & \text{if } t \in [-3\pi/28, \pi/28] \\ -7t/6 - 5\pi/24 & \text{if } t \in [\pi/28, \pi/4] \end{cases}
$$

□

3.3.4 Existence of Solutions

In this section we briefly discuss two complications that can occur. It may happen that we have a correct problem statement, in the sense that we have conservation of energy, but that still there is no solution to the problem. One obstacle for existence of real solutions is that of multiple reflections which may occur (in the case of decreasing solutions). Another obstacle may be the following.

It is easily seen that when $t_1 + \theta_1 < -\pi$ or that $t_2 + \theta_2 > \pi$, then an increasing solution does not exist. But what happens if $t_1 + \theta_1$ approximates $-\pi$ or if $t_2 + \theta_2$ approximates π? We then have a problem as well, because in the cases that $t_1 + \theta_1 = -\pi$ or that $t_2 + \theta_2 = \pi$, the problem has no increasing solution. In order to see why, suppose for instance that $t_2 + \theta_2 = \pi$. For the increasing solution we then should have $\theta(t_2) = \theta_2$, which means that the reflected ray proceeds into the same direction as the incident ray, in other words, it is tangent to the reflector. Practically, this is impossible of course. Theoretically, it means that the curve representing the reflector is tangent to the line through the origin in direction t_2. This also follows from (3.13): if $t_2 + \theta_2 = \pi$ then $\tan((\theta(t_2) + t_2)/2) = \infty$ so $\dot{f}(t_2) = \infty$. In other words, the line through the origin in direction t_2 is

asymptotic to the curve $\mathbf{r}(t)$, and the reflector will be infinitely large. The other case that $t_1 + \theta_1 = -\pi$ is similar.

As for multiple reflections, we have seen that Example 3.3.4 has no decreasing solution because some reflected rays meet the reflector more than once. One can easily prove that this can never happen with increasing solutions. It would be pleasant when we could tell whether multiple reflections will occur in the decreasing case, from a simple criterion based on the knowledge of $\mathcal{G}$, $\mathcal{I}$, t_1 and t_2. Unfortunately, it seems that exact knowledge of $f_{\theta-}$ is required. Mathematically, the problem is to find out when the reflected ray from angle t, i.e. the half-line

$$f(t)\begin{pmatrix}\cos t\\ \sin t\end{pmatrix} + \lambda\begin{pmatrix}-\cos\theta(t)\\ \sin\theta(t)\end{pmatrix} \tag{3.47}$$

with $\lambda > 0$, intersects the reflector

$$\mathbf{r}(s) = f(s)(\cos s, \sin s)$$

for an $s \in [t_1, t_2]$ with $s \neq t$. A.J.E.M. Janssen suggested the following approach. Without loss of generality, let us concentrate on multiple reflections on the upper part ($s \geq 0$) of the reflector only. Now, suppose the halfline (3.47) intersects the line through the origin and the upper endpoint in the point $\mu(t)(\cos t_2, \sin t_2)$. It is then easily seen that we have multiple reflections if and only if $\mu(t) < f(t_2)$ for some t with $t < t_2 - \pi$ or $\mu(t) > f(t_2)$ for some t with $t > t_2 - \pi$. So, we only have to investigate the function

$$\mu(t) = f(t)\frac{\sin(t + \theta(t))}{\sin(t_2 + \theta(t))}.$$

We end this section with an example relevant to both the above phenomena. Suppose we have a cylindrically symmetric situation, with a uniform light source, and we want to obtain a uniform distribution between angles $[-\theta_2, \theta_2]$ by a reflector between angles $[-t_2, t_2]$. Now, if $t_2 + \theta_2 > \pi$, we ask for a reflected ray bundle of a wider angle than the aperture of the reflector. We know that this cannot be accomplished by an increasing solution, but the decreasing solution may exist if multiple reflections do not occur. Below we give two surprising examples of what is possible; see Figure 3.11. In the left picture, we have $t_2 = 0.7364\pi$ and $\theta_2 = \pi/2$ (so with an aperture of about 95°, we have a bundle of 180°), and in the right picture, we have $t_2 = 11\pi/12$ and $\theta_2 = \pi/4$ (so with an aperture of 30°, we have a bundle of 90°).

3.3.5 Caustics

In this section we give a formula for the caustic of a ray bundle. Although this is only interesting for the decreasing solution, the formula below holds for the

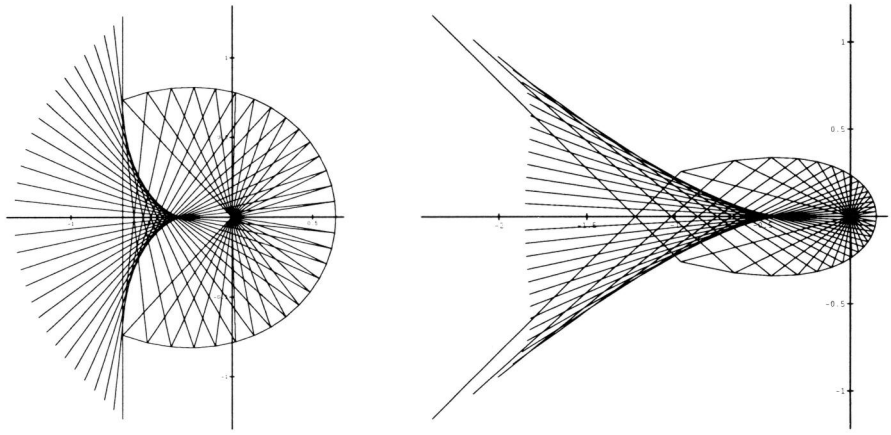

Figure 3.11: *Two examples of reflectors with reflected bundles that are wider than the apertures.*

virtual caustic of an increasing bundle as well. The following proposition shows that caustics are easily expressed in terms of $\theta(t)$ and $f(t)$.

Proposition 3.3.5. *The caustic of the ray bundle corresponding to θ is given by the parametrization*

$$t \to f(t) \begin{pmatrix} \cos t + \frac{\cos\theta(t)}{\dot{\theta}(t)} \\ \sin t - \frac{\sin\theta(t)}{\dot{\theta}(t)} \end{pmatrix}. \tag{3.48}$$

Proof. Mathematically, the collection of rays can be seen as a line bundle, parameterized by

$$(t, \lambda) \to f \begin{pmatrix} \cos t \\ \sin t \end{pmatrix} + \lambda \begin{pmatrix} -\cos\theta \\ \sin\theta \end{pmatrix}. \tag{3.49}$$

The caustic of the ray bundle is now precisely the singular locus of this mapping, i.e. the collection of points where the determinant of the Jacobian of this mapping equals zero. So in these points we have

$$\begin{vmatrix} \dot{f}\cos t - f\sin t + \lambda\dot{\theta}\sin\theta & -\cos\theta \\ \dot{f}\sin t + f\cos t + \lambda\dot{\theta}\cos\theta & \sin\theta \end{vmatrix} = 0,$$

which is equivalent to

$$(\cos t\sin\theta + \sin t\cos\theta)\dot{f} + (-\sin t\sin\theta + \cos t\cos\theta)f + \lambda\dot{\theta} = 0.$$

Using $\dot{f} = f\tan(\frac{t+\theta}{2})$, we obtain

$$(\tan(\frac{t+\theta}{2})\sin(t+\theta)+\cos(t+\theta))f+\lambda\dot{\theta}=0.$$

Now $\tan(\frac{t+\theta}{2})\sin(t+\theta)+\cos(t+\theta)=1$, so we finally get

$$f+\lambda\dot{\theta}=0.$$

Hence $\lambda=-f/\dot{\theta}$, which after substitution into (3.49) proves the proposition. □

3.4 General Solutions for Far Field Problems

3.4.1 Other Solutions

In the previous section, we have introduced and discussed the monotonic solutions to the reflector design problem. The applicability of the method we have discussed so far would have been very limited if the two monotonic solutions were the only ones that could be found this way. In this section we will see that the monotonic solutions can be used as the 'building blocks' to (infinitely) many other solutions which might be more suitable to meet all kinds of practical requirements.

It is easily explained how such an approach works: Suppose we have a cylindrical problem with $\mathcal{I}=1$ on $[t_1,t_2]$ (again for convenience only!) and that we have a required distribution $\mathcal{G}$ defined on $[\theta_1,\theta_2]$ as in the previous sections. Then we can subdivide the interval $[t_1,t_2]$ into n parts, as follows. Let

$$t_1=s_0<s_1<\ldots<s_{n-1}<s_n=t_2$$

and let

$$S_i:=[s_{i-1},s_i]. \tag{3.50}$$

Then $\cup S_i=[t_1,t_2]$. At the same time, we might 'subdivide' the required distribution into n parts. Let $\mathcal{G}_1,\ldots,\mathcal{G}_n:[\theta_1,\theta_2]\to\mathbb{R}$ be integrable functions such that

$$\mathcal{G}=\mathcal{G}_1+\ldots+\mathcal{G}_n. \tag{3.51}$$

Now suppose that for all $i\in\{1,\ldots,n\}$ we have

$$\int_{\theta_1}^{\theta_2}\mathcal{G}_i(\psi)\,d\psi=\int_{s_{i-1}}^{s_i}\mathcal{I}(s)\,ds=s_i-s_{i-1}, \tag{3.52}$$

then each part S_i of the reflector can realize the contribution $\mathcal{G}_i$ to the total required distribution. So, for fixed n, S_i and $\mathcal{G}_i$, we may consider solutions θ such

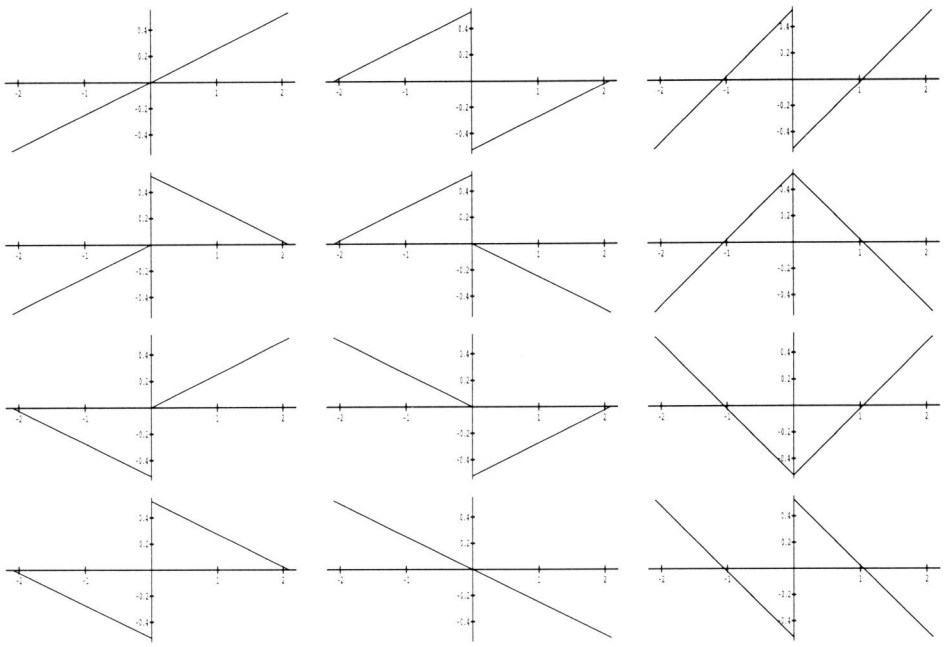

Figure 3.12: *The twelve θ's corresponding to the disjoint (first column), the crossing (second column) and the overlapping (third column) subdivisions.*

that θ is smooth (and thus monotonic) on each open interval (s_{i-1}, s_i) and such that S_i realizes the contribution $\mathcal{G}_i$ to $\mathcal{G}$. Since on each interval we can choose either the increasing or the decreasing solution, this generally leads to 2^n possible solutions for this particular choice of the intervals S_i and the functions $\mathcal{G}_i$. Needless to say, there are infinitely many ways of choosing these. In order to investigate subdivisions in more detail, let us consider subdivisions into 2 parts only. Note that any n-part subdivision can be obtained by repeatedly using these subdivisions. In order to subdivide the reflector, we must specify the subdivision direction $s_1 \in [t_1, t_2]$. The functions $\mathcal{G}_1$ and $\mathcal{G}_2$ should then be chosen such that (3.52) holds. Again, there are infinitely many possible choices, but there are some straightforward ones which are easily computed and practically relevant. These will be described below and illustrated by the corresponding solutions to Example 3.3.2.

(i) The *disjoint* subdivision. In this subdivision, we let the lower and upper part of the reflector realize the lower and upper part of the required distribution, respectively. To that end, we have to find a direction σ such that

$$\int_{\theta_1}^{\sigma} \mathcal{G}(\psi)\, d\psi = s_1 - t_1. \tag{3.53}$$

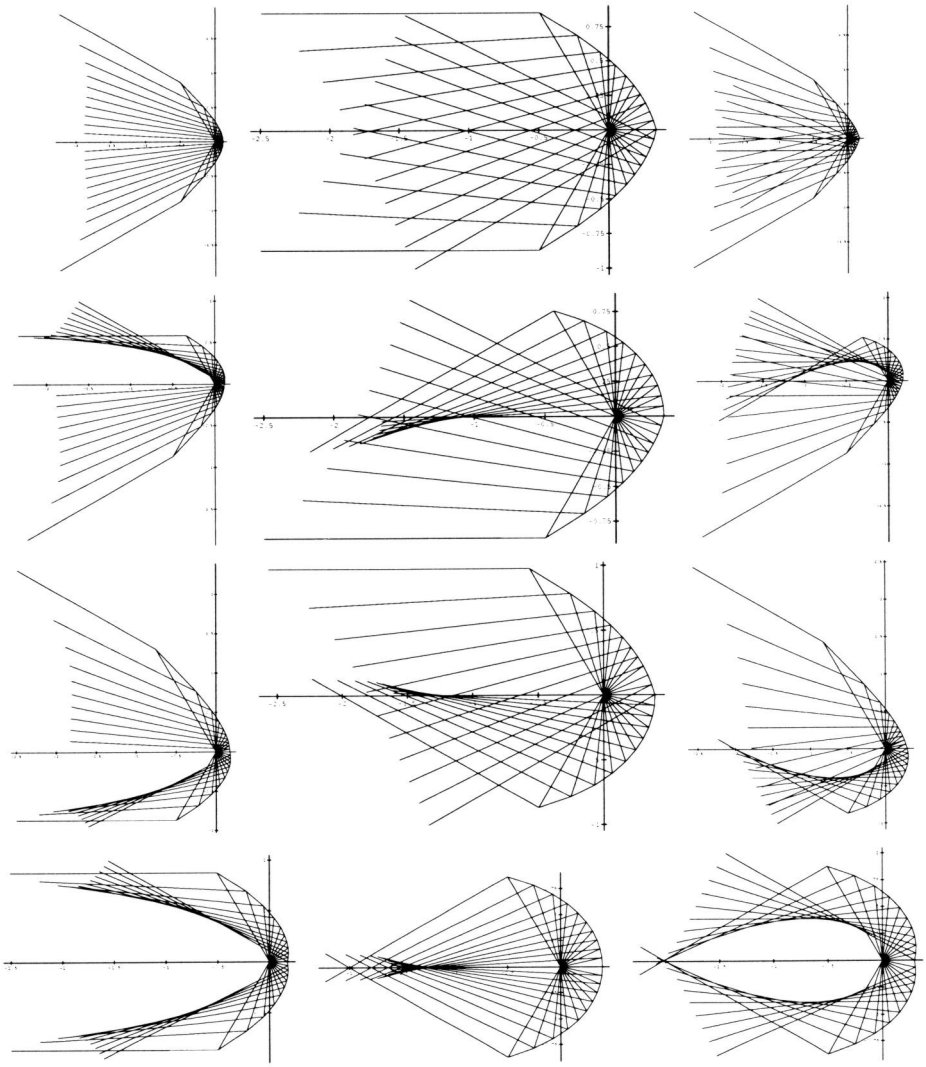

Figure 3.13: *The twelve reflectors corresponding to the disjoint (first column), the crossing (second column) and the overlapping (third column) subdivisions.*

Then we can set

$$\mathcal{G}_1(\psi) = \begin{cases} \mathcal{G}(\psi) & \text{if } \psi < \sigma, \\ 0 & \text{otherwise,} \end{cases} \tag{3.54}$$

$$\mathcal{G}_2(\psi) = \begin{cases} 0 & \text{if } \psi < \sigma, \\ \mathcal{G}(\psi) & \text{otherwise.} \end{cases} \tag{3.55}$$

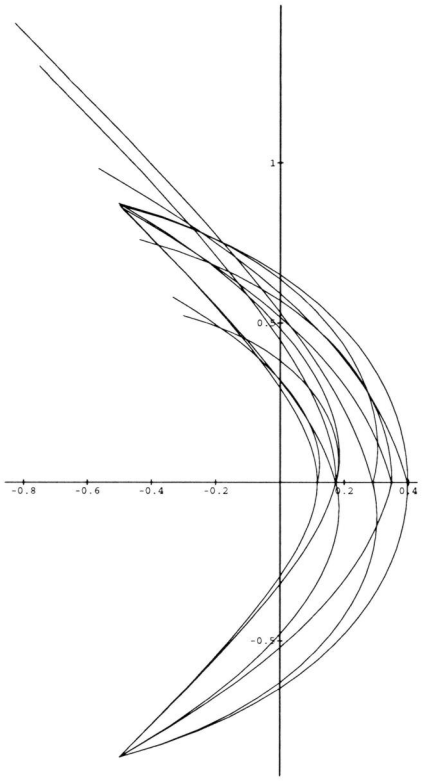

Figure 3.14: *The twelve solutions to Example 3.3.2.*

(ii) The *crossing* subdivision. In this subdivision, we let the lower and upper part of the reflector realize the upper and lower part of the required distribution, respectively. Again, the two parts of the reflector realize disjoint parts of the required distribution, but this time the two ray bundles cross. To subdivide the intensity distribution correspondingly, we have to find a direction τ such that

$$\int_{\theta_1}^{\tau} \mathcal{G}(\psi)\, d\psi = t_2 - s_1. \tag{3.56}$$

Then we can set

$$\mathcal{G}_1(\psi) = \begin{cases} 0 & \text{if } \psi < \tau, \\ \mathcal{G}(\psi) & \text{otherwise,} \end{cases} \tag{3.57}$$

$$\mathcal{G}_2(\psi) = \begin{cases} \mathcal{G}(\psi) & \text{if } \psi < \tau, \\ 0 & \text{otherwise.} \end{cases} \tag{3.58}$$

(iii) The *overlapping* subdivision. In this subdivision, we let the lower and upper part of the reflector both take care of proportional parts of $\mathcal{G}$, as follows.

	disjoint	*crossing*	*overlapping*
$t < s_1$, *incr.*	$\theta^+(t)$	$\theta^+(t_2 - s_1 + t)$	$\theta^+(\frac{t_2-t_1}{s_1-t_1}(t - t_1) + t_1)$
$t < s_1$, *decr.*	$\theta^+(t_1 + s_1 - t)$	$\theta^+(t_1 + t_2 - t)$	$\theta^+(\frac{t_2-t_1}{s_1-t_1}(s_1 - t) + t_1)$
$t \geq s_1$, *incr.*	$\theta^+(t)$	$\theta^+(t_1 - s_1 + t)$	$\theta^+(\frac{t_2-t_1}{t_2-s_1}(t - s_1) + t_1)$
$t \geq s_1$, *decr.*	$\theta^+(s_1 + t_2 - t)$	$\theta^+(t_1 + t_2 - t)$	$\theta^+(\frac{t_2-t_1}{t_2-s_1}(t_2 - t) + t_1)$

Table 3.1: *Subdivided solutions expressed in terms of* θ^+.

Let

$$\mathcal{G}_1(\psi) = \frac{s_1 - t_1}{t_2 - t_1}\mathcal{G}(\psi), \tag{3.59}$$

$$\mathcal{G}_2(\psi) = \frac{t_2 - s_1}{t_2 - t_1}\mathcal{G}(\psi). \tag{3.60}$$

When we apply all these subdivisions to Example 3.3.2 with $s_1 = 0$, we obtain the 12 corresponding functions θ and reflectors as shown in Figures 3.12 and 3.13. In these figures, the disjoint, crossing and overlapping solutions are shown in the first, second and third columns, respectively. In the first row, both lower and upper parts yield increasing ray paths; in the second row, the lower and upper parts yield increasing and decreasing ray paths, etc.

We see that the two monotonic solutions are present here as well, and that there are two more smooth reflectors corresponding to the symmetric overlapping subdivisions. In two solutions, we see that no reflected ray goes through the origin. Such solutions may be important when one wishes to take the finite dimensions of real light sources into account and when one wants to avoid that reflected rays re-enter the source. Note furthermore that the shapes of these reflectors, which all have a fixed lower endpoint $\mathbf{r}(t_1)$, differ significantly. In Figure 3.14 all 12 reflectors are drawn. In Section 3.6 we will discuss shape and dimensions of reflectors in more detail.

We conclude this section with Table 3.1 which shows how the θ's corresponding to the above 12 solutions can be expressed in terms of the increasing solution θ^+. For instance, to find the θ corresponding to the overlapping case with an increasing bundle on the lower part and a decreasing one on the upper part, we should take the first and fourth expressions in the overlapping column for $t < s_1$ and $t \geq s_1$, respectively.

3.4.2 The Rotationally Symmetric Problem Revisited

In this section we will reconsider the reduction of a 3D rotationally symmetric problem to a 2D problem. In Proposition 3.2.4, this restriction was in fact accomplished by restricting the 3D problem to the half-plane $H := \{(x, y, z) \mid z = 0,\ y \geq 0\}$. By doing so, we unnecessarily restricted ourselves to a smaller class of solutions! Keeping in mind the crossing, disjoint and overlapping solutions of the previous section, we may note that there is no reason why the rays that are emitted into the 'upper' part of the reflector should also realize the 'upper' part of the illumination. Indeed, when we restrict the 3D situation to the whole plane $P := \{(x, y, z) \mid z = 0\}$, we see that the restriction proposed in Proposition 3.2.4 only covers disjoint solutions. Obviously, we can generalize it as follows.

Proposition 3.4.1. *Suppose we have a 3D rotationally symmetric problem as in Section 3.2.1, with intensity I and with required illumination $E(y, z) = e(y^2 + z^2)$ on the disk $S = \{(x, y, z) \mid x = -h,\ y^2 + z^2 \leq y_2^2\}$. Now let $\mathcal{E}$ be an integrable function on $[-y_2, y_2]$ such that*

$$\mathcal{E}(y) + \mathcal{E}(-y) = e(y^2)|y| \tag{3.61}$$

for all y, and let

$$\mathcal{I}(t) = I_2(t) \sin t \qquad \text{for all } t \in [t_1, t_2].$$

Then, if $f(t)$ is a function that solves the 2D problem for this $\mathcal{E}$ and $\mathcal{I}$, then the reflector surface

$$\mathbf{r}(t, u) = f(t)(\cos t, \sin t \cos u, \sin t \sin u)$$

for $t \in [t_1, t_2]$ and $u \in [0, 2\pi]$, solves the 3-dimensional problem for E and I as above.

In analogy with the previous section, we will speak of the *disjoint, crossing* and *overlapping restriction* if

$$\mathcal{E}(y) = \begin{cases} 0 & \text{if } y < 0, \\ e(y^2)y & \text{otherwise,} \end{cases} \tag{3.62}$$

$$\mathcal{E}(y) = \begin{cases} -e(y^2)y & \text{if } y < 0, \\ 0 & \text{otherwise,} \end{cases} \qquad \text{and} \tag{3.63}$$

$$\mathcal{E}(y) = \frac{1}{2}e(y^2)|y| \quad \text{for all } y \in [-y_2, y_2], \tag{3.64}$$

respectively. Similar definitions hold for the corresponding far field problems. An example will be given in Section 3.6.2.

3.5 Near Field Problems

The design method for near field problems is very similar to that for far field problems. For far fields the method consisted of two steps. In the first step, one chooses and computes the function $\theta(t)$, and then $f(t)$ follows immediately from (3.13), which we can write explicitly in the form (3.37). For near field problems, our approach is similar. First we choose and compute a function $y(t)$, and then we determine $f(t)$ from (3.15). The major difference with the far field problem is this second step. First of all, we generally cannot express $f(t)$ explicitly in terms of $y(t)$ and t. Secondly, we do not have scale invariance in the near field case. This means that different begin points will lead to reflectors of different shapes.

Since the first step, i.e. that of determining $y(t)$, is similar to the far field case, we will not go through all details again. Instead of this, we give an example of the solution of a near field problem in the following section, and we only briefly discuss the similarities and the differences of near and far field problems.

3.5.1 An Example of a Near Field Problem

Let us consider a 2D problem as sketched in Sections 3.2.3 and 3.2.5. The interval to be illuminated is at a distance $h = 1$, and between heights 0 and 2. We assume we have a source of intensity $\mathcal{I} = 1$, and a reflector between angles 0 and $\pi/2$. The required illumination for the reflected light is given by $\mathcal{E} = \pi/4$. Note that (3.26) is satisfied, so there is conservation of energy. Now, consider the function $y^+ : [0, \pi/2] \to [0, 2]$, defined by

$$\int_0^{y^+(t)} \mathcal{E}(y)\, dy = \int_0^t \mathcal{I}(s)\, ds. \tag{3.65}$$

This function can be written explicitly as $y^+(t) = 4t/\pi$. It describes the ray paths for the increasing solution. Note that, although no two reflected rays intersect before they reach the screen, it does *not* necessarily imply that the reflected ray bundle is divergent. Indeed, it may as well be convergent, unlike the situation in the far field case. The decreasing solution, given by the function $y^-(t) = 2 - 4t/\pi$, produces a convergent bundle, as in the far field case.

In order to determine the reflector that realizes the above ray paths, we must find the function f that satisfies

$$\frac{\dot{f}(t)}{f(t)} = \tan\left(\frac{t}{2} + \frac{1}{2}\arctan\left(\frac{y(t) - f(t)\sin t}{1 + f(t)\cos t}\right)\right) \tag{3.66}$$

for $y(t)$ equal to $y^+(t)$ or $y^-(t)$. Generally, this differential equation cannot be solved analytically, so we have to use numerical methods; a Runge Kutta method

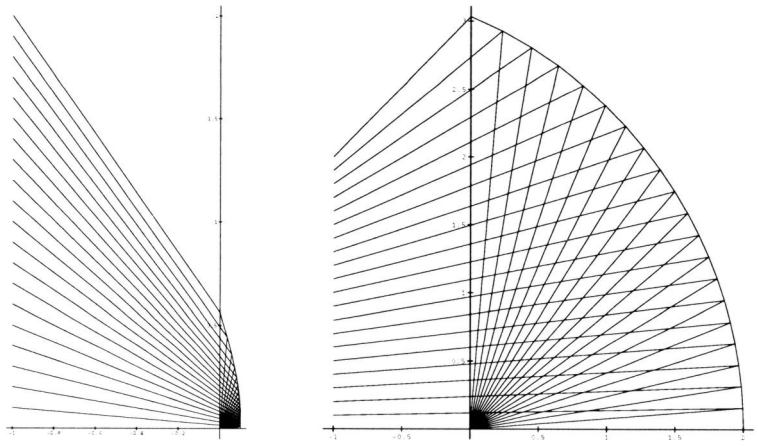

Figure 3.15: *Two* increasing *solutions to the same problem, with* $f(0) = 0.1$ *and* $f(0) = 2$*, respectively.*

will do. The solution of (3.66) requires a boundary condition, i.e. some initial value, say $f(0)$. In Figure 3.15, we see two increasing solutions with different starting values. In Figure 3.16, the reflectors of the increasing and decreasing solutions are plotted for various starting points, as well as the two monotonic solutions to the corresponding far field problem. Note that the solution looks more like that of the far field problem as the starting point $f(0)$ of the near field problem approaches zero, while the solutions look more circular as the starting point $f(0)$ is larger.

From the above example we see that the main strategy to solve the problem is similar for near and far field problems. First of all, the *monotonic solutions* are found roughly in the same way as sketched in (3.46). For the near field problem, the basic steps are as follows:

$$\left.\begin{array}{l} \mathcal{E} \xrightarrow{(a)} P \xrightarrow{(b)} P^{-1} \\ \mathcal{I} \xrightarrow{(a)} Q \end{array}\right\} \xrightarrow{(c)} \left\{\begin{array}{l} y^+ \xrightarrow{(d)} f_{y^+} \\ y^- \xrightarrow{(d)} f_{y^-} \end{array}\right. \tag{3.67}$$

Here (a) is an integration, (b) is an inversion, (c) is a substitution and (d) is solving a differential equation. The form of this differential equation implies that the solutions are not scale-invariant in the near field case. In other words, the choice of the starting point of the reflector will influence the shape of the reflector.

The two *complications* that were mentioned in Section 3.3.4 may occur in the near field case as well. In addition to these complications, there is a third one that may occur in very proximate lighting tasks (like LCD back-lighters), when

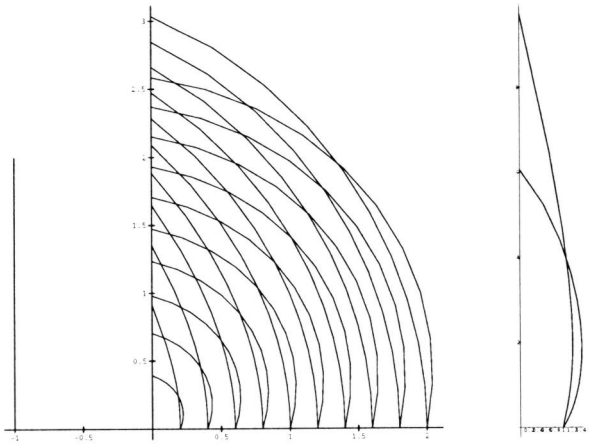

Figure 3.16: *Several monotonic solutions to the same problem, with different starting points, and the two monotonic solutions to the corresponding far field problem.*

one wants the reflector to 'fit onto' or to 'touch' the screen. In the mathematical description of that case, we might have problems, because the denominator of (3.14), which also appears in (3.15) equals 0 in a point where the reflector meets the screen. This is particularly annoying when that point is the one we would like to choose as a starting point for solving (3.15). We have to be careful in that case.

Finally, considering the *other solutions*, we can completely analogously define disjoint, crossing and overlapping subdivisions.

3.5.2 Uniform Illumination of a Disk

In this section we consider a special class of practically relevant rotationally symmetric problems. It is not our aim to present the complete solutions to these problems, but to illustrate the method for this class of problems. Indeed, we have not yet seen any example of the application of the theory we presented to a more or less realistic rotationally symmetric problem. This section provides such an example.

Assume we have a disk $S = \{(x, y, z) | x = -h,\ y^2 + z^2 \leq y_2^2\}$ which we want to illuminate uniformly, by means of a uniform light source with intensity $I = 1$ in all directions, combined with a reflector of the form

$$\mathbf{r}(t, u) = f(t)(\cos t, \sin t \cos u, \sin t \sin u)$$

for $t \in [0, t_2]$ and $u \in [0, 2\pi]$, and with reflection coefficient ρ. The direct

illumination E_1 on S follows immediately from (3.3), which gives

$$E_1(y,z) = \frac{h}{(y^2+z^2+h^2)^{3/2}}.$$

The total illumination $E = E_1 + E_2$ should be constant, let us say $E(y,z) = k$, so the required illumination for the reflected light equals

$$E_2(y,z) = k - \frac{h}{(y^2+z^2+h^2)^{3/2}}. \tag{3.68}$$

Of course, E_2 should be positive, so since E_2 is minimal for $y = z = 0$, we must have

$$k \geq \frac{1}{h^2}. \tag{3.69}$$

The precise value for k can be obtained from the energy conservation condition (3.28), which here gives

$$\int_0^{2\pi}\int_0^{y_2}(k - \frac{h}{(r^2+h^2)^{3/2}})r\,dr\,d\phi = \int_0^{2\pi}\int_0^{t_2}\rho\sin t\,dt\,du, \tag{3.70}$$

so after integration we find

$$\frac{1}{2}ky_2^2 + \frac{h}{\sqrt{y_2^2+h^2}} - 1 = \rho(1-\cos t_2).$$

Writing $h/\sqrt{y_2^2+h^2} = \cos\theta_2$, we get

$$k = \frac{2}{y_2^2}(1 - \cos\theta_2 + \rho(1-\cos t_2)). \tag{3.71}$$

Now before we continue with the solution of the design problem, we give the following result.

Proposition 3.5.1. *A disk at distance h from a uniform point source can only be illuminated uniformly if it has a radius smaller than $2h$.*

Proof. One way to prove this is as follows: in an ideal situation, where no light is lost, we have $\rho = 1$ and $\theta_2 = \pi - t_2$. Then (3.71) gives $k = 4/y_2^2$, and the result follows from (3.69).

In fact, we didn't have to calculate (3.71) to obtain this result. The following way to obtain it is more straightforward: The total amount of light, emitted by the source of intensity $I = 1$, equals $\int_0^{2\pi}\int_0^{\pi}\sin t\,dt\,du = 4\pi$. The direct illumination in $(-h,0,0)$ equals $1/h^2$. So if a disk of radius y_2 has this illumination everywhere, then we must have $\pi y_2^2 \cdot 1/h^2 = 4\pi$, from which the proposition follows as well. □

Let us now try to solve the corresponding 2D problem for the disjoint restriction. In order to find the monotonic solutions, we have to find an anti-derivative of

$$\mathcal{E}(r) = (k - \frac{h}{(r^2 + h^2)^{3/2}})r \tag{3.72}$$

with $P(0) = 0$. We find

$$P(r) = -1 + \frac{kr^2}{2} + \frac{h}{\sqrt{h^2 + r^2}}. \tag{3.73}$$

The next step towards the solution of the problem would now be the inversion of this function. In principle, this can be done, even analytically! However, it involves the solution of a polynomial equation of degree 3, and computations tend to get long. And then, if we have an analytical expression for $y^+(t)$, we perhaps still have to proceed numerically in order to compute f from y^+. The same holds for the crossing and the overlapping solutions.

The corresponding 2D far field problem is similar; we have

$$\mathcal{G}(\psi) = (k - \frac{h}{(h^2 \tan^2 \psi + h^2)^{3/2}}) \cdot \frac{h^2 \sin \psi}{\cos^3 \psi} = \frac{kh^2 \sin \psi}{\cos^3 \psi} - \sin \psi. \tag{3.74}$$

The anti-derivative P of $\mathcal{G}$ with $P(0) = 0$ is given by

$$P(\psi) = \frac{1}{2} kh^2 \tan^2 \psi + \cos \psi - 1. \tag{3.75}$$

Again, inversion of P requires the solution of a third degree polynomial.

3.5.3 Uniform Illumination of a Strip

In this section we consider the cylindrically symmetric analogue of the example in the previous section. Assume we have a strip

$$S = \{(x, y, z) | x = -h, \ -y_2 \leq y \leq y_2\} \tag{3.76}$$

which we want to illuminate uniformly, by means of a uniform linear light source which at each position has an intensity $I = 1$ in all directions, combined with a reflector of the form

$$\mathbf{r}(t, z) = (f(t) \cos t, \ f(t) \sin t, \ z)$$

for $t \in [-t_2, t_2]$ and $z \in \mathbb{R}$, and of reflection coefficient ρ. The direct illumination on S follows immediately from (3.8), which gives

$$E_1(y, z) = \frac{2h}{y^2 + h^2}.$$

The total illumination $E = E_1 + E_2$ should be constant, let us say $E(y, z) = k$, so the required illumination for the reflected light equals

$$E_2(y, z) = k - \frac{2h}{y^2 + h^2}. \tag{3.77}$$

Of course, E_2 should be positive, so since E_2 is minimal for $y = 0$, we must have

$$k \geq \frac{2}{h}. \tag{3.78}$$

The precise value for k can be obtained from the energy conservation condition (3.30), which here gives

$$\int_{-y_2}^{y_2} k - \frac{2h}{(y^2 + h^2)}\, dy = \int_{-t_2}^{t_2} 2\rho\, dt, \tag{3.79}$$

so after integration we find

$$k = \frac{2\rho t_2 + 2 \arctan \frac{y_2}{h}}{y_2}. \tag{3.80}$$

The following result is the equivalent of Proposition 3.5.1. Its proof is similar.

Proposition 3.5.2. *A strip S, given by (3.76), can only be illuminated uniformly by a parallel linear source of uniform illumination combined with a cylindrical reflector if $y_2 < \pi h$.*

3.6 Shape and Dimensions

We now investigate shape aspects of reflectors in more detail. In the previous sections we have seen how to find many different reflectors that all produce exactly the same illumination. In practical situations, we usually do not aim at an exact illumination, but rather at one that resembles an ideal illumination closely enough. At the same time however, we may have very strict restrictions on the shape and the dimensions of the reflector. Usually, small, compact reflectors are to be preferred, for both aesthetic and economic reasons.

3.6.1 The Area of a Reflector Surface

A good measure for the size, or the compactness of a reflector is its surface area. For cylindrical and rotational surfaces, this area can easily be computed from the

descriptions (3.1) and (3.6). Let us first express the length L of a curve $\mathbf{r}(t) = f(t)(\cos(t), \sin(t))$, for $t \in [t_1, t_2]$. This length is given by

$$L = \int_{t_1}^{t_2} ||\dot{\mathbf{r}}(t)|| \, dt. \tag{3.81}$$

So here we have

$$L = \int_{t_1}^{t_2} \sqrt{f^2(t) + \dot{f}^2(t)} \, dt. \tag{3.82}$$

Using (3.13), we find

$$L = \int_{t_1}^{t_2} \frac{f(t)}{\cos(\frac{t+\theta(t)}{2})} \, dt. \tag{3.83}$$

Now, a (finite length) cylindrical surface of the form

$$\mathbf{r}(t, z) = (f(t)\cos t, \, f(t)\sin t, \, z)$$

for $t \in [-t_2, t_2]$ and $z \in [z_1, z_2]$ has an area A equal to

$$A = (z_2 - z_1) \int_{t_1}^{t_2} \frac{f(t)}{\cos(\frac{t+\theta(t)}{2})} \, dt.$$

A rotationally symmetric surface of the form (3.1) has area

$$A = 2\pi \int_{t_1}^{t_2} \frac{f^2(t)\sin t}{\cos(\frac{t+\theta(t)}{2})} \, dt.$$

3.6.2 Examples and some Observations

To get an idea of the impact of the choice of $\theta(t)$ or $y(t)$ on the shape of the reflector, we will present some examples in this section. We usually consider the 12 reflectors that are obtained by the disjoint, crossing and overlapping subdivisions. Unless indicated otherwise, the subdivision direction is chosen to be $s_1 = (t_1 + t_2)/2$. We present three sets of examples, and then we draw some general conclusions. Let us first consider the far field examples of Section 3.3.3. In Figure 3.17, the 12 solutions to these 4 problems are shown. (These are drawn such that the axes do not necessarily coincide with the lines $x = 0$ and $y = 0$, so the position of the light source is not visualized.) Next, considering the near field problem of Section 3.5.1, we find reflectors as in Figure 3.18 (where the solutions are not drawn on the same scale). The figure illustrates how the situation depends on the starting point of the reflector. The third set of examples we consider is one that illustrates the different subdivisions possible for the restriction of a 3D rotationally symmetric problem to a 2D problem.

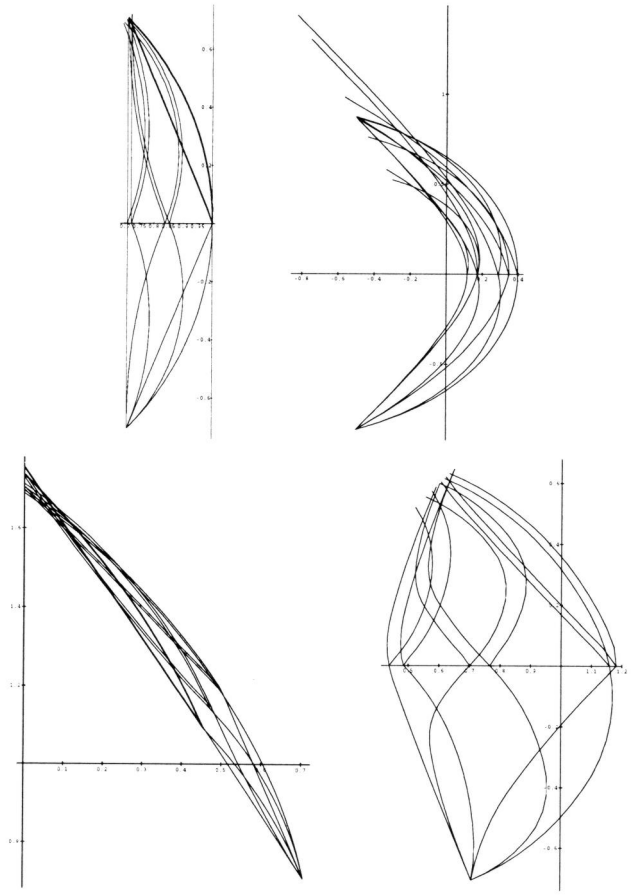

Figure 3.17: *The twelve solutions to the examples in Section 3.3.3.*

Example 3.6.1. In this example we assume a situation as in Section 3.4.2, with a uniform required illumination for the reflected light, so $e(y) = k$ for all $y \in [0, y_2]$, and a uniform light source with intensity $I_2(t) = 1$ for all $t \in [0, t_2]$. Conservation of energy implies

$$\int_0^{y_2} ky\, dy = \int_0^{t_2} \sin t\, dt,$$

so we should have

$$k = \frac{2 - 2\cos t_2}{y_2^2}.$$

The disjoint, crossing and overlapping monotonic solutions lead to 6 different reflectors for a given starting point. The functions $y(t)$ according to these are the

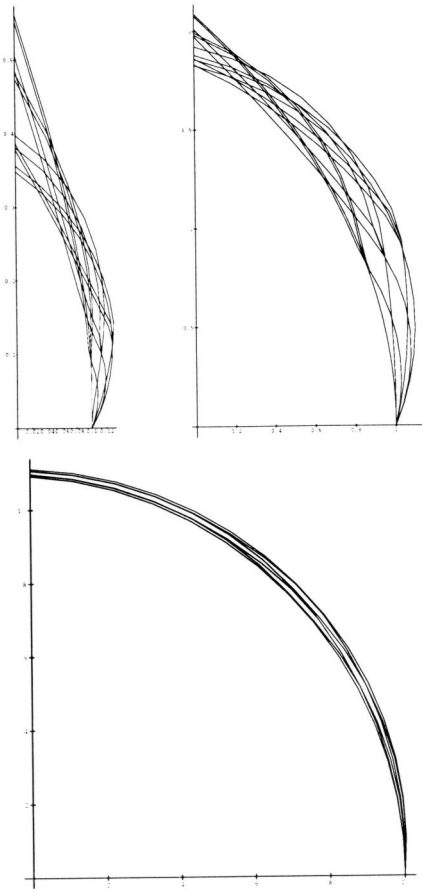

Figure 3.18: *The twelve solutions to the example of Section 3.5.1, with starting points* $f(0)$ *equal to* $1/10$, 1 *and* 10, *respectively.*

following,

$$y^{+}_{\text{disj}}(t) = \sqrt{\frac{2}{k}(1-\cos t)}, \tag{3.84}$$

$$y^{-}_{\text{disj}}(t) = \sqrt{y_2^2 - \frac{2}{k}(1-\cos t)}, \tag{3.85}$$

$$y^{+}_{\text{cros}}(t) = -\sqrt{y_2^2 - \frac{2}{k}(1-\cos t)}, \tag{3.86}$$

$$y^{-}_{\text{cros}}(t) = -\sqrt{\frac{2}{k}(1-\cos t)}, \tag{3.87}$$

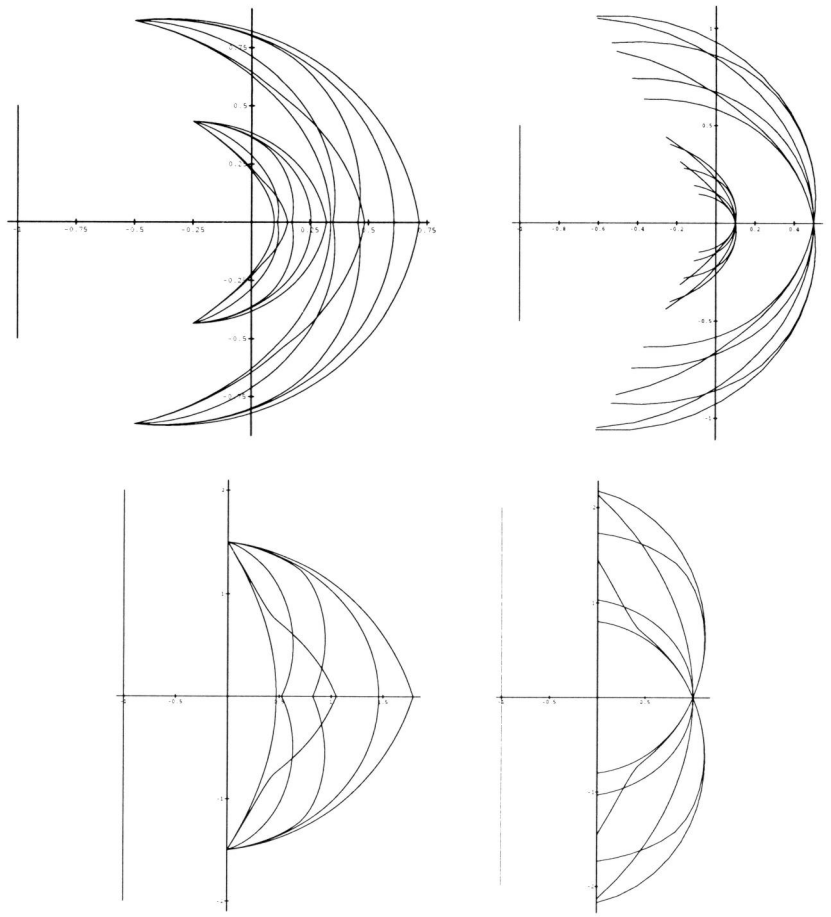

Figure 3.19: *Solutions corresponding to different restrictions of rotationally symmetric problems of Example 3.6.1.*

$$y^{+}_{\text{over}}(t) = -\text{sign}(y_2^2 - \frac{4}{k}(1-\cos t)) \cdot \sqrt{|y_2^2 - \frac{4}{k}(1-\cos t)|}, \quad (3.88)$$

$$y^{-}_{\text{over}}(t) = \text{sign}(y_2^2 - \frac{4}{k}(1-\cos t)) \cdot \sqrt{|y_2^2 - \frac{4}{k}(1-\cos t)|}, \quad (3.89)$$

where $\text{sign}(0) := 0$ and $\text{sign}(x) := x/|x|$ for all $x \neq 0$. These functions describe the ray paths of the 'upper' parts of six different reflectors.

In Figure 3.19, some solutions to two special cases of this example are shown. In all four pictures, the intervals to be illuminated are drawn as well.

In the upper two pictures, we have $h = 1$, $y_2 = 1/2$ and $t_2 = 2\pi/3$. For endpoints $f(t_2) = 1/2$ and $f(t_2) = 1$, the six solutions are shown in the left

picture, while in the right picture, we have the six solutions with $f(0) = 1/5$ and $f(0) = 1/2$, respectively.

In the lower two pictures, we have $h = 1$, $y_2 = 2$ and $t_2 = \pi/2$. For the endpoint $f(t_2) = 3/2$, the six solutions are shown in the left picture, while in the right picture, we have the six solutions with $f(0) = 1$. □

Note that not all reflectors shown above are correct solutions. Multiple reflections may occur in most reflectors of the fourth picture in Figure 3.17, as well as in some of the rotationally symmetric examples. Note also that we have to be careful when we try to say what type of solution will lead to more compact reflectors. This strongly depends on which point of the reflector one keeps fixed: consider the lower two pictures of Figure 3.19. In the left picture, the increasing disjoint solution gives the most compact reflector, and one of the crossing solutions gives the least compact reflector. However, in the right picture, one of the crossing solutions gives the most compact reflector, and the non-increasing disjoint solution gives the largest reflector.

An interesting observation from the above examples is the following. *The convex hull rule of thumb: if one endpoint is fixed, then all solutions lie approximately within the convex hull of the two monotonic solutions.* It should be noted that this observation is not based on this set of examples alone, but on many others as well. Also, although in the above examples the subdivision direction is chosen to be $s_1 = (t_1 + t_2)/2$, this observation holds for other subdivision directions as well.

Further research is needed for a thorough analysis of this observation, and of other consequences of the subdivision choice. In particular, we would like to know how to choose the subdivisions in order to meet certain constraints on the shape of the reflector. In Chapter 4, we will discuss one such constraint for a limited class of problems. This will already illustrate how very difficult these problems are. On the other hand, with the various subdivision strategies as design tools, a designer will soon have an intuitive idea what constraints can or cannot be met in a certain problem.

3.6.3 Convex and Concave Reflectors

In Example 3.3.4, we have seen that convex reflectors can also occur as the increasing solution to the design problem. Let us investigate the precise conditions under which this occurs. The notion of convexity or concavity of plane curves can be made precise by introducing the *curvature* of a curve. See any textbook on the geometry of (plane) curves for details on the notion of curvature. Here we restrict ourselves to introducing, for any curve of the form $\mathbf{r}(t) = f(t)(\cos t, \sin t)$

θ	$\dot{\theta}$	*intensity* $\mathcal{G}$	*curvature* K	*reflector*
decreasing	$\dot{\theta} < 0$	any	$K < 0$	concave
constant	$\dot{\theta} = 0$	δ_{θ_0}		parabola
increasing	$0 < \dot{\theta} < 1$	$\mathcal{G} > 1$		concave
	$\dot{\theta} = 1$	$\mathcal{G} = 1$	$K = 0$	plane
	$\dot{\theta} > 1$	$\mathcal{G} < 1$	$K > 0$	convex

Table 3.2: *The relations between intensity and convexity properties in the cylindrically symmetric far field case with* $\mathcal{I}(t) = 1$ *for all* t.

defined by a function $f(t)$ which is twice differentiable, the curvature $K(t)$ by

$$K(t) = \frac{\ddot{f} f - 2\dot{f}^2 - f^2}{(f^2 + \dot{f}^2)^{3/2}}. \tag{3.90}$$

It can be shown that the geometrical meaning of $K(t)$ is the following: $|K(t)|^{-1}$ is the radius of the 'best fitting' circle to the curve at the point $\mathbf{r}(t)$.

Now, a curve is concave ('when viewed from the origin') if $K(t)$ is negative for all t, it is convex when $K(t)$ is positive for all t, and for straight lines we have $K(t) \equiv 0$.

In the far field case we can relate the curvature to the function θ: note that from (3.17) and (3.90) it follows that

$$2\sqrt{f^2 + \dot{f}^2}\, K(t) = \dot{\theta}(t) - 1. \tag{3.91}$$

Furthermore, if $\mathcal{I}(t) = 1$ for all t, then the relations between K, θ and $\mathcal{G}$ are now easily derived from this equation and from (3.19). In the Table 3.2, the possible situations are listed. Remember that this analysis holds for *differentiable* θ's only, which we have shown to be strictly decreasing or strictly increasing.

Chapter 4

An Optimization Problem in 2D Reflector Design[1]

4.1 Introduction

In this chapter we consider a special topic associated with the design of 2D reflectors, namely that of finding 'smallest' and 'largest' reflectors that solve a given 2D far field problem.

For a large part, this chapter is independent of the others. The problem we consider is formulated as a more general optimization problem. Its solution requires some dedicated mathematics. We also use some notation which is specific for this chapter. Because the mathematics becomes somewhat involved, we present a flavour of the results in the following section. Next, we present the problem formulation and a summary of the results at the end of the introduction.

4.1.1 Designing a Reflector Between Fixed Endpoints

In the previous chapter we have seen some examples of the variety of shapes of reflectors that all produce the same required intensity or illumination. Choosing the function $y(t)$ or $\theta(t)$ so as to meet certain requirements on the shape of the reflector is, however, a very difficult problem. In this section we will consider a special constraint: we investigate the problem of designing a reflector under the additional constraint that *two* endpoints are prescribed. This is likely to occur in practical situations. For instance, in the rotationally symmetric case, the 'depth'

[1]This chapter has resulted from joint work with A.J.E.M. Janssen, and it has been published in an almost identical form in [13].

$f(0)$ and the radius $f(t_2)\sin t_2$ of the opening of the reflector may be prescribed, or at least they will usually have to lie within certain bounds.

Since for a fixed endpoint $f(t_1)$, there are usually infinitely many reflectors, we are led to ask: what possible values for $f(t_2)$ can occur, and how do we choose $y(t)$ or $\theta(t)$ in order to obtain a certain value for $f(t_2)$? In this chapter we will thoroughly study this problem for a limited class of situations, viz. cylindrically symmetric far field problems with light sources of uniform radiation (i.e. $\mathcal{I}$ is constant). The considerable mathematical effort that is needed to obtain the results for these cases indicates that the problem for e.g. rotationally symmetric cases will be very hard to solve exactly. On the other hand, in these cases we can solve the problem adequately by *discretizing* the problem; see Section 4.2. Also, knowledge of the results for the cylindrically symmetric far field case may be helpful in other cases. For a summary of the results that are obtained, we refer to the following section.

Here we restrict ourselves to an example and the following theorem.

Theorem 4.1.1. *Assume we have a cylindrically symmetric far field problem as in Section 3.3.1, with required distribution $\mathcal{G}$ and with $\mathcal{I}(t) = 1$ for all t. Because of the scale invariance property, we only have to consider solutions to this problem with $f(t_1) = 1$. Now, if $t_1 + \theta_1 \geq 0$, then we have the following.*

(a) For all solutions $f(t)$, the endpoint $f(t_2)$ is bounded by those of the monotonic solutions, i.e.

$$f_{\theta^-}(t_2) \leq f(t_2) \leq f_{\theta^+}(t_2). \tag{4.1}$$

(b) For each value f_2 between these extreme values $f_{\theta^-}(t_2)$ and $f_{\theta^+}(t_2)$, there exists a solution with $f(t_2) = f_2$.

(c) The extreme values $f_{\theta^-}(t_2)$ and $f_{\theta^+}(t_2)$ can be expressed in terms of P as follows (where $P(\psi) = \int_{\theta_1}^{\psi} \mathcal{G}(\phi)\,d\phi$)

$$f_{\theta^-}(t_2) = \frac{\cos^2(\frac{t_1+\theta_2}{2})}{\cos^2(\frac{t_2+\theta_1}{2})} \exp\Big(\int_{\theta_1}^{\theta_2} \tan\Big(\frac{\psi - P(\psi) + t_2}{2}\Big)\,d\psi\Big), \tag{4.2}$$

$$f_{\theta^+}(t_2) = \frac{\cos^2(\frac{t_1+\theta_1}{2})}{\cos^2(\frac{t_2+\theta_2}{2})} \exp\Big(-\int_{\theta_1}^{\theta_2} \tan\Big(\frac{\psi + P(\psi) + t_1}{2}\Big)\,d\psi\Big). \tag{4.3}$$

Proof.
(a) See [22], or the proof of the more general case in the next section.
(b) Consider the disjoint subdivision, with subdivision direction s_1, that is decreasing for $t_1 \leq t \leq s_1$, and increasing for $s_1 \leq t \leq t_2$. Let θ_{s_1} be the function that

describes the corresponding ray paths. From (3.37) and from Table 3.1 it follows that

$$f_{\theta_{s_1}}(t_2) = \exp\left(\int_{t_1}^{s_1} \tan\left(\frac{s+\theta^+(t_1+s_1-s)}{2}\right) ds + \int_{s_1}^{t_2} \tan\left(\frac{s+\theta^+(s)}{2}\right) ds\right)$$

depends continuously on s_1. Since for $s_1 = t_1$ and for $s_1 = t_2$ the function θ_{s_1} coincides with the increasing and the decreasing solution, the result then follows from the mean value theorem.
(c) We will only prove (4.3), the other equality is proved similarly. We know $\theta^+(t) = P^{-1}(t - t_1)$, so

$$f_{\theta^+}(t_2) = \exp\left(\int_{t_1}^{t_2} \tan\left(\frac{s+P^{-1}(s-t_1)}{2}\right) ds\right).$$

We now substitute $\psi = P^{-1}(s - t_1)$, so $s = P(\psi) + t_1$ and $ds = P'(\psi)\, d\psi$, which gives

$$\int_{t_1}^{t_2} \tan\left(\frac{s+P^{-1}(s-t_1)}{2}\right) ds = \int_{\theta_1}^{\theta_2} \tan\left(\frac{\psi+P(\psi)+t_1}{2}\right) P'(\psi)\, d\psi.$$

The rest of the proof is calculus. We can write

$$\tan\left(\frac{\psi+P(\psi)+t_1}{2}\right) P'(\psi) = 2\tan\left(\frac{\psi+P(\psi)+t_1}{2}\right)\frac{P'(\psi)+1}{2} - \tan\left(\frac{\psi+P(\psi)+t_1}{2}\right), \tag{4.4}$$

and integrating the first term of the right-hand side of (4.4) gives the result in a few steps. □

Some remarks about this theorem should be made. First of all, we assumed that all reflectors we considered above had endpoint $f(t_1) = 1$. Because the far field problem is scale invariant, this actually means that the above results tell us something about the ratio $f(t_2)/f(t_1)$. Note the condition $t_1 + \theta_1 \geq 0$ in the theorem above. This condition implies that both reflector and all rays lie within a half-plane with the origin on its boundary. This is essential for the result of (a). If we replace this condition by $t_2 + \theta_2 \leq 0$, then the inequality signs in (4.1) should be reversed.

The result of (b) can be generalized in the following way: if two different endpoints can be realized, then so can all endpoints that lie between these two. This result holds for all 2D problems discussed here. The proof of the general case is much more involved than the one given above (which specifically used

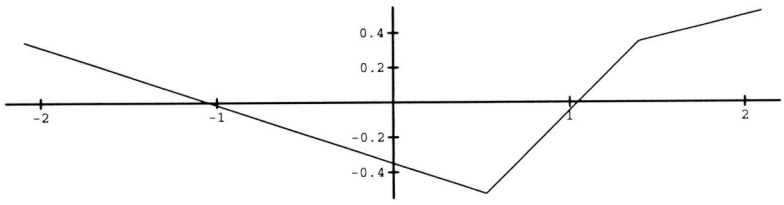

Figure 4.1: *The function $\theta_{\max}$ that maximizes $f(t_2)$ in the problem of Example 3.3.2.*

that the two endpoints were those of the monotonic solutions). Also, it should again be noted that some endpoints can only be reached by reflectors that suffer from multiple reflections.

Note that in the proof of (c) we didn't use the condition $t_1 + \theta_1 \geq 0$. The result of (c) can be used to determine the endpoints of the monotonic solutions quickly, without actually computing the reflector. This cannot be done for near field tasks.

We conclude this section with an example of the solution of the above problem in the case that the condition $t_1 + \theta_1 \geq 0$ is not satisfied. From the results of the present chapter it can be shown that, in the case of Example 3.3.2, $f(t_2)$ is maximum and minimum for $\theta(t)$ equal to

$$\theta_{\max}(t) = \begin{cases} -t/3 - \pi/9 & \text{if } t \in [-2\pi/3, \pi/6], \\ t - \pi/3 & \text{if } t \in [\pi/6, 4\pi/9], \\ t/4 & \text{if } t \in [4\pi/9, 2\pi/3], \end{cases} \tag{4.5}$$

and $\theta_{\min}(t) = -\theta_{\max}(t)$, respectively. The function $\theta_{\max}$ is shown in Figure 4.1. Note that it is obtained by a disjoint subdivision in direction $4\pi/9$, followed by an overlapping subdivision of the lower part in direction $\pi/6$. In Figure 4.2, the two reflectors with extreme endpoints are drawn in one picture, together with the two monotonic ones. Also, their ray paths are shown.

4.1.2 Mathematical Problem Formulation and Summary of Results

Please note that from now on in this chapter, notation is different from other chapters. In particular, f refers to the function to be optimized, and not to that describing the reflector surface.

In strict mathematical terms we will consider the maximization and the minimization of the functional

$$J(\theta) := \int_{t_1}^{t_2} f(s + \theta(s))\, ds \tag{4.6}$$

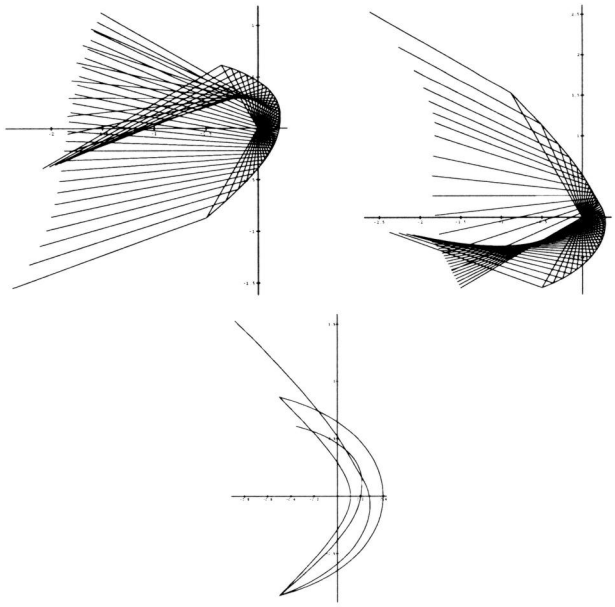

Figure 4.2: *The two reflectors that achieve extreme values for $f(t_2)$ in the problem of Example 3.3.2, and their ray paths. In the bottom, these reflectors are plotted together with the reflectors corresponding to the monotonic solutions.*

over all measurable functions $\theta : [t_1, t_2] \to \mathbb{R}$ that are equimeasurable with a prescribed smooth function $\bar{\theta} : [t_1, t_2] \to \mathbb{R}$. Here f is a smooth, odd function with convex, non-negative derivative f', such as $f(t) = \tan(t/2)$ on $(-\pi, \pi)$. The condition of *equimeasurability* means that for all ϕ_1, ϕ_2 with $\phi_1 < \phi_2$ the sets of all t with $\phi_1 < \theta(t) < \phi_2$ and with $\phi_1 < \bar{\theta}(t) < \phi_2$ have equal Lebesgue measure. For definiteness we always take $\bar{\theta}$ to be non-decreasing and thus ask for the extreme values of $J(\theta)$ over all θ having $\bar{\theta}$ as their common non-decreasing rearrangement. We refer to Hardy, Littlewood and Pólya [12, Secs. 10.12-16] for more details concerning rearrangements.

We shall concentrate on the maximization of (4.6); the minimization of (4.6) is easily transformed into a maximization problem of the considered type by replacing t_2 by $-t_1$, t_1 by $-t_2$, and $\bar{\theta}(t)$ by $-\bar{\theta}(-t)$ for $-t_2 \le t \le -t_1$.

The answer to the maximization problem is particularly easy in two special cases, viz. when $t_1 + \bar{\theta}(t_1) \ge 0$ or $t_2 + \bar{\theta}(t_2) \le 0$. We will show that when $t_1 + \bar{\theta}(t_1) \ge 0$, then we have

$$\int_{t_1}^{t_2} f(s + \theta(s))\, ds \le \int_{t_1}^{t_2} f(s + \bar{\theta}(s))\, ds, \tag{4.7}$$

and that when $t_2 + \bar{\theta}(t_2) \leq 0$, we have

$$\int_{t_1}^{t_2} f(s + \theta(s))\, ds \leq \int_{t_1}^{t_2} f(s + \bar{\theta}(t_1 + t_2 - s))\, ds \tag{4.8}$$

for all allowed θ. Hence the non-decreasing rearrangement $\bar{\theta}(s)$ and the non-increasing rearrangement $\bar{\theta}(t_1 + t_2 - s)$ solve the respective maximization problems. In the reflector design context, these solutions correspond to the monotonic ray paths. In [22], a proof for the special case that $f(t) = \tan(t/2)$ is presented. In Section 4.3.1 we derive a similar result for more general functions f.

Unfortunately, the results for the case that $t_1 + \bar{\theta}(t_1) < 0 < t_2 + \bar{\theta}(t_2)$ are not so easy to state, and the proofs are in keeping with it. Firstly, it may very well happen that the maximization problem does not admit a solution in the space of all measurable functions θ having $\bar{\theta}$ as their common non-decreasing rearrangement. Also, in the cases that there does exist a solution, it may be discontinuous at many places and its actual form, which can be rather complicated, usually depends on f. (If θ has n discontinuities, then the corresponding reflector will consist of $n+1$ smooth facets.)

On the other hand we have certain not too restrictive conditions under which we can show the optimal θ's to be reasonably well-behaved (what this means will be explained below). These conditions are that $\bar{\theta}'(t) < 2$ for all $t \in [t_1, t_2]$, and that $\bar{\theta}'(t) = 1/2$ for only finitely many points $t \in [t_1, t_2]$. In reflector design applications, both these conditions are usually satisfied.

Let us summarize the results of this chapter. In Section 4.2 we consider the discrete version of the maximization problem. That is, given increasing sequences $s_1, \ldots s_n$ and $\bar{\theta}_1, \ldots, \bar{\theta}_n$, together with a smooth, odd function f for which f' is (strictly) convex and non-negative, then we want to maximize

$$J(\theta) := \sum_{i=1}^{n} f(s_i + \theta(s_i)), \tag{4.9}$$

over all bijections $\theta : \{s_1, \ldots, s_n\} \to \{\bar{\theta}_1, \ldots, \bar{\theta}_n\}$. This problem can be seen as a matching problem, and it is solvable in $O(n^3)$ time. However, due to the conditions on f, several properties of optimizers can be deduced. For instance, denoting $\theta_i = \theta(s_i)$, it will be shown that for any maximizer θ and any k, m with $1 \leq k \leq m \leq n$ we have

$$\{\theta_k, \theta_m\} \cap \{\min_{k \leq l \leq m} \theta_l, \max_{k \leq l \leq m} \theta_l\} \neq \emptyset. \tag{4.10}$$

Furthermore, when

$$\max_{1 \leq i \leq n-1} (\bar{\theta}_{i+1} - \bar{\theta}_i) < \min_{1 \leq i \leq n-2} (s_{i+2} - s_i), \tag{4.11}$$

it turns out that for any maximizer and any k, m with $1 \leq k \leq m \leq n$ we have

$$\{\theta_k, \theta_m\} \cap \{\max_{k \leq l \leq m} \theta_l\} \neq \emptyset. \tag{4.12}$$

The latter property is equivalent with θ being V-*shaped*: there is an n_0 with $1 \leq n_0 \leq n$, such that

$$\theta_1 > \theta_2 > \ldots > \theta_{n_0-1} > \theta_{n_0} = \bar{\theta}_1 < \theta_{n_0+1} < \ldots < \theta_{n-1} < \theta_n. \tag{4.13}$$

(If θ has the converse property, i.e. if $-\theta$ is V-shaped, then θ is usually said to be unimodal.) Also, the deviation of the maximizing θ from being V-shaped in the general case can be quantified in terms of the extent to which (4.11) is violated; see Proposition 4.2.7. Finally we show that under the condition that

$$\max_{1 \leq i \leq n-2} (\bar{\theta}_{i+2} - \bar{\theta}_i) < \min_{1 \leq i \leq n-1} (s_{i+1} - s_i), \tag{4.14}$$

we can even solve the discrete problem by a greedy $O(n)$ algorithm.

In Section 4.3.1 we present existence results for the maximization of

$$J_\phi(\theta) := \int_{t_1}^{t_2} f(\phi(s) + \theta(s))\, ds, \tag{4.15}$$

over all measurable θ having $\bar{\theta}$ as their common non-decreasing rearrangement. Here ϕ is a given bounded function. We shall show the result announced in connection with (4.7) and (4.8) for the case that $\phi(t)$, $\theta(t) \geq 0$ for all $t \in [t_1, t_2]$. Furthermore we show the following. Let the *variation* $\mathrm{Var}(\theta;\, t_1, t_2)$ *of* θ *over* $[t_1, t_2]$ be defined by

$$\mathrm{Var}(\theta;\, t_1, t_2) = \sup\{\sum_{k=1}^{n-1} |\theta(s_{k+1}) - \theta(s_k)| \,|\, t_1 = s_1 < \ldots < s_n = t_2; n \in \mathbb{N}\}. \tag{4.16}$$

Then we show that for any $V \geq \bar{\theta}(t_2) - \bar{\theta}(t_1)$ there exists an allowed θ_V with

$$\mathrm{Var}(\theta_V;\, t_1, t_2) \leq V$$

such that $J_\phi(\theta_V) \geq J_\phi(\theta)$ for all allowed θ with $\mathrm{Var}(\theta;\, t_1, t_2) \leq V$. Although in actual reflector design problems the restriction to mappings θ of finite variation is quite natural, this existence result is unsatisfactory in the sense that it does not exclude (and indeed, it happens) that $\mathrm{Var}(\theta_V;\, t_1, t_2) \to \infty$ as $V \to \infty$. A further result that we present in Section 4.3.1 is that $\sup_\theta J_{\bar{\phi}}(\theta) = \sup_\phi J_{\bar{\theta}}(\phi)$, where the suprema are over all θ and ϕ with common non-decreasing rearrangements

$\bar{\theta}$ and $\bar{\phi}$, respectively. This result is useful when one of the optimizations is easier than the other. Finally, a result is presented showing that the continuous problem can be considered as a limit case of the discrete problem, so that the results of Section 4.2 can be carried over to the continuous problem.

In Section 4.3.2 we consider the case $\phi(s) = s$ for all s in (4.15) in more detail, and we analyze the optimizers θ under the condition that their variation (4.16) is finite. For instance, it is shown that these optimizers are V-shaped. Also, with the aid of Section 4.3.1 it is shown that there exist optimizers of finite variation whenever $\bar{\theta}'(s) < 2$ for all $s \in [t_1, t_2]$. Furthermore, it is shown that V-shaped optimizers are continuous on the left leg of the V and that the number of discontinuities of θ on the right leg is bounded from above in terms of the number of s with $\bar{\theta}'(s) = 1/2$, if that number is finite. For instance, when $\bar{\theta}'(s) < 1/2$ for all $s \in [t_1, t_2]$, we find that the optimizer θ is continuous. Also, the form of θ, both on the left leg and between the discontinuities on the right leg, is determined analytically in terms of the discontinuities of θ and the values of θ assumed at t_1 and t_2. This allows us to express $J(\theta)$ as a finite series of integrals involving known functions, with integration bounds that are to be chosen so as to yield the highest possible value for $J(\theta)$. The latter problem can get quite complicated.

In Section 4.4 we present, again under the condition that the optimizers are of finite variation, analytical results for the case that there is at most one point s with $\bar{\theta}'(s) = 1/2$. (In reflector design problems, this will often be the case.) Finally, in Section 4.5 we present examples, both for the discrete and the continuous case, some of which are relevant to the reflector design problem. These examples also serve to illustrate a curious duality between the existence of non-injective solutions of the continuous problem when $\bar{\theta}'(s) < 1/2$ for all s, and the non-existence of solutions of this problem when $\bar{\theta}'(s) \geq 2$ is allowed to occur.

4.2 The Discrete Problem

4.2.1 The Discrete Problem Seen as a Matching Problem

In this section we consider an increasing sequence $s_1, \ldots, s_n$ and an increasing sequence $\bar{\theta}_1, \ldots, \bar{\theta}_n$, together with a smooth, odd function f for which f' is (strictly) convex and non-negative, and we want to maximize

$$J(\theta) := \sum_{i=1}^{n} f(s_i + \theta(s_i)), \tag{4.17}$$

over all bijections $\theta : \{s_1, \ldots, s_n\} \to \{\bar{\theta}_1, \ldots, \bar{\theta}_n\}$. This problem is a special case of a well-known matching problem. In order to formulate this matching problem,

we briefly recall some notions from graph theory. For more details, we refer to Lovász and Plummer [21].

A graph $G = (V, E)$ is called *bipartite* if $V = A \cup B$ for two disjoint non-empty subsets A and B of V such that all edges in E join a vertex of A to a vertex of B. A bipartite graph is called *complete* if each vertex in A is adjacent to each vertex in B. A subset of edges $M \subset E$ of a graph G is called a *matching of* G if no two edges in M have a vertex in common. A matching M is called *perfect* if each vertex is covered by an edge in M. If the graph G is weighted, i.e. if each edge $e \in E$ has a weight $w_e \in \mathbb{R}$ associated with it, then the weight of a matching M is defined to be $\sum_{e \in M} w_e$. A *maximum weight perfect matching* is a perfect matching that has the greatest weight among all perfect matchings.

It is easily seen that maximizing (4.17) is precisely the problem of finding a maximum weight perfect matching in a weighted complete bipartite graph. Specifically, let $A = \{s_1, s_2, \ldots, s_n\}$, $B = \{\bar{\theta}_1, \bar{\theta}_2, \ldots, \bar{\theta}_n\}$, $E = \{(s_i, \bar{\theta}_j) \mid s_i \in A,\ \bar{\theta}_j \in B\}$, and $w_e = f(s_i + \bar{\theta}_j)$ for $e = (s_i, \bar{\theta}_j)$. This problem is solvable in polynomial time: Gabow [10], Lawler [18], and Cunningham and Marsh [6] have developed algorithms which take $O(|V|^3)$ time. In our problem however, the 'weight function' has some special properties. From this we can deduce several properties of optimal mappings θ (i.e. optimal matchings). It might be interesting to investigate whether these properties may lead to a faster matching algorithm for these special weight functions. This topic, however, is not addressed here.

What is more important here is that the results of this section provide us with insight as to when the continuous problem is solvable (and when not), and what the optimal $\theta(t)$ looks like. It is also for this reason that the problem above is formulated as that of finding an optimal mapping, rather than one of finding an optimal permutation, another way to present the problem which would have emphasized the symmetry of the problem (in the sense that the s_i's and the $\bar{\theta}_i$'s play similar roles). Finally, the restriction to increasing sequences is for convenience only; the results of this section can be applied to non-decreasing sequences as well.

4.2.2 Basic Properties of Maximizers

From now on, we assume that θ is a bijection that maximizes (4.17), and we will write $\theta_i = \theta(s_i)$ for all $i \in \{1, \ldots, n\}$. In this section we will see that θ maps at least one of the extreme points s_1, s_n onto one of the extreme points $\bar{\theta}_1, \bar{\theta}_n$. We will also investigate conditions under which any of these situations may occur. The following result is basic to the remainder of this section.

Proposition 4.2.1. *Let* $1 \le k < l \le n$. *Then we have*

$$\begin{aligned} &(a) \quad \theta_k < \theta_l \quad \Rightarrow \quad -(\theta_k + \theta_l) \le s_k + s_l, \\ &(b) \quad \theta_k > \theta_l \quad \Rightarrow \quad -(\theta_k + \theta_l) \ge s_k + s_l. \end{aligned}$$

Proof. By optimality of θ, we have

$$f(s_k + \theta_k) + f(s_l + \theta_l) \ge f(s_k + \theta_l) + f(s_l + \theta_k). \tag{4.18}$$

The assumptions on f (see the beginning of Section 4.2.1) imply that the function

$$\phi_{\eta,\tau}(s) = f(s + \eta) - f(s + \tau), \qquad s \in \mathbb{R}, \tag{4.19}$$

is even, i.e. it is symmetric about the point $s = -(\eta + \tau)/2$. Furthermore, $\phi_{\eta,\tau}$ is positive and strictly convex when $\eta > \tau$, while it is negative and strictly concave when $\eta < \tau$. Hence (4.18) together with $s_k < s_l$ imply that

$$-(s_l + (\theta_k + \theta_l)/2) \le s_k + (\theta_k + \theta_l)/2 \tag{4.20}$$

or

$$-(s_l + (\theta_k + \theta_l)/2) \ge s_k + (\theta_k + \theta_l)/2 \tag{4.21}$$

according as $\theta_k < \theta_l$ or $\theta_k > \theta_l$, as required. □

The next result involves three different points; we only present the most significant conclusions that one can draw concerning three points.

Proposition 4.2.2. *Let* $1 \le k < l < m \le n$. *Then we have*

$$\begin{aligned} &(a) \quad \theta_k > \theta_m > \theta_l \quad \Rightarrow \quad \theta_k - \theta_l \le s_l - s_k, \\ &(b) \quad \theta_l > \theta_k > \theta_m \quad \Rightarrow \quad \theta_k - \theta_m \ge s_m - s_k, \\ &(c) \quad \theta_l > \theta_m > \theta_k \quad \textit{does not occur.} \end{aligned}$$

Proof.
(a) Because $\theta_k > \theta_m$ and $\theta_m > \theta_l$ it follows from Proposition 4.2.1 that

$$-(\theta_k + \theta_m) \ge s_k + s_m \text{ and } -(\theta_l + \theta_m) \le s_l + s_m. \tag{4.22}$$

By combining these two inequalities, implication (a) follows.
(b) Because $\theta_l > \theta_k$ and $\theta_l > \theta_m$ it follows from Proposition 4.2.1 that

$$-(\theta_k + \theta_l) \le s_k + s_l \text{ and } -(\theta_l + \theta_m) \ge s_l + s_m. \tag{4.23}$$

By combining these two inequalities, implication (b) follows.
(c) In the proof of (b) it was not used that $\theta_k > \theta_m$, but this follows already from the right hand side of (b). Hence $\theta_l > \theta_m > \theta_k$ does not occur. □

The next result is an important characteristic of a maximizing θ. It says that θ maps at least one of the extreme points s_1, s_n onto one of the extreme points $\bar{\theta}_1, \bar{\theta}_n$.

Theorem 4.2.3. *For a maximizing θ we have*

$$\{\theta_1, \theta_n\} \cap \{\bar{\theta}_1, \bar{\theta}_n\} \neq \emptyset. \tag{4.24}$$

Proof. Suppose that (4.24) is not true. Then there are i, j with $1 < i, j < n$ such that

$$\theta_i = \bar{\theta}_1 < \theta_1 \text{ and } \theta_j = \bar{\theta}_n > \theta_n. \tag{4.25}$$

It follows from Proposition 4.2.2(b) and (c) with $k = 1,\ l = j,\ m = n$ that

$$\theta_1 - \theta_n \geq s_n - s_1. \tag{4.26}$$

Next it follows from Proposition 4.2.2(a) with $k = 1,\ l = i,\ m = n$ that

$$\theta_1 - \bar{\theta}_1 \leq s_i - s_1. \tag{4.27}$$

However, $s_i < s_n$ and $\theta_n > \bar{\theta}_1$, and this shows that (4.26) and (4.27) yield a contradiction. □

An immediate consequence of this proposition is the following.

Corollary 4.2.4. *Let $1 \leq k < m \leq n$. Then we have*

$$\{\theta_k, \theta_m\} \cap \{\min_{k \leq l \leq m} \theta_l, \max_{k \leq l \leq m} \theta_l\} \neq \emptyset. \tag{4.28}$$

Now that we know that an optimal θ 'matches' at least one pair of extremal points, we can investigate necessary and sufficient conditions under which any of these matchings occur. The following proposition gives some of these conditions.

Proposition 4.2.5. *For a maximizing θ we have*

$$\begin{array}{lllll}
(a) & -(\bar{\theta}_1 + \bar{\theta}_2) & < s_1 + s_2 & \Rightarrow & \theta_1 = \bar{\theta}_1, \\
(b) & -(\bar{\theta}_{n-1} + \bar{\theta}_n) & > s_1 + s_n & \Rightarrow & \theta_1 = \bar{\theta}_n, \\
(c) & -(\bar{\theta}_1 + \bar{\theta}_n) & > s_{n-1} + s_n & \Rightarrow & \theta_n = \bar{\theta}_1, \\
(d) & -(\bar{\theta}_1 + \bar{\theta}_n) & < s_1 + s_n & \Rightarrow & \theta_n = \bar{\theta}_n, \\
(e) & -(\bar{\theta}_{n-1} + \bar{\theta}_n) & < s_1 + s_2 & \Rightarrow & \theta_1 \neq \bar{\theta}_n, \\
(f) & -(\bar{\theta}_1 + \bar{\theta}_2) & > s_1 + s_n & \Rightarrow & \theta_1 \neq \bar{\theta}_1.
\end{array}$$

Proof. We will only prove (a) and (b). The rest is proven similarly. (a) Suppose that the left member of the implication (a) is valid, and that $\theta_1 > \bar{\theta}_1 = \theta_k$ for some $k > 1$. Then by Proposition 4.2.1(b) we have

$$-(\bar{\theta}_1 + \bar{\theta}_2) \geq -(\theta_1 + \theta_k) \geq s_1 + s_k \geq s_1 + s_2, \tag{4.29}$$

a contradiction.
(b) Suppose that the left member of the implication (b) is valid, and that $\theta_1 < \bar{\theta}_n = \theta_k$ for some $k > 1$. Then by Proposition 4.2.1(a) we have

$$-(\bar{\theta}_{n-1} + \bar{\theta}_n) \leq -(\theta_1 + \theta_k) \leq s_1 + s_k \leq s_1 + s_n, \tag{4.30}$$

a contradiction. □

We conclude this section with the discrete analogue of the result in [13], which is generalized in Proposition 4.3.1.

Corollary 4.2.6. *If* $s_1 + s_2 + 2\bar{\theta}_1 \geq 0$ *then* $\theta_i = \bar{\theta}_i$ *for all* $i \in \{1, \ldots, n\}$. *If* $s_n + s_{n-1} + 2\bar{\theta}_n \leq 0$ *then* $\theta_i = \bar{\theta}_{n+1-i}$ *for all* $i \in \{1, \ldots, n\}$.

Proof. Repeatedly apply Proposition 4.2.5(a) and (c) for the first and second statement, respectively. □

4.2.3 V-Shaped Maximizers

In the previous section we have seen that θ satisfies condition (4.28). From this one can deduce that the number of mappings

$$\theta : \{s_1, \ldots, s_n\} \to \{\bar{\theta}_1, \ldots, \bar{\theta}_n\}$$

that can possibly be a maximizer, is reduced from $n!$ to $\lceil \frac{1}{2}(2 + \sqrt{2})^{n-1} \rceil$. Unfortunately, this is the best one can do: for each function f and for each mapping θ that satisfies condition (4.28), one can find numbers

$$s_1, \ldots, s_n \text{ and } \bar{\theta}_1, \ldots, \bar{\theta}_n$$

such that θ is a maximizer (the proof uses Proposition 4.2.5 and induction).

Nevertheless, there is a tendency of the θ's towards being V-*shaped*. By V-shaped we mean that there is an n_0 with $1 \leq n_0 \leq n$, such that

$$\theta_1 > \theta_2 > \ldots > \theta_{n_0-1} > \theta_{n_0} = \bar{\theta}_1 < \theta_{n_0+1} < \ldots < \theta_{n-1} < \theta_n. \tag{4.31}$$

Note that θ is V-shaped if and only if for all k, m with $1 \leq k \leq m \leq n$, we have (compare with (4.28)),

$$\max_{k \leq l \leq m} \theta_l \in \{\theta_k, \theta_m\}. \tag{4.32}$$

We will now show that the deviation from being V-shaped puts strong restrictions on the sets $\{s_1, \ldots, s_n\}$ and $\{\bar{\theta}_1, \ldots, \bar{\theta}_n\}$. To this end, first note that if θ is not V-shaped, then there is an l with $1 < l < n$ such that $\theta_l > \theta_{l-1}$ and $\theta_l > \theta_{l+1}$. From Proposition 4.2.2 it then follows that $\theta_l > \theta_{l-1} > \theta_{l+1}$. The following proposition is formulated, mainly for convenient graphical display in Figure 4.3, for the case $s_i = i$ for all i. The generalization to the case of arbitrary increasing s_i is straightforward.

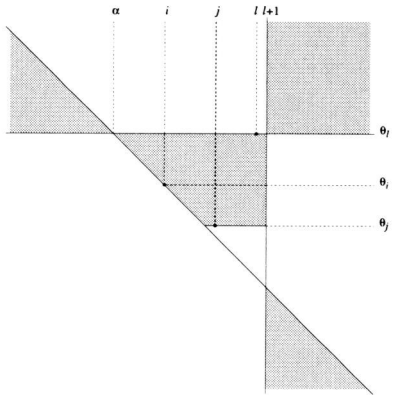

Figure 4.3: *In the case that θ is not V-shaped, its graph is restricted to the shaded regions.*

Proposition 4.2.7. *Let $s_i = i$ for all $i \in \{1, \ldots, n\}$. Assume that θ is not V-shaped, so that there is an l with $1 < l < n$ such that $\theta_l > \theta_{l-1} > \theta_{l+1}$. Let i and j be such that*

$$\theta_i + i = \min_{k \le l, \theta_k < \theta_l} (\theta_k + k), \quad \text{and} \quad \theta_j = \min_{k \le l} \theta_k. \tag{4.33}$$

Note that, by definition $i \le j$. Now put $\alpha = \theta_i + i - \theta_l$. Then the graph $\{(k, \theta_k) \mid k \in \{1, \ldots, n\}\}$ of θ is restricted to the shaded regions in Figure 4.3. More precisely, we have

$$\begin{array}{lll} (a) \quad k < \alpha & \Rightarrow & \theta_l < \theta_k \le \theta_l + \alpha - k, \\ (b) \quad \alpha < k < l & \Rightarrow & \theta_l > \theta_k \ge \max\{\theta_j, \theta_l + \alpha - k\}, \\ (c) \quad l < k & \Rightarrow & \theta_k > \theta_l \text{ or } \theta_k \le \theta_l + \alpha - k. \end{array}$$

Moreover, we have

$$(d) \quad l < k < m;\ \theta_l > \theta_k \text{ and } \theta_l > \theta_m \quad \Rightarrow \quad \theta_k > \theta_m.$$

Finally, θ is increasing between j and l, and decreasing before α.

Proof.
(a) Let $k < \alpha$. Suppose that $\theta_k < \theta_l$. Then

$$\theta_k + k < \theta_k + \alpha = \theta_k + \theta_i + i - \theta_l < \theta_i + i, \tag{4.34}$$

violating the definition of i. So $\theta_k > \theta_l$. Now assume $\theta_k > \theta_l$. Then $\theta_k > \theta_l > \theta_i$, so that $\theta_k - \theta_i \le i - k$ by Proposition 4.2.2(a), i.e. $\theta_k \le \theta_l + \alpha - k$.

(b) Let $\alpha < k < l$. By definition of i and j, we have $\theta_k \geq \max\{\theta_j, \theta_l + \alpha - k\}$. This leaves us to show that $\theta_k < \theta_l$. To this end, first suppose that we have a k with $\alpha < k < i$ and $\theta_k > \theta_l$. Then $\theta_k > \theta_l > \theta_i$, so that by Proposition 4.2.2(a) we have $\theta_k - \theta_i \leq i - k$, i.e. $\theta_k \leq \theta_l + \alpha - k \leq \theta_l$, a contradiction. Next, suppose we have a k with $i < k < l$ such that $\theta_k > \theta_l > \theta_i$. Then by Proposition 4.2.2(b) we have $\theta_i - \theta_l \leq l - i$, i.e. $\theta_l \leq \theta_l + \alpha - l < \theta_l$, a contradiction.
(c) Let $l < k$. When $\theta_k < \theta_l$, we have by Proposition 4.2.2(b) that $\theta_i - \theta_k \geq k - i$, i.e. $\theta_k \leq \theta_l + \alpha - k$.
(d) Let $l < k < m$ with $\theta_l > \theta_k$ and $\theta_l > \theta_m$, and suppose that $\theta_k < \theta_m$. Then we have by Proposition 4.2.2(a) that $\theta_l - \theta_k \leq k - l$, i.e. $\theta_k \geq \theta_l + l - k > \theta_l + \alpha - k$, which contradicts (c). This proves monotonicity of θ in the region to the right of l, below θ_l.

Finally, monotonicity in the region between j and l and before α are proved similarly, by applying Proposition 4.2.2. □

In the situation of the Proposition 4.2.7 it follows that either θ is increasing from j onwards, or that the sequence θ_n exhibits a gap of at least $l + 1 - j \geq 2$. Also, when n_0 is such that $\theta_{n_0} = \bar{\theta}_1$, we have that θ is increasing from n_0 onwards (so this holds for any optimal θ, V-shaped or not). An immediate consequence of the existence of the gap for non-V-shaped maximizers is that θ is V-shaped whenever

$$\max_{1 \leq i \leq n-1} (\bar{\theta}_{i+1} - \bar{\theta}_i) < 2. \tag{4.35}$$

For arbitrary s_i, the analogue of this is given by the following corollary. Its proof is the same as for the case that $s_i = i$ for all i.

Corollary 4.2.8. *The maximizer θ is V-shaped if*

$$\max_{1 \leq i \leq n-1} (\bar{\theta}_{i+1} - \bar{\theta}_i) < \min_{1 \leq i \leq n-2} (s_{i+2} - s_i). \tag{4.36}$$

In the remainder of this section we shall analyze optimal V-shaped θ's a bit further for the case that $s_i = i$, for all i. This special case arises naturally when the continuous problem of Section 4.3 is discretized. So assume that θ is V-shaped and that n_0 is such that $\theta_{n_0} = \bar{\theta}_1$. The following proposition tells us something about how the points on the left and right leg of the V are relatively situated.

Proposition 4.2.9. *Let $k < n_0$. There is at most one $l > n_0$ such that*

$$\theta_k > \theta_l > \theta_{k+1}. \tag{4.37}$$

When such an l exists, then we have for all $m \geq k$

$$\theta_m - \theta_k \geq -(m - k), \tag{4.38}$$

in particular, $\theta_k - \theta_{k+1} \leq 1$. *Furthermore, when* p *is such that*

$$\theta_k > \theta_l > \theta_{k+1} > \ldots > \theta_{k+p} > \theta_{l-1} > \theta_{k+p+1}, \tag{4.39}$$

then we have

$$\frac{1}{2}p - 1 < \frac{1}{2}(\theta_k + \theta_{k+1}) - \frac{1}{2}(\theta_{k+p} + \theta_{k+p+1}) < \frac{1}{2}p. \tag{4.40}$$

Proof. Let $l > n_0$ be such that (4.37) holds. It follows from Proposition 4.2.1 that

$$-(\theta_k + k) \geq \theta_l + l \geq -(\theta_{k+1} + k + 1) > -(\theta_k + k) - 1. \tag{4.41}$$

Now since

$$\theta_{l-1} + (l-1) + 1 \leq \theta_l + l \leq \theta_{l+1} + (l+1) - 1, \tag{4.42}$$

we see from (4.41) that

$$\theta_{l-1} + (l-1) \leq -(\theta_k + k) - 1, \text{ and } \theta_{l+1} + (l+1) > -(\theta_k + k). \tag{4.43}$$

Hence (4.41), and therefore (4.37), is not satisfied when l is replaced by $l \pm 1$.

The validity of (4.38) follows from Proposition 4.2.2(a).

To show (4.40) from (4.39), we observe that Proposition 4.2.1, together with $\theta_k > \theta_l > \theta_{k+1}$, and $\theta_{k+p} > \theta_{l-1} > \theta_{k+p+1}$ imply that

$$k + l < -(\theta_k + \theta_{k+1}) < k + l + 1, \tag{4.44}$$

and

$$k + p + l - 1 < -(\theta_{k+p} + \theta_{k+p+1}) < k + p + l. \tag{4.45}$$

Combination of these two inequalities yields (4.40). □

We will complete this section with a special case in which a greedy $O(n)$ algorithm solves the matching problem.

Proposition 4.2.10. *Assume that*

$$\max_{1 \leq i \leq n-1} (\bar{\theta}_{i+1} - \bar{\theta}_i) < \min_{1 \leq i \leq n-2} (s_{i+2} - s_i). \tag{4.46}$$

Then

$$\begin{array}{lrcll} (a) & -(\bar{\theta}_{n-1} + \bar{\theta}_n) & > & s_1 + s_n & \Rightarrow \quad \theta_1 = \bar{\theta}_n, \\ (b) & -(\bar{\theta}_{n-1} + \bar{\theta}_n) & < & s_1 + s_n & \Rightarrow \quad \theta_n = \bar{\theta}_1. \end{array}$$

Proof. The implication (a) is the same as 4.2.5(b). To prove (b), assume that $-(\bar{\theta}_{n-1} + \bar{\theta}_n) < s_1 + s_n$ and that $\theta_n < \bar{\theta}_n$, so $\theta_n = \bar{\theta}_{n-k}$ for some $k \geq 1$. Note that

(4.46) implies (4.36), so θ is V-shaped, and consequently, we have $\theta_k = \bar{\theta}_{n-k+1}$. From Proposition 4.2.1(b) it then follows that

$$-(\bar{\theta}_{n-k+1} + \bar{\theta}_{n-k}) \geq s_k + s_n. \tag{4.47}$$

On the other hand, we have

$$\begin{aligned} -(\bar{\theta}_{n-k+1} + \bar{\theta}_{n-k}) &= -(\bar{\theta}_n + \bar{\theta}_{n-1}) + (\bar{\theta}_n - \bar{\theta}_{n-2}) + (\bar{\theta}_{n-1} - \bar{\theta}_{n-3}) + \dots \\ &\quad + (\bar{\theta}_{n-k+2} - \bar{\theta}_{n-k}) \\ &< (s_n + s_1) + (s_2 - s_1) + (s_3 - s_2) + \dots + (s_k - s_{k-1}) \\ &= s_k + s_n, \end{aligned} \tag{4.48}$$

by (b) and (4.46). This contradicts (4.47). □

Note that, in the proposition above, in the case that $-(\bar{\theta}_{n-1} + \bar{\theta}_n) = s_1 + s_n$, we get $\{\theta_1, \theta_n\} = \{\bar{\theta}_1, \bar{\theta}_n\}$; both possible assignments yield the same value of the functional. It is clear that the above proposition can be applied repeatedly, and we get the following result.

Corollary 4.2.11. *If*

$$\max_{1 \leq i \leq n-1} (\bar{\theta}_{i+1} - \bar{\theta}_i) < \min_{1 \leq i \leq n-2} (s_{i+2} - s_i), \tag{4.49}$$

then we can find a maximizer in $O(n)$ time.

4.3 The Continuous Problem

We consider in this section the maximization of

$$J(\theta) := \int_{t_1}^{t_2} f(s + \theta(s))\, ds. \tag{4.50}$$

Here f is a smooth, odd function with non-negative, convex derivative f', and θ is equimeasurable with a given, smooth, non-decreasing function $\bar{\theta}$ defined on $[t_1, t_2]$, i.e. the sets

$$S_\theta(a, b) := \{t \mid a < \theta(t) < b\} \text{ and } S_{\bar{\theta}}(a, b) := \{t \mid a < \bar{\theta}(t) < b\} \tag{4.51}$$

have equal measure for all $a, b \in \mathbb{R}$. The set of all functions θ equimeasurable with $\bar{\theta}$ will be denoted $\bar{\Theta}$. In solving this problem we are strongly inspired by the results of Section 4.2 on the discrete problem. However, there are also conspicuous differences between the two problems, the most important one being the non-trivial matter of the existence of maximizers in the continuous problem.

The continuous problem can be discretized so that a discrete problem of the type dealt with in Section 4.2 is obtained. For instance, when $n \in \mathbb{N}$, then let

$$\delta^{(n)} := \frac{t_2 - t_1}{2n}, \tag{4.52}$$

and let for all $i \in \{1, \ldots, n\}$

$$s_i^{(n)} := t_1 + (2i - 1)\delta^{(n)}, \quad \text{and} \quad \bar{\theta}_i^{(n)} := \bar{\theta}(s_i^{(n)}). \tag{4.53}$$

That is, the interval $[t_1, t_2]$ is divided into n equally sized subintervals, and the midpoints of these intervals are chosen as $s_i^{(n)}$. We can now consider the corresponding discrete optimization problem (4.17). If $\theta^{(n)}$ is a maximizer of this problem, we can associate with it a step function

$$\theta_{\text{step}}^{(n)} := \sum_{i=1}^{n} \theta_i^{(n)} I_i^{(n)}, \tag{4.54}$$

where $\theta_i^{(n)} = \theta^{(n)}(s_i^{(n)})$, and where $I_i^{(n)}$ is the indicator function of the interval $(s_i - \delta^{(n)}, s_i + \delta^{(n)}]$ for all i with $1 < i \leq n$, and $I_1^{(n)}$ is the indicator function of $[s_1 - \delta^{(n)}, s_1 + \delta^{(n)}]$. Now we can hope that

$$J(\theta_{\text{step}}^{(n)}) \to \sup\{J(\theta) \mid \theta \in \bar{\Theta}\}, \tag{4.55}$$

and that (a subsequence of) $\theta_{\text{step}}^{(n)}$ converges to a θ maximizing $J(\theta)$ as $n \to \infty$, when such a θ exists.

This section is subdivided as follows. In Section 4.3.1 we present the solution of the problem in case that $0 \notin (t_1 + \bar{\theta}(t_1), t_2 + \bar{\theta}(t_2))$, which is a generalization of the result in [13]. Furthermore, we show existence of a maximizer among all functions $\theta \in \bar{\Theta}$, whose variation

$$\text{Var}(\theta;\, t_1, t_2) := \sup_{n \in \mathbb{N}} \{ \sum_{k=1}^{n-1} |\theta(s_{k+1}) - \theta(s_k)| \,|t_1 = s_1 < \ldots < s_n = t_2\}, \tag{4.56}$$

does not exceed a prescribed threshold. We will denote by $\bar{\Theta}_V$ the set of all $\theta \in \Theta$ with $\text{Var}(\theta;\, t_1, t_2) \leq V$. Also, a statement concerning the convergence of the solution of the discretized problem is given and special attention is paid to the case that $\bar{\theta}'(t) < 2$, for all $t \in [t_1, t_2]$.

In Section 4.3.2 we assume that there is a θ with finite variation $\text{Var}(\theta;\, t_1, t_2)$ such that $J(\theta) \geq J(\eta)$ for all $\eta \in \bar{\Theta}$. Then we present the basic properties of this θ such as being V-shaped, and continuity on the left leg of the V. We conclude it with a more detailed analysis of these θ's, and we attempt to describe them and their functional value $J(\theta)$ analytically.

4.3.1 Some Existence Results

We present in this section some existence results for the slightly more general problem of maximizing (over θ)

$$J_\phi(\theta) := \int_{t_1}^{t_2} f(\phi(s) + \theta(s))\, ds, \tag{4.57}$$

where ϕ has a smooth non-decreasing rearrangement $\bar{\phi}$, see Hardy, Littlewood and Pólya [12, Sec. 10.12]. The set of all functions ϕ equimeasurable with $\bar{\phi}$ will be denoted $\bar{\Phi}$.

Proposition 4.3.1. *Let $f : [0, \infty) \to [0, \infty)$ be a non-decreasing, smooth, convex function with $f(0) = 0$, and let ϕ and θ be two bounded, measurable non-negative functions defined on* [0, 1]. *Then*

$$\int_0^1 f(\bar{\phi}(s)+\underline{\theta}(s))\, ds \le \int_0^1 f(\phi(s)+\theta(s))\, ds \le \int_0^1 f(\bar{\phi}(s)+\bar{\theta}(s))\, ds. \tag{4.58}$$

Here $\underline{\theta}(s) = \bar{\theta}(1-s)$ and $\underline{\phi}(s) = \bar{\phi}(1-s)$ are the non-increasing rearrangements of θ and ϕ, respectively.

Proof. For all $t \ge 0$, we have

$$f(t) = \int_0^\infty f''(u) \max(0, t-u)\, du + tf'(0). \tag{4.59}$$

We can assume that $f'(0) = 0$ since there is equality in (4.58) for linear f's, and then we get by Fubini's theorem

$$\int_0^1 f(\phi(s)+\theta(s))\, ds = \int_0^\infty f''(u)\Big(\int_0^1 \max(0,\ \phi(s)+\theta(s)-u)\, ds\Big)\, du. \tag{4.60}$$

Since $\max(0,\ x-u) = \max(u, x) - u$, it suffices to show that

$$\int_0^1 \max(u, \bar{\phi}(s) + \underline{\theta}(s))\, ds \le \int_0^1 \max(u, \phi(s) + \theta(s))\, ds \le \int_0^1 \max(u, \bar{\phi}(s) + \bar{\theta}(s))\, ds \tag{4.61}$$

for any $u \ge 0$.

We shall first prove (4.61) for functions ϕ and θ of the form

$$\phi(s) = \sum_{k=1}^n \phi_k I_k(s), \qquad \theta(s) = \sum_{k=1}^n \theta_k I_k(s), \tag{4.62}$$

where $I_k(s)$ is the indicator function of $[(k-1)/n, k/n]$. In this case the inequality to be proved reduces to

$$\sum_{k=1}^{n} \max(u, \bar{\phi}_k + \underline{\theta}_k) \leq \sum_{k=1}^{n} \max(u, \phi_k + \theta_k) \leq \sum_{k=1}^{n} \max(u, \bar{\phi}_k + \bar{\theta}_k) \tag{4.63}$$

for any $u \geq 0$, where $\bar{\phi}_1, \ldots \bar{\phi}_n$ is the non-decreasing ordering of the sequence $\phi_1, \ldots \phi_n$, etc.

The elementary inequality

$$\begin{array}{ccc} a \leq b & \text{and} & c \leq d \\ & \Downarrow & \\ \max(u, a+c) + \max(u, b+d) & \geq & \max(u, b+c) + \max(u, a+d) \end{array} \tag{4.64}$$

for $u \geq 0$ gives what is required for proving (4.63). To show (4.64) we just note that for all $y, u \in \mathbb{R}$, we have

$$\max(u, y) = \frac{1}{2}(y + u + |y - u|), \tag{4.65}$$

and that the function $x \to |c+x| - |d+x|$ is non-increasing in $x \in \mathbb{R}$ when $c \leq d$.

The proof of (4.61) for the general case can now be completed as follows. We can find sequences of functions $\phi^{(n)}, \theta^{(n)}$ of the form (4.62) such that as $n \to \infty$, we have

$$\int_0^1 |\phi(s) - \phi^{(n)}(s)|\, ds \to 0, \text{ and } \int_0^1 |\theta(s) - \theta^{(n)}(s)|\, ds \to 0. \tag{4.66}$$

Now for any two integrable functions f and g defined on $[0, 1]$ and for any $a \in \mathbb{R}, \epsilon > 0$ we have

$$\mu(\{s \mid f(s) \geq a,\ g(s) \leq a - \epsilon\}) \leq \frac{1}{\epsilon} \int_0^1 |f(s) - g(s)|\, ds. \tag{4.67}$$

This implies that as $n \to \infty$, we have

$$\int_0^1 |\bar{\phi}(s) - \overline{\phi^{(n)}}(s)|\, ds \to 0, \text{ and } \int_0^1 |\bar{\theta}(s) - \overline{\theta^{(n)}}(s)|\, ds \to 0, \tag{4.68}$$

and then the result follows in a few lines. □

The following is an easy consequence.

Corollary 4.3.2. *Let f satisfy the properties that were required in connection with (4.50). Then*

$$\int_{t_1}^{t_2} f(t+\bar{\theta}(t_1+t_2-t))\,dt \le \int_{t_1}^{t_2} f(t+\theta(t))\,dt \le \int_{t_1}^{t_2} f(t+\bar{\theta}(t))\,dt \quad (4.69)$$

when $t_1+\bar{\theta}(t_1) \ge 0$, and the inequality signs are reversed when $t_2+\bar{\theta}(t_2) \le 0$.

Proposition 4.3.3. *Let $V > 0$ and assume $\bar{\Theta}_V \neq \emptyset$. Then there is a $\theta \in \bar{\Theta}_V$ such that $J_\phi(\theta) \ge J_\phi(\eta)$ for all $\eta \in \bar{\Theta}_V$.*

Proof. Let $M = \sup\{J_\phi(\eta) \mid \eta \in \bar{\Theta}_V\}$, and let $(\theta^{(k)})_{k\in\mathbf{N}}$ be a sequence in $\bar{\Theta}_V$ such that $J_\phi(\theta^{(k)}) \to M$, as $k \to \infty$. We can write

$$\theta^{(k)}(s) = \theta_+^{(k)}(s) - \theta_-^{(k)}(s), \text{ for all } s \in [t_1, t_2], \quad (4.70)$$

where $\theta_\pm^{(k)}(s)$ are non-decreasing in s, and

$$\theta_+^{(k)}(t_2) - \theta_+^{(k)}(t_1) + \theta_-^{(k)}(t_2) - \theta_-^{(k)}(t_1) \le V. \quad (4.71)$$

By Helly's theorem, see Loève [19, Sect. 11.2], we can find subsequences (denoted by $\theta^{(k)}$, etc.) and non-decreasing functions $\theta_\pm(s)$ such that $\theta_\pm^{(k)}(s) \to \theta_\pm(s)$ in all but countably many points $s \in [t_1, t_2]$. At the same time it can be arranged that

$$\theta_+(t_2) - \theta_+(t_1) + \theta_-(t_2) - \theta_-(t_1) \le V, \quad (4.72)$$

just by taking care that t_1 and t_2 are among the points s with $\theta_\pm^{(k)}(s) \to \theta_\pm(s)$. When we let $\theta(s) = \theta_+(s) - \theta_-(s)$, we thus see that $\mathrm{Var}(\theta; t_1, t_2) \le V$, and, by dominated convergence, that

$$\int_{t_1}^{t_2} f(\phi(s)+\theta(s))\,ds = M. \quad (4.73)$$

Finally, for any $a, b \in \mathbb{R}$, we have that

$$\mu(\{s \mid a < \theta^{(k)}(s) < b\}) \to \mu(\{s \mid a < \theta(s) < b\}) \quad (4.74)$$

when $k \to \infty$, again by dominated convergence. Since the numbers at the left hand side of (4.74) are all equal to $\mu(\{s \mid a < \bar{\theta}(s) < b\})$, we thus see that $\theta \in \bar{\Theta}_V$, as required. □

The two following results, whose proofs are omitted, can be shown to hold by employing the same sort of arguments that were used to prove Proposition 4.3.1.

Proposition 4.3.4. *We have*

$$\sup_{\theta\in\bar{\Theta}} \int_{t_1}^{t_2} f(\bar{\phi}(s) + \theta(s))\, ds = \sup_{\phi\in\bar{\Phi}} \int_{t_1}^{t_2} f(\phi(s) + \bar{\theta}(s))\, ds. \tag{4.75}$$

We now return to the case that $\phi(s) = s$ for all s (for convenience only).

Proposition 4.3.5. *Let $n \in \mathbb{N}$, and let δ, $s_i^{(n)}$, $\bar{\theta}_i^{(n)}$ and $\theta_{\text{step}}^{(n)}$ be defined as in (4.52), (4.53) and (4.54). Then we have*

$$\sup_{\theta\in\bar{\Theta}} \int_{t_1}^{t_2} f(s + \theta(s))\, ds = \lim_{n\to\infty} J(\theta_{\text{step}}^{(n)}). \tag{4.76}$$

Note that in this last proposition, there does not have to be a θ such that $J(\theta) = \lim_{n\to\infty} J(\theta_{\text{step}}^{(n)})$. Although Proposition 4.3.4 shows that within the set $\bar{\Theta}_V$ there is a maximizer, say θ_V, it may well happen that $\text{Var}(\theta_V;\, t_1, t_2) \to \infty$ as $V \to \infty$. See also Example 4.5.5.

From Proposition 4.3.5 it follows that the continuous problem has a well-behaved solution when

$$\max_s \bar{\theta}'(s) < 2. \tag{4.77}$$

To see this, note that in this case we have for all $n \in \mathbb{N}$

$$\max_{1\le i\le n-1} (\bar{\theta}_{i+1}^{(n)} - \bar{\theta}_i^{(n)}) < \min_{1\le i\le n-2} (s_{i+2}^{(n)} - s_i^{(n)}), \tag{4.78}$$

see (4.36), whence the optimal $\theta^{(n)}$ are all V-shaped. It thus follows that the step functions $\theta_{\text{step}}^{(n)}$ have uniformly bounded variation, they are asymptotically equimeasurable with $\bar{\theta}$, and

$$\lim_{n\to\infty} J(\theta_{\text{step}}^{(n)}) = \sup_{\theta\in\bar{\Theta}} J(\theta). \tag{4.79}$$

Now proceed as in the proof of Proposition 4.3.1 to conclude the existence of a maximizer $\theta \in \bar{\Theta}$. Summarizing, we get the following.

Corollary 4.3.6. *If $\max_s \bar{\theta}'(s) < 2$, then a V-shaped maximizer exists.*

4.3.2 Maximizers with Finite Variation

In this section we assume that $\phi(s) = s$ for all s, and that we have a $\theta \in \bar{\Theta}$, of finite variation such that $J(\theta) \ge J(\eta)$ for all $\eta \in \bar{\Theta}$ of finite variation. As we see from Proposition 4.3.1 this may occur without condition (4.77) being satisfied. Such a θ is continuous at all but at most countably many points. We can

redefine θ so that it is continuous from the right on $[t_1, t_2)$ and continuous from the left at t_2, without violating the condition of being equimeasurable with $\bar{\theta}$ or changing the value $J(\theta)$ of the functional. We start by establishing versions of Propositions 4.2.1 and 4.2.2 for the present case.

Proposition 4.3.7. *Let $t_1 \le u < v \le t_2$. Then we have*

$$\begin{aligned} &(a) \quad \theta(u) < \theta(v) \quad \Rightarrow \quad -(\theta(u) + \theta(v)) \le u + v, \\ &(b) \quad \theta(u) > \theta(v) \quad \Rightarrow \quad -(\theta(u) + \theta(v)) \ge u + v. \end{aligned}$$

Proof.
(a) Suppose that $\theta(u) < \theta(v)$, and that $-(\theta(u) + \theta(v)) > u + v$. We can find two non-overlapping closed intervals I_u and I_v of equal length contained in $[t_1, t_2]$ such that $u \in I_u$, $v \in I_v$ and such that for all $s \in I_u$ and $t \in I_v$, we have

$$\theta(s) < \theta(t) \text{ and } -(\theta(s) + \theta(t)) > s + t. \tag{4.80}$$

Denoting $I_u = [a, a + \delta]$ and $I_v = [b, b + \delta]$, we have

$$\int_{I_u} f(s + \theta(s))\, ds + \int_{I_v} f(s + \theta(s))\, ds = \int_0^\delta f(a + x + \theta(a + x)) + f(b + x + \theta(b + x))\, dx. \tag{4.81}$$

Now because of (4.80), compare with the proof of Proposition 4.2.1, we have

$$\begin{aligned} &f(a + x + \theta(a + x)) + f(b + x + \theta(b + x)) < \\ &\quad f(a + x + \theta(b + x)) + f(b + x + \theta(a + x)) \end{aligned} \tag{4.82}$$

for all $x \in (0, \delta)$. Hence

$$\int_0^\delta f(a + x + \theta(a + x)) + f(b + x + \theta(b + x))\, dx < \int_0^\delta f(a + x + \theta(b + x)) + f(b + x + \theta(a + x))\, dx. \tag{4.83}$$

This shows that θ is not a maximizer since interchanging the values of θ on the intervals I_u and I_v increases the functional J. Contradiction.
(b) is proved similarly. □

Proposition 4.3.8. *Let $t_1 \le u < v < w \le t_2$. Then we have*

$$\begin{aligned} &(a) \quad \theta(u) > \theta(w) > \theta(v) \quad \Rightarrow \quad \theta(u) - \theta(v) \le v - u, \\ &(b) \quad \theta(v) > \theta(u) > \theta(w) \quad \Rightarrow \quad \theta(u) - \theta(w) \ge w - u, \\ &(c) \quad \theta(v) > \theta(w) > \theta(u) \quad \textit{does not occur.} \end{aligned}$$

Proof. The proof is the same as that of Proposition 4.2.2. □

We are now ready to prove the following result.

Theorem 4.3.9. *If the maximizer θ is of finite variation, then it is V-shaped.*

Proof. First note that it suffices to prove the following:
Let $t_1 \leq u < v < w \leq t_2$. Then we have

$$\theta(v) > \theta(u) \Rightarrow \theta(w) \geq \theta(v). \tag{4.84}$$

To prove (4.84), suppose that $\theta(v) > \theta(u)$ and $\theta(w) < \theta(v)$. Let

$$\theta_0 := \inf\{\theta(x) \mid x < v\}. \tag{4.85}$$

Since θ is right-continuous at v, there is a $\delta > 0$ such that

$$\theta(z) > \theta_0, \text{ for all } z \text{ with } 0 \leq z - v < \delta. \tag{4.86}$$

We shall show that $\theta(w) \leq \theta_0 - \delta$. This implies that θ, and therefore $\bar{\theta}$, does not assume values between $\theta_0 - \delta$ and θ_0, which contradicts smoothness of $\bar{\theta}$.

To show that $\theta(w) \leq \theta_0 - \delta$, we let $\epsilon > 0$ and $y < v$ be such that $\theta(y) < \theta_0 + \epsilon < \theta(v)$. By Proposition 4.3.8(b) and (c) we see that

$$\theta(w) \leq \theta(y) - (w - y) < \theta_0 + \epsilon - (w - v). \tag{4.87}$$

Hence, by letting $\epsilon \downarrow 0$, we get that

$$\theta(w) \leq \theta_0 - (w - v). \tag{4.88}$$

From (4.86) it then follows that $w - v \geq \delta$, so that indeed $\theta(w) \leq \theta_0 - \delta$, which completes the proof. □

So, the optimal θ is V-shaped, and consequently there is a $v_0 \in [t_1, t_2]$ such that $\theta(v_0) = \bar{\theta}(t_1)$ or $\lim_{t \uparrow v_0} \theta(t) = \bar{\theta}(t_1)$. The following theorem proves continuity of θ on the left leg of the V, provided that there is a left leg.

Theorem 4.3.10. *If $v_0 > t_1$, then θ is continuous on $[t_1, v_0)$.*

Proof. Let $u \in (t_1, v_0)$ be such that

$$\theta(u) < \lim_{t \uparrow u} \theta(t). \tag{4.89}$$

By Theorem 4.3.9 and by smoothness of $\bar{\theta}$ there is a $v \geq v_0$, such that

$$\theta(y) \geq \lim_{t \uparrow u} \theta(t) > \theta(v) > \theta(u), \text{ for all } y \text{ such that } t_1 \leq y < u. \tag{4.90}$$

But then by Proposition 4.3.8(a) we get that

$$0 \leq \theta(y) - \theta(u) \leq y - u, \text{ for all } y \text{ such that } t_1 \leq y < u, \tag{4.91}$$

showing $\lim_{t \uparrow u} \theta(t) = \theta(u)$, a contradiction. Hence θ is continuous on (t_1, v_0). Since θ is right-continuous at t_1, the proof is complete. □

We continue the analysis of θ by studying its behaviour on the right leg of the V. In order to simplify the analysis somewhat, we assume that $\bar{\theta}$ is strictly increasing on $[t_1, t_2]$. As a consequence, θ is strictly decreasing on $[t_1, v_0)$ and strictly increasing on $[v_0, t_2]$. The following result then follows immediately from Proposition 4.3.7.

Corollary 4.3.11. *Let $\bar{\theta}$ be strictly increasing on $[t_1, t_2]$ and let u and v with $t_1 \leq u < v \leq t_2$ be such that $\theta(u) = \theta(v)$. Then we have $\theta(u) = \theta(v) = -\frac{1}{2}(u + v)$ whenever $u > t_1$ or when θ is continuous at v.*

From now on, we assume that $t_1 < v_0 < t_2$; other cases are trivial. In order to formulate the forthcoming results, it is necessary to introduce some more notations.

Firstly, let

$$\hat{v} := \begin{cases} \inf\{t \in [v_0, t_2] \mid \theta(t) \geq \theta(t_1)\}, & \text{if } \theta(t_2) > \theta(t_1) \\ t_2 & \text{otherwise.} \end{cases} \tag{4.92}$$

So, if $\theta(t_2) > \theta(t_1)$, then we have $\theta(\hat{v}) = \theta(v_1)$ and it follows that $\theta(v) = \bar{\theta}(v)$ for all $v > \hat{v}$. Now, let

$$\hat{\theta}_+ := \theta(\hat{v}), \qquad \hat{\theta}_- := \lim_{v \uparrow \hat{v}} \theta(v), \tag{4.93}$$

and let $\hat{u}_+$ and $\hat{u}_-$ be the unique solutions $u \in [t_1, v_0]$ of the equations $\theta(u) = \hat{\theta}_+$ and $\theta(u) = \hat{\theta}_-$, respectively. (So $\hat{u}_+ = t_1$ when $\theta(t_2) > \theta(t_1)$.)

Secondly, set

$$\theta_{0,+} := \theta(v_0), \qquad \theta_{0,-} := \lim_{v \uparrow v_0} \theta(v) = \bar{\theta}(t_1), \tag{4.94}$$

let $u_{0,+}$ be the unique solution $u \in [t_1, v_0]$ of the equation $\theta(u) = \theta_{0,+}$ and let $u_{0,-} = v_0$.

Finally, let $(v_k)_{k \geq 1}$ be an enumeration of the discontinuities of θ in $(v_0, \hat{v})$, let for all $k \geq 1$

$$\theta_{k,+} := \theta(v_k), \qquad \theta_{k,-} := \lim_{v \uparrow v_k} \theta(v), \tag{4.95}$$

and let $u_{k,+}$ and $u_{k,-}$ be the unique solutions $u \in [t_1, v_0]$ of the equations $\theta(u) = \theta_{k,+}$ and $\theta(u) = \theta_{k,-}$, respectively.

In Figure 4.4 we have plotted a case where θ is discontinuous at $\hat{v} < t_2$, at v_0 and at two other points $v_1, v_2 \in (v_0, \hat{v})$. Of course, all sorts of degeneracies can occur in the definitions of $\hat{v}$, $\hat{u}_\pm$, $v_{k,\pm}$, etc.

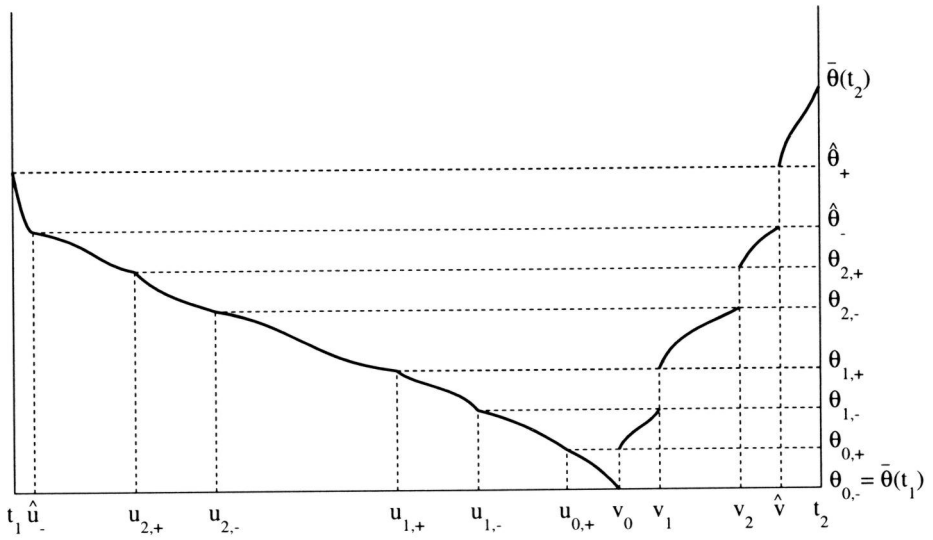

Figure 4.4: *The graph of a V-shaped θ, illustrating some definitions.*

Theorem 4.3.12. *We have*

$$-\theta_{k,-} = \frac{1}{2}(u_{k,-} + v_k), \qquad \text{for all } k \geq 1, \tag{4.96}$$

$$-\theta_{k,+} = \frac{1}{2}(u_{k,+} + v_k), \qquad \text{for all } k \geq 1, \tag{4.97}$$

$$-\theta_{0,+} = \frac{1}{2}(u_{0,+} + v_0), \tag{4.98}$$

$$-\hat{\theta}_- = \frac{1}{2}(\hat{u}_- + \hat{v}). \tag{4.99}$$

Furthermore, we have $-\theta_{0,-} \geq v_0 \geq -\frac{1}{2}(\theta_{0,-} + \theta_{0,+})$, *and, if* $\theta(t_2) > \theta(t_1)$, *then*

$$-\theta(t_1) = -\theta(\hat{v}) \leq \frac{1}{2}(t_1 + \hat{v}). \tag{4.100}$$

Proof. First we prove (4.100), which follows from Proposition 4.3.7(b) by taking $v \downarrow \hat{v}$ in the inequality

$$-(\theta(t_1) + \theta(v)) \leq t_1 + v. \tag{4.101}$$

Similarly, one proves that $-\theta_{0,-} \geq v_0 \geq -\frac{1}{2}(\theta_{0,-} + \theta_{0,+})$.

Now (4.96) and (4.97) follow immediately from Corollary 4.3.11. This leaves us to show that

$$-\hat{\theta}_- = \frac{1}{2}(\hat{u}_- + \hat{v}), \tag{4.102}$$

because (4.98) is proved similarly. Let $\epsilon > 0$ and take a $u \in (\hat{u}_-, \hat{u}_- + \epsilon)$ such that $\hat{\theta}_- - \epsilon < \theta(u) < \hat{\theta}_-$. Next, take a $v \in (\hat{v} - \epsilon, \hat{v})$ such that $\theta(u) < \theta(v) < \hat{\theta}_-$. Then Proposition 4.3.7 shows that

$$-\hat{\theta}_- > -\frac{1}{2}(\hat{\theta}_- + \theta(v)) - \frac{\epsilon}{2} \geq \frac{1}{2}(\hat{u}_- + v) - \frac{\epsilon}{2} > \frac{1}{2}(\hat{u}_- + \hat{v}) - \epsilon, \tag{4.103}$$

and

$$-\hat{\theta}_- < -\frac{1}{2}(\theta(u) + \theta(v)) \leq \frac{1}{2}(u + v) < \frac{1}{2}(\hat{u}_- + \hat{v}) - \frac{\epsilon}{2}. \tag{4.104}$$

Now let $\epsilon \downarrow 0$ to obtain (4.102). □

Note that if $t_1 < v_0 < t_2$ and if θ is continuous, then it follows that $v_0 = -\theta(t_1)$. Another consequence of this theorem is the following.

Corollary 4.3.13. *For each $k \geq 1$ there is at least one $u \in (u_{k,+}, u_{k,-})$ such that $\theta'(u) = -1/2$. Consequently, the number of discontinuities of θ is finite whenever the number of points $t \in [t_1, t_2]$ with $\bar{\theta}'(t) = 1/2$ is finite.*

Proof. Note that θ is smooth on each interval $(u_{k,+}, u_{k,-})$, and that

$$\theta(u_{k,-}) - \theta(u_{k,+}) = -\frac{1}{2}(u_{k,-} - u_{k,+}), \tag{4.105}$$

so that the result follows from the mean value theorem. □

Now that we know the conditions on the boundaries of the intervals into which $[t_1, t_2]$ is divided, we will describe θ in more detail in terms of $\bar{\theta}$ on each of these intervals. From now on, assume that the number of points $t \in [t_1, t_2]$ with $\bar{\theta}'(t) = 1/2$ is finite, so that we have discontinuities at, say, $v_1, \ldots v_K$, with $v_1 < v_2 < \ldots < v_K$. (Here v_K may or may not be equal to $\hat{v}$, if $\hat{v} < t_2$.)

It is straightforward to express θ on the intervals

$$(u_{k,+}, u_{k,-}),\ (u_{0,+}, u_{0,-}),\ (\hat{v}, t_2),\ (\hat{u}_+, \hat{u}_-) \text{ or } (t_1, \hat{u}_+) \tag{4.106}$$

in terms of $\bar{\theta}$, and so is their contribution to $J(\theta)$. This is not true for the remaining intervals $(u_{k+1,-}, u_{k,+})$ and (v_k, v_{k+1}), which will be treated as pairs, and for which the following result is relevant.

Proposition 4.3.14. *Let $U = (u_\lambda, u_\rho)$, $V = (v_\lambda, v_\rho)$ be one of the above mentioned pairs of intervals, and let $S = (s_\lambda, s_\rho)$, where s_λ and s_ρ are the solutions s of $\bar{\theta}(s) = \theta(v_\lambda)(= \theta(u_\rho))$ and $\bar{\theta}(s) = \theta(v_\rho)(= \theta(u_\lambda))$, respectively. Define functions $u : S \to U$ and $v : S \to V$ by (see Figure 4.5)*

$$\theta(u(s)) = \theta(v(s)) = \bar{\theta}(s), \qquad \text{for all } s \in S. \tag{4.107}$$

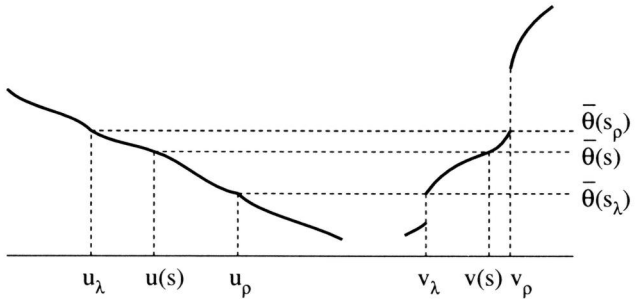

Figure 4.5: *Illustration of the intervals* (u_λ, u_ρ) *and* (v_λ, v_ρ) *of Proposition 4.3.14.*

Then we have for all $s \in S$

$$u(s) = -\frac{1}{2}(s - t_1) - \bar{\theta}(s), \qquad v(s) = \frac{1}{2}(s - t_1) - \bar{\theta}(s). \tag{4.108}$$

Furthermore, for all $s \in S$ *we have* $\bar{\theta}'(s) \leq 1/2$, *and*

$$\theta'(u(s)) = \frac{-\bar{\theta}'(s)}{\frac{1}{2} + \bar{\theta}'(s)} \in [-\frac{1}{2}, 0], \tag{4.109}$$

and

$$\theta'(v(s)) = \frac{\bar{\theta}'(s)}{\frac{1}{2} - \bar{\theta}'(s)} \in [0, \infty]. \tag{4.110}$$

Finally,

$$\int_U f(u + \theta(u))\, du + \int_V f(v + \theta(v))\, dv = -2 \int_S f(\frac{1}{2}(s - t_1))\bar{\theta}'(s)\, ds. \tag{4.111}$$

Proof. We have for any two points $u \in U$ and $v \in V$ with $\theta(u) = \theta(v)$ that

$$-\theta(u) = -\theta(v) = \frac{1}{2}(u + v). \tag{4.112}$$

Hence $u(s)$ and $v(s)$ of (4.107) satisfy

$$u(s) + v(s) = -2\bar{\theta}(s), \tag{4.113}$$

for all s. Furthermore, since $[u(s), v(s)] = \{u \mid \theta(u) \leq \bar{\theta}(s)\}$, we have

$$v(s) - u(s) = s - t_1. \tag{4.114}$$

Now (4.108) follows from these two equalities.

To show $\bar{\theta}'(s) \leq 1/2$, we note that $v(s)$ is non-decreasing and is related to $\bar{\theta}(s)$ by the second formula in (4.108).

To show (4.109) and (4.110), we note that

$$\theta'(u(s)) = \frac{1}{u'(s)} \frac{d}{ds}[\theta(u(s))] = \frac{-\bar{\theta}'(s)}{\frac{1}{2} + \bar{\theta}'(s)} \in [-\frac{1}{2}, 0], \tag{4.115}$$

and

$$\theta'(v(s)) = \frac{1}{v'(s)} \frac{d}{ds}[\theta(v(s))] = \frac{\bar{\theta}'(s)}{\frac{1}{2} - \bar{\theta}'(s)} \in [0, \infty]. \tag{4.116}$$

Finally, to show (4.111), we note that by the substitutions $u = u(s)$, $v = v(s)$, we get

$$\int_U f(u + \theta(u))\, du = -\int_S f(u(s) + \bar{\theta}(s))u'(s)\, ds, \tag{4.117}$$

and

$$\int_V f(v + \theta(v))\, dv = \int_S f(v(s) + \bar{\theta}(s))v'(s)\, ds, \tag{4.118}$$

respectively. Adding these two equalities, and using (4.108) and oddness of f we get the required result. □

A further result is the following. Suppose there is an interval $(u_{k,+}, u_{k,-})$ as above. Then $\bar{\theta}$ has at least two points s where $\bar{\theta}'(s) = 1/2$. This is seen as follows. From (4.105) it follows that there are s_λ and s_ρ such that

$$\bar{\theta}(s_\lambda) - \bar{\theta}(s_\rho) = \frac{1}{2}(s_\lambda - s_\rho); \quad \text{and } \bar{\theta}'(s_\lambda), \bar{\theta}'(s_\rho) \leq 1/2, \tag{4.119}$$

where for the last two inequalities Proposition 4.3.14 has been used. Therefore, in the cases that $\bar{\theta}'(s) = 1/2$ for only one s, there is at most one interval to which the analysis of Proposition 4.3.14 applies. These cases are worked out further in the next section.

4.4 Analytic Results for the Continuous Case

In the previous section we have indicated how we can express $J(\theta)$, in case of finitely many points s with $\bar{\theta}'(s) = 1/2$ and under the assumption that the optimizers are of finite variation, as a series of integrals involving f and $\bar{\theta}$, with integration bounds (determined by the discontinuities of θ) satisfying certain constraints. Hence the problem has been reduced to a finite-dimensional constrained optimization problem. However, this problem can get quite involved since the

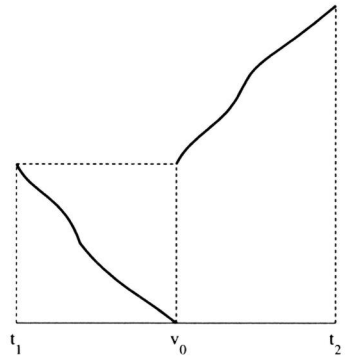

Figure 4.6: *The optimal θ for the case that $\bar{\theta}'(s) > \frac{1}{2}$ for all s.*

constraints are not so easy to deal with. In this section we present analytic results for the case that $\bar{\theta}'(s) = 1/2$ for at most one $s \in [t_1, t_2]$, again under the assumption that the optimizers are of finite variation (which is for instance true if $\bar{\theta}'(s) < 2$ for all s). This already shows that analytic solution of the problem quickly gets cumbersome.

4.4.1 The Case $\bar{\theta}'(s) > 1/2$ for all s

Suppose that $\bar{\theta}'(s) > 1/2$ for all $s \in [t_1, t_2]$. Then θ can have at most one discontinuity: at v_0. Furthermore, θ must be injective, otherwise there would be two intervals to which the analysis of Proposition 4.3.14 applies. This would imply that $\bar{\theta}'(s) \leq 1/2$ on a certain interval, contradicting our assumption on $\bar{\theta}$. Therefore, the optimal θ is of the form as depicted in Figure 4.6; where the degenerate cases $v_0 = t_1$ or $v_0 = t_2$ may also occur. In this subsection, we will write v instead of v_0. The value of $J(\theta)$ is given by

$$\psi(v) := \int_{t_1}^{v} f(t_1 + v - s + \bar{\theta}(s))\, ds + \int_{v}^{t_2} f(s + \bar{\theta}(s))\, ds \tag{4.120}$$

where v is constrained so as to satisfy (see Theorem 4.3.12)

$$-\bar{\theta}(v) \leq \frac{1}{2}(t_1 + v), \tag{4.121}$$

unless $v = t_1$ or $v = t_2$. Hence we should maximize $\psi(v)$ over $v \in [t_1, t_2]$ satisfying (4.121).

We shall show that $\psi''(v) < 0$ whenever $v \in (t_1, t_2)$ and $-\bar{\theta}(v) \leq \frac{1}{2}(t_1 + v)$. To that end we note that we have

$$\psi'(v) = f(t_1 + \bar{\theta}(v)) - f(v + \bar{\theta}(v)) + \int_{t_1}^{v} f'(-s + t_1 + v + \bar{\theta}(s))\, ds \tag{4.122}$$

Figure 4.7: *In the case that* $\bar{\theta}'(s) < \frac{1}{2}$ *for all* s*, discontinuities at* v_0 *will* not *occur.*

and

$$\psi''(v) = \int_{t_1}^{v} f''(t_1 + v - s + \bar{\theta}(s))\, ds + (1 + \bar{\theta}'(v))(f'(t_1 + \bar{\theta}(v)) - f'(v + \bar{\theta}(v))). \tag{4.123}$$

So

$$\psi''(v) = \int_{t_1}^{v} f''(t_1 + v - s + \bar{\theta}(s))\, ds - (1 + \bar{\theta}'(v)) \int_{t_1}^{v} f''(t_1 + v - s + \bar{\theta}(v))\, ds. \tag{4.124}$$

Now, by (4.121) and the fact that f'' is increasing,

$$\int_{t_1}^{v} f''(t_1 + v - s + \bar{\theta}(v))\, ds \geq \int_{t_1}^{v} f''(\frac{1}{2}(t_1 + v) - s)\, ds = 0. \tag{4.125}$$

Therefore, since $\bar{\theta}'(v) \geq 0$, we have

$$\psi''(v) \leq \int_{t_1}^{v} f''(t_1 + v - s + \bar{\theta}(s)) - f''(t_1 + v - s + \bar{\theta}(v))\, ds. \tag{4.126}$$

Finally, $\bar{\theta}(s) < \bar{\theta}(v)$ for $s \in [t_1, v)$ and f'' is increasing, whence $\psi''(v) < 0$, as required.

It follows that the optimal θ has $v = t_1$ or $v = t_2$, unless there is a $v \in (t_1, t_2)$ with $\psi'(v) = 0$. (To see whether there is such a v, first solve $-\bar{\theta}(w) = \frac{1}{2}(t_1 + w)$. Then for this w we have $\psi'(w) > 0$. Now also check whether $\psi'(t_2) < 0$.)

4.4.2 The Case $\bar{\theta}'(s) < 1/2$ for all s

Suppose that $\bar{\theta}'(s) < 1/2$ for all $s \in [t_1, t_2]$. Note that in this case the condition of the optimizer being of finite variation is automatically fulfilled. Then, as in

Figure 4.8: *Two possibilities for the optimal θ for the case that $\bar{\theta}'(s) < \frac{1}{2}$ for all s.*

the previous section, θ can have at most one discontinuity: at v_0. We will show that θ has no discontinuity at all. To this end, consider the situations depicted in Figures 4.7(a) and (b). We will show that none of these situations can occur, so that θ must be of the form as depicted in Figure 4.8(a) or (b), where, again, the degenerate cases $v_0 = t_1$ or t_2 may occur. We will consider the situation of Figure 4.7(a) only; the other case is treated completely similarly.

Let us introduce some notation. Let, as in Section 4.3, $u_{0,+}$ be such that $\theta(u_{0,+}) = \theta(v_0)$. Also, let s_λ be such that $\bar{\theta}(s_\lambda) = \theta(v_0)$, and let s_ρ be such that $\bar{\theta}(s_\rho) = \theta(t_1)$. Then Proposition 4.3.14 applies to the intervals $(u_\lambda, u_\rho) := (t_1, u_{0,+})$ and $(v_\lambda, v_\rho) := (v_0, \hat{v})$. It follows from Proposition 4.3.14 that then $J(\theta)$ can be written as

$$\psi(s_\lambda) := C - 2\int_{s_\lambda}^{s_\rho} f(\frac{1}{2}(s - t_1))\bar{\theta}'(s)\,ds + \int_{t_1}^{s_\lambda} f(t_1 + v(s_\lambda) - u + \bar{\theta}(u))\,du, \tag{4.127}$$

where C does not depend on s_λ, and where v is the function (see (4.108)) defined by

$$v(s) = \frac{1}{2}(s - t_1) - \bar{\theta}(s). \tag{4.128}$$

We will show that $\psi'(s_\lambda) < 0$ for all $s_\lambda < s_\rho$, so that $s_\lambda = t_1$ yields the maximum value for (4.127), which implies that the optimal θ is continuous at v_0.

Lemma 4.4.1. *We have $\psi'(s_\lambda) < 0$.*

Proof. Differentiating (4.127) gives

$$\psi'(s_\lambda) = \int_{t_1}^{s_\lambda} f'(t_1 + v(s_\lambda) - u + \bar{\theta}(u))v'(s_\lambda)\,du + 2f(\frac{1}{2}(s_\lambda - t_1))\bar{\theta}'(s_\lambda) + f(t_1 + v(s_\lambda) - s_\lambda + \theta(s_\lambda)). \tag{4.129}$$

It follows from the definition of v and from the oddness of f that this equals

$$\psi'(s_\lambda) = -(\frac{1}{2} - \bar{\theta}'(s_\lambda))[2f(\frac{1}{2}(s_\lambda - t_1)) - \int_{t_1}^{s_\lambda} f'(t_1 + v(s_\lambda) - u + \bar{\theta}(u))\,du]. \tag{4.130}$$

We will show that the expression in (4.130) between square brackets is positive. Define for all $u \in [t_1, s_\lambda]$

$$\omega(u) := -(t_1 + v(s_\lambda) - u + \bar{\theta}(u)) \tag{4.131}$$

and let

$$a := \omega(t_1); \qquad b := \frac{1}{2}(s_\lambda - t_1) = \omega(s_\lambda). \tag{4.132}$$

Then, since f' is even, we get by substituting $x = \omega(u)$,

$$\int_{t_1}^{s_\lambda} f'(t_1 + v(s_\lambda) - u + \bar{\theta}(u))\, du = \int_a^b f'(x)h(x)\, dx, \tag{4.133}$$

where $h(x) = [\omega'(\omega^{-1}(x))]^{-1}$. Since $\frac{1}{2} < \omega'(u) < 1$, we have $-b < a < 0$ and $1 < h(x) < 2$ for $x \in [a, b]$. Also

$$\int_a^b h(x)\, dx = 2b. \tag{4.134}$$

From the properties of f' (even, increasing on $[0, \infty)$) it then follows that

$$\int_a^b f'(x)h(x)\, dx < \int_{-b}^b f'(x)\, dx = 2f(b) = 2f(\frac{1}{2}(s_\lambda - t_1)), \tag{4.135}$$

as required. □

So the optimal θ is of the form as depicted in Figure 4.8(a) and (b), where the degenerate cases $v_0 = t_1$ or $v_0 = t_2$ and $\hat{v} = t_2$ or $\hat{u} = t_1$ should be expected to occur. Note that $v_0 = -\bar{\theta}(t_1)$.

The points $\hat{v}, \hat{u}$ are found by solving v, u from

$$-\bar{\theta}(v) = \frac{1}{2}(t_1 + v), \qquad -\bar{\theta}(t_1 + t_2 - u) = \frac{1}{2}(u + t_2), \tag{4.136}$$

respectively. At most one of these equalities has a solution. The precise situation can easily be read off from a picture of $\bar{\theta}$: the first equation in (4.136) has a (unique) solution $\hat{v} \in (t_1, t_2)$ if and only if

$$\bar{\theta}(t_1) < -t_1 \text{ and } \bar{\theta}(t_2) > -\frac{1}{2}(t_1 + t_2), \tag{4.137}$$

and the second equation in (4.136) has a (unique) solution $\hat{u} \in (t_1, t_2)$ if and only if

$$\bar{\theta}(t_1) > -t_2 \text{ and } \bar{\theta}(t_2) < -\frac{1}{2}(t_1 + t_2). \tag{4.138}$$

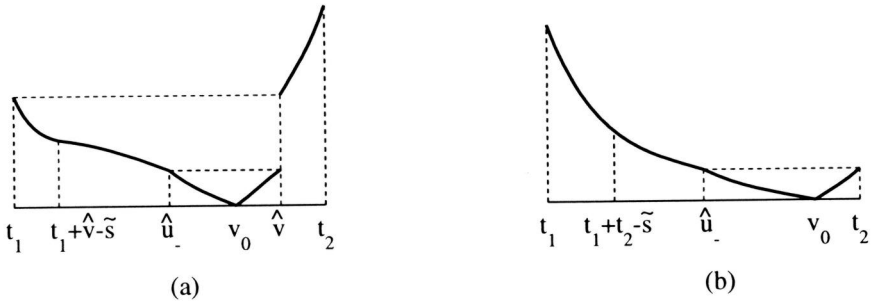

Figure 4.9: *Two possibilities for the optimal θ for the case that $\bar{\theta}'(s) < 1/2$ for $s < \tilde{s}$, $\bar{\theta}'(s) > 1/2$ for $s > \tilde{s}$.*

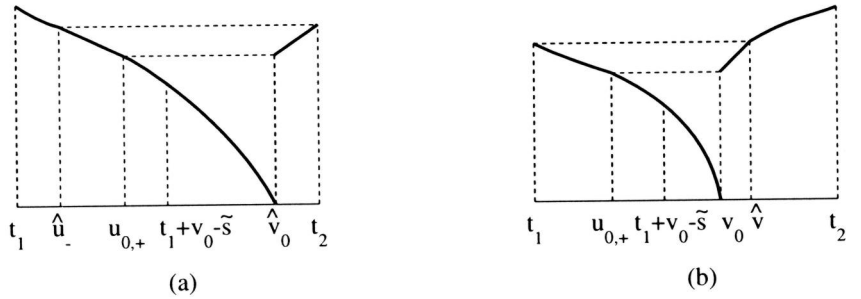

Figure 4.10: *Two possibilities for the optimal θ for the case that $\bar{\theta}'(s) > 1/2$ for $s < \tilde{s}$, $\bar{\theta}'(s) < 1/2$ for $s > \tilde{s}$.*

Note that at most one of the conditions (4.137) and (4.138) can be fulfilled. If none of these conditions is fulfilled, we have the following. If $\bar{\theta}(t_2) = -\frac{1}{2}(t_1 + t_2)$, then we get the degenerate solution $\hat{u} = t_1$. If $\bar{\theta}(t_2) > -\frac{1}{2}(t_1 + t_2)$ and $\bar{\theta}(t_1) \geq -t_1$, then we get the degenerate solution $\hat{v} = t_1$. Finally, if $\bar{\theta}(t_2) < -\frac{1}{2}(t_1 + t_2)$ and $\bar{\theta}(t_1) \leq -t_2$, then we get the degenerate solution $\hat{u} = t_1$.

4.4.3 The Case of One Point $\tilde{s}$ with $\bar{\theta}'(\tilde{s}) = 1/2$

We distinguish two subcases.

Case 1. Suppose $\bar{\theta}'(s) < 1/2$ for $s < \tilde{s}$ and $\bar{\theta}'(s) > 1/2$ for $s > \tilde{s}$.
In this case the optimal θ has the form as depicted in Figure 4.9(a) and (b) or several degeneracies thereof. For instance in Figure 4.9(a), for given $\hat{v}$ the point $\hat{u}_-$ is determined as the solution u of

$$-\bar{\theta}(t_1 + t_2 - \hat{v} + u) = \frac{1}{2}(u + \hat{v}), \tag{4.139}$$

or $\hat{u}_- = \hat{v}$ when no solution exists. Then the corresponding value of the functional J should be maximized as a function of $\hat{v}$, using pretty much the same methods as in the previous sections.

Case 2. Suppose $\bar{\theta}'(s) > 1/2$ for $s < \tilde{s}$ and $\bar{\theta}'(s) < 1/2$ for $s > \tilde{s}$.
In this case the optimal θ has the form as depicted in Figure 4.10(a) and (b) or several degeneracies thereof. For instance in Figure 4.10(a), the point $\hat{u}_-$ is determined as the solution u of

$$-\bar{\theta}(t_1 + t_2 - u) = \frac{1}{2}(u + t_2). \tag{4.140}$$

To determine the points $u_{0,+}$ and v_0, we should use the approach of Section 4.4.2. To that end we consider for $s_\lambda \geq \tilde{s}$, see (4.130),

$$\phi(s_\lambda) := 2f(\frac{1}{2}(s_\lambda - t_1)) - \int_{t_1}^{s_\lambda} f'(t_1 + v(s_\lambda) - u + \bar{\theta}(u))\, du. \tag{4.141}$$

As in (4.127-4.135) it can be shown that $\phi(\tilde{s}) < 0$, and that for $s > s_\lambda$ we have

$$\phi'(s_\lambda) = (\frac{1}{2} - \theta'(s_\lambda)) \int_{t_1}^{s_\lambda} f''(t_1 + v(s_\lambda) - u + \bar{\theta}(u))\, du > 0. \tag{4.142}$$

It is then easy to see that $-(\frac{1}{2} - \bar{\theta}'(s_\lambda))\phi(s_\lambda)$ has at most one zero $s_\lambda > \tilde{s}$, and that we should set $u_{0,+} = t_1 + v_0 - s_\lambda$ if such an s_λ exists and $u_{0,+} = t_1 + v_0 - \tilde{s}$ otherwise.

4.5 Examples

In this section we present some examples that exhibit a number of features we have shown the optimal θ to possess, both for the discrete and the continuous maximization problem. It turns out that the cases of uniform reflected angle distribution (i.e. such that $\bar{\theta}'(t)$ or $\bar{\theta}_n - \bar{\theta}_{n-1}$ is constant) already provide a good picture of the various phenomena. These cases can be treated analytically, and are of practical relevance to the reflector design problem.

Example 4.5.1. Let $0 < \alpha < 1/2$, let $b > 0$, and consider the function $\bar{\theta}_\alpha : [-b, b] \to \mathbb{R}$, defined by

$$\bar{\theta}_\alpha(s) = \alpha(s - b). \tag{4.143}$$

Considering (4.136), note that we have $-\bar{\theta}(b) = \frac{1}{2}(-b + b)$, so $\hat{v} = b = t_2$. Furthermore, we have $v_0 = -\bar{\theta}(t_1) = 2\alpha b$. Now (see Proposition 4.3.14), we

have

$$u(s) = -\tfrac{1}{2}(s - t_1) - \bar{\theta}(s) = -(\tfrac{1}{2} + \alpha)s + (-\tfrac{1}{2} + \alpha)b, \quad (4.144)$$

$$v(s) = \tfrac{1}{2}(s - t_1) - \bar{\theta}(s) = (\tfrac{1}{2} - \alpha)s + (\tfrac{1}{2} + \alpha)b. \quad (4.145)$$

It easily follows from (4.107) that

$$\theta_\alpha(u) = \begin{cases} \frac{-\alpha}{\frac{1}{2}+\alpha}(u + b) & \text{for all } u \in [-b, 2\alpha b], \\ \frac{\alpha}{\frac{1}{2}-\alpha}(u - b) & \text{for all } u \in [2\alpha b, b]. \end{cases} \quad (4.146)$$

For the functional we get

$$J(\theta_\alpha) = -2\int_{-b}^{b} f(\frac{1}{2}(s + b))\alpha \, ds = -4\alpha \int_0^b f(u) \, du. \quad (4.147)$$

Note that

$$\lim_{\alpha \uparrow \frac{1}{2}} \theta_\alpha(u) = -\frac{1}{2}(u + b) = \bar{\theta}_{\frac{1}{2}}(-u), \quad (4.148)$$

for all $u \in [-b, b]$. □

The more general case, where, instead of θ_α, we consider

$$\bar{\theta}_{\alpha,\beta}(s) = \alpha s + \beta \quad (4.149)$$

with $\beta \in \mathbb{R}$ and $0 < \alpha < 1/2$, can be reduced to the one above, but we shall not work this out in detail here.

Example 4.5.2. Let $1 \neq \alpha > 1/2$, $\beta \in \mathbb{R}$ and $b > 0$, and consider $\bar{\theta}_{\alpha,\beta} : [-b, b] \to \mathbb{R}$, defined by (4.149). In case $\alpha \geq 2$, it may happen that there does not exist a maximizer of finite variation; we come back to this point in Example 4.5.5. When we assume, however, the existence of such a maximizer, we can apply the analysis of Sections 4.3.2 and 4.4.1, and this we do below. Stated differently, we determine the maximum of $J(\theta)$ over all V-shaped θ equimeasurable with $\bar{\theta}_{\alpha,\beta}$. When

$$-\alpha b + \beta - b \geq 0 \text{ or } \alpha b + \beta + b \leq 0, \quad (4.150)$$

the maximizer is given as $\theta(u) = \bar{\theta}_{\alpha,\beta}(u)$ or $\theta(u) = \bar{\theta}_{\alpha,\beta}(-u)$. Otherwise, that is, when

$$|\beta| < (1 + \alpha)b, \quad (4.151)$$

we should look for a solution v of the equation

$$-f(v + \bar{\theta}(v)) + f(-b + \bar{\theta}(v)) + \int_{-b}^{v} f'(v - b - s + \bar{\theta}(s)) \, ds = 0, \quad (4.152)$$

or, in the present case, of

$$f(v - \alpha b + \beta) = \alpha f(\alpha v - b + \beta) + (1 - \alpha) f((1 + \alpha)v + \beta). \tag{4.153}$$

Here v is constrained by

$$-\bar{\theta}(v) \leq \frac{1}{2}(v - b), \tag{4.154}$$

so, in the present case, by

$$v \geq \frac{\frac{1}{2}b - \beta}{\frac{1}{2} + \alpha}. \tag{4.155}$$

There is at most one such v; if such a v exists we have $v_0 = \min(v, b)$, and otherwise $v_0 = b$, see Figure 4.6. Note that the "obvious" solution $v = -b$ of (4.153) does not meet the constraint (4.155) when (4.151) is valid. Having found v_0, we get for the functional

$$J = \int_{-b}^{v_0} f((1 - \alpha)s + \beta + \alpha v_0 - \alpha b)\, ds + \int_{v_0}^{b} f((1 + \alpha)s + \beta)\, ds. \tag{4.156}$$

We note that the limiting case $\alpha = 1/2$, $\beta = -b/2$ (see Example 4.5.1) has $v = b$ as a solution of (4.153) satisfying the constraint (4.155) with equality. This agrees with (4.148). □

Example 4.5.3. Let $\alpha = 1$, $\beta \in \mathbb{R}$ and consider $\bar{\theta}_{1,\beta} : [-b, b] \to \mathbb{R}$, defined by

$$\bar{\theta}_{1,\beta}(s) = s + \beta. \tag{4.157}$$

The analysis of this case is the same as in the previous example, except that (4.153) has to be replaced by

$$f(2v + \beta) = f(v - b + \beta) + (v + b) f'(v - b + \beta). \tag{4.158}$$

For instance, in the case $\beta = 0$, $f(s) = s^3$, Equation (4.153) reads

$$(b - 2v)(b + v)^2 = 0,$$

so we have $v_0 = b/2$, and we find

$$J(\theta_{1,0}) = \frac{7}{4}b^4. \tag{4.159}$$

□

Now before we consider a case with $\bar{\theta}'(s) > 2$ for some s, we consider a discrete problem.

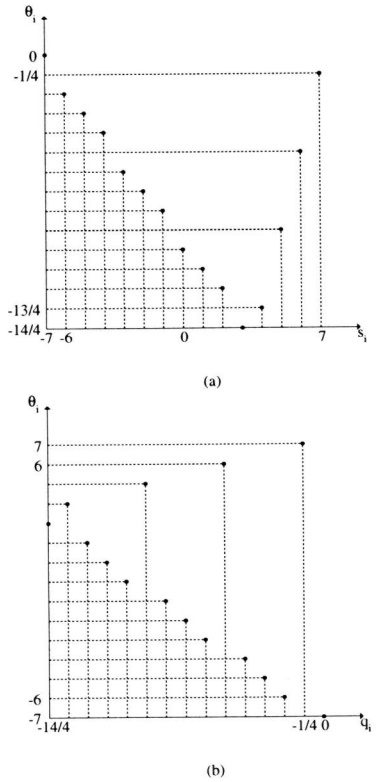

Figure 4.11: *Graphs of the optimizers of Example 4.5.4 for* $k = 7$.

Example 4.5.4. Let $n = 2k + 1$, and let

$$s_i := i - 1 - k, \qquad \bar{\theta}_i = \frac{1}{4}(i - n). \tag{4.160}$$

Then it can be shown by Proposition 4.2.10 that the optimal θ is as plotted in Figure 4.11(a). When we exchange the roles of the s_i's and the $\bar{\theta}_i$'s, i.e. if $\bar{\theta}_i := i - 1 - k$ and $s_i = \frac{1}{4}(i - n)$, then the optimal θ, depicted in Figure 4.11(b), is of course the inverse of the one above. □

Example 4.5.5. Let $b > 0$ and consider $\bar{\theta}_{4,-\frac{1}{4}} : [-b/4, b/4] \to \mathbb{R}$, defined by

$$\bar{\theta}(s) = \bar{\theta}_{4,-\frac{1}{4}}(s) = 4s - \frac{1}{4}. \tag{4.161}$$

We wish to calculate

$$\sup_{\theta \in \bar{\Theta}} \int_{-b/4}^{b/4} f(s + \theta(s))\, ds. \tag{4.162}$$

To that end, let $\bar{\phi} : [-b/4, b/4] \to \mathbb{R}$ be defined by

$$\bar{\phi}(s) = s, \tag{4.163}$$

and we get by Proposition 4.3.4 and Example 4.5.1 that

$$\sup_{\theta\in\bar{\Theta}} \int_{-b/4}^{b/4} f(s+\theta(s))\,ds = \sup_{\phi\in\bar{\Phi}} \int_{-b/4}^{b/4} f(4s+\phi(s)-b/4)\,ds = \frac{1}{4}\sup_{\phi\in\bar{\Phi}} \int_{-b}^{b} f(s+\phi(s/4)-b/4)\,ds = -\frac{1}{4}\int_0^b f(u)\,du. \tag{4.164}$$

Here, $\sup_\phi$ is assumed by ϕ given by

$$\phi(s/4) - b/4 = \theta_{\frac{1}{4}}(s); \tag{4.165}$$

see Example 4.5.1. For instance, in the special case that $b = 1$, $f(s) = s^3$, we find that the supremum in (4.164) equals -0.0625 while the value of (4.156), the supremum of $J(\theta)$ over all V-shaped θ's, equals -0.0664. It should be noted that this optimal ϕ is not injective. Hence the measure preserving mapping $\pi = \bar{\phi}^{-1} \circ \phi$ of $[-b, b]$ onto itself is not injective. This explains why the supremum in (4.162) is not assumed: the only possible candidate would be $\bar{\theta}(\pi^{-1}(s))$, but this is not properly defined as a one-valued function. In Fig. 4.12 we have plotted $\theta_{\frac{1}{4}}$ on $[-b, b]$, ϕ on $[-b/4, b/4]$, the two-valued inverse $\phi^{-1}$of ϕ on $[-b/4, b/4]$, and the two-valued "optimal"

$$\theta(s) = 4\pi^{-1}(s) - b/4 = 4\phi^{-1}(s) - b/4 \tag{4.166}$$

on $[-b/4, b/4]$. If one denotes by θ_V an optimal element of $\bar{\Theta}_V$, see Proposition 4.3.3, one would observe that θ_V goes back and forth between the two straight lines in Figure 4.12(d) at a rate that tends to infinity as $V \to \infty$. □

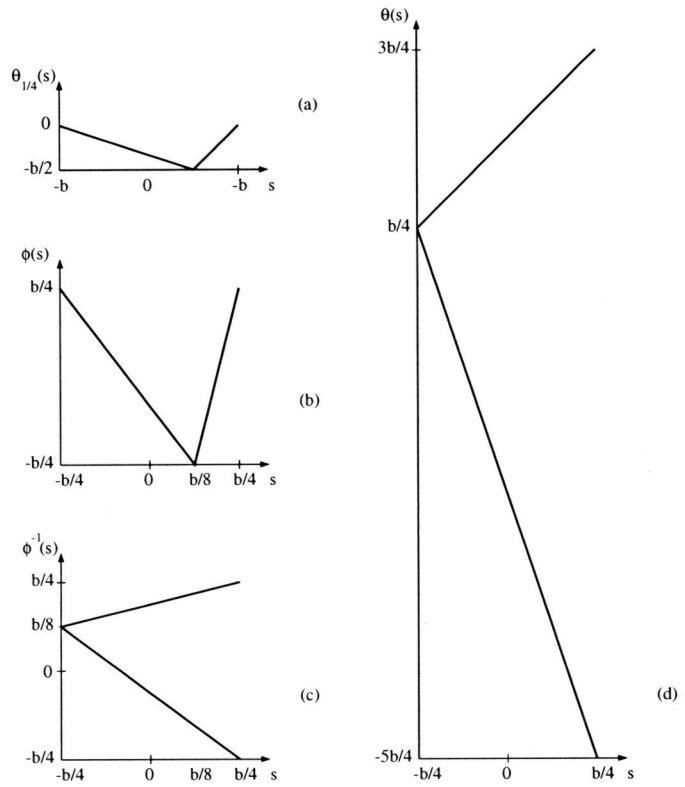

Figure 4.12: *Illustration (d) of the 'two-valued' optimizer of Example 4.5.5, and three auxiliary 'functions'.*

Chapter 5

2D Light Distributions of Area Sources

5.1 Introduction

In this chapter we consider special cases of the *direct* problem in reflector design: i.e. the problem of computing the light distribution for a given source and reflector. Consequently, this chapter is more or less independent of the other chapters.

In Chapter 3 we have seen that in the 2D case, the design problem can be solved by solving an ordinary differential equation, and therefore this allows a very fast implementation. When designers work with a computer tool for reflector design, an implementation of the forward computation is very important as well. Fast verification of the validity of computed reflectors, possibly with more realistic features taken into account, adds to the credibility of a tool which would otherwise seem like a black box. Therefore, the direct problem was considered for rotationally and cylindrically symmetric problems with area sources: Lambertian spheres and cylinders respectively (cf. Section 2.2).

We restrict ourselves in this chapter to rotationally or cylindrically symmetric reflectors that are represented by 2D curves consisting of straight line segments. The contents of this chapter is as follows. In Section 5.2, the general expressions in terms of integrals are given for the illuminance on a screen or the intensity distribution for arbitrary perfectly diffuse light sources, and arbitrary specular reflectors. In Section 5.3, we consider cylindrically symmetric problems with a circular cylindrical light source and facetted reflectors. It turns out that very simple, closed formulae for the required light distributions can be given. In Section 5.4, we consider rotationally symmetric problems with a spherical light source. It is shown how a double integral can be reduced to a single one, and some typical geometric

features of the ray bundles of these reflectors are illustrated.

5.2 Light Distributions for Non-Point Sources

5.2.1 Illuminance and Form Factor Calculation

We will consider perfectly diffuse light sources only. For a perfect diffuser, the fraction of the flux that leaves the source that is incident on another surface—usually called the *form*, *configuration* or *view factor*—depends only on the shape, size, position and orientation of the two surfaces involved. In other words, it only depends on their geometrical features. There is a close relation between form factors (as we will call them) and illuminances, to be explained below.

Let us consider the situation with two surface elements ΔS_1 and ΔS_2, where ΔS_1 is a perfectly diffuse light source with luminance L_0. We will compute the illumination of ΔS_2. Let us denote the distance between the elements by d, and the angles between the normals to the elements and the line joining them by α_1 and α_2, respectively. Then the luminous intensity of ΔS_1 in the direction of ΔS_2 is given by

$$L_0 \Delta S_1 \cos\alpha_1,$$

and it follows from the inverse square law that the illuminance $E(\Delta S_2)$ of ΔS_2 equals

$$E(\Delta S_2) = \frac{L_0 \Delta S_1 \cos\alpha_1 \cos\alpha_2}{d^2}. \tag{5.1}$$

The total flux incident on ΔS_2 is therefore equal to

$$\frac{L_0 \Delta S_1 \Delta S_2 \cos\alpha_1 \cos\alpha_2}{d^2}.$$

Since the total flux emitted by ΔS_1 is equal to $\pi L_0 \Delta S_1$, we find that the fraction of the emitted flux that is incident on ΔS_2, in other words the form factor denoted $F_{\Delta S_1 - \Delta S_2}$, is equal to

$$F_{\Delta S_1 - \Delta S_2} = \frac{\Delta S_2 \cos\alpha_1 \cos\alpha_2}{\pi d^2}. \tag{5.2}$$

For a curved, uniformly diffuse surface S_1, we then find for the illuminance E of ΔS_2, and for the form factor $F_{S_1 - \Delta S_2}$ the expressions

$$E = L_0 \int_{S_1} \frac{\cos\alpha_1 \cos\alpha_2}{d^2} \, dS_1, \tag{5.3}$$

$$F_{S_1 - \Delta S_2} = \frac{\Delta S_2}{S_1} \int_{S_1} \frac{\cos\alpha_1 \cos\alpha_2}{\pi d^2} \, dS_1. \tag{5.4}$$

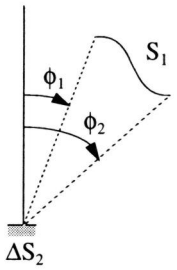

Figure 5.1: *Form factor computation in 2D scenes.*

The relation between form factors and illuminances that we will use is

$$E(\Delta S_2) = \frac{\pi L_0 S_1}{\Delta S_2} F_{S_1 - \Delta S_2}, \tag{5.5}$$

or equivalently,

$$E(\Delta S_2) = \frac{\Phi}{\Delta S_2} F_{S_1 - \Delta S_2}, \tag{5.6}$$

where Φ is the total luminous flux of S_1. Form factors are often used in Heat Transfer and also in 3D Graphics. There are many papers and books devoted to the calculation of form factors for the cases where geometrically special surfaces (like planes, spheres or cylinders) are involved. The calculation of form factors is very easy in cylindrically symmetric (and thus 2D) scenes. In Section 5.3 we will use the following result which can be found in [36][Appendix C]. (We changed the notation.)

Lemma 5.2.1. *Given an area ΔS_2 of infinitesimal width and any length, and a cylindrical surface S_1 generated by a line of infinite length moving parallel to itself and parallel to the plane of ΔS_2; see Figure 5.1. Then we have*

$$F_{S_1 - \Delta S_2} = \frac{\sin \phi_2 - \sin \phi_1}{2 S_1} \Delta S_2. \tag{5.7}$$

We will use this formula for the calculation of illuminances in the cylindrically symmetric case.

5.2.2 General Formulas

In this section we present the general formulas for illuminance and intensity distributions for both the direct and the reflected light of a uniformly diffuse light source. We do not yet restrict ourselves to facetted reflectors here. Let us first introduce some notation that we use throughout the chapter.

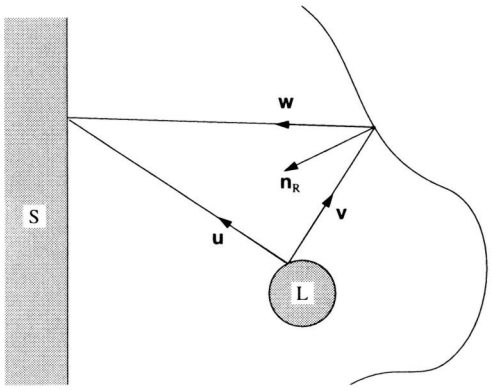

Figure 5.2: *The vectors* **u**, **v** *and* **w**.

We assume that the light source is a convex, smooth surface L. A point on L is denoted $\mathbf{x}_L$, and the (outward) normal to L in $\mathbf{x}_L$ is denoted $\mathbf{n}_L$. The luminance of the source is denoted L_0. The reflector R is also a smooth surface, and a point on R is called $\mathbf{x}_R$, with normal $\mathbf{n}_R$ (where the proper normal should be taken). The reflection coefficient of the reflector is denoted ρ. Also, when we want to calculate the illuminance on a screen S, a point on S is called $\mathbf{x}_S$, and has normal $\mathbf{n}_S$.

It turns out to be convenient to introduce the following vectors of unit length, that represent the directions of light rays. Let

$$\mathbf{u}(\mathbf{x}_L, \mathbf{x}_S) := \frac{\mathbf{x}_S - \mathbf{x}_L}{|\mathbf{x}_S - \mathbf{x}_L|}, \tag{5.8}$$

$$\mathbf{v}(\mathbf{x}_L, \mathbf{x}_R) := \frac{\mathbf{x}_R - \mathbf{x}_L}{|\mathbf{x}_R - \mathbf{x}_L|}, \tag{5.9}$$

$$\mathbf{w}(\mathbf{x}_R, \mathbf{x}_S) := \frac{\mathbf{x}_S - \mathbf{x}_R}{|\mathbf{x}_S - \mathbf{x}_R|}. \tag{5.10}$$

We usually simply write $\mathbf{u}$ for $\mathbf{u}(\mathbf{x}_L, \mathbf{x}_S)$, and likewise for $\mathbf{v}$ and $\mathbf{w}$. Figure 5.2 illustrates these vectors.

We are now ready to present the formulas for four relevant light distributions. The formula for the direct light has been derived in the previous section. The expressions for the intensity distributions follow easily from those for the illuminance by taking limits when the screen is moved to infinity.

In the remainder of this chapter, we will write $\cos(\mathbf{a}, \mathbf{b})$ for the cosine of the angle between vectors $\mathbf{a}$ and $\mathbf{b}$.

The direct light contribution to the illuminance on a screen.
Let $\mathbf{x}_S$ be a point on S. Then the illuminance E_1 caused by the direct light in $\mathbf{x}_S$ equals

$$E_1(\mathbf{x}_S) = L_0 \int_L \frac{\cos(\mathbf{u}, \mathbf{n}_L)\cos(-\mathbf{u}, \mathbf{n}_S)}{|\mathbf{x}_L - \mathbf{x}_S|^2} K_{E_1}(\mathbf{x}_L, \mathbf{x}_S)\, dL. \tag{5.11}$$

Here $K_{E_1}(\mathbf{x}_L, \mathbf{x}_S)$ is 1 or 0 according to whether $\mathbf{x}_L$ and $\mathbf{x}_S$ 'see each other'. More formally:

$$K_{E_1}(\mathbf{x}_L, \mathbf{x}_S) = \begin{cases} 1 \text{ if } \mathbf{u}.\mathbf{n}_L > 0 \text{ and } \mathbf{u}.\mathbf{n}_S < 0, \\ 0 \text{ otherwise.} \end{cases} \tag{5.12}$$

So the factor K_{E_1} actually describes the integration bounds, which usually depend on the point $\mathbf{x}_S$.

The reflected light contribution to the illuminance on a screen.
Let $\mathbf{x}_S$ be a point on S. Then the illuminance E_2 caused by the reflected light in $\mathbf{x}_S$ equals

$$E_2(\mathbf{x}_S) = \rho L_0 \int_R \frac{\cos(\mathbf{w}, \mathbf{n}_R)\cos(-\mathbf{w}, \mathbf{n}_S)}{|\mathbf{x}_R - \mathbf{x}_S|^2} K_{E_2}(\mathbf{x}_R, \mathbf{x}_S)\, dR. \tag{5.13}$$

Here $K_{E_2}(\mathbf{x}_R, \mathbf{x}_S)$ is 1 or 0 according to whether a 'back-traced' ray from $\mathbf{x}_S$ to $\mathbf{x}_R$ would meet the light source L after reflection. Note that the integration is to be done over the reflector surface, and that all geometrical information of the light source is incorporated in the factor K_{E_2}. Formally, this factor can be defined as follows. We have $K_{E_2}(\mathbf{x}_R, \mathbf{x}_S) = 1$ if there exists a point $\mathbf{x}_L$ on L such that $\mathbf{v}.\mathbf{n}_L < 0$ and such that the law of reflection holds, i.e.

$$\mathbf{v} = \mathbf{w} - 2(\mathbf{w}.\mathbf{n}_R)\mathbf{n}_R. \tag{5.14}$$

If no such point exists then $K_{E_2}(\mathbf{x}_R, \mathbf{x}_S) = 0$.

Contribution of the direct light to the intensity distribution.
Let $\boldsymbol{\omega}$ be a unit vector (a direction). Then the intensity I_1 caused by the direct light in this direction equals

$$I_1(\boldsymbol{\omega}) = L_0 \int_L \cos(\boldsymbol{\omega}, \mathbf{n}_L) K_{I_1}(\mathbf{x}_L, \boldsymbol{\omega})\, dL, \tag{5.15}$$

where $K_{I_1}(\mathbf{x}_L, \boldsymbol{\omega})$ is given by

$$K_{I_1}(\mathbf{x}_L, \boldsymbol{\omega}) = \begin{cases} 1 \text{ if } \boldsymbol{\omega}.\mathbf{n}_L > 0, \\ 0 \text{ otherwise.} \end{cases} \tag{5.16}$$

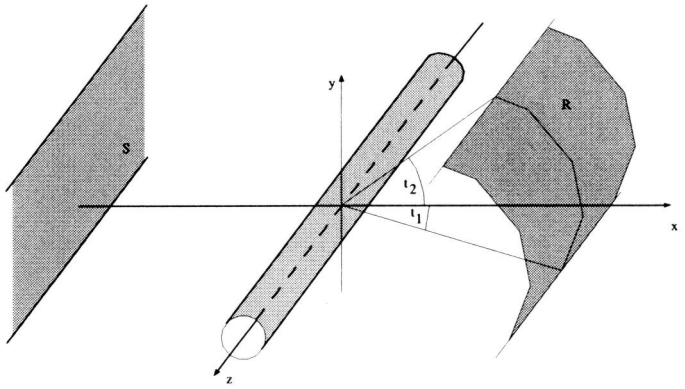

Figure 5.3: *The cylindrically symmetric case.*

Contribution of the reflected light to the intensity distribution.
Let $\boldsymbol{\omega}$ be a unit vector (a direction). Then the intensity I_2 caused by the reflected light in this direction equals

$$I_2(\boldsymbol{\omega}) = \rho L_0 \int_R \cos(\boldsymbol{\omega}, \mathbf{n}_R) K_{I_2}(\mathbf{x}_R, \boldsymbol{\omega})\, dR. \tag{5.17}$$

Here $K_{I_2}(\mathbf{x}_R, \boldsymbol{\omega})$ is 1 or 0 according to whether a 'back-traced' ray coming from direction $-\boldsymbol{\omega}$ and meeting the reflector in $\mathbf{x}_R$ would meet the light source L after reflection. Formally, this can be defined as follows. We have $K_{I_2}(\mathbf{x}_R, \boldsymbol{\omega}) = 1$ if there exists a point $\mathbf{x}_L$ on L such that $\mathbf{v}, \mathbf{n}_L < 0$ and such that

$$\mathbf{v} = \boldsymbol{\omega} - 2(\boldsymbol{\omega}.\mathbf{n}_R)\mathbf{n}_R, \tag{5.18}$$

and $K_{I_2}(\mathbf{x}_R, \boldsymbol{\omega}) = 0$ if no such point exists.

5.3 The Cylindrically Symmetric Case

In this chapter we consider the special case of a cylindrical light source and reflector, both of infinite length and parallel to each other. In this case the problem is equivalent to a 2D problem, and we can use the result of Lemma 5.2.1. Let us first present the geometrical situation and introduce some notation. Suppose that we have a rectangular xyz-coordinate system in $\mathbb{R}^3$, and that we have an infinitely long circular cylindrical light source L with axis coinciding with the z-axis, and with radius r.

Furthermore, suppose we have fixed angles $t_1, t_2 \in (-\pi, \pi)$ with $t_1 < t_2$. Then a cylindrical reflector parallel to L between angles t_1 and t_2 can be described

by a surface of the form

$$\mathbf{r}(t, z) = (f(t)\cos t, f(t)\sin t, z) \tag{5.19}$$

for $t \in [t_1, t_2]$, where f is a smooth positive function. In the case that we consider here, the reflector consists of straight facets. It then suffices to concentrate on one facet only, and we may assume that the function f describes a straight line, i.e. it is of the form

$$f(t) = f_0/\cos(t - t_0), \tag{5.20}$$

for some positive constant f_0 (which is the distance of the origin to the line through the facet) and angle t_0 (which is the direction of the normal to this line). With this choice for $f(t)$, the description (5.19) only makes sense if $t_0 - \pi/2 < t_1 < t_2 < t_0 + \pi/2$.

Finally, if there is a screen, then it is represented by the plane

$$S := \{(x, y, z) \mid x = -d\}, \tag{5.21}$$

for a fixed distance d.

Now, in order to present the light distributions corresponding to this situation, we do not use the formulas of the previous chapter, but instead we will profit from existing knowledge from radiation heat transfer. Indeed, the result for the direct light is well-known, and that for the reflected light is easily calculated once it is realized that any cylindrically symmetric scene is equivalent to a 2D scene, and we can use standard methods for the calculation of the form factors that determine the light distributions.

In a similar fashion as in Chapter 3, the following 2D situation can be considered. The source is the circle

$$L := \{(r\cos u, r\sin u) \mid u \in [0, 2\pi]\}, \tag{5.22}$$

the reflector is given by

$$\mathbf{r}(t) = f(t)(\cos t, \sin t) \tag{5.23}$$

with f as in (5.20) and the screen S is represented by the line $x = -d$. From now on, we write $f_1 := f(t_1)$ and $f_2 := f(t_2)$. We will also use the Cartesian coordinates of the endpoints of the segment:

$$x_1 := f_1\cos t_1, \tag{5.24}$$

$$y_1 := f_1\sin t_1, \tag{5.25}$$

$$x_2 := f_2\cos t_2, \tag{5.26}$$

$$y_2 := f_2\sin t_2. \tag{5.27}$$

We assume that the total flux of the source equals 1. So $\Phi = \pi L_0 S_1 = 1$, where we have to be a little careful about the exact meaning of this: we use the 2D equivalents of the notions that were defined in a 3D context, so S_1 is the perimeter of the 2D source. (The equivalent assumption on the 3D source would be that $\Phi = \pi L_0 S_1 = 1$ for any part of the source of unit length in the z-direction.) Also, the reflection coefficient is chosen without loss of generality equal to 1.

The formula for the direct light is well-known. After some erroneous results had been published, Feingold and Gupta [9] gave the correct formula as follows. In a point $(-d, y) \in S$ (or a point $(-d, y, z) \in S$ in the 3D scene), we have

$$\mathcal{E}_1(y) = \frac{d}{2\pi(y^2 + d^2)}. \tag{5.28}$$

Note that this formula is independent of r, and it is similar for a line source (with $r = 0$).

For the intensity distribution, we again measure the directions θ of outgoing rays clockwise relative to the left (negative) side of the x-axis. It is obvious that in the 2D-situation, we have for all θ

$$\mathcal{I}_1(\theta) = \frac{1}{2\pi}. \tag{5.29}$$

For the reflected light, things are a little bit more involved. When the light source is reflected in the segment, the image of the reflected source has centre

$$C = (c_1, c_2) = 2\frac{x_2 y_1 - x_1 y_2}{(x_1 - x_2)^2 + (y_1 - y_2)^2}(y_1 - y_2, x_2 - x_1). \tag{5.30}$$

Now consider the image of the source when reflected in the segment, and imagine the line through the segment to be a wall with a gap at the position of the segment. Then the light distribution caused by this scene is equal to that of the reflected light we are looking for. (When we ignore interaction of reflected light with the lamp.)

It is more convenient to consider this new scene, and we shift the coordinate system to the centre C of the reflected source. Relative to the reflected source, the screen is at a distance $\tilde{d} = d + c_1$, and the endpoints of the gap are $(\tilde{x}_1, \tilde{y}_1)$ and $(\tilde{x}_2, \tilde{y}_2)$. It is from this scene that we will calculate the illuminance and intensity distributions in the next two sections.

5.3.1 The Illuminance by the Reflected Light

In order to calculate the illuminance on S, we can determine the form factor from the source to the screen, taking into account the obstacles around the gap. The illuminance is easily calculated when we use Lemma 5.2.1 in combination with (5.5).

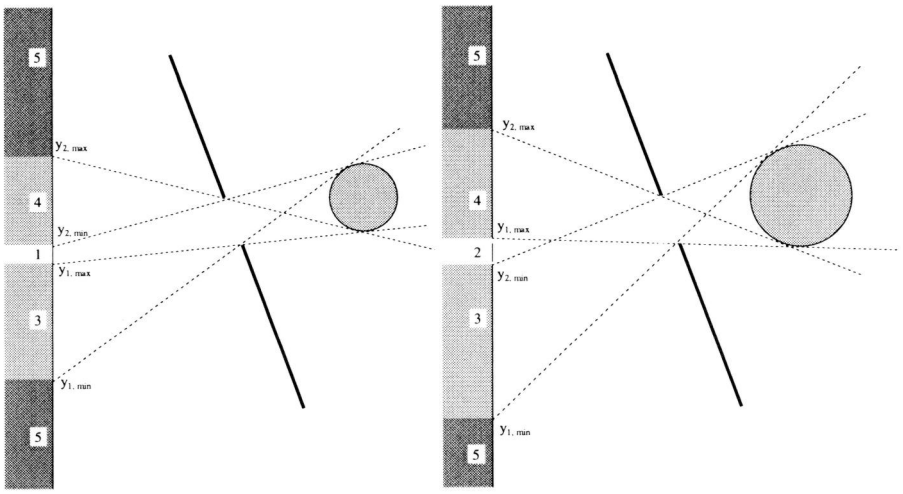

Figure 5.4: *Visibility types for illuminance calculation.*

It follows that all we have to do is to determine the directions of the lines that bound the visible part of the source. To do this, we must distinguish between different situations that can occur; see Figure 5.4. The areas on the screen drawn here illustrate various different *visibility types*. These are the following.

- Type 1: The source is completely visible and the bounding lines of interest are the tangent lines to the circle.
- Type 2: Both lines through the point on the screen and the endpoints of the gap intersect the source. The directions of these lines determine the illuminance. (Either type 1 or type 2 can occur, depending on the relative sizes of the source and the gap, as well as the position of the screen.)
- Type 3: Only the line through the point on the screen and the lower endpoint of the gap intersects the source. The other line relevant for the illuminance is the upper tangent line to the source.
- Type 4: Only the line through the point on the screen and the upper endpoint of the gap intersects the source. The other line relevant for the illuminance is the lower tangent line to the source.
- Type 5: The source is not visible and has contribution 0.

Now, the areas on the screen on which the visibility type does not change, are bounded by the values $y_{i,min}$ and $y_{i,max}$ for $i = 1, 2$. These values are obtained

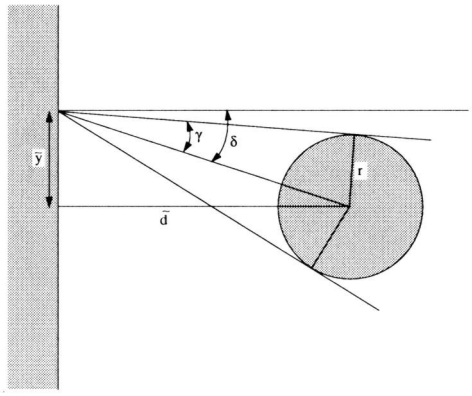

Figure 5.5: *Illustration of the angles relevant for the form factor calculation for visibility types 3 and 4.*

by taking the intersection with the screen of the tangent lines to the circle through the endpoints of the gap; see Figure 5.4. On each of these areas, we can give explicit analytical formulas for the illuminance. Before we give these, we need a few elementary results.

Lemma 5.3.1. *Let $(-\tilde{d}, \tilde{y})$ be a point on S. Let ψ_i be the angle with the x-axis of the line through $(-\tilde{d}, \tilde{y})$ and $(\tilde{x}_i, \tilde{y}_i)$ for $i = 1$ or $i = 2$. Then we have*

$$\sin \psi_i = \frac{\tilde{y}_i - \tilde{y}}{\sqrt{(\tilde{d} + \tilde{x}_i)^2 + (\tilde{y} - \tilde{y}_i)^2}} = \frac{y_i - y}{\sqrt{(d + x_i)^2 + (y - y_i)^2}}. \tag{5.31}$$

Lemma 5.3.2. *Let $\psi_\pm$ be the angles with the x-axis of the tangent lines to the circle through the point $(-\tilde{d}, \tilde{y})$. Then*

$$\sin \psi_\pm = \frac{-\tilde{y}\sqrt{\tilde{d}^2 + \tilde{y}^2 - r^2} \pm r\tilde{d}}{\tilde{d}^2 + \tilde{y}^2}. \tag{5.32}$$

Proof. Consider Figure 5.5, and note that $\sin \psi_\pm = \sin(\delta \pm \gamma)$. Then note that $\delta = -\arctan(\tilde{y}/\tilde{d})$ and that $\gamma = \arcsin(r/\sqrt{\tilde{d}^2 + \tilde{y}^2})$. The rest is elementary calculus. □

We are now ready to apply Lemma 5.2.1 and (5.5) to each visibility type. For a point $(-\tilde{d}, \tilde{y})$ on S, we find that

$$\mathcal{E}_2(\tilde{y}) = \frac{\sin \phi_2 - \sin \phi_1}{4\pi r}, \tag{5.33}$$

where the angles ϕ_i should be chosen appropriately:

- Type 1: Note that this type only occurs if $y_{1,max} < y_{2,min}$. For a point $(-\tilde{d}, \tilde{y})$ with $y_{1,max} < \tilde{y} < y_{2,min}$ we have $\phi_2 = \psi_+$ and $\phi_1 = \psi_-$, so

$$\begin{aligned}\mathcal{E}_2(\tilde{y}) &= \frac{\sin\phi_2 - \sin\phi_1}{4\pi r} \\ &= \frac{1}{4\pi r}\left(\frac{-\tilde{y}\sqrt{\tilde{d}^2+\tilde{y}^2-r^2}+r\tilde{d}}{\tilde{d}^2+\tilde{y}^2} - \frac{-\tilde{y}\sqrt{\tilde{d}^2+\tilde{y}^2-r^2}-r\tilde{d}}{\tilde{d}^2+\tilde{y}^2}\right) \\ &= \frac{1}{2\pi}\frac{\tilde{d}}{\tilde{d}^2+\tilde{y}^2},\end{aligned}$$

  which is precisely the formula for the direct light contribution (5.28)!

- Type 2: Note that this type only occurs if $y_{1,max} > y_{2,min}$. For a point $(-\tilde{d}, \tilde{y})$ with $y_{2,min} < \tilde{y} < y_{1,max}$ we have $\phi_2 = \psi_2$ and $\phi_1 = \psi_1$, so

$$\mathcal{E}_2(\tilde{y}) = \frac{\sin\psi_2 - \sin\psi_1}{4\pi r}.$$

- Type 3: In this situation we have

$$\mathcal{E}_2(\tilde{y}) = \frac{\sin\psi_+ - \sin\psi_1}{4\pi r}.$$

- Type 4: In this situation we have

$$\mathcal{E}_2(\tilde{y}) = \frac{\sin\psi_2 - \sin\psi_-}{4\pi r}.$$

5.3.2 The Intensity of the Reflected Light

As in the previous section, there are several cases to be considered, when we wish to calculate the intensity in a certain direction; see Figure 5.6. The range of all directions can again be subdivided in ranges of different visibility types.

- Type 1: The source is completely visible from directions in this range.
- Type 2: Given a direction in this range, then the two lines through the endpoints of the gap in this direction both intersect the source. The source is not completely visible. (Either type 1 or type 2 can occur, depending on the relative sizes of the source and the gap.)
- Type 3: For a direction in this range, only the line through the the lower endpoint of the gap intersects the source. The upper part of the source is completely visible.

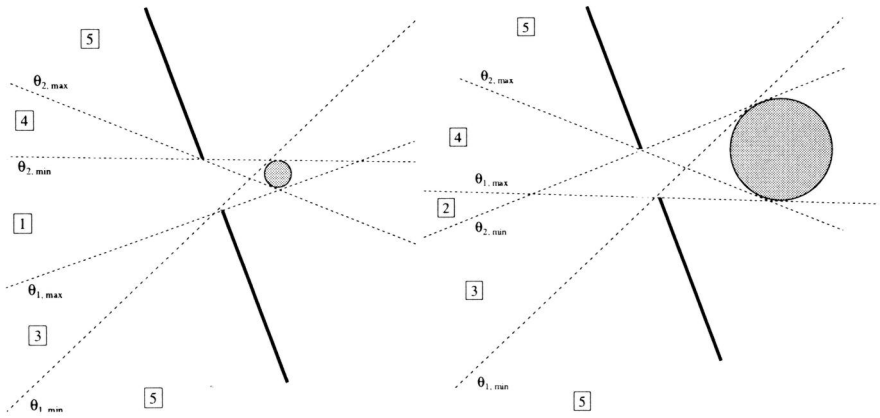

Figure 5.6: *Visibility types for the calculation of the intensity distribution.*

- Type 4: For a direction in this range, only the line through the the upper endpoint of the gap intersects the source. The lower part of the source is completely visible.

- Type 5: The source is not visible from directions in this range.

It is clear from the figure that the directions that bound the various ranges of a given visibility type are determined by the tangent lines to the source through the endpoints of the gap. Let us introduce, for $i = 1, 2$ the angles

$$\psi_i := \arcsin \frac{r}{f_i}, \tag{5.34}$$

$$\theta_{i,\min} := t_i - 2t_0 - \psi_i, \tag{5.35}$$

$$\theta_{i,\max} := t_i - 2t_0 + \psi_i. \tag{5.36}$$

Then $\theta_{i,\min}$ and $\theta_{i,\max}$ are the smallest and largest angle of the rays that pass (x_i, y_i), respectively. Visibility type 1 occurs if and only if

$$\theta_{1,\max} < \theta_{2,\min}. \tag{5.37}$$

This means that from all angles between $\theta_{1,\max}$ and $\theta_{2,\min}$, the whole source is visible. The total intensity distribution is then as sketched in Figure 5.7.

Similarly, type 2 can only occur if and only if

$$\theta_{1,\max} > \theta_{2,\min}. \tag{5.38}$$

The total intensity distribution is then as sketched in Figure 5.8.

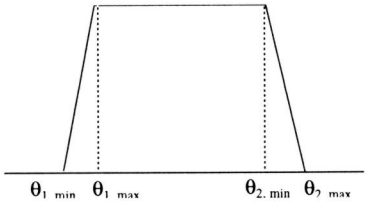

Figure 5.7: *Sketch of a typical intensity distribution when visibility type 1 occurs.*

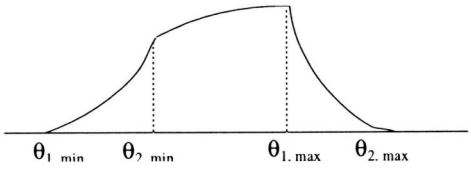

Figure 5.8: *Sketch of a typical intensity distribution when visibility type 2 occurs.*

It may happen that the radius r is such that the lower tangent line through (x_1, y_1) to the circle and the upper tangent line through (x_2, y_2) to the circle are parallel. Then we have

$$\theta_{1,\max} = \theta_{2,\min}, \tag{5.39}$$

or equivalently,

$$t_1 + \arcsin\frac{r}{f_1} = t_2 - \arcsin\frac{r}{f_2}. \tag{5.40}$$

This is approximately the case if

$$r \approx \frac{f_1 f_2 (t_2 - t_1)}{f_1 + f_2}. \tag{5.41}$$

Then type 2 and 3 do not occur and the distribution is 'triangularly' shaped; see Figure 5.9.

Finally, analytical expressions for the intensity on the ranges of constant visibility type are easily given. For visibility type 2, we have

$$I_2(\theta) = \frac{(\tilde{y}_2 - \tilde{y}_1)\cos\theta + (\tilde{x}_2 - \tilde{x}_1)\sin\theta}{4\pi r}. \tag{5.42}$$

Note that $(\tilde{y}_2 - \tilde{y}_1)\cos\theta + (\tilde{x}_2 - \tilde{x}_1)\sin\theta$ is precisely the width of the bundle through the gap in direction θ. For visibility type 3 and 4, we find

$$\mathcal{I}_2(\theta) = \frac{-\tilde{y}_1\cos\theta - \tilde{x}_1\sin\theta + r}{4\pi r}, \tag{5.43}$$

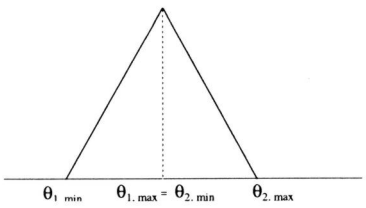

Figure 5.9: *Sketch of a typical intensity distribution when visibility types 2 and 3 both do not occur.*

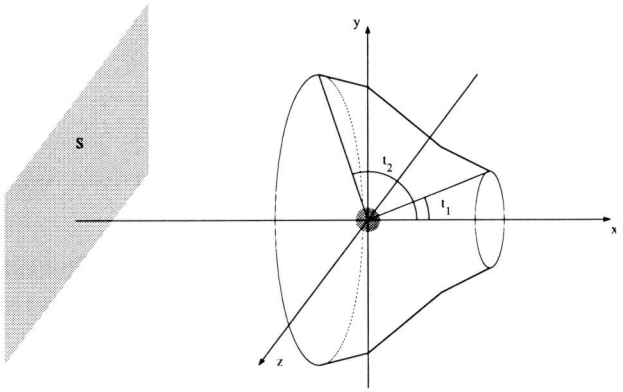

Figure 5.10: *The rotationally symmetric case.*

and

$$\mathcal{I}_2(\theta) = \frac{\tilde{y}_2 \cos\theta + \tilde{x}_2 \sin\theta + r}{4\pi r}, \tag{5.44}$$

respectively.

5.4 The Rotationally Symmetric Case

In this section we consider a problem that has rotational symmetry. We have a spherical light source, and a reflector that is rotationally symmetric around a line through the centre of the sphere. If there is a screen, then this is perpendicular to this line.

More precisely, we have a rectangular xyz-coordinate system in $\mathbb{R}^3$, and the light source is given by

$$L := \{(x, y, z) \mid x^2 + y^2 + z^2 = r^2\}, \tag{5.45}$$

for a fixed radius r. The reflector is a surface that is rotationally symmetric around

the x-axis, and can be described as

$$\mathbf{r}(t, u) = f(t)(\cos t, \sin t \cos u, \sin t \sin u) \tag{5.46}$$

for $t \in [t_1, t_2]$ and $u \in [0, 2\pi]$, for fixed angles $t_1, t_2 \in [0, \pi)$ with $t_1 < t_2$. If there is a screen, it is again of the form

$$S := \{(x, y, z) \mid x = -d\}, \tag{5.47}$$

for a fixed distance d. Because of the rotational symmetry, it is convenient to introduce polar coordinates on S, so a point $(-d, y, z)$ is written as

$$(-d, p\cos\phi, p\sin\phi),$$

where p is non-negative, and $\phi \in [0, 2\pi)$.

Since the geometry of the 3D scene is completely determined by the intersection with a plane through the x-axis, we may hope that the calculation of the light distributions can be done in an equivalent 2D scene as well. In the special case that we consider here we will indeed see that the computation can be reduced from a double integral to a single one. This special case is that the reflector is facetted, or more precise: that the intersection of the reflector surface with a plane through the x-axis is facetted, i.e. it consists of straight line segments. So f is of the same form as before in (5.20) and consequently we must have $t_2 < t_0 + \pi/2$.

The expressions for the direct light are well known. In [9] it is shown that the form factor from the sphere L to a differential area ΔS in S located at

$$(-d, p\cos\phi, p\sin\phi)$$

equals

$$F_{L-\Delta S} = \frac{d}{4\pi}(d^2 + p^2)^{-3/2}\Delta S. \tag{5.48}$$

So if the total flux Φ of the source equals 1, we find

$$E_1(-d, p\cos\phi, p\sin\phi) = \frac{d}{4\pi}(d^2 + p^2)^{-3/2}. \tag{5.49}$$

Note that this formula is independent of ϕ, and of the radius of the source. Furthermore, for the intensity in a direction

$$\boldsymbol{\omega} = (-\cos\theta, \sin\theta\cos\phi, \sin\theta\sin\phi) \tag{5.50}$$

we obviously have

$$I_1(\boldsymbol{\omega}) = \frac{1}{4\pi}. \tag{5.51}$$

5.4.1 The Intensity of the Reflected Light

In this section we will use the formulae of Section 5.2 to calculate the intensity distribution of the reflected light. We will write K for K_{I_2}. Let $\boldsymbol{\omega}$ be a direction as in (5.50). We restrict ourselves to directions in one hemisphere, so we let $\theta \in [0, \pi/2)$. We now recall formula (5.17):

$$I_2(\boldsymbol{\omega}) = \rho L_0 \int_R \cos(\boldsymbol{\omega}, \mathbf{n}_R) K(\mathbf{x}_R, \boldsymbol{\omega})\, dR.$$

For notational convenience, we take $\rho L_0 = 1$ in this section. In terms of the coordinates of the parametric description (5.46) for R, we have the following.

$$\mathbf{x}_R = \frac{f_0}{\cos(t - t_0)}(\cos t, \sin t \cos u, \sin t \sin u), \tag{5.52}$$

$$\mathbf{n}_R = -(\cos t_0, \sin t_0 \cos u, \sin t_0 \sin u), \tag{5.53}$$

$$dR = \frac{f_0^2 \sin t}{\cos^3(t - t_0)}\, du\, dt. \tag{5.54}$$

It is easily calculated that

$$\cos(\boldsymbol{\omega}, \mathbf{n}_R) = \cos\theta \cos t_0 - \sin\theta \sin t_0 \cos(u - \phi). \tag{5.55}$$

When we substitute all this in (5.17), we find

$$I_2(\boldsymbol{\omega}) = \int_t \int_u (\cos\theta \cos t_0 - \sin\theta \sin t_0 \cos(u - \phi))\; K(\mathbf{x}_R, \boldsymbol{\omega}) \frac{f_0^2 \sin t}{\cos^3(t - t_0)}\, du\, dt. \tag{5.56}$$

So this is the expression that it is all about in this section. It is a double integral, containing a discontinuous factor K. We will show that this double integral can be reduced to a single one. Since the factor K equals 0 or 1, we can remove it by choosing the proper integration bounds. Once these are determined, the integrand is integrated with respect to u. The rest of this section is completely dedicated to the further investigation of this. First the precise condition for K being equal to 1 in terms of the coordinates is derived. The result follows in Proposition 5.4.2. Then from this result, the integration bounds for u in terms of the other parameters are derived. This latter part is rather involved, since various cases have to be distinguished. Although this investigation is mathematically somewhat involved, it is interesting to see that it provides the basis for a complete understanding of which parts of the reflector will reflect light into which directions. For instance, it will be shown that, when looking from a certain direction to the reflector, the enlightened part (if there is one) may consist of one or two connected areas. We now turn to the investigation of the factor K.

Lemma 5.4.1. *Let L be the sphere given by (5.45), and let* $\mathbf{a}$ *be a point outside the sphere. Let* $\mathbf{b}$ *be a vector of unit length. Then the half-line l in $\mathbb{R}^3$, given by the parametric description $\lambda \to \mathbf{a} + \lambda\mathbf{b}$ for $\lambda \in \mathbb{R}^+$ intersects L if and only if*

$$\mathbf{a}.\mathbf{b} \leq -\sqrt{|\mathbf{a}|^2 - r^2}. \tag{5.57}$$

Proof. The angle between the line through the origin and the point $\mathbf{a}$ and any tangent line to the sphere through $\mathbf{a}$ equals

$$\arcsin \frac{r}{|\mathbf{a}|}.$$

So the half-line $\mathbf{a} + \lambda\mathbf{b}$ intersects the sphere if and only if

$$\cos(-\mathbf{a}, \mathbf{b}) \geq \cos \arcsin \frac{r}{|\mathbf{a}|}.$$

and the result follows. □

We can now apply this lemma to the current situation where $\mathbf{a} = \mathbf{x}_R$, and $\mathbf{b}$ is the direction of the back-traced ray after reflection; so we get from (5.18)

$$\mathbf{b} = -\mathbf{v} = 2(\boldsymbol{\omega}.\mathbf{n}_R)\mathbf{n}_R - \boldsymbol{\omega}. \tag{5.58}$$

Thus we find

$$K(\mathbf{x}_R, \boldsymbol{\omega}) = 1 \iff (2(\boldsymbol{\omega}.\mathbf{n}_R)\mathbf{n}_R - \boldsymbol{\omega}).\mathbf{x}_R \leq -\sqrt{|\mathbf{x}_R|^2 - r^2}. \tag{5.59}$$

In order to work this out further in coordinates, we note that

$$(2(\boldsymbol{\omega}.\mathbf{n}_R)\mathbf{n}_R - \boldsymbol{\omega}).\mathbf{x}_R = 2(\boldsymbol{\omega}.\mathbf{n}_R)(\mathbf{n}_R.\mathbf{x}_R) - \boldsymbol{\omega}.\mathbf{x}_R,$$

and we have

$$\begin{aligned}
\boldsymbol{\omega}.\mathbf{n}_R &= \cos\theta\cos t_0 - \sin\theta\sin t_0\cos(u-\phi),\\
\boldsymbol{\omega}.\mathbf{x}_R &= -f(t)(\cos\theta\cos t - \sin\theta\sin t\cos(u-\phi)),\\
\mathbf{n}_R.\mathbf{x}_R &= -f_0.
\end{aligned}$$

Using $f(0) = f(t)cos(t - t_0)$, we then find

$$\begin{aligned}
2(\boldsymbol{\omega}, \mathbf{n}_R)(\mathbf{n}_R, \mathbf{x}_R) - \boldsymbol{\omega}.\mathbf{x}_R &= -2f_0(\cos\theta\cos t_0 - \sin\theta\sin t_0\cos(u-\phi)) +\\
&\quad f(t)(\cos\theta\cos t - \sin\theta\sin t\cos(u-\phi))\\
&= f(t)\cos\theta\,(-2\cos(t-t_0)\cos t_0 + \cos t) +\\
&\quad f(t)\sin\theta\,(2\cos(t-t_0)\sin t_0 - \sin t)\\
&= -f(t)(\cos\theta\cos(t-2t_0) +\\
&\quad \sin\theta\sin(t-2t_0)\cos(u-\phi)).
\end{aligned}$$

It follows that condition (5.57) is equivalent to the inequality

$$\cos\theta\cos(t-2t_0)+\sin\theta\sin(t-2t_0)\cos(u-\phi)\geq\sqrt{1-\frac{r^2}{f(t)^2}}. \tag{5.60}$$

So we have proved the following.

Proposition 5.4.2. *For the 'visibility' factor K we have*

$$K(\mathbf{x}_R,\boldsymbol{\omega})=1 \iff$$
$$\cos\theta\cos(t-2t_0)+\sin\theta\sin(t-2t_0)\cos(u-\phi)\geq\sqrt{1-\frac{r^2}{f(t)^2}} \tag{5.61}$$

The rest of the section is devoted to the further analysis of this condition in order to deduce the integration bounds for u to further calculate the integral (5.56) analytically. But it will also give us a geometrical insight in the situation. To start with, note the geometric meaning of the occurrence of the angle $t-2t_0$ in (5.61): for a point source, we have that a ray in direction $f(t)(\cos t,\sin t\cos u,\sin t\sin u)$ is reflected in direction $(-\cos(t-2t_0),\sin(t-2t_0)\cos u,\sin(t-2t_0)\sin u)$.

Now, we want to deduce the bounds for u. Since θ is assumed to be non-negative, it is clear from (5.61) that the sign of $\sin(t-2t_0)$ and thus of $t-2t_0$ is important. We therefore distinguish various cases below.

But let us first consider a sketch of the situation in Figure 5.11. In this figure, the intersection of a reflector with $t_1=0$ and $t_0=\pi/4$ with a plane through the x-axis is sketched. Let us assume this is the plane given by the equation $z=0$. Then note that the upper part consists of the points with $t>0$ and $u=0$. The lower part corresponds to points with $t>0$, but now $u=\pi$. Similarly, all reflected rays have non-negative angles θ, but the rays 'going down' have $\phi=\pi$. This should be kept in mind in the discussion below. When we speak of 'the upper part' of the reflector, then this is the part where $u=\phi$, while 'the lower part' of the reflector is the part with $u=\phi+\pi$. It is clear from the figure that, given a direction $\boldsymbol{\omega}$, this direction may receive light from both the upper and lower part (relative to the direction). Let us return to a more formal description of these features.

Case 1. If $t=2t_0$.
If $t=2t_0$, then for a point source all reflected rays would have $\theta=0$; see Figure 5.11 which also illustrates the following. We find that (5.61) is equivalent to

$$K(\mathbf{x}_R,\boldsymbol{\omega})=1 \iff \cos\theta\geq\sqrt{1-\frac{r^2}{f(2t_0)^2}}=\cos\arcsin(\frac{r}{f(2t_0)}).$$

In other words, $K(\mathbf{x}_R, \boldsymbol{\omega}) = 1$ if and only if

$$\theta \leq \arcsin(\frac{r \cos t_0}{f_0}). \tag{5.62}$$

Note that this condition is independent of u. We see that for relatively small values of θ, the whole 'ring' $t = 2t_0$ reflects light in direction θ, while for larger values such that condition (5.62) does not hold, no part of that ring does. It will be clear that condition (5.62) now occurs naturally in the further investigation of the various cases.

Case 2. If $t < 2t_0$ and $\theta < \arcsin(\frac{r \cos t_0}{f_0})$.
If $t < 2t_0$, then $\sin(t - 2t_0) < 0$ (for relevant values of t), so we find the following condition

$$\cos(u - \phi) \leq \frac{\cos \arcsin(\frac{r}{f(t)}) - \cos\theta \cos(t - 2t_0)}{\sin\theta \sin(t - 2t_0)}. \tag{5.63}$$

So if t is such that the right hand side of (5.63) is less than -1, no u can be found such that the condition holds. Also, if the right hand side is larger than 1, all u satisfy. For values between -1 and 1, the condition is satisfied for u in a fixed interval around $\phi + \pi$. (Note that this is the lower side of the reflector relative to the view direction.)

To investigate this further, we consider the following lemma, which is also useful for the other cases.

Lemma 5.4.3. *a) For the right hand side of (5.63) we find the following condition for the occurrence of the critical values* ± 1,

$$\frac{\cos \arcsin(\frac{r}{f(t)}) - \cos\theta \cos(t - 2t_0)}{\sin\theta \sin(t - 2t_0)} = 1 \iff$$
$$\theta = t - 2t_0 \pm \arcsin(\frac{r}{f(t)}), \tag{5.64}$$
$$\frac{\cos \arcsin(\frac{r}{f(t)}) - \cos\theta \cos(t - 2t_0)}{\sin\theta \sin(t - 2t_0)} = -1 \iff$$
$$\theta = 2t_0 - t \pm \arcsin(\frac{r}{f(t)}). \tag{5.65}$$

b) The function $t \to t + \arcsin(\frac{r}{f(t)})$ *is increasing on* $[0, t_0 + \pi)$, *and the function* $t \to -t + \arcsin(\frac{r}{f(t)})$ *is decreasing on* $[0, t_0 + \pi)$.

The proof of this lemma is elementary calculus. Let us return to the above analysis. Combining (5.63) and (5.64), we find that the smallest $t_a < 2t_0$ for

which all u satisfy (5.63) is determined by

$$\theta = t_a - 2t_0 + \arcsin(\frac{r}{f(t_a)}). \tag{5.66}$$

Note that of the two possibilities ($\pm$) in (5.64), only this one (+) is relevant if $t < 2t_0$, since θ is positive by definition.

Combining (5.63) and (5.65), we find that the largest t_n such that no u satisfies (5.63) is determined by

$$\theta = 2t_0 - t_n - \arcsin(\frac{r}{f(t_n)}). \tag{5.67}$$

Summarizing Case 2, we find that the segment $[0, 2t_0]$ can be divided into $[0, t_n]$, $[t_n, t_a]$ and $[t_a, 2t_0]$, consisting of rings on which no, some or all u satisfy (5.63), respectively. (If the only t_n would be negative, the first interval does not occur.)

Case 3. If $t < 2t_0$ and $\theta > \arcsin(\frac{r\cos t_0}{f_0})$.
Having done most of the work in the previous case, we can now present the results to this case much faster. First of all, if $\theta > \arcsin(\frac{r\cos t_0}{f_0})$, then no value of $t < 2t_0$ can be found such that all u satisfy (5.63). This is easily seen in Figure 5.11, and it can be proved by combining a) and b) of Lemma 5.4.3. The boundaries of the t-range for which at least some u satisfy (5.63) are given by (5.65). One or both of these boundaries may be negative, and can be ignored (i.e. set to $t = 0$) then.

Case 4. If $t > 2t_0$ and $\theta < \arcsin(\frac{r\cos t_0}{f_0})$.
If $t > 2t_0$, then $\sin(t - 2t_0) > 0$ (for relevant values of t), so we find the following condition

$$\cos(u - \phi) \geq \frac{\cos\arcsin(\frac{r}{f(t)}) - \cos\theta\cos(t - 2t_0)}{\sin\theta\sin(t - 2t_0)}. \tag{5.68}$$

So all u satisfy (5.68) if the right hand side of this inequality is less than -1. The largest t_a for which this holds is given by

$$\theta = 2t_0 - t_a + \arcsin(\frac{r}{f(t_a)}). \tag{5.69}$$

Also, no u satisfies (5.68) if t is larger than the critical value t_n given by

$$\theta = t_n - 2t_0 - \arcsin(\frac{r}{f(t_n)}). \tag{5.70}$$

So for $t > 2t_0$ and $\theta < \arcsin(\frac{r\cos t_0}{f_0})$, the different ranges of interest are $[2t_0, t_a]$, and $[t_a, t_n]$.

Case 5. If $t > 2t_0$ and $\theta > \arcsin(\frac{r\cos t_0}{f_0})$.
As in Case 3, if $\theta > \arcsin(\frac{r\cos t_0}{f_0})$, then no value of $t > 2t_0$ can be found such that all u satisfy (5.68). The boundaries of the t-range for which at least some u satisfy (5.63) are given by (5.64).

The above five cases completely describe how the integration bounds for u are determined in terms of the other parameters involved. So at this point, we have all the knowledge needed to carry out the integration with respect to u analytically. The very lengthy and complicated expressions then obtained are integrals with respect to t. Whether these single integrals allow an analytical solution as well, is not yet known.

5.4.2 The Illuminance by the Reflected Light

We now calculate the illuminance on S by the reflected light. In this section we write K instead of K_{E_2}. Let $\mathbf{x}_S$ be a point on S. We have seen in the Section 5.2 that

$$E_2(\mathbf{x}_S) = \rho L_0 \int_R \frac{\cos(\mathbf{w}, \mathbf{n}_R)\cos(-\mathbf{w}, \mathbf{n}_S)}{|\mathbf{x}_R - \mathbf{x}_S|^2} K(\mathbf{x}_R, \mathbf{x}_S)\, dR. \tag{5.71}$$

For convenience we take $\rho L_0 = 1$. By definition of $\mathbf{w}$, we find

$$E_2(\mathbf{x}_S) = \int_R \frac{((\mathbf{x}_S - \mathbf{x}_R).\mathbf{n}_R)((\mathbf{x}_R - \mathbf{x}_S).\mathbf{n}_S)}{|\mathbf{x}_R - \mathbf{x}_S|^4} K(\mathbf{x}_R, \mathbf{x}_S)\, dR. \tag{5.72}$$

In terms of the coordinates that were introduced above, we have

$$\begin{aligned}
\mathbf{x}_S &= (-d,\, p\cos\phi,\, p\sin\phi), && (5.73)\\
\mathbf{n}_S &= (1, 0, 0), && (5.74)\\
\mathbf{x}_R &= \frac{f_0}{\cos(t - t_0)}(\cos t,\, \sin t\cos u,\, \sin t\sin u), && (5.75)\\
\mathbf{n}_R &= -(\cos t_0,\, \sin t_0\cos u,\, \sin t_0\sin u), && (5.76)\\
dR &= \frac{f_0^2\sin t}{\cos^3(t - t_0)}\, du\, dt. && (5.77)
\end{aligned}$$

We find

$$\begin{aligned}
\mathbf{x}_S.\mathbf{n}_R &= d\cos t_0 - p\sin t_0\cos(u - \phi), && (5.78)\\
\mathbf{x}_R.\mathbf{n}_R &= -f_0, && (5.79)\\
\mathbf{x}_S.\mathbf{n}_S &= -d, && (5.80)\\
\mathbf{x}_R.\mathbf{n}_S &= f(t)\cos t, && (5.81)\\
|\mathbf{x}_R - \mathbf{x}_S| &= \sqrt{d^2 + p^2 + f(t)^2 + 2df(t)\cos t - 2pf(t)\sin t\cos(u - \phi)}.
\end{aligned}$$

Substituting these identities into (5.72) gives the following expression for $E_2(\mathbf{x}_S)$:

$$\int_t \int_u \frac{(f_0 + d\cos t_0 - p\sin t_0 \cos(u-\phi))(f(t)\cos t + d)}{(d^2 + p^2 + f(t)^2 + 2df(t)\cos t - 2pf(t)\sin t\cos(u-\phi))^2} K \frac{f_0^2 \sin t}{\cos^3(t-t_0)}\, du\, dt.$$

Again, this can be worked out further analytically, once we know more about the factor K. Indeed, in terms of u, the inner integral is of the form

$$\int_u e \frac{a - b\cos(u-\phi)}{(c - d\cos(u-\phi))^2} K\, du, \tag{5.82}$$

and

$$\frac{a - b\cos\alpha}{(c - d\cos\alpha)^2}$$

has anti-derivative (with respect to α)

$$\frac{(bc-ad)\sin\alpha}{(c^2-d^2)(d\cos\alpha - c)} + \frac{2(ac-bd)}{(c^2-d^2)^{3/2}} \arctan\left(\frac{(c+d)\sin\alpha}{\sqrt{c^2-d^2}(1+\cos\alpha)}\right).$$

So again we should investigate the factor K. This can be done along the same lines as in the previous section, and we can then deduce an inequality which is quadratic in $\cos(u-\phi)$. Thus, in principle, the integration bounds of u in terms of the other variables can be calculated.

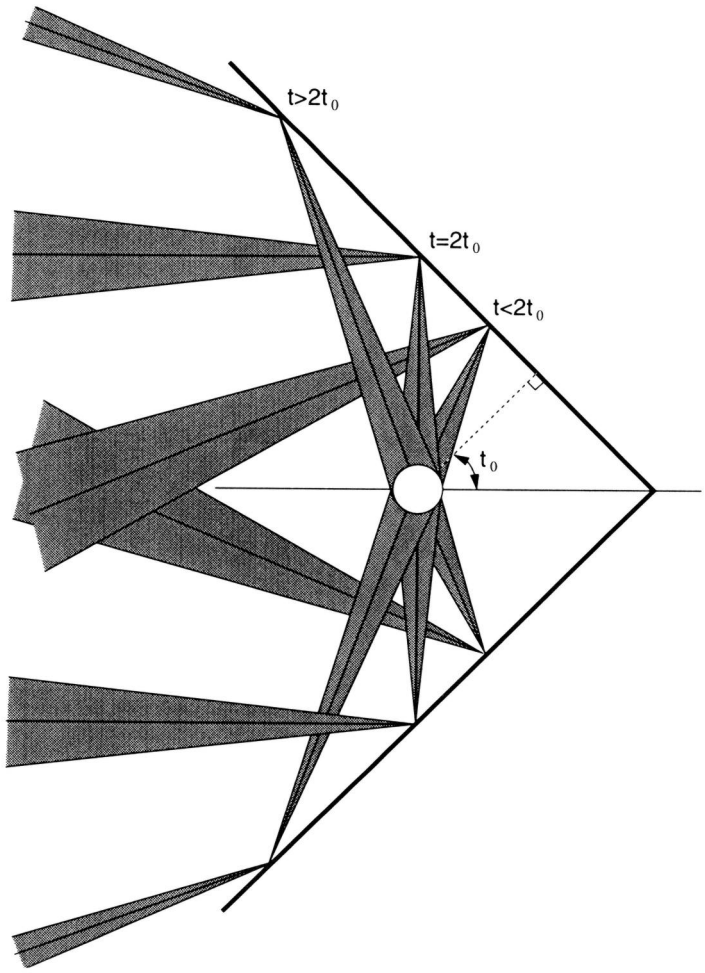

Figure 5.11: *Illustration of ray paths in the rotationally symmetric case.*

Chapter 6

3D Problems With Point Sources

6.1 Introduction to 3D Problems

In this chapter we take up the 3D far field reflector design problem formulated in Chapter 2. We will see that the problem can be formulated in terms of a non-linear partial differential equation of the Monge-Ampère type. We will not try to solve this differential equation as has been done in the literature (see Section 1.2). Rather, we will focus on trying to understand the problem geometrically in terms of ray paths. We will classify the sorts of ray paths that can be achieved with smooth reflectors, and deduce some properties of these ray paths that have proved to be very helpful in heuristic approaches to solve 3D problems.

6.2 The Basics of Smooth Reflector Design

In this section, we will present some basic formulas and we will have a closer look at the two laws that a solution of a reflector design problem has to comply with: the Law of Reflection and Conservation of Energy. We will look at this from two different viewpoints. The first approach is that we consider the reflector surface, described by a function f, and we will derive the exact conditions f has to satisfy in order to represent a reflector that solves our problem. The second approach is to look at the problem in terms of the mapping between incident and reflected rays, which we will also call the ray path. This approach is equivalent to the above one, but has the advantage that it gives more insight in geometrical features of the problem.

6.2.1 Some Basic Formulas

Let us recall the notation from Chapter 2. Suppose we have a Euclidean xyz-coordinate system in $\mathbb{R}^3$, with a point source located at the origin. Outgoing rays are represented by unit vectors

$$\mathbf{v} := \mathbf{v}(t, u) := (\cos t, \sin t \cos u, \sin t \sin u), \tag{6.1}$$

for $t \in [t_1, t_2] \subset [0, \pi]$ and $u \in [u_1, u_2] \subset [0, 2\pi]$. The reflector surface $\mathbf{r}(t, u)$ is given by

$$\mathbf{r} := \mathbf{r}(t, u) := f(t, u)\mathbf{v}(t, u), \tag{6.2}$$

where f is twice differentiable, strictly positive, and where $f(t, 0) = f(t, 2\pi)$ for all t. The function f and the surface $\mathbf{r}$ are defined on some fixed t, u domain, usually of the form $t \in [t_1, t_2]$ and $u \in [0, 2\pi]$. Note that the representation (6.2) is well-defined for $t = 0$ only if $f_u = 0$ at $t = 0$, i.e. $f(0, u)$ is constant.

A reflected ray is denoted by the vector $\mathbf{w}$ (of unit length), which is often given in spherical coordinates θ, ϕ as follows,

$$\mathbf{w} := \mathbf{w}(\theta, \phi) := (-\cos\theta, \sin\theta \cos\phi, \sin\theta \sin\phi), \tag{6.3}$$

for $\theta \in [\theta_1, \theta_2] \subset [0, \pi]$ and $\phi \in [\phi_1, \phi_2] \subset [0, 2\pi]$.

Furthermore, we have given a luminous intensity $I(t, u)$ of the light source, as well as a required far field intensity distribution $G(\theta, \phi)$ for the reflected light (we may assume that the direct light contribution has already been subtracted). Both these intensities are positive functions (infinite intensities are not considered). We also assume that the intensity I is corrected to account for the reflection coefficient ρ of the reflector.

Finally, we assume that there is global conservation of energy, i.e.

$$\int_{\theta_1}^{\theta_2} \int_{\phi_1}^{\phi_2} G(\theta, \phi) \sin\theta \, d\theta \, d\phi = \int_{u_1}^{u_2} \int_{t_1}^{t_2} I(t, u) \sin t \, dt \, du. \tag{6.4}$$

The problem is then to find a reflector, given by a function f, such that for the given source, the required light has the prescribed intensity pattern. We limit ourselves to solutions where there is a *one-to-one correspondence between incident and reflected rays*. In the further modelling of this problem, we neglect multiple reflections, and we don't go into boundary conditions and constraints on the dimensions of the reflector. Rather, we will focus on what types of solutions we may expect, in case there are any solutions at all.

Some basic expressions involving v and w. We have the following expressions for the partial derivatives of the vector $\mathbf{v}(t, u)$, where we abbreviate expressions like $\frac{\partial}{\partial t}\mathbf{v}(t, u)$ by $\mathbf{v}_t$,

$$\begin{aligned}
\mathbf{v}_t &= (-\sin t, \cos t \cos u, \cos t \sin u), && (6.5)\\
\mathbf{v}_u &= (0, -\sin t \sin u, \sin t \cos u), && (6.6)\\
\mathbf{v}_{tt} &= -\mathbf{v}, && (6.7)\\
\mathbf{v}_{uu} &= -\sin^2 t\, \mathbf{v} - \sin t \cos t\, \mathbf{v}_t, && (6.8)\\
\mathbf{v}_{ut} &= \mathbf{v}_{tu} = \mathbf{v}_u / \tan t. && (6.9)
\end{aligned}$$

Note that for $t = 0$, some of these vectors vanish. Because of this, we will sometimes need to treat the case $t = 0$ separately in forthcoming expressions and results. The following formulas for inner products will be used,

$$\begin{aligned}
\mathbf{v}.\mathbf{v} = \mathbf{v}_t.\mathbf{v}_t &= 1, && (6.10)\\
\mathbf{v}.\mathbf{v}_t = \mathbf{v}.\mathbf{v}_u = \mathbf{v}_t.\mathbf{v}_u &= 0, && (6.11)\\
\mathbf{v}_u.\mathbf{v}_u &= \sin^2 t. && (6.12)
\end{aligned}$$

Next we have the following expressions for the cross products,

$$\begin{aligned}
\mathbf{v} \times \mathbf{v}_t &= \mathbf{v}_u / \sin t, && (6.13)\\
\mathbf{v} \times \mathbf{v}_u &= -\sin t\, \mathbf{v}_t, && (6.14)\\
\mathbf{v}_t \times \mathbf{v}_u &= \sin t\, \mathbf{v}. && (6.15)
\end{aligned}$$

The scalar triple product $[\mathbf{v}, \mathbf{v}_t, \mathbf{v}_u] = \mathbf{v}.(\mathbf{v}_t \times \mathbf{v}_u)$ is given by

$$[\mathbf{v}, \mathbf{v}_t, \mathbf{v}_u] = \sin t. \tag{6.16}$$

We will need the following expressions concerning $\mathbf{w}$:

$$\begin{aligned}
\mathbf{w}_\theta &= (\sin\theta, \cos\theta \cos\phi, \cos\theta \sin\phi), && (6.17)\\
\mathbf{w}_\phi &= (0, -\sin\theta \sin\phi, \sin\theta \cos\phi), && (6.18)\\
\mathbf{w} \times \mathbf{w}_\theta &= -\mathbf{w}_\phi / \sin\theta, && (6.19)\\
\mathbf{w} \times \mathbf{w}_\phi &= \sin\theta\, \mathbf{w}_\theta. && (6.20)
\end{aligned}$$

The normal to the reflector surface.
The reflector surface $\mathbf{r}(t, u) = f(t, u)\mathbf{v}(t, u)$ has normal

$$\mathbf{n} = \mathbf{n}(t, u) = \frac{\mathbf{r}_t \times \mathbf{r}_u}{|\mathbf{r}_t \times \mathbf{r}_u|}. \tag{6.21}$$

For $t \neq 0$ we have

$$\begin{aligned} \mathbf{r}_t \times \mathbf{r}_u &= (f_t \mathbf{v} + f\mathbf{v}_t) \times (f_u \mathbf{v} + f\mathbf{v}_u) \\ &= f f_t\, \mathbf{v} \times \mathbf{v}_u + f f_u\, \mathbf{v}_t \times \mathbf{v} + f^2\, \mathbf{v}_t \times \mathbf{v}_u \\ &= f(f \sin t\, \mathbf{v} - f_t \sin t\, \mathbf{v}_t - \frac{f_u}{\sin t}\mathbf{v}_u), \end{aligned} \tag{6.22}$$

and therefore

$$|\mathbf{r}_t \times \mathbf{r}_u| = |f|\sqrt{(f^2 + f_t^2)\sin^2 t + f_u^2}. \tag{6.23}$$

Since $f > 0$ we obtain

$$\mathbf{n} = \frac{f \sin t\, \mathbf{v} - f_t \sin t\, \mathbf{v}_t - \frac{f_u}{\sin t}\mathbf{v}_u}{\sqrt{(f^2 + f_t^2)\sin^2 t + f_u^2}}. \tag{6.24}$$

6.2.2 The Law of Reflection; Existence of Reflectors

Suppose we have a mapping R of vectors $\mathbf{v}$ to vectors $\mathbf{w}$, for instance in terms of a mapping of the coordinates $(t, u) \to (\theta, \phi)$. Such a mapping can be seen as a mapping between incident and reflected rays, and will be called a *ray path*. Not every ray path can be realized by a reflector. In this section we will give the conditions for the existence of a reflector that realizes a certain ray path. If a ray path can be realized by a reflector, then it will be called a *feasible ray path* or a *reflector mapping*.

The law of reflection. The law of reflection relates the incident ray $\mathbf{v}$ and the reflected ray $\mathbf{w}$ in terms of the normal to the surface. We recall from Chapter 2 that

$$\mathbf{w} = \mathbf{v} - 2(\mathbf{v}.\mathbf{n}).\mathbf{n}. \tag{6.25}$$

Using (6.25), we can express $\mathbf{w}$ in terms of the reflector surface and the incident ray $\mathbf{v}$. From (6.24) it follows that

$$\mathbf{v}.\mathbf{n} = \frac{f \sin t}{\sqrt{(f^2 + f_t^2)\sin^2 t + f_u^2}}$$

and that

$$\begin{aligned} \mathbf{w} &= \mathbf{v} - 2(\mathbf{v}.\mathbf{n}).\mathbf{n} \\ &= \mathbf{v} - 2\frac{f \sin t}{\sqrt{(f^2 + f_t^2)\sin^2 t + f_u^2}} \frac{f \sin t\, \mathbf{v} - f_t \sin t\, \mathbf{v}_t - \frac{f_u}{\sin t}\mathbf{v}_u}{\sqrt{(f^2 + f_t^2)\sin^2 t + f_u^2}} \end{aligned}$$

$$= \frac{((f_t^2 - f^2)\sin^2 t + f_u^2)\,\mathbf{v} + 2ff_t \sin^2 t\,\mathbf{v}_t + 2ff_u\,\mathbf{v}_u}{(f^2 + f_t^2)\sin^2 t + f_u^2}. \tag{6.26}$$

So, if we have the ray path defined by prescribing $\mathbf{w}$ in terms of t and u, it is feasible if and only if there is a function f such that (6.26) holds. An alternate formulation of the reflector existence condition will be given in the next paragraph.

Reflector existence for w as a function of t and u. Given the mapping $\mathbf{w}(t, u)$, the question is whether there exists a surface $\mathbf{r}(t, u) = f(t, u)\mathbf{v}(t, u)$ with normal $\mathbf{n} = (\mathbf{v} - \mathbf{w})/\sqrt{2 - 2(\mathbf{v}.\mathbf{w})}$. This is the case precisely if

$$\mathbf{r}_t.\mathbf{n} = \mathbf{r}_u.\mathbf{n} = 0.$$

By definition of $\mathbf{r}$ this is equivalent to the two equations

$$\begin{aligned}(\mathbf{v}.\mathbf{n})f_t &= -(\mathbf{v}_t.\mathbf{n})f,\\ (\mathbf{v}.\mathbf{n})f_u &= -(\mathbf{v}_u.\mathbf{n})f,\end{aligned}$$

which can be written as

$$\frac{\partial}{\partial t}(\log f) = \frac{-\mathbf{v}_t.\mathbf{n}}{\mathbf{v}.\mathbf{n}} = \frac{\mathbf{v}_t.\mathbf{w}}{1 - \mathbf{v}.\mathbf{w}}, \tag{6.27}$$

$$\frac{\partial}{\partial u}(\log f) = \frac{-\mathbf{v}_u.\mathbf{n}}{\mathbf{v}.\mathbf{n}} = \frac{\mathbf{v}_u.\mathbf{w}}{1 - \mathbf{v}.\mathbf{w}}. \tag{6.28}$$

By differentiating these two equations with respect to u and t respectively, we obtain

$$\frac{\partial}{\partial u}\left(\frac{\mathbf{v}_t.\mathbf{n}}{\mathbf{v}.\mathbf{n}}\right) = \frac{\partial}{\partial t}\left(\frac{\mathbf{v}_u.\mathbf{n}}{\mathbf{v}.\mathbf{n}}\right),$$

or equivalently,

$$\frac{\partial}{\partial u}\left(\frac{\mathbf{v}_t.\mathbf{w}}{1 - \mathbf{v}.\mathbf{w}}\right) = \frac{\partial}{\partial t}\left(\frac{\mathbf{v}_u.\mathbf{w}}{1 - \mathbf{v}.\mathbf{w}}\right), \tag{6.29}$$

which can be reduced to

$$(\mathbf{v}.\mathbf{w}_u)(\mathbf{v}_t.\mathbf{w}) - (\mathbf{v}_t.\mathbf{w}_u)(\mathbf{v}.\mathbf{w}) + \mathbf{v}_t.\mathbf{w}_u = \tag{6.30}$$

$$(\mathbf{v}.\mathbf{w}_t)(\mathbf{v}_u.\mathbf{w}) - (\mathbf{v}_u.\mathbf{w}_t)(\mathbf{v}.\mathbf{w}) + \mathbf{v}_u.\mathbf{w}_t. \tag{6.31}$$

Using cross products, this can be written in the form

$$(\mathbf{v}_t \times \mathbf{v}).(\mathbf{w} \times \mathbf{w}_u) + \mathbf{v}_t.\mathbf{w}_u = (\mathbf{v}_u \times \mathbf{v}).(\mathbf{w} \times \mathbf{w}_t) + \mathbf{v}_u.\mathbf{w}_t. \tag{6.32}$$

Reflector existence in terms of a mapping $(t, u) \to (\theta, \phi)$. Suppose the ray path is given as a mapping $(t, u) \to (\theta, \phi)$. Using the known expressions for the cross products involving $\mathbf{v}$, we can rewrite equation (6.32) as

$$\mathbf{v}_t.(\mathbf{w}_u - \sin t\,(\mathbf{w} \times \mathbf{w}_t)) = \mathbf{v}_u.(\mathbf{w}_t - \frac{1}{\sin t}\,(\mathbf{w} \times \mathbf{w}_u)).$$

We have

$$\mathbf{w}_t = \mathbf{w}_\theta \frac{\partial \theta}{\partial t} + \mathbf{w}_\phi \frac{\partial \phi}{\partial t}, \tag{6.33}$$

$$\mathbf{w}_u = \mathbf{w}_\theta \frac{\partial \theta}{\partial u} + \mathbf{w}_\phi \frac{\partial \phi}{\partial u}. \tag{6.34}$$

Using this and writing out all cross products gives

$$\begin{aligned}\mathbf{v}_t.(\mathbf{w}_\theta \theta_u + \mathbf{w}_\phi \phi_u + \frac{\sin t}{\sin \theta}\mathbf{w}_\phi \theta_t - \sin t \sin\theta\, \mathbf{w}_\theta \phi_t) = \\ \mathbf{v}_u.(\mathbf{w}_\theta \theta_t + \mathbf{w}_\phi \phi_t + \frac{1}{\sin t \sin\theta}\mathbf{w}_\phi \theta_u - \frac{\sin\theta}{\sin t}\mathbf{w}_\theta \phi_u).\end{aligned}$$

By writing out the inner products and some basic calculus we eventually find

$$\begin{aligned}0 \;=\; & \theta_u\,(-\sin t \sin\theta + (1 + \cos t \cos\theta)\cos(u - \phi)) + \\ & \theta_t\,(\sin t\,(\cos t + \cos\theta)\sin(u - \phi)) + \\ & \phi_t\,(-\sin t \sin\theta(-\sin t \sin\theta + (1 + \cos t \cos\theta)\cos(u - \phi))) + \\ & \phi_u\,(\sin\theta\,(\cos t + \cos\theta)\sin(u - \phi)),\end{aligned} \tag{6.35}$$

which we can also write as

$$\begin{aligned}0 \;=\; & (\theta_u - \phi_t \sin t \sin\theta)(-\sin t \sin\theta + (1 + \cos t \cos\theta)\cos(u - \phi)) + \\ & (\theta_t \sin t + \phi_u \sin\theta)(\cos t + \cos\theta)\sin(u - \phi).\end{aligned} \tag{6.36}$$

Note that if we have a mapping that satisfies this equation, then we can also find the corresponding reflector surface by integration, using (6.27) or (6.28).

6.2.3 Conservation of Energy

Let us recall from Chapter 2 that, *under the assumption that we have a one-to-one correspondence between incident and reflected rays*, the required far field pattern is realized if in all directions $\mathbf{v}$ with corresponding reflected ray $\mathbf{w}$ we have

$$G(\mathbf{w})|d\Omega| = I(\mathbf{v})|d\Omega'|, \tag{6.37}$$

where $d\Omega'$ and $d\Omega$ are solid angles corresponding to incident and reflected ray cones around $\mathbf{v}$ and $\mathbf{w}$, respectively. We have

$$d\Omega' = [\mathbf{v}, \mathbf{v}_t, \mathbf{v}_u]\,\mathrm{d}t\,\mathrm{d}u = \sin t\,\mathrm{d}t\,\mathrm{d}u, \tag{6.38}$$

$$d\Omega = [\mathbf{w}, \mathbf{w}_\theta, \mathbf{w}_\phi]\,\mathrm{d}\theta\,\mathrm{d}\phi = -\sin\theta\,\mathrm{d}\theta\,\mathrm{d}\phi. \tag{6.39}$$

So we can write the energy conservation equation as

$$G(\mathbf{w})\sin\theta\,\mathrm{d}\theta\,\mathrm{d}\phi = I(\mathbf{v})\sin t\,\mathrm{d}t\,\mathrm{d}u. \tag{6.40}$$

Now suppose we have a mapping $(t, u) \to (\theta, \phi)$, then

$$\mathrm{d}\theta\,\mathrm{d}\phi = \left|\frac{\partial(\theta, \phi)}{\partial(t, u)}\right| \mathrm{d}t\,\mathrm{d}u,$$

so (6.40) becomes

$$\theta_t\phi_u - \theta_u\phi_t = \pm\frac{\sin t\, I(\mathbf{v})}{\sin\theta\, G(\mathbf{w})}. \tag{6.41}$$

If a reflector surface is given by the function f, then we can express $\mathbf{w}$ in terms of t and u as shown in (6.26), and we find the far field distribution by

$$G(\mathbf{w}) = \frac{\sin t\, I(\mathbf{v})}{|[\mathbf{w}, \mathbf{w}_t, \mathbf{w}_u]|}. \tag{6.42}$$

The Monge-Ampère equation. In the literature, the design problem is often described in terms of the so-called Monge-Ampère equation, which is a non-linear second order partial differential equation. The highest order term of this equation in terms of the function f is of the form

$$k(f_{uu}f_{tt} - f_{tu}^2) \tag{6.43}$$

where k is a function of t, u, f, f_t and f_u. This term arises when the vector triple product $[\mathbf{w}, \mathbf{w}_t, \mathbf{w}_u]$ is evaluated in terms of f. We will return to this expression in more detail in Sections 6.4.4 and 6.4.5.

6.3 Types of Ray Paths

In this section we will look at reflector mappings in more detail, and will distinguish three types of mappings for a certain class of reflectors. The definition of these types as given here shows very well what is going on in terms of the ray path, but is inconvenient to extend to a broader class of reflectors. Therefore, the following sections will give a more mathematically sound classification, based on the shape of the wave front of the reflected light. Later on, we will show that the two definitions are in fact equivalent.

6.3.1 Special Cases of Reflector Mappings and Examples

In this section, we consider an example which illustrates the three types of ray paths that we distinguish later on. We consider mappings of the form $\theta = \theta(t)$ and $\phi = \phi(u)$. For these mappings, the Energy Conservation and the Reflector Existence equations read

$$\theta_t \phi_u = \pm \frac{\sin t \, I(\mathbf{v})}{\sin\theta \, G(\mathbf{w})} \tag{6.44}$$

and

$$(\theta_t \sin t + \phi_u \sin\theta)(\cos t + \cos\theta)\sin(u - \phi) = 0, \tag{6.45}$$

respectively.

Rotationally symmetric ray paths. It follows from (6.45) that a ray path is feasible if $\phi(u) = u$ or $\phi(u) = u + \pi$. These mappings are realized by rotationally symmetric reflectors and they produce rotationally symmetric far fields.

Example 6.3.1. Suppose we have a required far field distribution for the reflected light that is given by $G(\mathbf{w}(\theta, \phi)) = 1$ for all $\theta \in [0, \pi/4]$ and $\phi \in [0, 2\pi]$. Let the intensity of the source be given by $I(\mathbf{v}(t, u)) = 1$ for all $t \in [0, \pi/4]$ and $u \in [0, 2\pi]$, and let the reflector be located in this t, u range. Then we have the following solutions.
(i) The mapping $\theta(t) = t$, $\phi(u) = u$. It is easily verified that this mapping satisfies both conditions (6.44) and (6.45). The reflector surface can be found from (6.27) or (6.28), and is given by

$$f(t, u) = c/\cos t$$

for all t and u and any constant c. The reflector is a flat disc, and the corresponding reflected ray bundle is divergent.
(ii) The mapping $\theta(t) = t$, $\phi(u) = u + \pi$. The reflector surface is now given by

$$f(t, u) = c$$

for all t and u and any constant c. The reflector surface is part of a sphere, and the corresponding reflected ray bundle is convergent. □

Non-rotationally symmetric ray paths. The following example shows that rotationally symmetric far fields can also be realized by reflectors that lack this kind of symmetry.

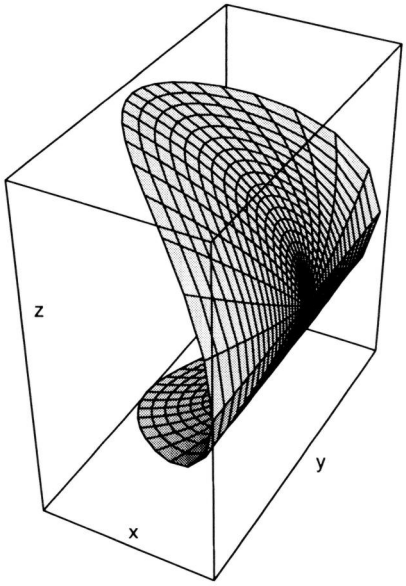

Figure 6.1: *A cylindrical reflector surface.*

Example 6.3.2. Consider the same required far field distribution as in the previous example. This time we will consider two types of non-rotationally symmetric ray paths that would produce the required distribution, provided that they are feasible.
(i) The mappings of the form $\theta(t) = t,\ \phi(u) = \phi_0 - u$, for any constant ϕ_0. Again it is easily verified that these mappings satisfy conditions (6.44) and (6.45). Now consider the case that $\phi_0 = 0$. For the reflector surface, we then have

$$\frac{\partial}{\partial u}(\log f) = \frac{\mathbf{v}_u.\mathbf{n}}{\mathbf{v}.\mathbf{n}} = \frac{-\sin^2 t \sin 2u}{1 + \cos^2 t - \sin^2 t \cos 2u}$$

which gives

$$f(t, u) = \frac{c}{\sqrt{1 - \sin^2 t \cos^2 u}}$$

for all t and u and any constant c. The corresponding reflector surface is part of the circular cylinder given by the equation

$$x^2 + z^2 = c^2.$$

See Figure 6.1. Note that the reflector surface is not rotationally symmetric.
(ii) A mapping that satisfies the energy conservation condition but which is not

feasible is the mapping $\theta(t) = t$ and $\phi(u) = \phi_0 + u$ for any ϕ_0 not of the form $k\pi$ for an integer k. Indeed, the feasibility condition (6.45) gives

$$4 \sin t \cos t \sin \phi_0 = 0,$$

which proves the assertion. □

Let us now look at the reflector existence condition (6.45) in more detail. The following analysis has been done by Brickell and Westcott [3, p. 118]. It follows from (6.45) that if we don't have $\phi(u) = u$ or $\phi(u) = u + \pi$, then we must have

$$\theta_t \sin t + \phi_u \sin \theta = 0. \tag{6.46}$$

Suppose we have $t \in [0, t_2]$ and $u \in [0, 2\pi]$. Then it follows from the above equation that $\theta(0) = 0$. We can rewrite (6.46) as

$$\theta_t \frac{\sin t}{\sin \theta} = -\phi_u.$$

We can solve this equation by separating variables and we obtain

$$\theta(t) = 2 \arctan(c \tan^k(\frac{t}{2})), \tag{6.47}$$

$$\phi(u) = -ku + \phi_0, \tag{6.48}$$

where c and ϕ_0 are to be determined from boundary conditions, and k should be a positive integer, as follows from $\theta(0) = 0$ and from the periodicity of ϕ as a function of u. From (6.48) and from (6.44) it follows that all required far fields are rotationally symmetric, while the ray paths are not. For $k = 1$, we obtain ray paths that are generalizations of the one in (i) in Example 6.3.2. Let us now consider the case that $k = 2$, $c = 1$ and $\phi_0 = 0$. Note that in this case we do not have a one-to-one correspondence between incident and reflected rays, which we generally have assumed in this thesis.

Example 6.3.3. Consider the mapping defined by

$$\theta(t) = 2 \arctan(\tan^2(\frac{t}{2})) = \pi/2 - 2 \arctan \cos t,$$
$$\phi(u) = -2u.$$

Then we obtain

$$\frac{\mathbf{v}_u.\mathbf{w}}{1 - \mathbf{v}.\mathbf{w}} = \frac{\sin t \sin \theta \sin(\phi - u)}{1 + \cos t \cos \theta - \sin t \sin \theta \cos(\phi - u)}$$
$$= \frac{-\sin 3u \sin^3 t}{4 - 3 \sin^2 t - \sin^3 t \cos 3u}.$$

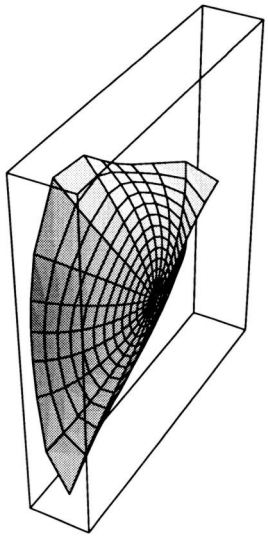

Figure 6.2: *The reflector surface defined by (6.49).*

By integration with respect to u we find the following expression for the reflector surface

$$f(t, u) = (4 - 3\sin^2 t - \sin^3 t \cos 3u)^{-1/3}. \tag{6.49}$$

See Figure 6.2.

The corresponding far field is given by

$$G(\mathbf{w}(\theta, \phi)) = \frac{1}{2\sin\theta(1 + \sin\theta)},$$

and has an infinite intensity in direction $\theta = 0$. Note also that if we restrict (6.49) to a domain $t \in [t_1, \pi/2]$, $u \in [0, 2\pi]$, with $0 < t_1 < \pi/2$, so we have a hole in the back of the reflector, then we obtain a far field pattern with a hole, where each reflected direction corresponds to two different incident directions. □

6.3.2 Different Types of Reflector Mappings

In the 2D case, ray bundles belonging to smooth reflectors are locally either convergent or divergent, and these notions can be defined either in terms of the monotonicity of the mapping between incident and reflected rays, or in terms of the curvature of the reflector curve. We would like to classify feasible ray paths in the 3D case in a similar way. Example 6.3.2 (i) shows a reflector that produces a ray

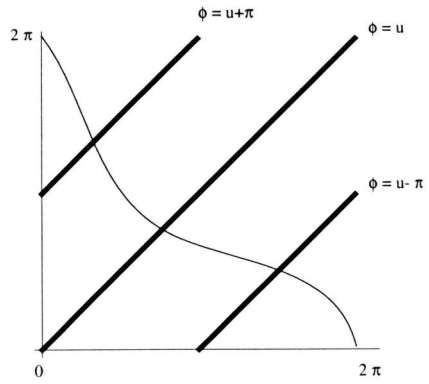

Figure 6.3: *A decreasing function ϕ, corresponding to a hyperbolic ray path, has two fixed and two antipodal points.*

path that is convergent in one direction, and divergent in the other. We will see in this section that under certain restrictions we can distinguish three types of ray paths. In Example 6.3.2 (ii) we have also seen an example of a rotated ray path that was not feasible. The following lemma shows that we have a stronger result about the impossibility of 'rotating' a ray bundle.

Lemma 6.3.4. (Fixed Point Lemma) *Let $(t, u) \to (\theta, \phi)$ be a reflector mapping. Then for each $t \neq 0$ there exist at least two angles u such that*

$$\sin(u - \phi(t, u)) = 0. \tag{6.50}$$

Proof. Let f be the function that describes the reflector surface that realizes the mapping. For fixed $t \neq 0$, the function $f(t, u)$ is periodic in u, so there are at least two angles u such that $f_u(t, u) = 0$. From (6.24) it follows that

$$f_u = 0 \Leftrightarrow \mathbf{v}_u.\mathbf{n} = 0 \Leftrightarrow \mathbf{v}_u.\mathbf{w} = 0 \Leftrightarrow \sin t \sin\theta \sin(u - \phi) = 0.$$

So we have $\sin(u - \phi) = 0$ at these points. This proves the lemma. □

In order to see what this means, let us consider a fixed $t \neq 0$, and consider ϕ as a function of u only, so we write $\phi(u)$ instead of $\phi(t, u)$. We can then regard the mapping ϕ as a mapping from the unit circle into itself, by associating the point $(\cos u, \sin u)$ with u. The angle u (or the pair (t, u)) is called a *fixed* point of ϕ if $\phi(u) = u$, and it is called an *antipodal* point of ϕ if $\phi(u) = u + \pi$.

Now suppose we have a reflector surface such that for each $t \neq 0$, the mapping ϕ corresponds to a one-to-one mapping of the unit circle onto itself, i.e. as a

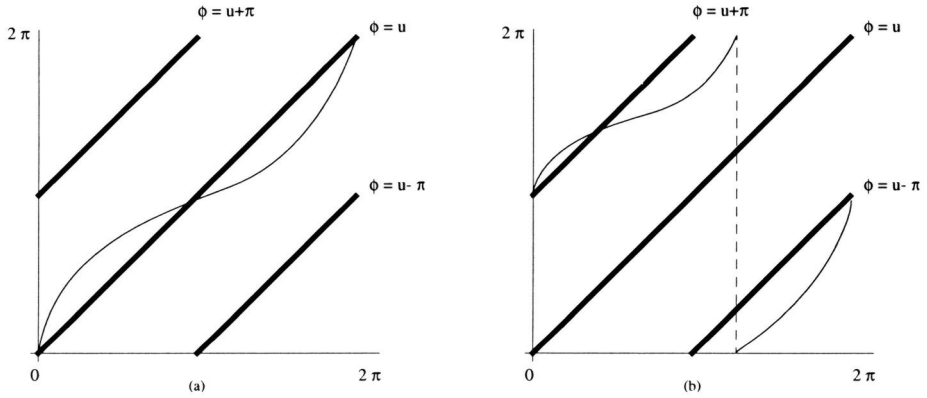

Figure 6.4: *(a) An increasing function ϕ corresponding to a divergent ray path has fixed points only. (b) An increasing function ϕ corresponding to a convergent ray path has antipodal points only.*

mapping $\phi : [0, 2\pi) \to [0, 2\pi)$. It follows from the above lemma that this mapping has at least two fixed or antipodal points. We will distinguish several types of mappings below, but let us first explain the corresponding figures.

In Figures 6.3, 6.4 and 6.5 examples of *periodic* functions ϕ are plotted on the $[0, 2\pi]$ domain. The heavy straight lines correspond to the loci of fixed and antipodal points. Note that there is also a fixed point in $(0, 2\pi) \equiv (2\pi, 0)$. The examples are chosen such that there is a fixed or antipodal point for $u = 0$, except for Figure 6.5(a) which shows a function without fixed points.

We now distinguish the following cases.

1. The case that $\phi'(u) \leq 0$ for all u. Then it is easily seen that ϕ has precisely two fixed points and two antipodal points. See Figure 6.3. If we have a reflector mapping such that for each $t \neq 0$ the mapping ϕ is of this type, the ray bundle is called *hyperbolic*.

2. The case that $\phi'(u) \geq 0$ for all u. If we have a reflector mapping such that for each $t \neq 0$ the mapping ϕ is of this type, the ray bundle is called *elliptic*. In the elliptic case, we can have the following situations.

   - If ϕ has fixed points but no antipodal points, as in Figure 6.4(a), the ray path is called *divergent*.
   - Conversely, if ϕ has antipodal points but no fixed points, then we call the ray path *convergent*, see Figure 6.4(b).
   - Note that the case that ϕ has neither fixed nor antipodal points, as in Figure 6.5(a), does not occur, as follows from the Fixed Point Lemma.

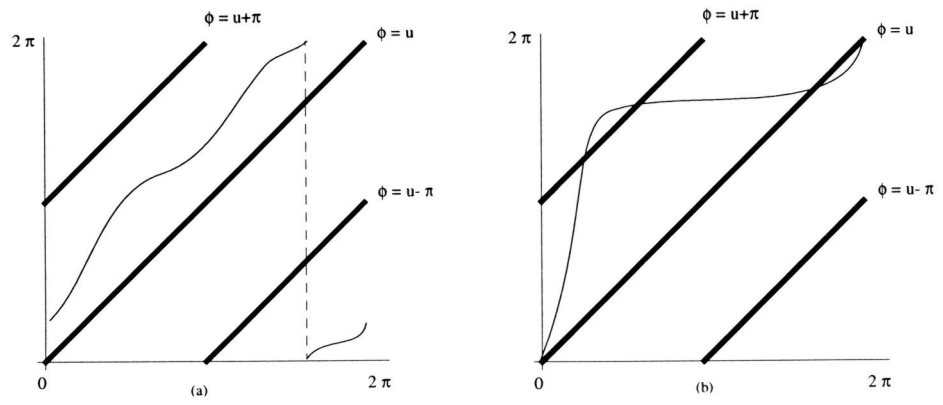

Figure 6.5: *(a) An increasing function without fixed or antipodal points (not feasible as reflector mapping). (b) An increasing function with both fixed and antipodal points.*

- Finally, we have the case that ϕ has both fixed and antipodal points, as in Figure 6.5(b). It is not known whether this may occur as a reflector mapping. It cannot occur *locally*, as we'll see in Section 6.5.4.

Example 6.3.5. A class of hyperbolic ray bundles is given by

$$\theta(t) = 2\arctan(c\tan\frac{t}{2}), \tag{6.51}$$

$$\phi(u) = \phi_0 - u, \tag{6.52}$$

for $c \in (0, 1]$. The corresponding reflector surface is (up to a constant scale factor) given by

$$f(t,u) = \frac{1}{\sqrt{(1+c^2)(1+\cos^2 t) + 2(1-c^2)\cos t - 2c\sin^2 t\cos(2u-\phi_0)}}. \tag{6.53}$$

For $c = 1$ and $\phi_0 = 0$, this is exactly the cylindrical surface of Example 6.3.2 (i), while for $c = 0$ this expression describes a paraboloid. For $c = 1/3$ and $\phi_0 = 0$, Figure 6.6 shows the reflector. □

It should be noted that the above definitions are only made for reflectors such that for each t the mapping $\phi(u)$ is a one-to-one mapping of the unit circle onto itself. Of course, this is only valid for a limited class of reflectors. For instance, the reflector of Example 6.3.3 does not satisfy this condition, and neither does a tilted parabola. In the following section we will present a more general definition, and in Section 6.5 we will show that the definitions are equivalent for the mappings we considered here.

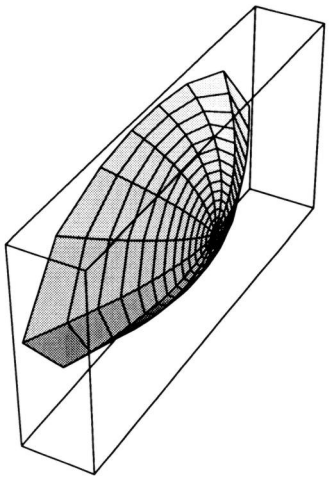

Figure 6.6: *A reflector surface that produces a hyperbolic ray bundle.*

6.4 Ray Path Types and Curvature of the Wave Front

We have seen in the previous section that we can distinguish hyperbolic and elliptic ray paths, and that elliptic ray paths can be further subdivided into convergent and divergent ray paths. In this section we give a more general definition for these types. We will first recall the 2D case, and then summarize the basic notions of curvature properties of surfaces. In particular, we will derive the curvature of the reflector surface in spherical coordinates. Next, we will introduce the wave front of the reflected light, and define the various types of ray paths in terms of the principal curvatures of the wave front. We will then show some relations between the curvatures of the wave front and those of the reflector. Throughout this section, various examples will illustrate the definitions and results.

6.4.1 2D Ray Paths and Curvature

In this section we recall some results from Chapter 3, in particular from Section 3.6.3. Assume we have a point source in the 2D plane, where as usual emitted rays are represented by unit vectors $\mathbf{v}(t) = (\cos t, \sin t)$, and the reflector surface

is represented by the curve $\mathbf{r}(t) = f(t)\mathbf{v}(t)$. This curve has normal

$$\mathbf{n} = \frac{(\dot{f}\sin t + f\cos t, -\dot{f}\cos t + f\sin t)}{\sqrt{f^2 + \dot{f}^2}}. \tag{6.54}$$

The reflected ray $\mathbf{w}$ is then given by

$$\mathbf{w} = \frac{1}{f^2 + \dot{f}^2}((\dot{f}^2 - f^2)\cos t - 2f\dot{f}\sin t, (\dot{f}^2 - f^2)\sin t + 2f\dot{f}\cos t) \tag{6.55}$$

which can be written as

$$\mathbf{w} = (-\cos\theta(t), \sin\theta(t)), \tag{6.56}$$

where

$$\theta(t) = -t + 2\arctan\frac{\dot{f}}{f}. \tag{6.57}$$

The intensity of the reflected light is inversely proportional to $\dot{\theta}$, i.e. if the intensity of the source is uniform then we have

$$I(\mathbf{w}) = \frac{c}{\dot{\theta}} \tag{6.58}$$

for some constant c. We have

$$\dot{\theta} = \frac{2\ddot{f}f - 3\dot{f}^2 - f^2}{f^2 + \dot{f}^2}. \tag{6.59}$$

Now, consider the curve $\mathbf{r}(t) = (x(t), y(t)) = (f\cos t, f\sin t)$. This curve has *curvature*

$$K(t) = \frac{\ddot{x}\dot{y} - \ddot{y}\dot{x}}{(\dot{x}^2 + \dot{y}^2)^{3/2}} = \frac{\ddot{f}f - 2\dot{f}^2 - f^2}{(f^2 + \dot{f}^2)^{3/2}}. \tag{6.60}$$

It follows that

$$\dot{\theta} = 1 + 2\sqrt{f^2 + \dot{f}^2}K. \tag{6.61}$$

So the intensity of the reflected light, as well as the type of ray path (which is determined by the sign of $\dot{\theta}$), are related to the curvature of the reflector curve by (6.61). We now show that the information on the reflected light is even more conveniently expressed in terms of the curvature of the so-called *wave front*. To introduce the wave front, let us follow a ray, emitted in direction t, when it has travelled over a distance $\lambda \geq f(t)$. The position of the ray after it has travelled this distance is denoted $\mathbf{x}(\lambda)$. We have

$$\mathbf{x}(\lambda) = f\mathbf{v} + (\lambda - f)\mathbf{w}. \tag{6.62}$$

For each fixed λ, the vectors $\mathbf{x}(\lambda)$ as a function of t form a curve which will be called the *wave front* at distance λ. We list a few results without proof. In the following sections, the corresponding 3D results will be presented with proofs. An elementary but important property of the wave front is that the reflected rays $\mathbf{w}$ are normal to it.

Lemma 6.4.1. *The reflected rays* $\mathbf{w}$ *are normal to the wave front* $\mathbf{x}(\lambda)$.

We are interested in the curvature of the wave front, which depends on λ, and which we denote $K(\lambda)$. In particular, we are interested in the curvature of the wave front *immediately after reflection*, that is in $\tilde{K} = \lim_{\lambda \downarrow f} K(\lambda)$. We have the following theorem, which shows that the curvature $\tilde{K}$ is directly related to the intensity of the reflected light.

Theorem 6.4.2. *We have*

$$\tilde{K} = \frac{\dot{\theta}}{f}. \tag{6.63}$$

Corollary 6.4.3. *The curvature* $\tilde{K}$ *is related to the curvature of the reflector by*

$$\tilde{K} = \frac{1}{f} + 2\sqrt{1 + \frac{\dot{f}^2}{f^2}}K. \tag{6.64}$$

In particular, if $f_t = 0$, *that is if the reflector surface is perpendicular to the incident ray, then we have*

$$\tilde{K} = \frac{1}{f} + 2K. \tag{6.65}$$

6.4.2 Gaussian and Mean Curvature of a Surface

In this section we summarize some of the foundations of the theory of surfaces. In particular, we define the first and second fundamental forms, and the Gaussian and mean curvature of a surface. For more details we refer the reader to e.g. [16]. Suppose we have a surface $R : \mathbf{x}(u^1, u^2)$. Then we let

$$g_{11} = \mathbf{x}_1.\mathbf{x}_1, \tag{6.66}$$

$$g_{12} = g_{21} = \mathbf{x}_1.\mathbf{x}_2, \tag{6.67}$$

$$g_{22} = \mathbf{x}_2.\mathbf{x}_2. \tag{6.68}$$

Recall that we write $\mathbf{x}_1$ for $\frac{\partial \mathbf{x}}{\partial u^1}$, $\mathbf{x}_2$ for $\frac{\partial \mathbf{x}}{\partial u^2}$, etc. These coefficients are used to define a metric on the surface as follows

$$\mathrm{d}s^2 = g_{11}(\mathrm{d}u^1)^2 + 2g_{12}\mathrm{d}u^1\mathrm{d}u^2 + g_{22}(\mathrm{d}u^2)^2. \tag{6.69}$$

This quadratic form is called the *first fundamental form*. At regular points of the surface this form is positive definite, and we can define the *discriminant g of the first fundamental form* by

$$g = \begin{vmatrix} g_{11} & g_{12} \\ g_{21} & g_{22} \end{vmatrix} = g_{11}g_{22} - g_{12}^2 > 0. \tag{6.70}$$

It is easily seen that $|\mathbf{x}_1 \times \mathbf{x}_2|^2 = g$, so we have the following expression for the normal to R,

$$\mathbf{n} = \frac{\mathbf{x}_1 \times \mathbf{x}_2}{\sqrt{g}}.$$

We also define the components of the contravariant metric tensor by

$$g^{11} = g_{22}/g, \tag{6.71}$$

$$g^{12} = g^{21} = -g_{12}/g, \tag{6.72}$$

$$g^{22} = g_{11}/g. \tag{6.73}$$

The *second fundamental form*

$$b_{11}(\mathrm{d}u^1)^2 + 2b_{12}\mathrm{d}u^1\mathrm{d}u^2 + b_{22}(\mathrm{d}u^2)^2 \tag{6.74}$$

is defined by the coefficients

$$b_{11} = \mathbf{x}_{11}.\mathbf{n} = -\mathbf{x}_1.\mathbf{n}_1, \tag{6.75}$$

$$b_{12} = b_{21} = \mathbf{x}_{12}.\mathbf{n} = -\mathbf{x}_1.\mathbf{n}_2, \tag{6.76}$$

$$b_{22} = \mathbf{x}_{22}.\mathbf{n} = -\mathbf{x}_2.\mathbf{n}_2. \tag{6.77}$$

These coefficients are used to study the shape of the surface around any of its points. The *discriminant b of the second fundamental form* is defined as

$$b = \begin{vmatrix} b_{11} & b_{12} \\ b_{21} & b_{22} \end{vmatrix} = b_{11}b_{22} - b_{12}^2. \tag{6.78}$$

Now consider a point P on the surface S. A plane passing through P that contains the normal to S at P intersects the surface in a plane curve. Let κ denote the curvature at P of that plane curve. We consider the values of κ for all such planes. The maximum and minimum values of κ, say κ_1 and κ_2, are the *principal curvatures* of S at P. The directions of the corresponding planes are called principal directions. It can be shown that if a plane has an angle α with the principal direction corresponding to κ_1, then the curvature at P of the corresponding plane curve is given by

$$\kappa = \kappa_1 \cos^2\alpha + \kappa_2 \sin^2\alpha. \tag{6.79}$$

This is known as *Euler's Theorem*. In particular, the two principal directions are perpendicular. The *Gaussian curvature* K at P is defined to be the product

$$K = \kappa_1 \kappa_2 \tag{6.80}$$

of the two principal curvatures. It can be shown that

$$K = \frac{b}{g} \tag{6.81}$$

and also that

$$\sqrt{g}K = \pm[\mathbf{n}, \mathbf{n}_1, \mathbf{n}_2] = \pm\mathbf{n}.(\mathbf{n}_1 \times \mathbf{n}_2) \tag{6.82}$$

The *mean curvature* H at P is defined to be the arithmetic mean

$$H = \frac{\kappa_1 + \kappa_2}{2} \tag{6.83}$$

of the two principal curvatures. It can be shown that

$$H = \frac{1}{2}(b_{11}g^{11} + b_{22}g^{22} + 2b_{12}g^{12}). \tag{6.84}$$

Note that K and $|H|$ are independent of the choice of coordinates. A point P is called *hyperbolic* or a *saddle point* if $K < 0$, it is called *elliptic* if $K > 0$, and it is called *parabolic* if $\kappa = 0$ in exactly one direction (so one of the principal curvatures, and consequently $K = 0$ in that case). A point P is called a *parabolic umbilic* or a *flat point* if at P all the coefficients b_{11}, b_{22} and b_{12} of the second fundamental form vanish.

6.4.3 Curvature in Spherical Coordinates

In order to express curvature properties of reflector surfaces, we represent the surface in the usual spherical coordinates. Recall that these have to be handled with care when $t = 0$. We have $u^1 = t$, $u^2 = u$, and $\mathbf{x}(u^1, u^2) = \mathbf{r}(t, u) = f(t, u)\mathbf{v}(t, u)$ and we find

$$\begin{aligned} g_{11} &= f^2 + f_t^2, && (6.85)\\ g_{22} &= f^2 \sin^2 t + f_u^2, && (6.86)\\ g_{12} &= f_t f_u, && (6.87)\\ g &= f^2(f^2 \sin^2 t + f_t^2 \sin^2 t + f_u^2). && (6.88) \end{aligned}$$

To calculate the coefficients of the second fundamental form, we first note that

$$\mathbf{r}_{tt} = (f_{tt} - f)\mathbf{v} + 2f_t\mathbf{v}_t, \tag{6.89}$$

$$\mathbf{r}_{tu} = f_{tu}\mathbf{v} + f_u\mathbf{v}_t + (\frac{f}{\tan t} + f_t)\mathbf{v}_u, \tag{6.90}$$

$$\mathbf{r}_{tu} = (f_{uu} - f^2\sin^2 t)\mathbf{v} - f\cos t\sin t\,\mathbf{v}_t + 2f_t\mathbf{v}_u, \tag{6.91}$$

and we recall from (6.24) that

$$\mathbf{n} = \frac{f\sin t\,\mathbf{v} - f_t\sin t\,\mathbf{v}_t - \frac{f_u}{\sin t}\mathbf{v}_u}{\sqrt{f^2\sin^2 t + f_t^2\sin^2 t + f_u^2}}. \tag{6.92}$$

So we obtain

$$b_{11} = \mathbf{r}_{tt}.\mathbf{n} = \frac{(ff_{tt} - f^2 - 2f_t^2)\sin t}{\sqrt{f^2\sin^2 t + f_t^2\sin^2 t + f_u^2}}, \tag{6.93}$$

$$b_{12} = \mathbf{r}_{tu}.\mathbf{n} = \frac{ff_{tu}\sin t - ff_u\cos t - 2f_tf_u\sin t}{\sqrt{f^2\sin^2 t + f_t^2\sin^2 t + f_u^2}}, \tag{6.94}$$

$$b_{22} = \mathbf{r}_{uu}.\mathbf{n} = \frac{(ff_{uu} - 2f_u^2 + ff_t\cos t\sin t - f^2\sin^2 t)\sin t}{\sqrt{f^2\sin^2 t + f_t^2\sin^2 t + f_u^2}}. \tag{6.95}$$

And we find

$$\begin{aligned} b = \frac{f}{f^2\sin^2 t + f_t^2\sin^2 t + f_u^2}(& \\ & (f_{tt}f_{uu} - f_{tu}^2)f\sin^2 t + \\ & f_{tt}(f_tf\cos t\sin^3 t - f^2\sin^4 t - 2f_u^2\sin^2 t) + \\ & f_{tu}(2f_uf\cos t\sin t + 4f_tf_u\sin^2 t) + \\ & f_{uu}(-f^2\sin^2 t - 2f_t^2\sin^2 t) - \\ & 4f_tf_u^2\cos t\sin t + ff_u^2(3\sin^2 t - 1) - 2f_t^3\cos t\sin^3 t - \\ & f^2f_t\cos t\sin^3 t + 2ff_t^2\sin^4 t + f^3\sin^4 t). \end{aligned} \tag{6.96}$$

We have $K = b/g$, and for H we find the following expression

$$\begin{aligned} H = \frac{1}{2f(f^2\sin^2 t + f_t^2\sin^2 t + f_u^2)^{3/2}}(& \\ & f_{tt}(f^2\sin^3 t + f_u^2\sin t) + f_{uu}(f^2\sin t + f_t^2\sin t) + \\ & f_{tu}(-2f_tf_u\sin t) - 2f^3\sin^3 t + f_t^3\cos t\sin^2 t + \\ & 2f_tf_u^2\cos t - 3ff_u^2\sin t + f^2f_t\cos t\sin^2 t - 3ff_t^2\sin^3 t). \end{aligned} \tag{6.97}$$

Let us now look at some examples.

Example 6.4.4. Consider a sphere with radius ρ, i.e. $f(t,u) = \rho$ for all t and u. We find

$$g_{11} = \rho^2, \quad g_{12} = 0, \quad g_{22} = \rho^2 \sin^2 t, \quad g = \rho^2 \sin^2 t$$

and

$$b_{11} = -\rho, \quad b_{12} = 0, \quad b_{22} = -\rho \sin^2 t, \quad b = \rho^2 \sin^2 t.$$

So we have $K = 1/\rho^2$, $H = -1/\rho$, and consequently $\kappa_1 = \kappa_2 = -1/\rho$. □

Example 6.4.5. Consider the plane described by $f(t,u) = 1/\cos t$ for all t and u. We find

$$b_{11} = b_{12} = b_{22} = b = 0.$$

So we also have $K = H = \kappa_1 = \kappa_2 = 0$. This holds for any plane of course. □

Example 6.4.6. The cylindrical surface given by the equation $x^2 + y^2 = 1$ is described by

$$f(t,u) = \frac{1}{\sqrt{1 - \sin^2 t \cos^2 u}}.$$

Computations show $\kappa_1 = 0, \kappa_2 = -1$. □

Example 6.4.7. The parabola defined by $f(t,u) = 1/(2 + 2\cos t)$ has

$$\begin{aligned} g &= \frac{\sin^2 t}{8(1+\cos t)^5}, \\ b &= \frac{\sin^2 t}{8(1+\cos t)^3}, \\ K &= (1+\cos t)^2, \\ H &= -\frac{(3+\cos t)\sqrt{1+\cos t}}{4\sqrt{2}}, \\ \kappa_1 &= -\frac{(1+\cos t)^{(3/2)}}{\sqrt{2}}, \\ \kappa_2 &= -\sqrt{2+2\cos t}. \end{aligned}$$

□

Example 6.4.8. Consider the quadratic surface given by the equation

$$x = 1 + a_{11} y^2 + a_{12} yz + a_{22} z^2,$$

which is described by the function

$$f(t,u) = \frac{2}{\cos t + \sqrt{\cos^2 t - 4a(u)\sin^2 t}} \tag{6.98}$$

where

$$a(u) = a_{11}\cos^2 u + a_{12}\cos u \sin u + a_{22}\sin^2 u.$$

Then at the point $P = (1,0,0)$ (i.e. $t = 0$) we find (more easily by using carthesian rather than spherical coordinates)

$$\begin{aligned} K &= 4a_{11}a_{22} - a_{12}^2, \\ H &= a_{11} + a_{22}, \\ \kappa_1 &= a_{11} + a_{22} + \sqrt{(a_{11} - a_{22})^2 + a_{12}^2}, \\ \kappa_2 &= a_{11} + a_{22} - \sqrt{(a_{11} - a_{22})^2 + a_{12}^2}. \end{aligned}$$

□

6.4.4 The Wave Front

In this section we study the wave front of the reflected rays. We will see that the curvature of the wave front contains information on the intensity, as well as on the type of the ray path of the reflected light.

Let us follow a ray, emitted in direction (t,u), when it has travelled over a distance $\lambda \geq f(t,u)$. The position of the ray after it has travelled this distance is denoted $\mathbf{x}(\lambda)$. We have

$$\mathbf{x}(\lambda) = f\mathbf{v} + (\lambda - f)\mathbf{w}. \tag{6.99}$$

For each fixed λ, the vectors $\mathbf{x}(\lambda)$ as a function of t and u form a surface which is called the *wave front* at distance λ. An elementary but important property of the wave front is that the reflected rays $\mathbf{w}$ are normal to it.

Lemma 6.4.9. *If for a given λ, the wave front $\mathbf{x}(\lambda)$ is a differentiable surface, then the vector $\mathbf{w}$ is a normal to $\mathbf{x}(\lambda)$.*

Proof. We show that $\mathbf{x}(\lambda)_t.\mathbf{w} = \mathbf{x}(\lambda)_u.\mathbf{w} = 0$. We have

$$\mathbf{x}(\lambda)_t = f_t\mathbf{v} + f\mathbf{v}_t - f_t\mathbf{w} + (\lambda - f)\mathbf{w}_t, \tag{6.100}$$

so, keeping in mind that $\mathbf{w}$ is a unit vector, we obtain

$$\mathbf{x}(\lambda)_t.\mathbf{w} = f_t\mathbf{v}.\mathbf{w} + f\mathbf{v}_t.\mathbf{w} - f_t^2. \tag{6.101}$$

Using the expression (6.26) for $\mathbf{w}$, we find

$$\mathbf{v}.\mathbf{w} = \frac{-f^2 \sin^2 t + f_t^2 \sin^2 t + f_u^2}{f^2 \sin^2 t + f_t^2 \sin^2 t + f_u^2}, \tag{6.102}$$

$$\mathbf{v}_t.\mathbf{w} = \frac{2ff_t \sin^2 t}{f^2 \sin^2 t + f_t^2 \sin^2 t + f_u^2}, \tag{6.103}$$

$$\mathbf{v}_u.\mathbf{w} = \frac{2ff_u}{f^2 \sin^2 t + f_t^2 \sin^2 t + f_u^2}, \tag{6.104}$$

and elementary calculus shows that the right hand side of (6.101) vanishes. Similarly, it is shown that $\mathbf{x}(\lambda)_u.\mathbf{w} = 0$. □

Let us write $b_{11}(\lambda)$, $g_{11}(\lambda)$, $K(\lambda)$, etc. for the curvature and the coefficients of the fundamental forms of the wave front. From the above lemma, and from (6.82) it follows that

$$\sqrt{g(\lambda)}K(\lambda) = \pm[\mathbf{w}, \mathbf{w}_t, \mathbf{w}_u]. \tag{6.105}$$

Note that the right hand side of (6.105) is related to the intensity of the reflected light; cf. expression (6.42) in Section 6.2.3.

Let us now consider the wave front in direction (t, u) *immediately after reflection*. We define

$$\begin{aligned} \tilde{g}_{11} &= \lim_{\lambda \downarrow f} g_{11}(\lambda), \\ \tilde{b}_{11} &= \lim_{\lambda \downarrow f} b_{11}(\lambda), \\ \tilde{K} &= \lim_{\lambda \downarrow f} K(\lambda), \\ &\text{etc.} \end{aligned}$$

The curvatures $\tilde{K}, \tilde{H}, \tilde{\kappa}_1$ and $\tilde{\kappa}_2$ are called the (Gaussian, mean and principal) *curvatures of the wave front*. We are now ready to distinguish several types of ray paths.

Definition. A ray path is called *hyperbolic, elliptic* or *parabolic in* (t, u) if $\tilde{K} < 0$, $\tilde{K} > 0$ or $\tilde{K} = 0$ in (t, u), respectively. Note that this corresponds to the wave front $\mathbf{x}(\lambda)$ being hyperbolic, elliptic or parabolic in (t, u), immediately after reflection. We call a ray path *(globally) hyperbolic, elliptic* or *parabolic* if it is hyperbolic, elliptic or parabolic for all t and u. In the elliptic case, we can distinguish two cases (either locally or globally), depending on the signs of the principal curvatures $\tilde{\kappa}_1$ and $\tilde{\kappa}_2$. If both principal curvatures of the wave front are

Gaussian curvature	Signs of principal curvatures	Type of ray path
$\tilde{K} > 0$	$\tilde{\kappa}_1 > 0$ and $\tilde{\kappa}_2 > 0$	Elliptic, divergent
$\tilde{K} > 0$	$\tilde{\kappa}_1 < 0$ and $\tilde{\kappa}_2 < 0$	Elliptic, convergent
$\tilde{K} < 0$	$\tilde{\kappa}_1 > 0$ and $\tilde{\kappa}_2 < 0$	Hyperbolic
$\tilde{K} = 0$	$\tilde{\kappa}_1 = 0$ or $\tilde{\kappa}_2 = 0$	Parabolic

Table 6.1: *The types of ray paths corresponding to the principal curvatures of the wave front after reflection.*

positive, the ray path is called *divergent*. If both principal curvatures of the wave front are negative, the ray path is called *convergent*. See Table 6.1 for a summary of the types of ray paths. Let us consider some examples.

Example 6.4.10. Consider a sphere with radius ρ, i.e. $f(t, u) = \rho$ for all t and u. We then have

$$\mathbf{x}(\lambda) = (2\rho - \lambda)\mathbf{v}.$$

So we find $K(\lambda) = 1/(2\rho - \lambda)^2$, $H = -1/(2\rho - \lambda)$, and consequently $\kappa_1(\lambda) = \kappa_2(\lambda) = -1/(2\rho - \lambda)$. It follows that the corresponding ray path is globally convergent. □

Example 6.4.11. Consider the plane described by $f(t, u) = \rho/\cos t$ for all t and u. We find $K(\lambda) = 1/(2\rho - \lambda)^2$, $H = 1/(2\rho - \lambda)$, and consequently $\kappa_1(\lambda) = \kappa_2(\lambda) = 1/(2\rho - \lambda)$. It follows that the corresponding ray path is globally divergent. □

Example 6.4.12. For the parabola defined by $f(t, u) = 1/(2 + 2\cos t)$ we find

$$\mathbf{x}(\lambda) = (\lambda + 1/2, \frac{\sin t \cos u}{2 + 2\cos t}, \frac{\sin t \sin u}{2 + 2\cos t}),$$

so the wave front $\mathbf{x}(\lambda)$ lies in the plane $x = \lambda + 1/2$ and we find

$$K(\lambda) = H(\lambda) = \kappa_1(\lambda) = \kappa_2(\lambda) = 0$$

for all λ, so the ray path is parabolic. □

Now, recall from Section 6.2.3 that the intensity $G(\mathbf{w})$ of the reflected light in direction $\mathbf{w}$ can be expressed as

$$G(\mathbf{w}) = \frac{I(\mathbf{v}) \sin t}{|[\mathbf{w}, \mathbf{w}_t, \mathbf{w}_u]|}, \tag{6.106}$$

so from (6.105) we obtain

$$G(\mathbf{w}) = \frac{I(\mathbf{v}) \sin t}{|\tilde{K}|\sqrt{\tilde{g}}}. \tag{6.107}$$

From this we see the following.

Corollary 6.4.13. *The intensity $G(\mathbf{w})$ in direction $\mathbf{w}$ is infinitely large if and only if the ray path in that direction is parabolic. Furthermore, any ray path that has finite intensity in all directions, is globally hyperbolic, convergent or divergent.*

The latter part of this corollary follows from the observation that if the local type of the ray path is not the same for all (t, u), then one of the principal curvatures $\tilde{\kappa}_1, \tilde{\kappa}_2$ changes sign, so it has to be 0 at some point.

Caustics. It is well known that the curvature of the wave front is directly related to the caustics of the reflected bundle: the caustic surface is formed by the locus of the principal centres of curvature of the wave front! We won't go into that here however, and refer the interested reader to e.g. [37].

6.4.5 Curvatures of the Wave Front in Terms of the Reflector

We have seen that the principal curvatures of the wave front right after reflection determine both the intensity and the type of the reflected ray paths. We therefore want to express these in terms of the function f that describes the reflector surface. Next, we relate the principal curvatures of the wave front to those of the reflector surface.

Lemma 6.4.14. *The coefficients of the fundamental forms of the wave front are*

$$\tilde{g}_{11} = f^2, \tag{6.108}$$

$$\tilde{g}_{22} = f^2 \sin^2 t, \tag{6.109}$$

$$\tilde{g}_{12} = 0, \tag{6.110}$$

$$\tilde{b}_{11} = \frac{f(2ff_{tt}\sin^2 t - f^2\sin^2 - 3f_t^2\sin^2 t + f_u^2)}{f^2\sin^2 t + f_t^2\sin^2 t + f_u^2}, \tag{6.111}$$

$$\tilde{b}_{12} = \frac{2f\sin t\,(ff_{tu}\sin t - 2f_t f_u \sin t - ff_u\cos t)}{f^2\sin^2 t + f_t^2\sin^2 t + f_u^2}, \tag{6.112}$$

$$\tilde{b}_{22} = \frac{f\sin^2 t\,(2ff_{uu} + 2ff_t\cos t\sin t + (f_t^2 - f^2)\sin^2 t - 3f_u^2)}{f^2\sin^2 t + f_t^2\sin^2 t + f_u^2}, \tag{6.113}$$

which gives

$$\tilde{g} = f^4\sin^2 t, \tag{6.114}$$

$$
\begin{aligned}
\tilde{b} \;=\; & \frac{f^2 \sin^2 t}{(f^2 \sin^2 t + f_t^2 \sin^2 t + f_u^2)^2}(\\
& (f_{tt} f_{uu} - f_{tu}^2) 4 f^2 \sin^2 t + \\
& f_{tt}(4 f_t f^2 \cos t \sin^3 t - 2 f^3 \sin^4 t - 6 f f_u^2 \sin^2 t + 2 f f_t^2 \sin^4 t) + \\
& f_{tu}(8 f^2 f_u \cos t \sin t + 16 f f_t f_u \sin^2 t) + \\
& f_{uu}(-2 f^3 \sin^2 t - 6 f f_t^2 \sin^2 t + 2 f f_u^2) - \\
& 3 f_u^4 - 4 f^2 f_u^2 \cos^2 t - 14 f f_t f_u^2 \cos t \sin t + 2 f^2 f_u^2 \sin^2 t - \\
& 6 f_t^2 f_u^2 \sin^2 t - 2 f^3 f_t \cos t \sin^3 t - 6 f f_t^3 \cos t \sin^3 t + \\
& f^4 \sin^4 t + 2 f^2 f_t^2 \sin^4 t - 3 f_t^4 \sin^4 t), \qquad (6.115)
\end{aligned}
$$

$$
\tilde{H} \;=\; \frac{f_{uu} + f_{tt} \sin^2 t + f_t \cos t \sin t}{f^2 \sin^2 t + f_t^2 \sin^2 t + f_u^2} - \frac{1}{f}. \qquad (6.116)
$$

Proof. We only prove the expressions for $\tilde{g}_{11}$ and $\tilde{b}_{11}$, the others are proven similarly. We have

$$
\begin{aligned}
\tilde{g}_{11} &= g_{11}(\lambda)_{|\lambda=f} = (\mathbf{x}(\lambda)_t . \mathbf{x}(\lambda)_t)_{|\lambda=f} \\
&= (f_t \mathbf{v} + f \mathbf{v}_t - f_t \mathbf{w} + (\lambda - f)\mathbf{w}_t) . (f_t \mathbf{v} + f \mathbf{v}_t - f_t \mathbf{w} + (\lambda - f)\mathbf{w}_t)_{|\lambda=f} \\
&= f^2 + 2 f_t^2 - 2 f_t^2 (\mathbf{v}.\mathbf{w}) - 2 f f_t (\mathbf{v}_t . \mathbf{w}).
\end{aligned}
$$

Using (6.102) and (6.103) then gives the above result for $\tilde{g}_{11}$. To compute $\tilde{b}_{11}$, we use the right hand side of (6.75) and Lemma 6.4.9 and we find

$$
\begin{aligned}
\tilde{b}_{11} &= b_{11}(\lambda)_{|\lambda=f} = -(\mathbf{x}(\lambda)_t . -\mathbf{w}_t)_{|\lambda=f} \\
&= f_t (\mathbf{v}.\mathbf{w}_t) + f(\mathbf{v}_t . \mathbf{w}_t).
\end{aligned}
$$

The rest then follows from straightforward but tedious calculations. □

The Monge-Ampère equation. Now recall that a reflector surface described by a function f produces the required far field pattern if and only if (6.107) holds, that is if

$$
\frac{I(\mathbf{v}) \sin t}{G(\mathbf{w})} = |\tilde{K}| \sqrt{\tilde{g}},
$$

which by definition of $\tilde{K}$ can be written as

$$
\frac{I(\mathbf{v}) \sin t}{G(\mathbf{w})} \sqrt{\tilde{g}} = |\tilde{b}|.
$$

So, using the above expressions for $\tilde{b}$ and $\tilde{g}$ we obtain the Monge-Ampère equation, as given in the next proposition.

Proposition 6.4.15. *The reflector surface described by the function f produces the far field G when combined with a source of luminous intensity I if and only if*

$$\begin{aligned}\frac{I(\mathbf{v})}{G(\mathbf{w})} = \frac{1}{(f^2\sin^2 t + f_t^2\sin^2 t + f_u^2)^2}(& \\ (f_{tt}f_{uu} - f_{tu}^2)4f^2\sin^2 t + & \\ f_{tt}(4f_t f^2\cos t\sin^3 t - 2f^3\sin^4 t - 6ff_u^2\sin^2 t + 2ff_t^2\sin^4 t) + & \\ f_{tu}(8f^2 f_u\cos t\sin t + 16ff_t f_u\sin^2 t) + & \\ f_{uu}(-2f^3\sin^2 t - 6ff_t^2\sin^2 t + 2ff_u^2) - & \\ 3f_u^4 - 4f^2 f_u^2\cos^2 t - 14ff_t f_u^2\cos t\sin t + 2f^2 f_u^2\sin^2 t - & \\ 6f_t^2 f_u^2\sin^2 t - 2f^3 f_t\cos t\sin^3 t - 6ff_t^3\cos t\sin^3 t + & \\ f^4\sin^4 t + 2f^2 f_t^2\sin^4 t - 3f_t^4\sin^4 t). & \end{aligned} \tag{6.117}$$

Relating curvatures of the wave front to those of the reflector. Note that in both the expressions for b and for $\tilde{b}$ the quadratic term of the second order partial derivatives of f is of the form

$$f_{tt}f_{uu} - f_{tu}^2.$$

Since both K and $\tilde{K}$ have these same highest order terms, we can derive the following relation between K and $\tilde{K}$

$$\tilde{K} - 4K = \frac{2\tilde{H}}{f} - \frac{1}{f^2}. \tag{6.118}$$

Using $K = \kappa_1\kappa_2$, $\tilde{K} = \tilde{\kappa}_1\tilde{\kappa}_2$ and $\tilde{H} = \frac{1}{2}(\tilde{\kappa}_1 + \tilde{\kappa}_2)$, we obtain the following result.

Corollary 6.4.16. *The principal curvatures of the reflector and those of the wave front are related by*

$$(\tilde{\kappa}_1 - \frac{1}{f})(\tilde{\kappa}_2 - \frac{1}{f}) = 4\kappa_1\kappa_2. \tag{6.119}$$

As we did in the 2D case in Corollary 6.4.3, we would like to express the principal curvatures of the wave front in terms of those of the reflector surface. This is particularly easy in the case in directions where the reflector surface is perpendicular to the incident ray.

Proposition 6.4.17. *If the reflector surface is perpendicular to the incident ray in a certain direction, i.e. if $f_t = f_u = 0$ for a pair (t, u), then we have*

$$\tilde{\kappa}_1 = \frac{1}{f} + 2\kappa_1, \ \tilde{\kappa}_2 = \frac{1}{f} + 2\kappa_2. \tag{6.120}$$

Proof. If $f_t = f_u = 0$, then we have

$$\begin{aligned} H &= -\frac{1}{f} + \frac{f_{tt}\sin^2 t + f_{uu}}{2f^2 \sin^2 t}, \\ \tilde{H} &= -\frac{1}{f} + \frac{f_{tt}\sin^2 t + f_{uu}}{f^2 \sin^2 t}, \end{aligned}$$

so

$$\tilde{H} = \frac{1}{f} + 2H.$$

In terms of the principal curvatures, this implies

$$\tilde{\kappa}_1 + \tilde{\kappa}_2 = \frac{2}{f} + 2\kappa_1 + 2\kappa_2.$$

When we combine this equation with (6.119), we obtain the required result. □

Let us consider a few more examples.

Example 6.4.18. The cylindrical surface given by the equation $x^2 + y^2 = 1$ and described by

$$f(t, u) = \frac{1}{\sqrt{1 - \sin^2 t \cos^2 u}}$$

has $\tilde{H} = 0$, which is fairly easily computed from (6.116). So $\tilde{\kappa}_2 = -\tilde{\kappa}_1$. Note that $\kappa_1 = 0$, so from (6.119) we see that

$$\tilde{\kappa}_1 = 1/f = \sqrt{1 - \sin^2 t \cos^2 u} = -\tilde{\kappa}_2.$$

Note that $\tilde{K} = -1/f^2$, so the ray path is hyperbolic. □

Example 6.4.19. Consider again the quadratic surface given by the equation $x = 1 + a_{11}y^2 + a_{12}yz + a_{22}z^2$, described by the function

$$f(t, u) = \frac{2}{\cos t + \sqrt{\cos^2 t - 4a(u)\sin^2 t}}$$

where

$$g(u) = a_{11}\cos^2 u + a_{12}\cos u \sin u + a_{22}\sin^2 u.$$

Then at the point $P = (1, 0, 0)$ (i.e. $t = 0$) we find

$$\begin{aligned} \tilde{K} &= (1 + 4a_{11})(1 + 4a_{22}) - 4a_{12}^2, \\ \tilde{H} &= 1 + 2a_{11} + 2a_{22}, \\ \tilde{\kappa}_1 &= 1 + 2\kappa_1, \\ \tilde{\kappa}_2 &= 1 + 2\kappa_2. \end{aligned}$$

Note that the values for the principal curvatures follow directly from Proposition 6.4.17. □

Unlike the special case of perpendicular incidence of Proposition 6.4.17, in general we cannot nicely express the principal curvatures of the wave front explicitly in terms of those of the reflector. However, the following section shows that if we consider a more appropriate choice of curvatures of normal sections of the surface, then we can do better.

6.5 Equivalence of Definitions

In this section we introduce the parallel and normal curvatures of the reflector and the wave front. These notions have been used for the description of the wave front before and after refraction or reflection in e.g. Stavroudis [37]. They enable us to relate the curvatures of the wave front to those of the reflector in a convenient way. They also pave the way to show the equivalence of the different definitions of the types of ray paths that we gave in the previous two sections; this will be the subject of the final subsection of this section.

First we will consider the ray path in the neighborhood of a given point and introduce a natural coordinate system and corresponding parametrization of the surface. In the next section we introduce the parallel and normal curvature, and will show how they relate to the principal curvatures.

6.5.1 Plane of Incidence; a New Coordinate System

Let $\mathbf{x}_0$ be a point on the reflector surface, and let $\mathbf{v}_0 = \mathbf{x}_0/||\mathbf{x}_0||$ be the unit vector in the direction of $\mathbf{x}_0$. Let $\mathbf{n}_0$ be the normal to the reflector surface at $\mathbf{x}_0$, and let α_0 be the angle between $\mathbf{v}_0$ and $\mathbf{n}_0$. Let us assume that $\alpha_0 \neq 0$, i.e. that the incident ray $\mathbf{v}_0$ is not perpendicular to the reflector surface. The plane through the point $\mathbf{x}_0$ that contains the vectors $\mathbf{v}_0$ and $\mathbf{n}_0$ is called the *plane of incidence*, or the *parallel plane*. A normal to this plane is given by the vector

$$\mathbf{v}_\perp = \frac{\mathbf{n}_0 \times \mathbf{v}_0}{||\mathbf{n}_0 \times \mathbf{v}_0||}. \tag{6.121}$$

The plane through $\mathbf{x}_0$ parallel to $\mathbf{v}_\perp$ and $\mathbf{n}_0$ is called the *normal plane*. We also introduce the vector $\mathbf{v}_\parallel$, which lies in the plane of incidence and is perpendicular to $\mathbf{v}_0$, by

$$\mathbf{v}_\parallel = \mathbf{v}_\perp \times \mathbf{v}_0. \tag{6.122}$$

The three vectors $\mathbf{v}_0$, $\mathbf{v}_\parallel$ and $\mathbf{v}_\perp$ form an orthonormal basis, and we can describe the reflector surface around $\mathbf{x}_0$ in coordinates on this basis as follows,

$$\mathbf{x} = h(\beta, \gamma)\mathbf{v}_0 + \beta\mathbf{v}_\parallel + \gamma\mathbf{v}_\perp \tag{6.123}$$

for some positive function h of the parameters β and γ in some interval $[-\epsilon, \epsilon]$. It turns out that with this parametrization of the surface, expressions for the curvature have a simple form. Indeed, we have

$$\begin{aligned}
\mathbf{x}_\beta &= h_\beta \mathbf{v}_0 + \mathbf{v}_\parallel, \\
\mathbf{x}_\gamma &= h_\gamma \mathbf{v}_0 + \mathbf{v}_\perp, \\
\mathbf{x}_{\beta\beta} &= h_{\beta\beta}\mathbf{v}_0, \\
\mathbf{x}_{\gamma\gamma} &= h_{\gamma\gamma}\mathbf{v}_0, \\
\mathbf{x}_{\beta\gamma} &= h_{\beta\gamma}\mathbf{v}_0, \\
g_{11} &= 1 + h_\beta^2, \\
g_{22} &= 1 + h_\gamma^2, \\
g_{12} &= h_\beta h_\gamma, \\
g &= 1 + h_\beta^2 + h_\gamma^2.
\end{aligned}$$

The normal to the surface is given by

$$\mathbf{n} = \frac{\mathbf{x}_\beta \times \mathbf{x}_\gamma}{||\mathbf{x}_\beta \times \mathbf{x}_\gamma||} = \frac{\mathbf{v}_0 - h_\beta \mathbf{v}_\parallel - h_\gamma \mathbf{v}_\perp}{\sqrt{1 + h_\beta^2 + h_\gamma^2}}. \tag{6.124}$$

Note that we have $\mathbf{n}_0.\mathbf{v}_\perp = 0$, so for $\beta = \gamma = 0$, we have

$$h_\gamma(0, 0) = 0, \tag{6.125}$$

and for the angle between the incident ray and the normal at $\mathbf{x}_0$ we have

$$\cos\alpha_0 = \mathbf{v}_0.\mathbf{n}_0 = 1/\sqrt{1 + h_\beta^2(0, 0)}. \tag{6.126}$$

For the coefficients of the second fundamental form we obtain

$$b_{11} = \mathbf{x}_{\beta\beta}.\mathbf{n} = h_{\beta\beta}/\sqrt{1 + h_\beta^2 + h_\gamma^2},$$

$$
\begin{aligned}
b_{22} &= \mathbf{x}_{\gamma\gamma}.\mathbf{n} = h_{\gamma\gamma}/\sqrt{1+h_\beta^2+h_\gamma^2}, \\
b_{12} &= \mathbf{x}_{\beta\gamma}.\mathbf{n} = h_{\beta\gamma}/\sqrt{1+h_\beta^2+h_\gamma^2}, \\
b &= \frac{h_{\beta\beta}h_{\gamma\gamma}-h_{\beta\gamma}^2}{1+h_\beta^2+h_\gamma^2}.
\end{aligned}
$$

So for the Gaussian and mean curvature of the surface we find

$$
K = \frac{h_{\beta\beta}h_{\gamma\gamma}-h_{\beta\gamma}^2}{(1+h_\beta^2+h_\gamma^2)^2}, \tag{6.127}
$$

$$
H = \frac{h_{\beta\beta}(1+h_\gamma^2)+h_{\gamma\gamma}(1+h_\beta^2)-2h_{\beta\gamma}h_\beta h_\gamma}{2(1+h_\beta^2+h_\gamma^2)^{3/2}}. \tag{6.128}
$$

6.5.2 Parallel and Normal Curvature

Consider the intersection of the incident plane with the reflector surface. This intersection is a curve $C_\parallel$ that contains the point $\mathbf{x}_0$. The curvature of this curve at $\mathbf{x}_0$ is called the *parallel curvature* and denoted $\kappa_\parallel$. Analogously, the intersection of the normal plane with the surface is a curve $C_\perp$, and its curvature at $\mathbf{x}_0$ is called the *normal curvature* and denoted $\kappa_\perp$. These curvatures are related to the principal curvatures by

$$
H = \frac{\kappa_1+\kappa_2}{2} = \frac{\kappa_\parallel+\kappa_\perp}{2}, \tag{6.129}
$$

$$
K = \kappa_1\kappa_2 = \kappa_\parallel\kappa_\perp - \tau^2, \tag{6.130}
$$

where τ is the torsion of a geodesic curve through $\mathbf{x}_0$, see [37, p. 149, 182-185]. Note that when we consider the matrix

$$
\begin{pmatrix} \kappa_\parallel & \tau \\ \tau & \kappa_\perp \end{pmatrix} \tag{6.131}
$$

then K and H are the determinant and trace of the matrix respectively, while the principal curvatures κ_1 and κ_2 are its eigenvalues.

Let us now calculate the parallel and normal curvatures.

Lemma 6.5.1. *The parallel and normal curvatures and torsion τ at $\mathbf{x}_0$ are given by*

$$
\kappa_\parallel = \frac{h_{\beta\beta}}{(1+h_\beta^2)^{3/2}}\Big|_{\beta=\gamma=0}, \tag{6.132}
$$

$$\kappa_\perp = \frac{h_{\gamma\gamma}}{(1+h_\beta^2)^{1/2}}\Big|_{\beta=\gamma=0}, \tag{6.133}$$

$$\tau = \frac{h_{\beta\gamma}}{(1+h_\beta^2)}\Big|_{\beta=\gamma=0}. \tag{6.134}$$

Proof. We first calculate the parallel curvature. The incident plane consists of vectors of the form

$$\mu\mathbf{v}_0 + \nu\mathbf{v}_\parallel,$$

for any $\mu, \nu \in \mathbb{R}$. Its intersection with the surface as given by (6.123) is the curve

$$C_\parallel(\beta) = h(\beta, 0)\mathbf{v}_0 + \beta\mathbf{v}_\parallel. \tag{6.135}$$

The curvature $K(C)$ of this curve is

$$K(C) = \frac{\sqrt{(C'.C')(C''.C'') - (C'.C'')^2}}{(C'.C')^{3/2}},$$

where $C' = \frac{\partial}{\partial\beta}h(\beta, 0)\mathbf{v}_0 + \mathbf{v}_\parallel$ and $C'' = \frac{\partial^2}{\partial\beta^2}h(\beta, 0)\mathbf{v}_0$. It follows that $C'.C' = 1 + h_\beta^2$, $C''.C'' = h_{\beta\beta}^2$ and $C'.C'' = h_\beta h_{\beta\beta}$, so we obtain

$$\kappa_\parallel = \frac{h_{\beta\beta}}{(1+h_\beta^2)^{3/2}}\Big|_{\beta=\gamma=0}. \tag{6.136}$$

To obtain the expression for $\kappa_\perp$, first note that $h_\gamma(0, 0) = 0$, so from (6.128) we find

$$H_{|\beta=\gamma=0} = \frac{h_{\beta\beta} + h_{\gamma\gamma}(1+h_\beta^2)}{2(1+h_\beta^2)^{3/2}}\Big|_{\beta=\gamma=0}.$$

The result for $\kappa_\perp$ then follows from (6.129). The expression for τ then follows from the above and from (6.127) and (6.130). □

6.5.3 Reflected Rays in the New Coordinates

We now study reflection, and its effect on wave front curvatures, in terms of the coordinate system introduced in Section 6.5.1.

Let $\mathbf{w}_0$ be the direction of ray $\mathbf{v}_0$ after reflection, as usual given by

$$\mathbf{w}_0 = \mathbf{v}_0 - 2(\mathbf{v}_0.\mathbf{n}_0)\mathbf{n}_0. \tag{6.137}$$

Let us now also introduce an orthonormal basis for the reflected wave front as follows. Let

$$\mathbf{w}_{\|} = \mathbf{v}_{\|} - 2(\mathbf{v}_{\|}.\mathbf{n}_0)\mathbf{n}_0, \tag{6.138}$$

$$\mathbf{w}_{\perp} = \mathbf{v}_{\perp} - 2(\mathbf{v}_{\perp}.\mathbf{n}_0)\mathbf{n}_0 = \mathbf{v}_{\perp}. \tag{6.139}$$

Then by definition $\mathbf{w}_{\|}$ lies in the plane of incidence and $\mathbf{w}_{\perp}$ lies in the normal plane, and $\mathbf{w}_0$, $\mathbf{w}_{\|}$ and $\mathbf{w}_{\perp}$ form an orthonormal basis. We are interested in the curvatures of the wave front after reflection. As above, we define the *parallel and normal curvature of the wave front* as the curvature at $\mathbf{x}_0$ of the curve obtained by taking the intersection of the surface with the parallel and normal plane, respectively. They are denoted $\tilde{\kappa}_{\|}$ and $\tilde{\kappa}_{\perp}$, respectively. Again we have

$$\tilde{H} = \frac{\tilde{\kappa}_1 + \tilde{\kappa}_2}{2} = \frac{\tilde{\kappa}_{\|} + \tilde{\kappa}_{\perp}}{2}, \tag{6.140}$$

$$\tilde{K} = \tilde{\kappa}_1\tilde{\kappa}_2 = \tilde{\kappa}_{\|}\tilde{\kappa}_{\perp} - \tilde{\tau}^2, \tag{6.141}$$

where $\tilde{\tau}$ is the torsion of a geodesic curve through $\mathbf{x}_0$, see [37, p. 149, 182-185]. See this same reference or [5] for a proof of the following proposition, which relates the parallel and normal curvatures of the wave front to those of the reflector. Both references show a stronger result that also incorporates refraction, and arbitrary incident wave fronts.

Proposition 6.5.2. *We have the following relations between the curvatures of the reflector and the wave front,*

$$\tilde{\kappa}_{\|} = \frac{1}{h} + \frac{2}{(\mathbf{v}.\mathbf{n})}\kappa_{\|}, \tag{6.142}$$

$$\tilde{\kappa}_{\perp} = \frac{1}{h} + 2(\mathbf{v}.\mathbf{n})\kappa_{\perp}, \tag{6.143}$$

$$\tilde{\tau} = 2\tau. \tag{6.144}$$

Note that $\frac{1}{h}$ is actually the parallel or normal curvature of the (spherical) incident wave front. So, for $\beta = \gamma = 0$, we have

$$\tilde{\kappa}_{\|} = \frac{1}{h} + \frac{2h_{\beta\beta}}{1 + h_{\beta}^2}, \tag{6.145}$$

$$\tilde{\kappa}_{\perp} = \frac{1}{h} + \frac{2h_{\gamma\gamma}}{1 + h_{\beta}^2}, \tag{6.146}$$

$$\tilde{\tau} = \frac{2h_{\beta\gamma}}{1 + h_{\beta}^2}. \tag{6.147}$$

We now give a result that will prove to be useful to understand the types of ray paths in terms of the mapping between incident and reflected rays.

Proposition 6.5.3. *At* $\mathbf{x}_0$, *i.e. for* $\beta = \gamma = 0$, *we have*

$$\begin{pmatrix} \mathbf{w}_\beta \\ \mathbf{w}_\gamma \end{pmatrix} = \begin{pmatrix} \tilde{\kappa}_\parallel & \tilde{\tau} \\ \tilde{\tau} & \tilde{\kappa}_\perp \end{pmatrix} \begin{pmatrix} \mathbf{w}_\parallel \\ \mathbf{w}_\perp \end{pmatrix}. \tag{6.148}$$

Proof. First we write $\mathbf{w}$ on the basis $\mathbf{v}_0$, $\mathbf{v}_\parallel$ and $\mathbf{v}_\perp$. We find

$$\begin{aligned} \mathbf{w} = & \frac{1}{(1+h_\beta^2+h_\gamma^2)\sqrt{h^2+\beta^2+\gamma^2}}(\\ & (h(-1+h_\beta^2+h_\gamma^2)+2\beta h_\beta+2\gamma h_\gamma)\mathbf{v}_0 + \\ & (\beta(1-h_\beta^2+h_\gamma^2)+2hh_\beta-2\gamma h_\beta h_\gamma)\mathbf{v}_\parallel + \\ & (\gamma(1+h_\beta^2-h_\gamma^2)+2hh_\gamma-2\beta h_\beta h_\gamma)\mathbf{v}_\perp). \end{aligned} \tag{6.149}$$

Taking derivatives and inserting $\beta = \gamma = 0$ gives

$$\begin{aligned} \mathbf{w}_\beta = & \frac{2h_\beta(1+h_\beta^2+2hh_{\beta\beta})}{h(1+h_\beta^2)^2}\mathbf{v}_0 + \frac{(1-h_\beta^2)(1+h_\beta^2+2hh_{\beta\beta})}{h(1+h_\beta^2)^2}\mathbf{v}_\parallel + \\ & \frac{2h_{\beta\gamma}}{1+h_\beta^2}\mathbf{v}_\perp, \end{aligned} \tag{6.150}$$

$$\mathbf{w}_\gamma = \frac{4h_\beta h_{\beta\gamma}}{(1+h_\beta^2)^2}\mathbf{v}_0 + \frac{2(1-h_\beta^2)h_{\beta\gamma}}{(1+h_\beta^2)^2}\mathbf{v}_\parallel + (\frac{1}{h}+\frac{2h_{\gamma\gamma}}{1+h_\beta^2})\mathbf{v}_\perp, \tag{6.151}$$

while for $\mathbf{w}_0$, $\mathbf{w}_\parallel$, $\mathbf{w}_\perp$ we have (where again all functions are evaluated at $\beta = \gamma = 0$),

$$\begin{aligned} \mathbf{w}_0 &= \frac{-1+h_\beta^2}{1+h_\beta^2}\mathbf{v}_0 + \frac{2h_\beta}{1+h_\beta^2}\mathbf{v}_\parallel, \\ \mathbf{w}_\parallel &= \frac{2h_\beta}{1+h_\beta^2}\mathbf{v}_0 + \frac{1-h_\beta^2}{1+h_\beta^2}\mathbf{v}_\parallel, \\ \mathbf{w}_\perp &= \mathbf{v}_\perp. \end{aligned}$$

We can now easily express $\mathbf{w}_\beta$ and $\mathbf{w}_\gamma$ on the basis $\mathbf{w}_0$, $\mathbf{w}_\parallel$, $\mathbf{w}_\perp$ by taking inproducts, and the proposition follows. □

Perpendicular incidence. Note that in this section and in the previous one, so far we have only considered the case that the incident ray is not perpendicular to the reflector surface, because otherwise the incident plane would not be well-defined. Note however, that for perpendicular incidence we could choose any pair

of mutually perpendicular planes that contain $\mathbf{x}_0$ and $\mathbf{n}_0$, and choose vectors $\mathbf{v}_\parallel$ and $\mathbf{v}_\perp$ in these planes such that $\mathbf{v}_0$, $\mathbf{v}_\parallel$ and $\mathbf{v}_\perp$ form an orthonormal basis. Then all the above results carry over to this situation. In particular, we can choose the planes such that they are precisely the planes of the principal directions. The curvatures $\tilde{\kappa}_\parallel$ and $\tilde{\kappa}_\perp$ are then equal to the principal curvatures $\tilde{\kappa}_1$ and $\tilde{\kappa}_2$, and Proposition 6.5.2 is then clearly a generalization of Proposition 6.4.17.

6.5.4 Equivalence of Definitions of Ray Path Types

Let us now recall that in Section 6.4 we had defined a ray path to be hyperbolic or elliptic, depending on whether $\tilde{K}$ is negative or positive (the parabolic case that $\tilde{K} = 0$ results in infinite far field intensities and can be ignored). Moreover in the elliptic case we can distinguish divergent and convergent ray paths, depending on whether $\tilde{\kappa}_1$ and $\tilde{\kappa}_2$ are both positive or both negative. Under some additional constraints, we introduced the same notions in terms of fixed and antipodal point properties in Section 6.3. We now show that locally, the two different definitions are equivalent.

Now, from Proposition 6.5.3 it follows that we have the following linear approximation of $\mathbf{w}$ in terms of β and γ around $\mathbf{w}_0$, i.e., the Taylor expansion of $\mathbf{w}$ around $\beta = \gamma = 0$ ignoring $O(|\beta|^2 + |\gamma|^2)$ terms and higher,

$$\mathbf{w} \approx \mathbf{w}_0 + (\beta, \gamma) \begin{pmatrix} \tilde{\kappa}_\parallel & \tilde{\tau} \\ \tilde{\tau} & \tilde{\kappa}_\perp \end{pmatrix} \begin{pmatrix} \mathbf{w}_\parallel \\ \mathbf{w}_\perp \end{pmatrix}. \tag{6.152}$$

Let us write

$$M := \begin{pmatrix} \tilde{\kappa}_\parallel & \tilde{\tau} \\ \tilde{\tau} & \tilde{\kappa}_\perp \end{pmatrix}. \tag{6.153}$$

Recall that the principal curvatures of the wave front are the eigenvalues of M, and that the Gaussian curvature of the wave front equals the determinant of M. Let us now introduce spherical coordinates for incident and reflected rays around $\mathbf{x}_0$. We write

$$\mathbf{x} = g(t, u)(\cos t\, \mathbf{v}_0 + \sin t \cos u\, \mathbf{v}_\parallel + \sin t \sin u\, \mathbf{v}_\perp) \tag{6.154}$$

for $t \in [0, t_1]$ and $u \in [0, 2\pi]$. So we have

$$h(\beta, \gamma) = g(t, u) \cos t, \tag{6.155}$$

$$\beta = g(t, u) \sin t \cos u, \tag{6.156}$$

$$\gamma = g(t, u) \sin t \sin u. \tag{6.157}$$

Furthermore, let $\theta(t, u)$ and $\phi(t, u)$ be functions such that

$$\mathbf{w}(t, u) = \cos\theta(t, u)\mathbf{w}_0 + \sin\theta(t, u)\cos\phi(t, u)\mathbf{w}_{\|} + \sin\theta(t, u)\sin\phi(t, u)\mathbf{w}_{\perp}. \tag{6.158}$$

We then have the following result.

Theorem 6.5.4. *For t small enough, we have*

$$\operatorname{sign}(\frac{\partial}{\partial u}\phi(t, u)) = \operatorname{sign}\tilde{K}. \tag{6.159}$$

In particular this shows that locally, the definitions for elliptic and hyperbolic ray paths in terms of the curvature of the wave front, and in terms of fixed points of the mapping $(t, u) \to (\theta, \phi)$ as given in Section 6.3 are equivalent.

Proof. We have the Taylor expansion of $\mathbf{w}$ with respect to β and γ as follows,

$$\mathbf{w} = \mathbf{w}_0 + (\beta, \gamma)M\begin{pmatrix} \mathbf{w}_{\|} \\ \mathbf{w}_{\perp} \end{pmatrix} + O(|\beta|^2 + |\gamma|^2).$$

It follows that for $t = 0$ (so $\beta = \gamma = 0$) we have

$$\mathbf{w}_t = g_0(\cos u, \sin u)M\begin{pmatrix} \mathbf{w}_{\|} \\ \mathbf{w}_{\perp} \end{pmatrix},$$

where $g_0 = g(0, 0)$. So the Taylor expansion of $\mathbf{w}$ around $t = 0$ gives

$$\mathbf{w} = \mathbf{w}_0 + g_0(\cos u, \sin u)M\begin{pmatrix} \mathbf{w}_{\|} \\ \mathbf{w}_{\perp} \end{pmatrix} t + O(t^2).$$

Comparing this expression with (6.158), we find

$$\cos\theta = 1 + O(t^2) \tag{6.160}$$

$$\sin\theta\cos\phi = g_0(\tilde{\kappa}_{\|}\cos u + \tilde{\tau}\sin u)t + O(t^2) \tag{6.161}$$

$$\sin\theta\sin\phi = g_0(\tilde{\kappa}_{\perp}\sin u + \tilde{\tau}\cos u)t + O(t^2). \tag{6.162}$$

It follows from (6.161) and (6.162) that

$$\tan\phi = \frac{(\tilde{\kappa}_{\perp}\sin u + \tilde{\tau}\cos u)g_0 t + O(t^2)}{(\tilde{\kappa}_{\|}\cos u + \tilde{\tau}\sin u)g_0 t + O(t^2)} = \frac{\tilde{\kappa}_{\perp}\sin u + \tilde{\tau}\cos u}{\tilde{\kappa}_{\|}\cos u + \tilde{\tau}\sin u} + O(t)$$

so

$$\phi = \arctan(\frac{\tilde{\kappa}_{\perp}\sin u + \tilde{\tau}\cos u}{\tilde{\kappa}_{\|}\cos u + \tilde{\tau}\sin u}) + O(t),$$

and

$$\phi'(u) = \frac{\tilde{\kappa}_{\|}\tilde{\kappa}_{\perp} - \tilde{\tau}^2}{(\tilde{\kappa}_{\perp}\sin u + \tilde{\tau}\cos u)^2 + (\tilde{\kappa}_{\|}\cos u + \tilde{\tau}\sin u)^2} + O(t).$$

Since the denominator of this expression is positive, and the numerator equals $\tilde{K}$, this proves the proposition. □

So, we have seen that locally, the two definitions for hyperbolic and elliptic ray paths are equivalent. In the elliptic case, we can distinguish between convergent and divergent ray paths. It is easily seen that if the eigenvalues of M are both positive or both negative, then the function ϕ has fixed or antipodal points in the directions corresponding to the eigenvectors of M, respectively. This shows the equivalence for all three types locally.

In the wave front definition, we have seen that local definitions extend to global definitions easily (Corollary 6.4.13). Similarly, we would also like to show that if the function $\phi(t, u)$ has a certain behaviour in terms of fixed points for t small enough, then it should have that behaviour for all t (of course, under the usual condition that ϕ comes from a one-to-one reflector mapping). It can be shown using results from homotopy theory, that the sign of $\frac{\partial}{\partial u}\phi(t, u)$ cannot be different for two different values for t, because that would correspond to curves with different winding numbers. This argument then shows that we have global fixed point properties corresponding to elliptic and hyperbolic types.

6.6 Discussion

In this final section we mention a few items of interest for further study, and we will show some examples of applications of this work.

- In the previous section we have seen that we have global fixed point properties for elliptic and hyperbolic ray path types. In the wave front definition, we have seen that in the elliptic case we can further distinguish convergent and divergent ray paths. In the elliptic case, we would also like to have a corresponding distinction in terms of fixed points, so we would have to show that the function $\phi(t, u)$ should have either only fixed points or only antipodal points. But this is not obvious. Arguments of homotopy theory cannot be applied unless we know that an increasing mapping as in Figure 6.4(c) does not occur as the result of a reflector mapping.

- In the 2D case we have seen that smooth ray paths have to be one-to-one, otherwise infinite intensities may occur. We conjecture that if the reflector surface is *simply connected*, we have a similar property in 3D: if the reflector mapping $(t, u) \to (\theta, \phi)$ is differentiable and not one-to-one, then the corresponding light distribution has an infinite intensity. Note that this is not the case if the surface is not simply connected: Example 6.3.3 provides an example of a reflector which produces a smooth two-to-one ray path without infinite peaks, if we allow a hole around the $t = 0$ direction. A

study of a possible classification of global ray path types for reflectors with one or more holes is also of interest.

- The study of the different types of ray paths may perhaps be helpful in the study of the solutions of the Monge-Ampère equation (6.117) in the case that the reflector surface is simply connected. A heuristic approach to the reflector design problem based on the fixed point properties, suggests that with the proper boundary conditions, there are precisely 2 solutions in the elliptic case (corresponding to convergent and divergent ray paths), while in the hyperbolic case, a one-parametric family of solutions seems to exist. Perhaps the uniqueness and existence results of Marder [24] and Oliker [29], as mentioned in Section 1.2, can be generalized to more arbitrary cones, or to the hyperbolic case.

Appendix A

Practical Examples

A better theoretical understanding of ray paths produced by reflectors may also contribute to more heuristic approaches as mentioned in Section 1.2. Within Philips, this has indeed been the case. A heuristic design method has been developed, which proves that the different solution types can actually be found. The fixed point properties of the various solution types play an important role in our heuristic.

To lift a tip of the veil, consider Figure A.1. In this figure, part of a sphere is triangulated such that all triangles span equal solid angles with respect to the origin of the sphere. When we imagine a uniform point source to be located in the centre of the sphere, and the triangles to be the facets of a reflector, then all facets receive equal amounts of luminous flux from the source. In the above figure, we have 160 facets, ordered in strips and rings. For large numbers of facets, incident and reflected beams will both be contained within small solid angles with respect to the source.

Now suppose we have a required intensity distribution, with a total required luminous flux equal to the total flux reflected from the reflector. What we now can do is subdivide the total required intensity distribution into parts, such that all parts have equal flux, and such that they can be realized approximately by the reflected beams resulting from triangular facets. These parts will be called *required beams*.

Next we can assign each facet to a required beam, and we can change the orientation and size of each facet, such that its triangular solid angle with respect to the source remains fixed, and such that its reflected beam resembles the corresponding required beam. The reflector surface we obtain will then realize a distribution resembling the required distribution. However, the crucial difficulty here is to do this in such a way that a *connected* reflector surface is obtained!

Note that when we have n facets and n required beams, there are $n!$ ways of

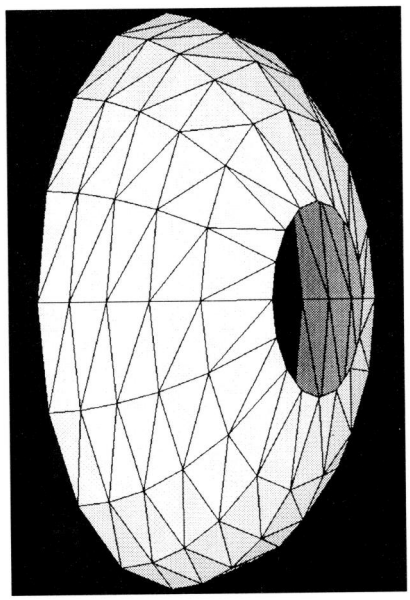

Figure A.1: *Part of a triangulated sphere, representing a facetted reflector.*

assigning the facets to the beams. A random assignment will generally lead to a chaotic, strongly disconnected collection of facets. In order to obtain a collection of facets resembling a connected surface, the assignment of (incident beams of) facets and required beams should satisfy "fixed point properties" similar to those derived for the one-to-one correspondence between incident and reflected rays for smooth surfaces in Section 6.3.

In the examples that follow, it should be noted that the required distribution is a near field distribution, i.e. it is defined as an illuminance on a screen. Furthermore, neither the reflector nor the required distribution are necessarily simply connected, as was assumed in the theory of Chapter 6.

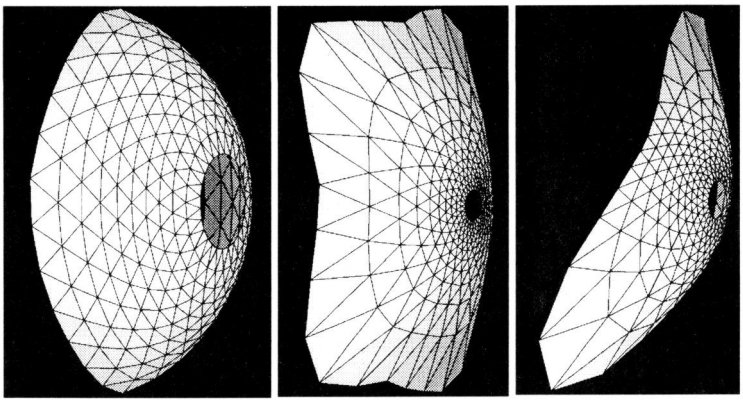

Figure A.2: *Convergent, divergent and hyperbolic reflectors which all illuminate a square uniformly.*

Example A.1.1. The uniform illumination of a rectangular square. This square is at 1 meter distance from the light source, and its size is 1 by 1 meter. The reflectors have an opening angle of 60 degrees, and a back opening of 30 degrees. They are about 0.1 meter in size. In Figure A.2 a convergent, a divergent and a hyperbolic solution are shown. They all realize similar distributions to the one in Figure A.3. □

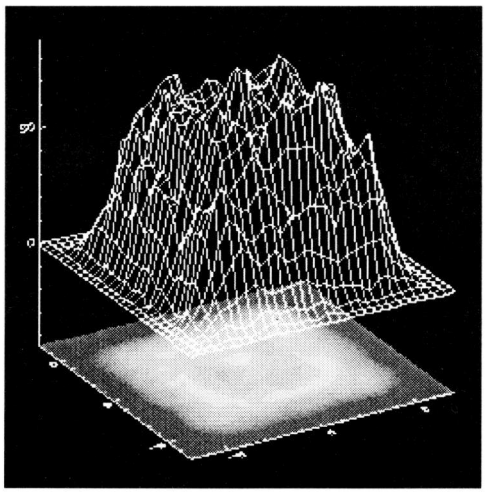

Figure A.3: *The illuminance achieved by the reflectors in Figure A.2.*

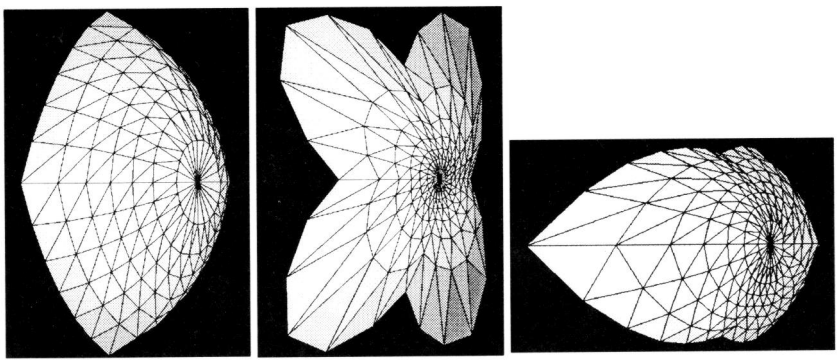

Figure A.4: *Convergent, divergent and hyperbolic reflectors which all produce four light peaks as in Figure A.5.*

Example A.1.2. In this example, the reflectors have realized 4 separate peaks of light at the corners of the screen of the previous example. See Figures A.4 and A.5. □

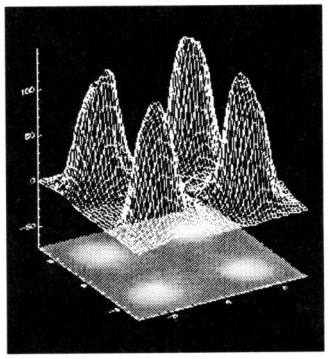

Figure A.5: *The illuminance achieved by the reflectors in Figure A.4.*

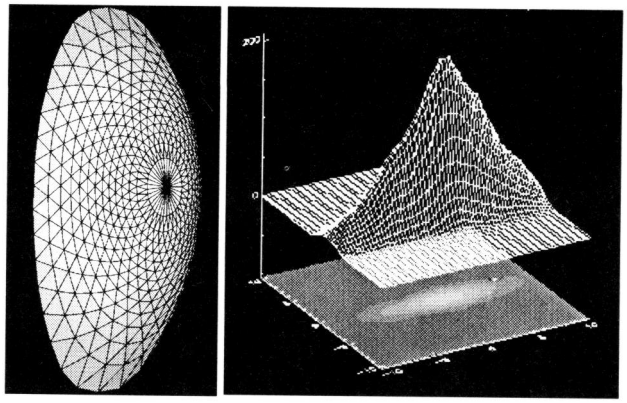

Figure A.6: *A convergent reflector realizing a car headlight profile.*

Example A.1.3. In Figure A.6, a distribution for car headlights is shown on a screen at a distance of 25 meter from the car, with a size of 10 by 10 meter. This distribution was achieved by the convergent reflector shown in the same figure, in combination with a realistic area source. □

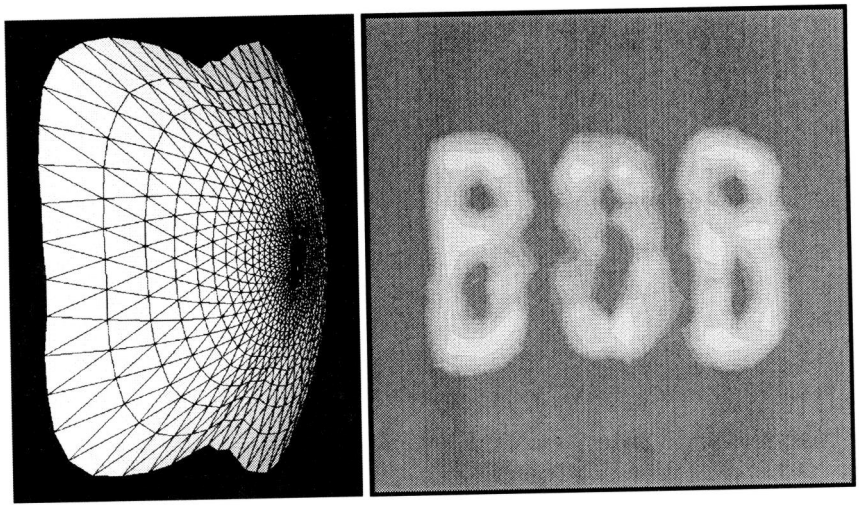

Figure A.7: *A divergent reflector which produces a light distributions that forms the name BOB.*

Example A.1.4. Figure A.7 shows the contour plot of the distribution corresponding to a divergent reflector that aims to produce the word BOB as its light distribution. Lighting tasks of this complexity are generally considered to be impossible to achieve with just a single reflector. □

References

[1] H.W. Bodman and B. Weis, Flux distribution with perfect specular reflectors, *Lighting Res. Techn.* **5**, No. 2, 1973, pp. 112-115.

[2] F. Brickell, L. Marder and B.S. Westcott, The geometrical optics design of reflectors using complex coordinates, *J. Phys. A: Math. Gen.* **10**, No. 2, 1977, pp. 245-260.

[3] F. Brickell and B.S. Westcott, Reflector design for two-variable beam shaping in the hyperbolic case, *J. Phys. A: Math. Gen.* **9**, No. 1, 1976, pp. 113-128.

[4] F. Brickell and B.S. Westcott, Phase and power density distributions on plane apertures of reflector antennas, *J. Phys. A: Math. Gen.* **11**, No. 4, 1978, pp. 777-789.

[5] D.G. Burkhard and D.L. Shealy, Simplified Formula for the Illuminance in an Optical System, *Applied Optics* **20**, No. 5, 1981, pp. 897-909.

[6] W.H. Cunningham and A.B. Marsh, A Primal Algorithm for Optimum Matching, *Polyhedral Combinatorics (dedicated to the memory of D.R. Fulkerson)*, Eds.: M.L. Balinski and A.J. Hoffman, Math. Programming Stud. No. 8, North-Holland, Amsterdam, 1978, pp. 50-72.

[7] W.B. Elmer, *The Optical Design of Reflectors*, John Wiley and Sons, New York, 1980.

[8] H.W. Engl and A. Neubauer, Reflector Design as an Inverse Problem, Proc. of the Fifth Europ. Conf. on Mathematics in Industry, June 6-9, 1990, Lahti, M. Heilio (ed.), pp. 13-24, Teubner, Stuttgart 1991.

[9] A. Feingold and K.G. Gupta, New Analytical Approach to the Evaluation of Configuration Factors in Radiation From Spheres and Infinitely Long Cylinders, *J. Heat Transfer*, **92**, No. 1, 1970, pp. 69-76.

[10] H.N. Gabow, *Implementation of Algorithms for Maximum Matching on Non-Bipartite Graphs*, Ph.D. Thesis, Stanford University Dept. Comput. Sci., 1973.

[11] V. Galindo-Israel, W.A. Imbriale and R. Mittra, On the theory of the synthesis of single and dual offset shaped reflector antennas, *IEEE Trans. Antenn. Prop.* **AP-35**, No. 8, 1987, pp. 887-896.

[12] G.H. Hardy, J.E. Littlewood and G. Pólya, *Inequalities*. Cambridge University Press, Cambridge, 2nd Ed. 1952.

[13] A.J.E.M. Janssen and M.J.J.J.B. Maes, An optimization problem in reflector design, *Philips Journal of Research* **47**, 1992, pp. 99-143.

[14] H.A.E. Keitz, *Light Calculations and Measurements*, MacMillan and Co. Ltd., London, 1971.

[15] J.B. Keller, The inverse scattering problem in geometrical optics and the design of reflectors, *IRE Trans. Antenn. Propag.*, 1958, pp. 146-149.

[16] E. Kreyszig, *Differential Geometry*, University Of Toronto Press, 1959, republication: Dover, New York, 1991.

[17] H.S.M. Kruijer, Mathematische modellen in de verlichtingskunde, Master's Thesis, Technical University of Eindhoven, The Netherlands, 1971.

[18] E.L. Lawler, *Combinatorial Optimization: Networks and Matroids*, Holt, Rinehart and Winston, New York, 1976.

[19] M. Loève, *Probability Theory*, 3rd Ed., Van Nostrand, 1963.

[20] G. Loos and M. Treiber, Optimierungsmethoden für optische Reflektorsysteme, *Optik*, **80**, No. 1, 1988, pp. 33-38.

[21] L. Lovász and M.D. Plummer, *Matching Theory*, Annals of Discrete Mathematics **29**, North-Holland, Amsterdam, New York, 1986.

[22] M.J.J.J.B. Maes and A.J.E.M. Janssen, A Note on cylindrical reflector design, *Optik* **88**, No. 4, 1991, pp. 177-181.

[23] M.J.J.J.B. Maes, Mathematical Methods for 2D Reflector Design, Proc. of the Conf. Inverse Problems and Optimal Design in Industry, July 8-10, 1993, Philadelphia, Pa., H.W. Engl, J. McLaughlin (Eds.), pp. 123-146, Teubner Stuttgart, 1994.

[24] L. Marder, Uniqueness in reflector mappings and the Monge-Ampère equation, *Proc. R. Soc. Lond. A* **378**, 1981, pp. 529-537.

[25] J.H. McDermit and T.E. Horton, Reflective optics for obtaining prescribed irradiative distributions from collimated sources, *Applied Optics* **13**, No. 6, 1974, pp. 1444-1450.

[26] M.Q. Montón and J.G. Vizmanos, Design of asymmetric reflecting surfaces, *Lighting Res. Techn.* **18**, No. 3, 1986, pp. 119-124.

[27] O. Myodo and M. Karino, A new method for computer aided design of luminaire reflectors, *Journal of IES*, Jan. 1982, pp. 98-105.

[28] A.P. Norris and B.S. Westcott, Computation of reflector surfaces for bivariate beamshaping in the elliptic case, *J. Phys. A: Math. Gen.* **9**, No. 12, 1976, pp. 2159-2169.

[29] V.I. Oliker, Near radially symmetric solutions of an inverse problem in geometric optics, *Inverse Problems* **3**, 1987, pp. 743-756.

[30] V.I. Oliker, On reconstructing a reflecting surface from the scattering data in the geometric optics approximation, *Inverse Problems* **5**, 1989, pp. 51-65.

[31] V.I. Oliker, E. Newman and L. Prussner, Formula for computing illumination intensity in a mirror optical system, *J. Opt. Soc. Am. A*, **10**, No.9, 1993, pp. 1895 - 1901.

[32] K. Petry, B. Weis and A. Willing, Beleuchtungsstärkeberechnung für ausgedehnte Lichtquellen und ideale Spiegelreflektoren, *Licht-Forschung* **3**, No. 2, 1981, pp. 89-96.

[33] A. Reiner and B. Weis, Zur Anwendung systemtheoretischer Methoden in der Lichttechnik, *Optik* **43**, No. 2, 1975, pp. 185-197.

[34] J.S. Schruben, Formulation of a reflector-design problem for a lighting fixture, *J. Opt. Soc.* **62**, No. 12, 1972, pp. 1498-1501.

[35] C. Scott, *Modern Methods of Reflector Antenna Analysis and Design*, Artech House, Boston, 1990.

[36] R. Siegel and J.R. Howell, Thermal Radiation Heat Transfer, 2nd Ed., McGraw-Hill Book Company, New York, 1981.

[37] O.N. Stavroudis, *The Optics of Rays, Wavefronts, and Caustics*, Academic Press, New York, London, 1972.

[38] V.V. Trembač: *Luminaires*. Soviet Union Publishing Institute for Energy Technology, Moscow, Leningrad 1958.

[39] J.M. Waldram, Some developments in the design of specular reflectors, *Lighting Res. Techn.* **2**, No. 3, 1970, pp. 164-173.

[40] B. Weis, Lichtverteilung idealer Spiegelreflektoren, *Lichttechnik* **24**, No. 9, 1972, pp. 455-459.

[41] B. Weis, Berechnung von Spiegelreflektoren, *Optik* **50**, No. 5, 1978, pp. 371-390.

[42] B.S. Westcott, *Shaped Reflector Antenna Design*, Letchworth, UK: Research Studies Press, 1983.

[43] B.S. Westcott and F. Brickell, Computation of reflector surfaces for two-variable beam shaping in the hyperbolic case, *J. Phys. A: Math. Gen.* **9**, No. 4, 1976, pp. 611-625.

[44] B.S. Westcott and A.P. Norris, Reflector synthesis for generalized far-fields, *J. Phys. A: Math. Gen.* **8**, No. 4, 1975, pp. 521-532.

[45] W. Wolber, Berechnung von Reflektoren für beliebige Lichtverteilungen, *Lichttechnik* **22**, No. 12, 1970, pp. 597-598.

Summary

Mathematical Methods for Reflector Design

This thesis discusses mathematical methods for reflector design. Reflectors are an important component in many lighting systems. They contribute to the realization of required light beams as well as to the efficient use of the yield of a lamp. From early days, Philips produces lighting systems for a variety of applications like street lighting, playground lighting, but also systems for Projection TV, LCD backlighters, or ordinary TL-tubes and spotlights.

For a long time, optical design has been a matter of craftsmanship and experience, where the drawing table and prototypes played a central role. Naturally, computer technology has changed this situation. The expensive process of manufacturing and measuring prototypes can partly be replaced by computer programs for simulation. When I met the optical designers of Central Development Lighting in 1990, simulations programs which compute a light distribution for a given light source and reflector, were already being used extensively. However, there were hardly any programs or methods available for the inverse problem, which is the problem to calculate a reflector for a given lamp and required light distribution.

In its full generality, this is a very difficult problem: one has to deal with complicated light sources, multiple reflections, but also for instance with geometrical constraints of the armature, aesthetical matters, or requirements with regards to the production of reflectors. Not all these practical aspects can be taken into account in the mathematical modelling of the problem. We have to simplify the problem in such a way that a mathematical approach is workable. Consequently, we assume in this thesis that reflection is specular and that light sources are small with respect to the reflector. We assume that required light distributions are well-defined and we neglect multiple reflections or reflected light re-entering the light source. The assumptions we make are similar to those made by designers in practice, and they don't limit the practical relevance of this research.

The literature on reflector design is also usually limited to small light sources and specular reflection. The methods described in the relatively scarce litera-

ture on this topic can roughly be divided in three classes: optimization methods, heuristic approaches, and studies based on mathematical analysis, in which the problem is formulated in terms of differential equations. What in my opinion is usually lacking in all these approaches is the geometrical insight in ray paths, or in other words, in the question: what light beams can actually be realized by reflectors? I think that an answer to this problem will be of use to all the above methods. To obtain a better geometrical understanding was one of the main issues I addressed, and the results of this research have led to this thesis. It discusses the mathematical aspects of the reflector design problem, which within Philips have been the basis for practical design methods.

A considerable simplification of the general reflector design problem is possible when the problem has rotational or cylindrical symmetry (TL-tubes for example). In these cases, a 2-dimensional (2D) approach to the problem becomes possible. Chapter 3 discusses the 2D problem. When one considers smooth (differentiable) ray paths only, then it is easy to show that 2D problems with point sources have precisely two solutions, corresponding to convergent and divergent ray paths. Things become more interesting when one drops the smoothness assumption. Then 2D problems appear to have infinitely many solutions and, by using the convergent and divergent beams as building blocks, it is possible to compute reflectors of varying shapes and sizes, which all produce the same light distribution. In particular, the extra freedom of choice can be exploited to fulfill the practically important geometrical constraints.

A special geometrical constraint is treated in Chapter 4, for cylindrical reflectors with a required light distribution defined on angles. It is described how one can find a 'most compact' reflector for a given required distribution. This chapter uses classical real analysis, in particular it applies the theory of 'rearrangements'.

The 2D design methods for point sources can be realized in very fast algorithms even on a simple computer. In order to check the validity of results for extended sources such as cylinders and spheres, it was desirable to have a fast method for the calculation of light distributions for these sources as well. In Chapter 5 it is shown that those light distributions can be computed analytically to a large extent, which has resulted in an implementation which is considerably faster than existing ray-tracing techniques. In this chapter we apply the calculation of 'view factors' which are also being used in Computer Graphics and Heat Transfer.

Chapter 6 is concerned with the 3D problem for point sources, and for required distributions defined on angles. We do not present a design method, but we aim at geometrical insight in the problem that can be useful in the development of actual design methods. Two laws play principal parts in the formulation of the reflector design problem: the law of reflection and the law of conservation of energy. Starting from these, and assuming that there is a one-to-one correspondence

between incident and reflected rays, a partial, non-linear, second-order differential equation can be deduced which describes the problem mathematically. This type of differential equation is called the Monge-Ampère equation. Methods based on the solution of this equation as described in the literature so far have had only limited results of practical relevance. Only little is known about the existence and the uniqueness of solutions, and for numerical solutions, good initial guesses are needed.

The highest order term of the Monge-Ampère equation, $f_{tt} f_{uu} - f_{tu}^2$, is related to the Gaussian curvature of a surface. Using elementary differential geometry, it is shown in Chapter 6 that the Monge-Ampère equation can be written in terms of the curvature of the wave front of the reflected light, immediately after reflection. The possible curvatures of this wave front (flat, convex, concave or saddle-shaped) lead to a classification of types of ray paths that can be realized by means of a reflector. We show that, when infinite intensities do not occur in the required distribution, there are three types of ray paths. These are the convergent, divergent and hyperbolic ray paths, which correspond to concave, convex and saddle-shaped wave fronts, respectively.

This classification can also be made by a completely different characterization of ray paths, which uses fixed point properties of reflector mappings. By this characterization one gains a better understanding on which ray paths are feasible. It is for instance impossible to rotate a ray path, by means of just one connected reflector without any cracks or holes. The equivalence between the definitions of the ray path types in terms of curvatures of the wave front and in terms of fixed point properties, is demonstrated locally. The practical relevance of the fixed point characterization is made plausible in the appendix, where a rough sketch of a heuristic design method is given, as well as several practical results from a method based on this theory.

Samenvatting

Wiskundige Methoden voor Reflector Ontwerp

Dit proefschrift behandelt wiskundige methoden voor reflector ontwerp. Reflectoren vormen een belangrijk onderdeel van veel verlichtingssystemen. Ze dragen er aan bij dat een voorgeschreven lichtbundel verkregen wordt en dat de lichtopbrengst van een lamp zo efficiënt mogelijk gebruikt wordt. Reeds van oudsher produceert Philips verlichtingssystemen voor zeer verschillende toepassingen, zoals straatverlichting, stadionverlichting, maar ook systemen voor Projectie TV, LCD backlighters, of voor gewone TL-buizen en spotjes.

Lange tijd is optisch ontwerp een kwestie van vakmanschap en ervaring geweest, waarbij de tekentafel en prototypes een centrale rol speelden. Uiteraard heeft computertechnologie in die situatie verandering gebracht. Het dure proces van het vervaardigen en doormeten van prototypes kan deels vervangen worden door simulatieprogramma's op de computer. Toen ik in 1990 met optiek ontwerpers van Central Development Lighting in contact kwam, werd reeds veel gebruik gemaakt van simulatieprogramma's, die voor een gegeven lamp en reflector de bijbehorende lichtverdeling uitrekenen. Echter, voor het omgekeerde probleem, om voor een gegeven lamp en gewenste lichtverdeling een reflector uit te rekenen, waren nauwelijks programma's of methoden voorhanden.

In zijn algemeenheid is dit ook een zeer moeilijk probleem, waarbij men niet alleen met ingewikkelde lichtbronnen, meervoudige reflecties enz. te maken heeft, maar bijvoorbeeld ook met geometrische beperkingen aan de optiek, esthetische wensen, of eisen met betrekking tot de productie van reflectoren. In een wiskundige modellering van het probleem kunnen we doorgaans dan ook niet alle praktische aspekten meenemen. We zijn genoodzaakt het probleem zodanig te vereenvoudigen dat een wiskundige aanpak rendabel is. Zo nemen we in dit proefschrift aan dat reflectie speculair is en dat lichtbronnen klein zijn ten opzichte van de optiek. We gaan uit van welgedefinieerde gewenste lichtverdelingen, en we verwaarlozen effecten zoals licht dat terugvalt op de lamp, of meervoudige reflecties. De in dit proefschrift gemaakte aannames lijken veel op de aannames die

ontwerpers in de praktijk maken bij de modellering van hun probleem en ze tasten de praktische relevantie van het onderzoek dan ook niet aan.

Ook in de literatuur over reflector ontwerp beperkt men zich doorgaans tot kleine lichtbronnen en speculaire reflectie. De methoden beschreven in de relatief schaarse literatuur over dit onderwerp kan men opdelen in drie klassen: optimaliseringsmethoden, heuristieke aanpakken en meer wiskundig analytische studies die het probleem in termen van differentiaalvergelijkingen formuleren. Wat mijns inziens vaak ontbreekt in al deze aanpakken is een geometrisch inzicht in stralengangen, ofwel in de vraag: wat voor soort lichtbundels kan men nu eigenlijk met reflectoren maken? Ik denk dat een antwoord op deze vraag voor alle methodes van nut zal zijn. Het verkrijgen van een duidelijker geometrisch inzicht was één van de taken die ik mezelf stelde, en de resultaten van dit onderzoek vinden hun weerslag in dit proefschrift. Het behandelt de mathematisch-theoretische aspecten van het reflector ontwerp probleem, die binnen Philips de basis zijn geweest voor praktische ontwerpmethoden.

Een significante vereenvoudiging van het algemene reflector ontwerp probleem is mogelijk wanneer er sprake is van rotatiesymmetrie of cylindersymmetrie (denk aan TL-buizen). In die gevallen is een 2-dimensionale (2D) aanpak van het probleem mogelijk. Het 2D probleem wordt behandeld in Hoofdstuk 3. Wanneer men zich beperkt tot gladde (differentieerbare) stralenbundels, is het eenvoudig af te leiden dat 2D problemen met puntbronnen precies twee oplossingen hebben, die overeenkomen met convergente en divergente bundels. Interessanter wordt het wanneer men de eis van differentieerbaarheid laat vallen. Dan blijken 2D problemen oneindig veel oplossingen te hebben, en is het mogelijk om, met de convergente en divergente bundels als bouwblokken, reflectoren van zeer verschillende vorm en afmetingen te berekenen, die allemaal dezelfde gewenste lichtverdeling opleveren. In het bijzonder kan men door de extra keuzevrijheid aan de praktisch zo belangrijke geometrische beperkingen proberen te voldoen.

Een speciaal geval van zo'n geometrische beperking is in Hoofdstuk 4 uitgezocht voor cylindrische reflectoren met een gewenste lichtverdeling gedefinieerd op hoeken. Er wordt beschreven hoe men in zekere zin een meest compacte reflector voor een gegeven gewenste verdeling kan vinden. In dit hoofdstuk wordt gebruik gemaakt van onderdelen van de klassieke reële analyse, onder andere van de theorie van 'rearrangements'.

De 2D ontwerpmethoden voor puntbronnen zijn in zeer snelle algorithmes op een eenvoudige computer te realizeren. Om de geldigheid van de resultaten voor uitgebreide bronnen als cylinders en bollen te kunnen verifiëren, bleek het wenselijk om ook een snelle methode te hebben voor de berekening van de lichtverdeling behorend bij die bronnen. In Hoofdstuk 5 laat ik zien dat die lichtverdelingen grotendeels analytisch berekend kunnen worden, wat heeft geresulteerd in

een implementatie die veel sneller is dan bestaande ray-tracing methoden. In dit hoofdstuk wordt gebruik gemaakt van de berekening van 'view factoren', zoals die ook voorkomen in Computer Graphics of bij de berekening van warmtestraling.

Hoofdstuk 6 behandelt het 3D probleem voor puntbronnen, en voor gewenste lichtverdelingen gedefinieerd op hoeken. Er wordt hier uiteindelijk geen ontwerpmethode afgeleid, maar wel worden geometrische inzichten in het probleem verkregen die bij het ontwikkelen van concrete ontwerpmethoden nuttig zijn. Twee wetten spelen een hoofdrol bij de formulering van het reflector ontwerp probleem: de reflectiewet en de wet van behoud van energie. Met deze ingrediënten, en met de aanname dat er een één-op-één-correspondentie tussen invallende en gereflecteerde stralen bestaat, kan men een partiële, niet-lineaire, tweede orde differentiaalvergelijking afleiden die het probleem wiskundig beschrijft. Dit type differentiaalvergelijking heet een Monge-Ampère vergelijking. De in de literatuur geboekte, praktisch relevante resultaten van methoden gebaseerd op het oplossen van deze vergelijking zijn beperkt. Over de existentie en de uniciteit van oplossingen is nog maar weinig bekend, en voor numerieke oplossingen zijn goede beginschattingen nodig.

De hoogste orde term van de Monge-Ampère vergelijking, $f_{tt} f_{uu} - f_{tu}^2$, is gerelateerd aan de Gaussische kromming van een oppervlak. Gebruik makend van elementaire differentiaalmeetkunde wordt in Hoofdstuk 6 getoond dat de Monge-Ampère vergelijking beschreven kan worden in termen van de kromming van het golffront van het gereflecteerde licht, onmiddellijk na reflectie. De mogelijke krommingen van dit golffront (vlak, convex, concaaf of zadelvormig) geven aanleiding tot een klassificatie van typen stralenbundels die met behulp van reflectoren gerealiseerd kunnen worden. We tonen aan dat, wanneer oneindige intensiteiten niet toegelaten worden, er drie typen stralenbundels bestaan. Dit zijn de convergente, divergente en hyperbolische bundels, die horen bij respectievelijk concave, convexe en zadelvormige golffronten.

Deze klassificatie kan men ook maken aan de hand van een geheel andere karakterisering van stralenbundels, die gebruik maakt van vaste punten stellingen over reflector afbeeldingen. Hierdoor krijgt men een beter inzicht in welke stralengangen mogelijk zijn. Het is bijvoorbeeld niet mogelijk om met behulp van een samenhangende reflector zonder scheuren of gaten een stralenbundel te roteren. De equivalentie tussen de definities van de typen bundels in termen van krommingen van golffronten en in termen van vaste punten, wordt locaal aangetoond. De praktische relevantie van de vaste punten formulering wordt aannemelijk gemaakt in de appendix, waar een zeer ruwe schets van een heuristische ontwerpmethode gegeven wordt, alsmede enkele praktische resultaten van een op deze theorie gebaseerde methode.

Biography

Maurice Maes was born in Maastricht, the Netherlands, on September 1, 1963. From 1981 to 1987 he studied mathematics at the University of Nijmegen. In September 1987 he received his Master's degree in mathematics with honours. The subject of his thesis was *The Mixed Hodge Structure on the Cohomology of the Complement of a Smooth Curve in* $P^1 \times P^1$.

In October 1987, he joined Philips Research Laboratories (PRL) as a member of the Mathematics Group. He has been working on geometrical problems in Computer Vision and IC Design, and from 1992 to 1996, his main research subject has been Reflector Design.

Presently, he is a member of the Information Technology group at PRL, and his main interests include Multimedia Asset Management and Digital Watermarking for copyright protection.